**SCIENTIFIC COMMITTEE**
**TWENTIETH REGULAR SESSION**

Manila, Philippines
14 – 21 August 2024

# Stock Assessment of Shortfin Mako Shark in the North Pacific Ocean through 2022

**WCPFC-SC20-2024/SA-WP-14**

**ISC**[1]

[1] International Scientific Committee for Tuna and Tuna-like Species in the North Pacific Ocean

# ANNEX 14

*24th Meeting of the*
*International Scientific Committee for Tuna*
*and Tuna-Like Species in the North Pacific Ocean*
*Victoria, British Columbia, Canada*
*June 17-24, 2024*

# STOCK ASSESSMENT OF SHORTFIN MAKO SHARK IN THE NORTH PACIFIC OCEAN THROUGH 2022[1]

**June 2024**

1 Prepared for the 24th Meeting of the International Scientific committee on Tuna and Tuna-like Species in the North Pacific Ocean (ISC) held June 17-24, 2024 at Victoria, British Columbia, Canada. Document should not be cited without permission of the authors.

Left Blank for Printing

# Table of Contents

*ANNEX 14*

# STOCK ASSESSMENT OF SHORTFIN MAKO SHARK IN THE NORTH PACIFIC OCEAN THROUGH 2022

*International Scientific Committee for Tuna and Tuna-Like Species in the North Pacific Ocean (ISC)*

## REPORT OF THE SHARK WORKING GROUP

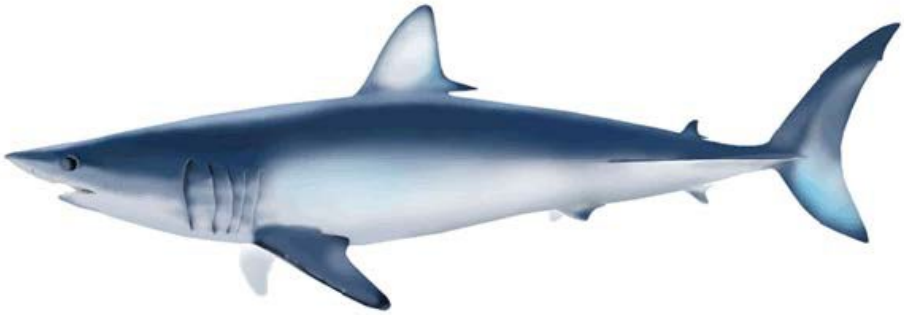

17-24 June 2024
Victoria, British Columbia, Canada

## EXECUTIVE SUMMARY

This document presents the results of the 2024 ISC SHARKWG stock assessment of shortfin mako shark (SMA, *Isurus oxyrinchus*) in the North Pacific Ocean (NPO). Previously an indicator analysis was performed in 2015 and an integrated, age-based stock assessment using the Stock Synthesis (SS3) modeling platform was conducted in 2018. Revision of historical catch data and removal of the early relative abundance index made it challenging to reconcile the recent catch and index data with the biological assumptions, and a strategic decision was made to use a Bayesian State-Space Surplus Production Model (BSPM) for the 2024 assessment to model stock status from 1994-2022.

### Stock Identification and Distribution

Current and previous stock assessment frameworks have assumed that SMA represent a single, distinct and well-mixed stock in the NPO. Within the NPO there is strong evidence to suggest, based on the presence of neonates (pups), distinct parturition sites: eastern (Southern California Bight, and Baja California) and western (waters east of Japan). Research within the Pacific indicates that female makos may have parturition site fidelity which could lead to discrete

population structure even if male gene flow exists. The available information appears to support the differentiation between separate NPO and south Pacific Ocean SMA stocks but more work is needed to identify the stock structure in the NPO (e.g., single well-mixed stock, or multiple stocks with varying connectivity as a result of females exhibiting site fidelity with distinct parturition sites).

**Catch History**

Fisheries have likely interacted with SMA in the NPO since the early 20$^{th}$ century, and certainly post-World War II with the expansion of industrial longlining into the high seas. However, fisheries impacts in terms of catch are highly uncertain as data on shark catches were largely unavailable prior to 1975 and species-specific records of shark catch were unavailable prior to 1994 for key fisheries. Species specific catch of sharks is available post-1994 however these catches are also uncertain given inconsistent reporting of shark catch and discards in commercial logbooks.

The previous assessment compiled catches for two periods, 1975-1993 and 1994-2016. When updating catches through 2022 for the current assessment, driftnet catches for the early period (1975-1993) were substantially revised and resulted in early period catches being lower than catches in subsequent periods. This revision made it difficult to explain recent period (1994-2022) increases in catch-per-unit-effort (CPUE), and a decision was made to model stock status from 1994-2022. Within the modeled period, catch generally increased from ~50,000 individuals per year in 1994 to ~80,000 individuals per year in 2022 (~94,000 individuals per year, average 2018-2022; Figure ES 1). Catches in the modeled period come predominantly from longline fisheries though catch from artisanal fisheries in Mexico and China make up an important component of the catch in more recent years.

**Data and Assessment**

As a first step, a conceptual model was developed to organize understanding of NPO SMA, identify plausible hypotheses for stock dynamics and fisheries structures, and to highlight key uncertainties (Figure ES 2). Using the conceptual model as a guide, a BSPM was developed to model the population from 1994-2022 in order to provide stock status information. Catch was aggregated into a single fishery and the model was fit to alternative standardized CPUE data (Figure ES 3), representing relative trends in abundance, provided by Japan, Chinese Taipei, and USA. Population dynamics are governed by a simplified parameter set: population carrying capacity, maximum intrinsic rate of increase, initial depletion relative to carrying capacity, and the shape of the production function. Informative priors were developed using numerical simulation based on NPO SMA biological characteristics in combination with a prior pushforward analysis. Additional estimated parameters included observation, process, and fishing mortality error terms.

Alternate configurations of the BSPM were developed to deal with uncertainty in catch estimates. Given that the BSPM simplifies the population dynamics, an age-structured simulation was developed to assess the possible level of bias when applying the BSPM.

An ensemble of 32 BSPMs was used to provide stock status and management advice. Models within the ensemble were defined based on alternate prior configurations, treatment of catch, and choice of standardized CPUE index used in model fitting. Models were retained in the final ensemble if they met convergence criteria (28 of 32), and the joint posterior distribution across models was used to characterize stock status.

**Future Projections**

Stochastic future projections were conducted for each BSPM in the ensemble. The SHARKWG used 4 exploitation rate ($U$) based scenarios to conduct 10-year future projections for NPO SMA: the average exploitation rate from 2018-2021 $U_{2018-2021}$, $U_{2018-2021} + 20\%$, $U_{2018-2021} - 20\%$, and the exploitation rate that produces maximum sustainable yield (MSY) $U_{MSY}$. Future projections were conducted using each set of parameters from the posterior distribution of BSPM models. The process error in the forecast period was resampled from the estimated values of process error from the model estimation period.

**Key Uncertainties**

Key uncertainties were identified through the conceptual model and development of the assessment model. While the model ensemble attempts to integrate over some of these uncertainties (catch, standardized CPUE, biology - through alternative priors), future work and research is needed in order to improve understanding of:

- *Stock structure in the NPO*: multiple parturition sites raise the possibility that multiple stocks exist depending on the level of genetic exchange between parturition sites.
- *Biology (age, growth, reproduction, and natural mortality)*: aging is uncertain due to differences in applied methodologies, limited utility of vertebral aging for large-sized individuals, and limited age validation. A general lack of observations for large mature females complicates understanding of biology.
- *Population scale*: Increasing trends in both the standardized CPUE and catch over the modeled period provide very little information from which to infer population scale.
- *Population trend*: There are no fisheries that operate across the entire range of SMA in the NPO and there are no fisheries that regularly capture and observe large females. This poses a challenge for modeling and indexing the status of the reproductive component of the stock.
- *Catch*: Fisheries related mortality (e.g., reported catch) is uncertain in the recent period due to uncertainties in how interactions with sharks (retained catch, live discards, and dead

discards) are reported in commercial logbooks, and is highly uncertain prior to 1994 due to the lack of species-specific shark information for many fisheries.

**Research Needs**

Future research is needed to resolve many of the highlighted uncertainties with the model and the input data. Research priorities include:

- Scoping study to develop and evaluate a genetic sampling plan for close-kin mark-recapture (CKMR).
- Improving aging estimates and methods used for determining age
- Improving catch estimates: Fishery removals should be calculated as the sum of landed catch, dead discards, and live discards which eventually succumb to release mortality for all fleets which interact with NPO SMA.
- Applying a joint spatiotemporal analysis of operational longline data to improve the spatial representativeness of the index
- Standardizing size composition if they are not collected representatively relative to either fishery removals or the population.
- Building on the BSPM and age-structured simulation by developing a Bayesian age-structured estimation model.

**Stock Status**

The current assessment provides the best scientific information available on North Pacific shortfin mako shark (SMA) stock status. Results from this assessment should be considered with respect to the management objectives of the Western and Central Pacific Fisheries Commission (WCPFC) and the Inter-American Tropical Tuna Commission (IATTC), the organizations responsible for management of pelagic sharks caught in international fisheries for tuna and tuna-like species in the Pacific Ocean. Target and limit reference points have not been established for pelagic sharks in the Pacific Ocean. In this assessment, stock status is reported in relation to maximum sustainable yield (MSY).

A Bayesian state-space production model (BSPM) ensemble was used for this assessment; therefore, the reproductive capacity of this population was characterized using total depletion (D) rather than spawning abundance as in the previous assessment. Total depletion is the total number of SMA divided by the unfished total number (i.e., carrying capacity). Recent D ($D_{2019-2022}$) was defined as the average depletion over the period 2019-2022. Exploitation rate (U) was used to describe the impact of fishing on this stock. The exploitation rate is the proportion of the SMA population that is removed by fishing. Recent U ($U_{2018-2021}$) is defined as the average U over the period 2018-2021.

During the 1994-2022 period, the median D of the model ensemble in the initial year

$D_{1994}$ was estimated to be 0.19 (95% CI: credible intervals = 0.08-0.44), and steadily improved over time and $D_{2019-2022}$ was 0.60 (95% CI = 0.23-1.00) (Table ES 1 and Figure ES 4). Although there are large uncertainties in the estimated population scale, the best available data for the stock assessment are four standardized abundance indices from the longline fisheries of Japan, Taiwan, and the US; and all four indices indicate a substantial (>100%) increase in the population during the assessment period. The population was likely heavily impacted prior to the start of the modeled period (1994), after which it has been steadily recovering. It is hypothesized that the fishing impact prior to the modeled period was likely due to the high-seas drift gillnet fisheries operating from the late 1970s until it was banned in 1993, though specific impacts from this fishery on SMA are uncertain as species specific catch data are not available for sharks. Consistent with the estimated trends in depletion, the exploitation rates were estimated to be gradually decreasing from 0.023 (95% CI = 0.004-0.09) in 1994 to the recent estimated exploitation rate ($U_{2018-2021}$) of 0.018 (95% CI = 0.004-0.07). The decreasing trends in estimated exploitation rates were likely due to the increase in estimated population size being greater than increases in the observed catch.

The median of recent D ($D_{2019-2022}$) relative to the estimated D at MSY ($D_{MSY}$ = 0.51, 95% CI = 0.40-0.70) was estimated to be 1.17 (95% CI = 0.46-1.92) (Table ES 1 and Figure ES 5). The recent median exploitation rate ($U_{2018-2021}$) relative to the estimated exploitation rate at MSY ($U_{MSY}$ = 0.05, 95% CI =0.03-0.09) was estimated to be 0.34 (95% CI = 0.07-1.20) (Table ES 1 and Figure ES 5). Surplus production models are a simplification of age-structured population dynamics and can produce biased results if this simplification masks important components of the age-structured dynamics (e.g., index selectivities are dome shaped or there is a long time-lag to maturity). Simulations suggest that under circumstances representative of the observed SMA fishery and population characteristics (e.g., dome-shaped index selectivity, long lag to maturity, and increasing indices), the BSPM ensemble may produce biased results. Representative simulations suggested that the $D_{2019-2022}$ estimate has a positive bias of approximately 7.3 % (median). The trajectories of stock status from the model ensemble revealed that North Pacific SMA had experienced a high level of depletion prior to the start of the model and was likely overfished in the 1990s and 2000s, relative to MSY reference points (Figure ES 5).

The following information on the status of the North Pacific SMA are provided:

**1. No biomass-based or fishing mortality-based limit or target reference points have been established for NPO SMA by the IATTC or WCPFC;**

**2. Recent median D ($D_{2019-2022}$) is estimated from the model ensemble to be 0.60 (95% CI = 0.23-1.00). The recent median $D_{2019-2022}$ is 1.17 times $D_{MSY}$ (95% CI = 0.46-1.92) and the stock is likely (66% probability) not in an overfished condition relative to MSY-based reference points.**

**3. Recent U ($U_{2018-2021}$) is estimated from the model ensemble to be 0.018 (95% CI**

**= 0.004-0.07). $U_{2018-2021}$ is 0.34 times (95% CI = 0.07-1.20) $U_{MSY}$ and overfishing of the stock is likely not occurring (95% probability) relative to MSY-based reference points.**

**4. The model ensemble results show that there is a 65% joint probability that the North Pacific SMA stock is not in an overfished condition and that overfishing is not occurring relative to MSY based reference points.**

**5. Several uncertainties may limit the interpretation of the assessment results including uncertainty in catch (historical and modeled period) and the biology and reproductive dynamics of the stock, and the lack of CPUE indices that fully index the stock.**

**Conservation Information**

Stock projections of depletion and catch of North Pacific SMA from 2023 to 2032 were performed assuming four different harvest policies: $U_{2018-2021}$, $U_{MSY}$, $U_{2018-2021} + 20\%$, and $U_{2018-2021} - 20\%$ and evaluated relative to MSY-based reference points (Figure ES 6). Based on these findings, the following conservation information is provided:

**1. Future projections in three of the four harvest scenarios ($U_{2018-2021}$, $U_{2018-2021} + 20\%$, and $U_{2018-2021} - 20\%$) showed that median D in the North Pacific Ocean will likely (>50% probability) increase; only the $U_{MSY}$ harvest scenario led to a decrease in median D.**

**2. Median estimated D of SMA in the North Pacific Ocean will likely (>50% probability) remain above $D_{MSY}$ in the next ten years for all scenarios except $U_{MSY}$; harvesting at $U_{MSY}$ decreases D towards $D_{MSY}$ (Figure ES 6).**

**3. Model projections using a surplus-production model may over simplify the age-structured population dynamics and as a result could be overly optimistic.**

366 *Table ES 1*. Summary of reference points and management quantities for the model ensemble of
367 North Pacific shortfin mako. Values in parentheses represent the 95% credible intervals when
368 available. Note that exploitation rate is defined relative to the carrying capacity.

| **Reference points** | **Symbol** | **Median (95% CI)** |
|---|---|---|
| **Unfished conditions** | | |
| Carrying capacity | $K$ (1000s sharks) | 12,541 (4,164 - 52,684) |
| **MSY-based reference points** | | |
| Maximum Sustainable Yield (MSY) | $C_{MSY}$ (1000s sharks) | 338 (134 - 1,338) |
| Depletion at MSY | $D_{MSY}$ | 0.51 (0.40 - 0.70) |
| Exploitation rate at MSY | $U_{MSY}$ | 0.055 (0.027 - 0.087) |
| **Stock status** | | |
| Recent depletion | $D_{2019-2022}$ | 0.60 (0.23 - 1.00) |
| Recent depletion relative to MSY | $D_{2019-2022}/D_{MSY}$ | 1.17 (0.46-1.92) |
| Recent exploitation rate | $U_{2018-2021}$ | 0.018 (0.004-0.07) |
| Recent exploitation rate relative to MSY level | $U_{2018-2021}/U_{MSY}$ | 0.34 (0.07-1.20) |

369
370

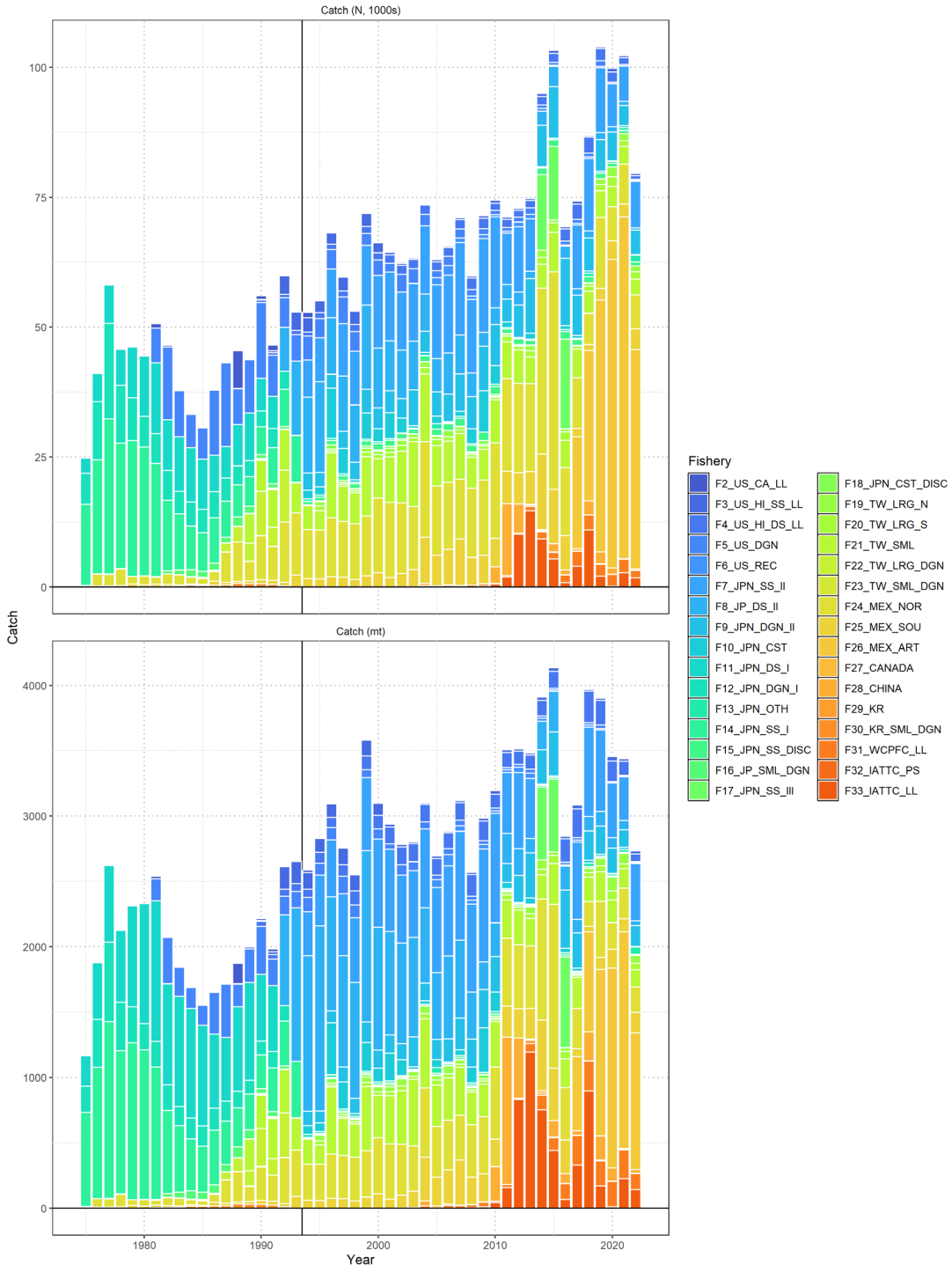


371

372 *Figure ES 1*. Catch of North Pacific shortfin mako by fishery as assembled by the SHARK
373 WORKING GROUP. Upper panel is catch in numbers (1000s) and lower panel is catch in
374 biomass (mt). The vertical black line indicates the start of the assessment period in 1994.

375

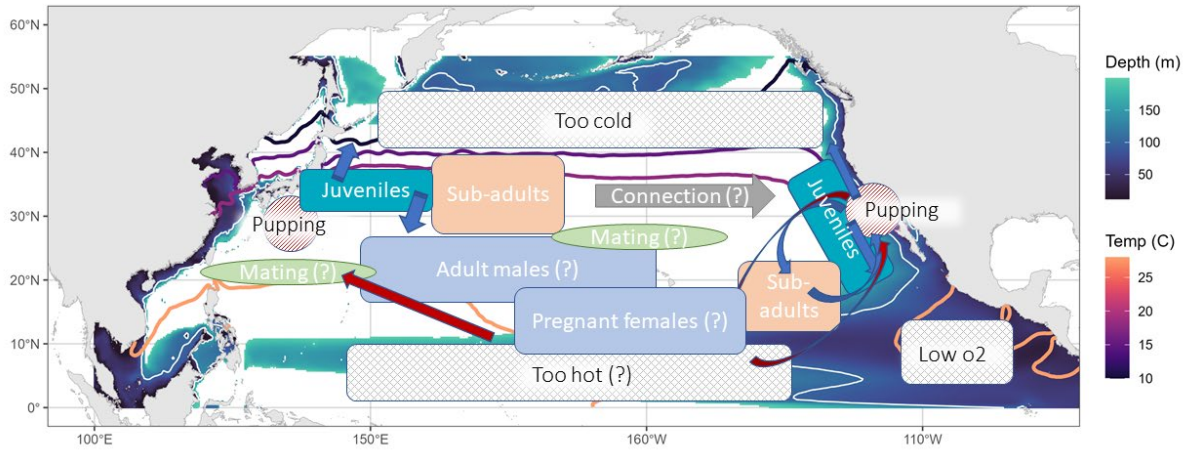


376

377 *Figure ES 2*. Conceptual model for North Pacific shortfin mako . Contour lines (warmer colors)
378 are shown for the average annual $10°, 15°, 18°,$ and $28°C$ sea surface temperature isotherms.
379 Background shading (cooler colors) shows the depth of the oxygen minimum zone ($3\ mL/L$), a
380 white isocline indicates a depth of 100m which could be limiting based on North Pacific shortfin
381 mako vertical dive profiles.

382

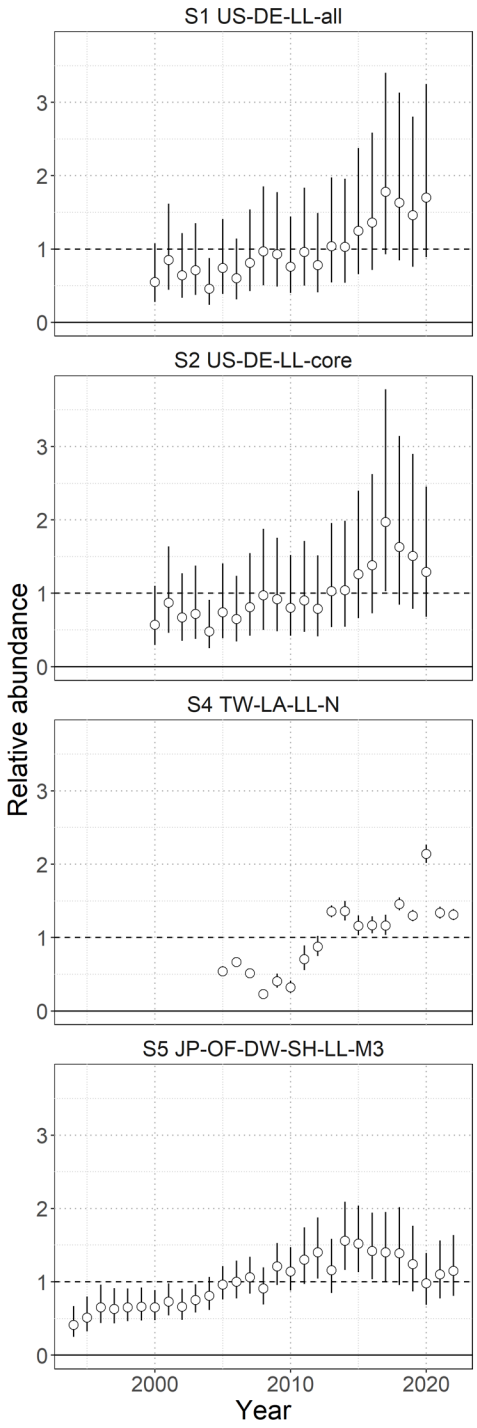


383

384 *Figure ES 3*. Standardized indices of relative abundance of North Pacific shortfin mako used in
385 the stock assessment model ensemble. Open circles show observed values (standardized to mean
386 of 1; black horizontal line) and the vertical bars indicate the observation error (95% confidence
387 interval).

388

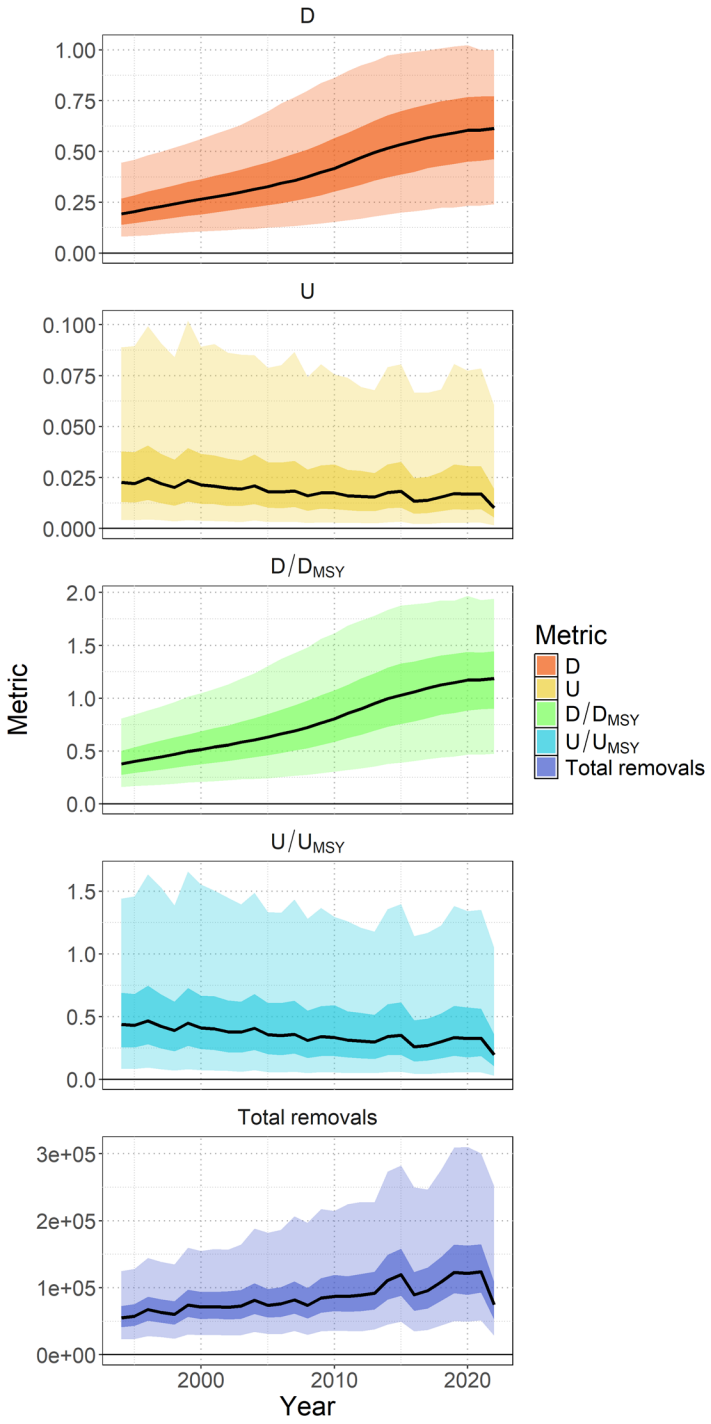


*Figure ES 4*. Time series (solid lines) of estimated: depletion (D), exploitation rate (U), depletion relative to the depletion at maximum sustainable yield (MSY) ($D/D_{MSY}$), exploitation rate relative to the exploitation rate that produces MSY ($U/U_{MSY}$), and total fishery removals (numbers) for North Pacific shortfin mako. Darker shading indicates 50% credible interval and lighter shading indicates 95% credible interval.

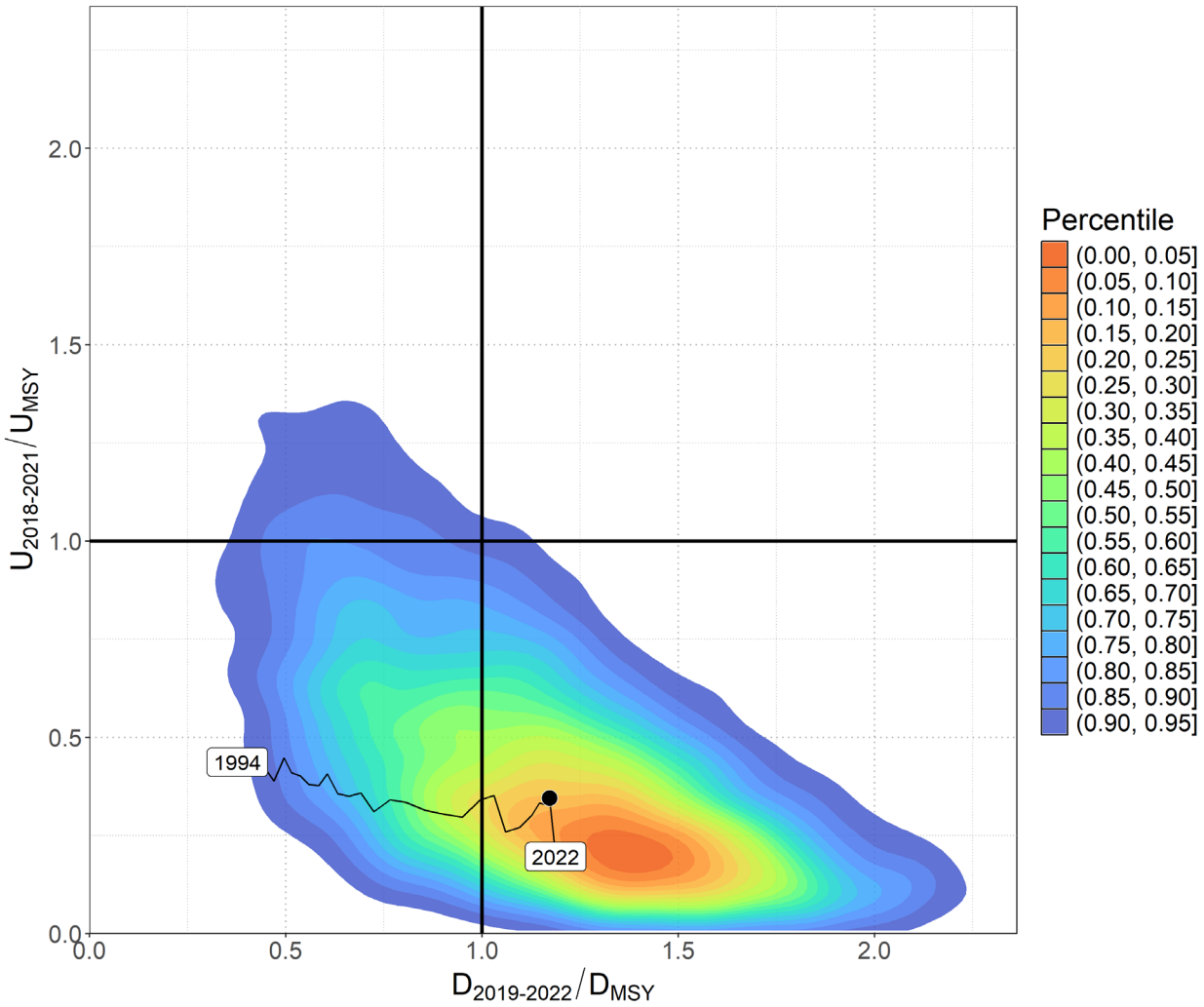


*Figure ES 5*. Kobe plot showing the bivariate distribution (shaded polygon) average recent depletion relative to the depletion at maximum sustainable yield (MSY) ($D_{2019-2022}/D_{MSY}$) against the average recent exploitation rate relative to the exploitation rate at MSY ($U_{2018-2021}/U_{MSY}$) for North Pacific shortfin mako. The median of this bivariate distribution is shown with the solid black point. The relative time series of annual ($t$) $D_t/D_{MSY}$ versus $U_t/U_{MSY}$ is shown from 1994 to 2022.

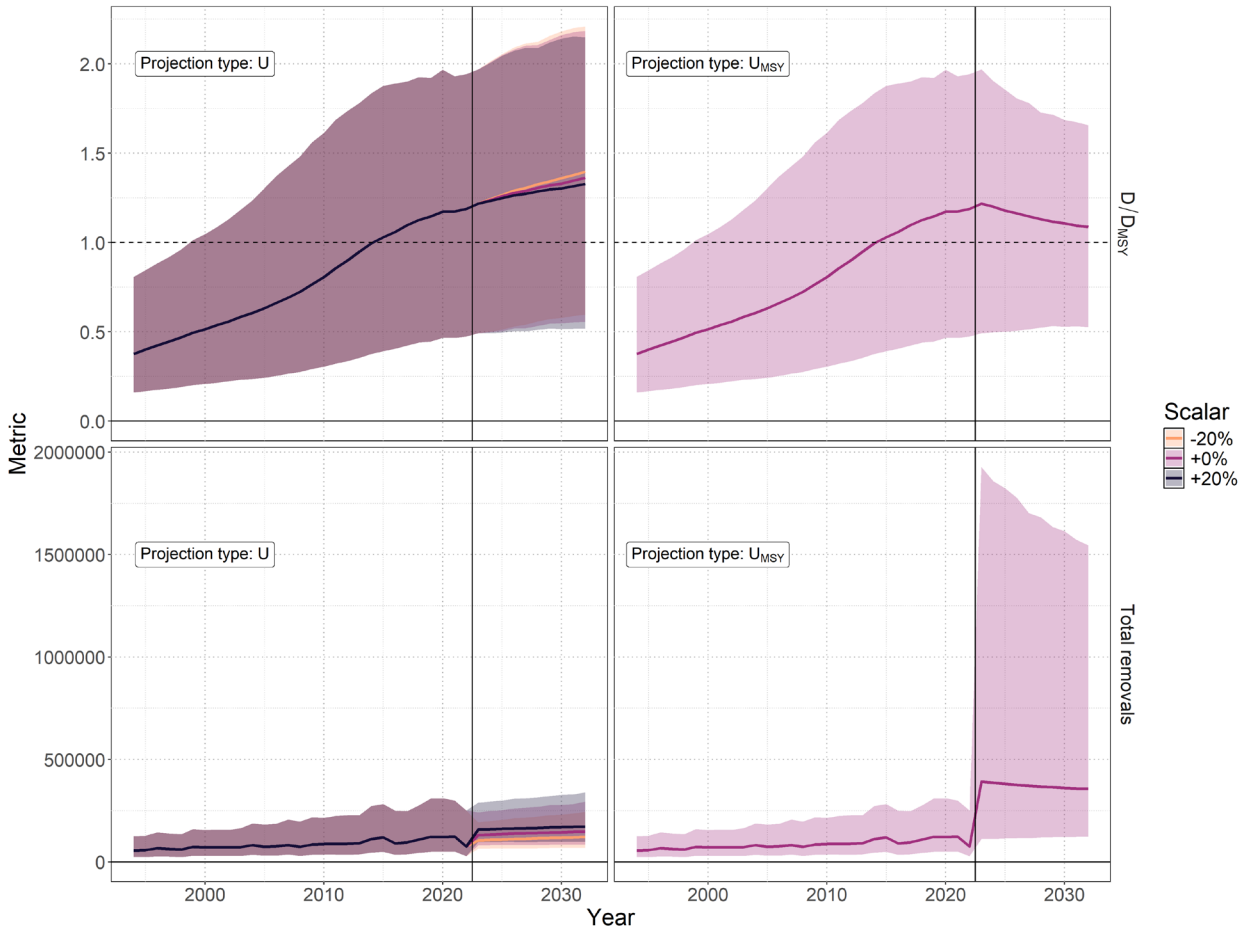


406

407 *Figure ES 6*. Stochastic stock projections of depletion relative to maximum sustainable yield
408 (MSY) ($D/D_{MSY}$) and catch (total removals) of North Pacific shortfin mako from 2023 to 2032
409 were performed assuming four different harvest rate policies: $U_{2018-2021}$, $U_{2018-2021} + 20\%$,
410 $U_{2018-2021} - 20\%$, and $U_{MSY}$. The 95% credible interval around the projection is shown by the
411 shaded polygon.

412

## 1. INTRODUCTION

Shortfin mako shark (SMA; *Isurus oxyrinchus*) are a highly migratory pelagic shark with a global distribution in tropical to temperate waters. For most fisheries, SMA are encountered incidentally during fishing operations, both longline and drift net fisheries. Retention rates of SMA vary historically and by fishing nation. SMA has higher quality flesh relative to other shark species and is retained by some fisheries either as a targeted species or as commercially valuable bycatch. SMA are currently understood to be a long-lived, late maturing, and low-fecundity species which may make them more susceptible to fishing pressure than teleosts (e.g., tunas and billfish) targeted by the same fisheries that incidentally encounter SMA. In 2019, the Convention on International Trade in Endangered Species of Wild Fauna and Flora (CITES) listed SMA on Appendix II limiting international trade.

To address uncertainty about the conservation status of high seas shark stocks in the North Pacific Ocean (NPO), the International Scientific Committee for Tuna and Tuna-like Species (ISC) created a Shark Working Group (SHARKWG or WG) in 2011 to begin compiling the necessary information to conduct stock assessments. The focus of the SHARKWG to date has been on the two most commonly encountered pelagic sharks, the blue shark (BSH, *Prionace glauca*) and SMA. In order to assess population status, SHARKWG members have been collecting biological and fisheries information on these key shark species in coordination and collaboration with regional fishery management organizations, national scientists and observers. The SHARKWG has conducted two prior assessments of NPO SMA: an indicator-based analysis (2015) and a benchmark full stock assessment (2018).

After the completion of the benchmark stock assessment for SMA in the NPO, which indicated a healthy stock condition (ISC, 2018a), ISC 20 Plenary approved a schedule change for the benchmark stock assessments. The schedule changed from 3 to 5 years to reduce the burden for stock assessment scientists, while also allowing more time to conduct research for the species between assessments (ISC, 2020). As a condition of the approval, ISC 20 Plenary requested the SHARKWG conduct an indicator-based analysis to monitor key fisheries indicators (i.e., catch, catch-per-unit-effort (CPUE), size frequency from the base case benchmark assessment) for changes that could warrant expediting the next scheduled benchmark assessments.

Following the request by ISC 20 Plenary, the SHARKWG conducted its second indicator-based analysis for SMA in the NP in 2021 based on updated data for the catch, abundance indices, and length frequencies (ISC, 2021). The SHARKWG concluded that no signs of shifts in the stock abundance or fisheries dynamics were apparent and decided to conduct the next benchmark stock assessment of NP SMA on schedule (2024).

## 2. BACKGROUND

### 2.1. Previous stock assessments

The SHARKWG conducted its first assessment of NPO SMA in 2015 using an indicator-based analysis (ISC, 2015). The 2015 analysis used a series of fishery indicators, such as CPUE and average length (AL), to assess the response of the population to fishing pressure. Such indicators are usually straightforward to compute and track over time, thus providing the opportunity to observe trends which can serve as early signals of overexploitation. Interpreted as a suite, indicators of stock status can be useful for initial assessments and/or for prioritizing future data collection or analytical work. After reviewing a suite of fishery indicators information, the SHARKWG concluded that stock status (overfishing and overfished) of NPO SMA could not be determined in 2015 because information on important fisheries were missing, validity of indicators for determining stock status were untested, and there were conflicts in the available data. The SHARKWG recommended that missing data (e.g., total annual catch) for all fisheries be developed for use in the next stock assessment scheduled for 2018.

The 2018 NPO SMA stock assessment (ISC, 2018a) used Stock Synthesis (SS3; Version 3.24U), an integrated statistical catch-at-age model, and fit to time series of standardized CPUEs (i.e., abundance indices) and sex-specific size composition data in a likelihood-based statistical framework. This model assumed a single, well-mixed stock in the NPO and partitioned data among 17 fisheries based on fishing nation and gear. Sex-specific growth curves and weight-at-length relationships were used to account for the sexual dimorphism of SMA. A Beverton-Holt stock recruitment relationship was used to characterize productivity of the stock based on plausible life history information available for NPO SMA. The model time-period spanned 1975-2016 and acknowledged that data for the early period (1975-1993) was highly uncertain given that species-specific shark catch was unavailable for major fisheries. This assessment characterized the NPO SMA stock to likely not be overfished and to likely not be undergoing overfishing. The SHARKWG identified that improvements to the catch, abundance indices, and size composition data were needed for the current assessment, and that there remained large uncertainties with respect to biological parameters.

As further background relative to the current modeling approach, it is worth noting that initial plans for the 2018 assessment were to begin the model in 1994 given that key fleets (e.g., Japan) lacked species-specific catch and CPUE data for sharks prior to 1994 (ISC, 2018b). SS3 models beginning in 1994 were unable to converge to reasonable estimates so 1975-1993 catches (Kai and Liu, 2018) and CPUEs (Kai and Kanaiwa, 2018) were developed after the 2017 SHARKWG data-prep workshop in order to test models beginning in 1975. In the absence of species-specific shark information prior to 1994, the early period CPUE was developed by applying average quarter-area

specific catch ratios of SMA to total shark catch (from 1994-1999) from the Japanese logbook for sets meeting filtering requirements (Kai and Kanaiwa, 2018). It was only after including the early CPUE that models were able to converge. However, it is uncertain how representative this index is of NPO SMA dynamics given that SMA is believed to have represented a small proportion of total shark catch (~1-2% of total shark catch from filtered logbooks from 1994-1999; Kai and Kanaiwa, 2018), and that the majority of the total shark catch is believed to be BSH, which have different life history and fishery interactions.

## 2.2. Biology

### *2.2.1. Genetic population structure*

Current and previous stock assessment frameworks have assumed that SMA represent a single, distinct and well-mixed stock in the NPO. Globally, multiple genetic studies show weak evidence of genetic spatial structure (Heist et al., 1996; Schrey and Heist, 2003; Corrigan et al., 2018). However, the techniques used (microsatellite and mitochondrial DNA) have weak power to distinguish functionally independent populations as 1-10 migrants per generation is enough to contaminate the signal (Allendorf and Phelps, 1981). Within the NPO there is strong evidence to suggest, based on the presence of neonates (pups), distinct parturition sites: eastern (Southern California Bight; Hanan et al., 1993, and Baja California; Carreón-Zapiain et al., 2018) and western (waters east of Japan; Kai et al., 2015). Recent research suggests that the eastern parturition site could have further sub-structure with distinct parturition sites in the Southern California Bight and Bahia Sebastian Vizcaino as indicated by vertebral chemistry (LaFreniere et al., 2023). Research within the Pacific indicates that female SMAs may have parturition site fidelity which could lead to discrete population structure even if male gene flow exists (Corrigan et al., 2018); however, more research is needed to confirm this (Schrey and Heist, 2003). The available information appears to support the differentiation between separate NPO and south Pacific Ocean (Corrigan et al., 2018) but more work is needed to identify the stock structure in the NPO (e.g., single well-mixed stock, or multiple stocks with varying connectivity as a result of females exhibiting site fidelity with distinct parturition sites).

### *2.2.2. Reproduction*

As mentioned in the previous section, there is evidence to suggest the presence of distinct parturition sites in the eastern and western NPO. However, uncertainty remains for many aspects of SMA reproductive biology. Parturition is believed to occur in winter through spring with some uncertainty in the exact timing (Pratt Jr. and Casey, 1983; Stevens, 1983; Fletcher, 1978; Joung and Hsu, 2005; Semba et al., 2011; Carreón-Zapiain et al., 2018). Pup size (~55-60cm PCL; pre-caudal length) appears consistent across ocean basins (Pratt Jr. and Casey, 1983; Stevens, 1983; Fletcher, 1978; Joung and Hsu, 2005). Sex-ratio is believed to be 1:1 at birth (Stevens, 1983; Joung

and Hsu, 2005; Fletcher, 1978; Semba et al., 2011) and average litter size appears to be ~12 pups per litter (Fletcher, 1978; Joung and Hsu, 2005; Semba et al., 2011) with some evidence that litter size increases with maternal length (Fletcher, 1978; Semba et al., 2011). Female SMA mature at a larger size than males with lengths at 50% maturity in the NPO of 233 cm PCL vs. 166 cm PCL, respectively for females and males (Semba et al., 2017). Mating may occur in summer months with uncertainty to either side (Fletcher, 1978; Joung and Hsu, 2005; Semba et al., 2011). Both mating and parturition periods can be protracted (Fletcher, 1978; Semba et al., 2011) though this is disputed (Joung and Hsu, 2005). Mating is hypothesized to occur in distinct geographical areas (Corrigan et al., 2015; Fletcher, 1978). From fisheries data, based on the simultaneous presence of mature-sized males and females, a potential mating ground could be north of the main Hawaiian Islands (near subtropical frontal zone) in the central NPO during the third quarter of the year (Ducharme-Barth et al., 2024). Joung and Hsu (2005) suggest that waters near the Taiwan and Ryukyu islands in the western NPO could be a mating ground. There is some evidence to suggest multiple-paternity within litters (Corrigan et al., 2015; Liu et al., 2020). Reproductive cycle, including gestation and "rest-period", is believed to be either two (Semba et al., 2011) or three (Fletcher, 1978; Joung and Hsu, 2005) years, with some evidence to suggest that pregnant females occupy warmer waters in earlier gestational stages (Semba et al., 2011). From a modeling standpoint, altering assumptions related to reproductive output (e.g., size at maturity, number of pups per litter, and/or reproductive cycle) can significantly affect the population rate of increase and the stock's ability to cope with fishing pressure.

#### *2.2.3. Growth*

There is considerable uncertainty in the growth of SMA due to difficulties in determining the age of individuals. Currently, age determination is based on detecting band-pairs from either whole or sectioned vertebral centra. However, there is uncertainty as to the deposition rate of vertebral band-pairs per year. Available research based on oxytetracycline (OTC) marked fish indicates that band-pairs may be deposited at the rate of two per year through age five (Wells et al., 2013) and one per year for older individuals (Natanson et al., 2006; Kinney et al., 2016). However, sample sizes (n=29 for Wells et al. 2013; and n=1 for both Kinney et al. 2016 and Natanson et al. 2006) and geographic ranges of the studies are small. Several other studies could not rule out a transition from multiple (two) to a single band-pair deposited per year (Ardizzone et al., 2006; Natanson et al., 2006). There is evidence to suggest that band-pair deposition is not a function of time but rather a structural component of the vertebrae related to somatic growth (Natanson et al., 2018) which could lead to underestimates of age in the largest individuals. Additionally, compression of band-pairs towards the outer edge of vertebrae may lead to further underestimates of age in larger individuals (Bishop et al., 2006; Natanson et al., 2006). More generally, sexual dimorphism is observed with females growing to larger sizes than males (Pratt

553 Jr. and Casey, 1983; Natanson et al., 2006; Cerna and Licandeo, 2009; Semba et al., 2009), with
554 similar growth rates between males and females through ~180-190cm PCL. Use of length
555 frequency data to determine growth rates from modal progression typically shows faster growth
556 than those based solely on vertebral age data (Kai et al., 2015), noting that those vertebral age
557 studies assumed one band-pair deposited per year.
558 Uncertainty in SMA growth has been a known issue for the SHARKWG as growth
559 estimates differ based on the sampling location and the method used to detect band-pairs.
560 Additionally, band-pair deposition was assumed to be different on either side of the NPO, one
561 band-pair per year in the west (Semba et al., 2009) and a transition from two to one band-pairs per
562 year in the east after age 5 (Wells et al., 2013; Kinney et al., 2016), noting that only the assumption
563 for the east was validated. Kinney et al. (2024) provide a helpful summary of the history of
564 SHARKWG efforts to address these issues, details the creation of an ISC vertebrae reference
565 collection, and the approaches used for developing growth curves for the current and 2018
566 assessments.
567 Briefly, key points from Kinney et al. (2024) are summarized here for convenience. The
568 2018 assessment used a growth curve developed from a Bayesian hierarchical model that
569 combined age and growth data from five vertebral data sources (using four different aging
570 methods) and two length frequency data sources (Takahashi et al., 2017). Despite acknowledging
571 that methodological differences between the four aging methods produced different counts when
572 applied to vertebrae from the same individual (ISC, 2018c), no adjustment or correction was made
573 when combining the age data to account for methodological differences or different assumptions
574 in the band-pair deposition. Additionally, the length frequency datasets were not used as length
575 frequencies in the Takahashi et al. (2017) model but rather as additional sources of age data, as the
576 length frequencies were converted to age data using a conversion equation from Kai et al. (2015).
577 In preparation for the current assessment, Kinney et al. (2024) improved upon the approach
578 from Takahashi et al. (2017) by explicitly addressing the issues mentioned in the previous
579 paragraph. Kinney et al. (2024) used the paired band-pair readings across methods from the ISC
580 vertebrae reference collection (ISC, 2018c) to develop lab-specific calibration factors. These were
581 then applied to age readings from each lab in order to develop *standardized* band-pair counts
582 relative to a reference aging method. Standardized band-pair counts were converted to age
583 according to the band-pair hypothesis which corresponded to the reference aging methodology,
584 either the US validated aging method (hard x-ray method & transition from two to one band-pair
585 per year after age 5) or Japanese (JP) aging method (centrum-face shadow method & one band-
586 pair per year). Development of the lab-specific calibration factors from the ISC vertebrae reference
587 collection in which all 4 aging methods were applied to sampled fish collected across the NPO
588 provides evidence that alternative band-pair deposition hypotheses are an artifact of the

589 methodology used (e.g., the hard x-ray method detects more band-pairs than the centrum-face
590 shadow method; ISC, 2018c). Kinney et al. (2024) also incorporated length frequency data via a
591 separate likelihood component (i.e., lengths were not converted to age-at-length data using external
592 growth curves). This allowed growth estimates to be based solely on length modal progression
593 information.
594 Based on the updated analysis from Kinney et al. (2024) the SHARKWG proposed two
595 alternative growth curve scenarios for the current assessment. The first scenario considered the US
596 validated aging method (hard x-ray) to be the "true" method for determining band-pairs and
597 standardized all other lab counts to this method. The corresponding band-pair deposition rate
598 hypothesis (two band-pairs per year to one band-pair per year after age 5) was applied. Length
599 data from the juvenile shark survey in the Southern California Bight (Runcie et al., 2016) was also
600 incorporated into this scenario. The second scenario considered the JP aging method (centrum-
601 face shadow method) to be the "true" method for determining band-pairs and standardized all other
602 lab counts to this method. The corresponding band-pair deposition rate hypothesis (one band-pair
603 per year) was applied, and no length frequency data was included.
604 ***2.2.4. Maximum age***
605 Related to the issues described above for growth, issues with determining age from band-
606 pairs deposited in vertebral centra may impact the ability to define a maximum age for this species,
607 and existing observations may be underestimated. Ability to determine a maximum age may be
608 further impacted by the lack of large (presumably old) SMA available in fisheries samples. Those
609 caveats aside, maximum age is believed to be 25+ years for both sexes (Cerna and Licandeo, 2009).
610 Natanson et al. (2006) directly observed maximum age values for females to be 32 and males to
611 be 29 in the northeast Atlantic Ocean. Bishop et al. (2006) directly observed maximum age values
612 for females to be 28 and males to be 29 in the southwest Pacific Ocean.
613 ***2.2.5. Natural mortality***
614 Natural mortality (M) is difficult to measure directly without large scale tagging studies.
615 Mucientes et al. (2023) estimated average annual survival of small SMA (n=132, size range 49-
616 163cm PCL, mean size = 80cm PCL) in the northeast Atlantic Ocean to be 0.618, and that
617 accounting for the component of total mortality due to fishing resulted in average annual M
618 estimates of ~0.28 (median ~0.22) for small/young SMA. Teo et al. (2024) used a meta-analytic
619 approach to derive sex-specific values for average annual adult M by combining the M estimates
620 derived from empirical relationships with maximum age (Hamel and Cope, 2022), age at maturity
621 (Charnov and Berrigan, 1990) or growth (Then et al., 2015; and accounting for the two growth
622 scenarios: JP aging or US aging). This resulted in average annual M estimates for females of 0.139
623 (JP aging) or 0.133 (US aging), and for males of 0.197 (JP aging) or 0.204 (US aging). This large
624 difference between average annual adult M by sex may be inconsistent with the lack of difference

seen in observed maximum age between sexes. Teo et al. (2024) also provide average annual adult M by sex using only the empirical relationship for maximum age (Hamel and Cope, 2022): 0.169 for females and 0.186 for males. These values corresponded to the maximum observed ages from Natanson et al. (2006) and reduced the difference in adult M between the sexes.

#### *2.2.6. Length-Weight relationship*

A number of studies within four different ocean basins (southwest Pacific Ocean, northeast Pacific Ocean, northwest Pacific Ocean, and northwest Atlantic Ocean) did not find significant differences in the length-weight relationship by sex (Stevens, 1983; Kohler et al., 1996; Joung and Hsu, 2005; Carreón-Zapiain et al., 2018). However, these studies did not contain large numbers of mature females given the nature of fisheries selectivity patterns. The available evidence does suggest that up to maturity there does not appear to be meaningful differences in either the length-weight or the growth relationship by sex.

#### *2.2.7. Movement dynamics*

Movement dynamics for SMA can be characterized in terms of their horizontal movements and their vertical movements. In either case, information is derived from tagging studies (conventional or satellite) where the majority of studied individuals are juveniles or sub-adults. SMA are capable of large trans-oceanic movements (Casey and Kohler, 1992; Vaudo et al., 2016). However, residency for juveniles along with cyclic seasonal migrations of sub-adults have been observed in both the north (Nasby-Lucas et al., 2019) and south (Francis et al., 2019, 2023) Pacific Ocean. Specifically within the NPO, residency has been observed in the Southern California Bight & California Current Large Marin Ecosystem during summer months with seasonal latitudinal migrations tracking higher sea surface temperatures (Nasby-Lucas et al., 2019). There is some evidence to suggest some large-scale movements from the eastern NPO to the central NPO and western NPO, and some movement from the central NPO to the eastern NPO (Musyl et al., 2011; Sippel et al., 2011). However, the limited tagging data in the western NPO does not indicate movement to the eastern NPO (Sippel et al., 2011). In the western NPO, spatiotemporal modeling of fisheries data also indicates a clear seasonal latitudinal migration for juveniles and sub-adults following higher sea surface temperatures (Kai et al., 2017a). Kai et al. (2015, 2017b) also used fisheries data to show patterns in spatial segregation by size in the western NPO which indicated a transition from smaller to larger individuals as fishing effort moved further offshore (east) of Japan.

With regards to vertical movement, SMA exhibit a diel diving behavior occupying deeper and cooler waters during the day time (Sepulveda et al., 2004; O'Brien and Sunada, 1994; Musyl et al., 2011; Vaudo et al., 2016; Nasby-Lucas et al., 2019). SMA appear to spend most of their time in epipelagic waters remaining predominantly in the upper 100-150 m of the water column (Sepulveda et al., 2004; O'Brien and Sunada, 1994; Abascal et al., 2011) with dives as deep as

500m (Casey and Kohler, 1992; Abascal et al., 2011; Vaudo et al., 2016) - 1400m (Francis et al., 2023) and maximum daytime and nighttime depths depend on body size and ambient water temperature (Sepulveda et al., 2004; Vaudo et al., 2016; Nasby-Lucas et al., 2019). This suggests that low temperatures could be limiting. Musyl et al. (2011) noted that SMA that transitioned into the cooler waters of the North Pacific Transition Zone (sea surface temperatures < ~18℃) spent more time at shallower depths. SMA tended to ascend rapidly from their deepest dives which perhaps is an indication of thermal or hypoxic stress at depth (Abascal et al., 2011).

#### *2.2.8. Environmental preferences*

SMA were observed to experience a wide range of temperatures across ocean basins and depth ranges (5 - 31℃; Vaudo et al., 2016). A number of studies suggest that 17 - 22℃ could be the preferred sea surface temperature band however these were all conducted in more temperate waters and usually based on fisheries dependent data (Stillwell and Kohler, 1982; Casey and Kohler, 1992; Kai et al., 2017a). Tagging studies based in temperate waters found sharks occupied waters with sea surface temperatures of ~14 - 24℃ (Abascal et al., 2011; Nasby-Lucas et al., 2019). One tagging study done in sub-tropical waters (Gulf of Mexico and northeast Atlantic Ocean) suggests that when available, SMA prefer waters 22 - 27℃, and avoid waters warmer than 28℃ (Vaudo et al., 2016). Temperature may not be the only environmental factor that limits vertical and horizontal distributions of SMA. Given the high routine and maximum oxygen metabolic consumption rates for SMA (Graham et al., 1990; Sepulveda et al., 2007), dissolved oxygen may also be a limiting factor. Vetter et al. (2008) and Abascal et al. (2011) suggest that dissolved oxygen concentrations below 1.25-3 ml/L may represent a lower environmental limit for SMA.

### 2.3. Fisheries

Given that SMA are encountered as incidental bycatch in both deep and shallow-set longline fisheries, large-scale fisheries interactions with SMA in the NPO have likely existed since the expansion of the Japanese distant-water longline fishing fleets in the 1950s. Other distant water large-scale longline fisheries (e.g., Chinese-Taipei and Korea) have also developed operations in the NPO. However, lack of species-specific catch records for sharks prior to the mid-1990s along with uncertain levels of shark reporting in logbooks (e.g., unreported discards) make it difficult to determine the exact impact of these longline fisheries before the mid-1990s. Since the mid-1990s catches are more certain however uncertainties remain around the level of discarding reported in logbooks. High-seas drift-net fisheries, both the small-mesh squid driftnet fishery and the large-mesh drift gillnet fishery, would have also interacted with SMA as they expanded operations from the western NPO in the late 1970s to the central NPO in the 1980s. The small-mesh squid driftnet fishery set at night in the upper 10m of the water column with operations by Japan, Chinese-Taipei, and Korea typically north of 35°N in the central NPO (Yatsu et al., 1993). Low-rates of SMA interactions relative to other sharks (BSH and salmon shark *Lamna ditropis*) were observed on

Japanese vessels operating in the central NPO in 1990 and 1991 (McKinnell and Seki, 1998). However, given the limited snapshot of observed fishing operations at the tail-end of the fishery it is unknown if these catch-rates are representative of SMA catch-rates throughout the duration of the fishery. High-seas large-mesh drift gillnet operations targeted surface waters (upper ~6-7m) of 15 - 24℃ and typically set nets at the end of the afternoon with retrieval beginning after midnight (Nakano et al., 1993). A high-seas moratorium was placed on driftnet fishing in 1992.

In the central NPO longline fishing based out of Hawai'i targeting tunas and billfish has existed since the 1930s, though post World War II landings declined from a peak in the mid-1950s until the 'modern' longline fishery was revitalized in the late 1980s (Boggs and Ito, 1993). Sectorization of the fishery occurred in the late 1980s with the development of the shallow-set sector targeting swordfish (*Xiphias gladius*). The shallow-set fishery set at night in the top ~60 m of the water column using squid bait prior to a fishery closure from 2003-2004. The fishery re-opened after the closure with additional restrictions (e.g., circle hooks and no use of squid bait) and substantially lower effort. The deep-set fishery targets predominantly bigeye tuna (*Thunnus obesus*) and is characterized by deep (~250m) daytime sets. Until recently the deep-set fishery was permitted to use wire-leaders (voluntary switching to monofilament in 2021 prior to a ban in 2022). Saury was the bait of choice though the fishery appears to have switched primarily to using milkfish since 2021.

In the eastern NPO SMA has primarily interacted with fisheries based in California (US) and Baja California (Mexico). A US domestic drift gillnet fishery developed in the late 1970s in the Southern California Bight where common thresher shark (*Alopias vulpinus*) was the initial target species but swordfish and SMA became important bycatch species (Hanan et al., 1993). The fishery expanded northwards towards San Francisco (California, USA) and offshore within the US Exclusive Economic Zone (EEZ) and effort peaked in the mid-1980s (Hanan et al., 1993). The US domestic drift gillnet fishery continues to exist though catches are very low relative to 1980 values. A US experimental drift longline fishery for sharks in the Southern California Bight occurred in the late 1980s – early 1990s using shallow sets (~10m) and wire leaders on a short longline attached to the boat (O'Brien and Sunada, 1994). Catch-rates for this fishery peaked seasonally in summer months and length-frequency data indicates 2 clear modes around ~95cm PCL and ~120cm PCL with very few individuals larger than ~155cm PCL (O'Brien and Sunada, 1994).

There is a long history of shark fisheries along the Pacific coast of Mexico with documented shark catches as early as the late 1880s (Sosa-Nishizaki et al., 2020). SMA interactions likely increased as fishing effort extended further offshore with the development of fiberglass panga vessels in the 1960s and development of large-scale domestic longline fisheries in the 1980s (Sosa-Nishizaki et al., 2020), and the development of a US style drift gillnet fishery operating off Baja California which lasted from the late-1980s to 2009 (Fernandez-Mendez et al., 2023). Currently

there are three primary fisheries from Mexico that interact with SMA: Ensenada (Baja California, Mexico) based longline, Mazatlán (Sinaloa, Mexico) based longline, and artisanal fisheries. Artisanal fishing (gillnet and small-scale longline) represents an important component of SMA catch by Mexican fisheries in recent years. While artisanal effort is primarily gillnet (~74% effort) SMA represent a small component (~1.4%) of sampled gillnet shark catch, though SMA represent ~23% of sampled small-scale longline shark catch (Ramirez-Amaro et al., 2013). Based on sampled length-frequency data, these artisanal fisheries primarily encounter juvenile SMA (mode ~100cm PCL; Ramirez-Amaro et al., 2013).

### 2.4. Conceptual model

Based on the available biological and fisheries data, the SHARKWG developed a conceptual model for NPO SMA following the approach described by Minte-Vera et al. (*In Review*). A summary of the model is shown in Figure 1. Briefly, the model specifies two parturition sites on either side of the NPO (Section 2.2.1), with a gradual offshore (cyclic) migration with age/size subject to seasonal latitudinal shifts to follow warmer waters (Section 2.2.7) such that the largest individuals are typically encountered in the central NPO. A tentative mating ground is identified in the central NPO north of Hawai'i (Section 2.2.1). Areas outside of the likely environmental envelope for SMA are identified (Section 2.2.8) with waters north of 35-40° N representing a seasonal northern extent, and waters in the Western Pacific Warm Pool (surface waters >28℃; De Deckker, 2016) likely representing a seasonal southern extent. Waters in the southeast NPO may be limiting due to the shallow depth of the oxygen minimum zone (depth of 3 ml/L < ~100m; Section 2.2.8). There is no single fishery that operates across the entire hypothesized distribution of SMA, or that routinely encounters mature females (see ISC, 2018a Figure 4 reproduced here as Figure 2).

The conceptual model is the foundational step in organizing information and developing both the modeling approach and structure for the current assessment. Additionally, it serves to highlight several key uncertainties. Stock structure in the NPO is unknown. Multiple parturition sites raise the possibility that multiple stocks exist depending on the level of genetic exchange between sites (e.g., degree of male straying and female site fidelity). Lack of information on adult SMA behavior (e.g., movements and mating grounds) makes this difficult to resolve. Biological uncertainties exist particularly as it relates to growth, maximum age, and natural mortality. As mentioned previously, the lack of observations for large females complicates the understanding of SMA biology. However, it also implies either a higher level of natural mortality or strong dome-shaped selectivity (gear contact selectivity or availability to the gear). Of these two hypotheses, it would seem unlikely for large females to see a dramatic increase in natural mortality following maturity given their trophic level and observed maximum ages. The dome-shaped selectivity hypothesis may be more plausible

as their large size (> 235cm PCL) may make them difficult to capture in conventional commercial fishing gear. Dome-shaped selectivity does reduce the information content (e.g., in the estimation of fishing mortality and scale) of size-frequency data if the descending limb of the selectivity curve is freely estimated.

The conceptual modeling exercise also identified key uncertainties related to stock assessment inputs: catch and indices of abundance. Fisheries related mortality (e.g., reported catch) is uncertain in the recent period due to uncertainties in the levels of discard reporting in logbooks, and is highly uncertain prior to 1994 due to the lack of species-specific shark information for many fisheries. Additionally, catch information for some fisheries are not complete for all years (e.g., Mexican artisanal shark fishery or Chinese longline fishery). Lastly, as mentioned previously there are no fisheries that operate across the entire range of SMA in the NPO and there are no fisheries that regularly capture and observe large females. This poses a challenge for modeling and indexing the status of the reproductive component of the stock.

## 3. DATA

Following development of the conceptual model, SHARKWG members assimilated available data in order to develop the current assessment model. Available time series of catch and abundance index data considered for use in this stock assessment model were assigned to "Extraction" and "Index" fisheries as summarized in Table 1 and Table 2.

### 3.1. Spatial stratification

For the purposes of the stock assessment, a single SMA stock was assumed in the NPO (noting the issues identified in the conceptual modeling phase), and available fisheries data were restricted to those corresponding to records located north of the equator.

### 3.2. Temporal stratification

Annual (January 1 – December 31) time series of fisheries data were produced with 2022 as the terminal year. Multiple model time periods were considered in the development of the current assessment. For consistency with previous approaches, a time series spanning 1975-2022 was developed. Additionally, a time series spanning 1994-2022 was developed given the uncertainties in early catches.

### 3.3. Catch data

Catches (metric tons; mt and/or numbers of sharks) were provided by ISC member nations and cooperating collaborators (Table 3 and Table 4; Figure 3). The primary sources of catch were from longline and drift gillnet fisheries, with smaller catches also estimated from purse seine, trap, troll, trawl and recreational fisheries. Catches are comprised of total dead removals, which include

802 landings and discards.

803 ***3.3.1. Japan***

804 SMA is incidentally caught by Japanese coastal and high seas (i.e., offshore and distant
805 waters) fisheries. The majority of SMA catch in Japanese fisheries is from either the high seas
806 longlines or large-mesh drift gillnet (ISC, 2018a). Offshore and distant water longline vessels are
807 split into two fisheries based on vessel gross registered tonnage (GRT), with smaller vessels (20 -
808 120 GRT) designated as offshore, and larger vessels (>120 GRT) deemed distant water (Kai,
809 2023a). These two-longline fisheries were further categorized as shallow-set (SS) and deep-set
810 (DS) based on the gear configuration (i.e., number of hooks between floats; HBF, with shallow-
811 set - HBF ≤5 and deep-set - HBF ≥6). In 1993, the Japanese large-mesh drift gill-net fishery was
812 banned in international waters (Miyaoka, 2004). The Japanese large-mesh drift gill-net fishery is
813 however still operating within the Japanese EEZ and therefore is still considered part of the
814 Japanese fisheries (Kai and Yano, 2023).

815 Japan provided SMA updated catch for the large-mesh high seas driftnet (1975-1993) and
816 following the approach used for the 2022 NPO BSH assessment developed catch estimates for the
817 small-mesh squid driftnet (1981-1992). For the large-mesh high-seas driftnet updated values were
818 provided due to the large uncertainty in the previous estimates and were based on the methods
819 (Fujinami et al., 2021a) adopted for the 2022 NPO BSH assessment (ISC, 2022). Briefly, species
820 compositions from scientific observers for the large-mesh driftnet (1990-1991) and a driftnet
821 survey for pomfret (1978-1984) were applied to Japanese statistical yearbook data for all sharks
822 to develop a catch time series for 1975-1993 (Semba and Kai, 2023). The estimated catch ranged
823 from 81.5 mt to 606.5 mt. These estimates are considerably smaller than those used in the previous
824 stock assessment, but the previous catch estimate of this fishery may have been overestimated
825 given that it assumed a ratio of SMA to BSH catch that was larger than what was seen in the
826 observer or survey data. Small-mesh squid driftnet catch used the methods (Fujinami et al., 2021b)
827 adopted for the 2022 NPO BSH assessment (ISC, 2022). The annual catch (in numbers) ranged
828 from 55 (1981) to 1,768 (1988), corresponding to 2.1 mt in 1981 to 67.6 mt in 1988 (Semba et al.,
829 2023). The estimated catch for the squid driftnet fishery was much smaller than that of the large-
830 mesh driftnet fishery, and combined were much lower than the driftnet catches used in the previous
831 assessment.

832 For the period 1994-2022, Japan provided estimated catch for five sectors of their fisheries,
833 categorized by vessel tonnage and gear configurations: 1) offshore and distant water longline
834 shallow-set; 2) offshore and distant water longline deep-set; 3) coastal waters longline and other
835 longline fisheries; 4) large-mesh drift gillnet; and 5) trap and other fisheries (Kai, 2023a; Kai and
836 Yano, 2023).

837 The annual catch of SMA caught by Japanese offshore and distant-water longline fisheries

was estimated using annual standardized CPUE multiplied by the total fishing effort. The annual catch of shallow-set and deep-set was estimated using two CPUEs for shallow-set (Kai, 2023b) and deep-set (Kai, 2023c), respectively. The estimated catch was stable between 1200 and 1700 mt until 2017, and then it gradually decreased and reached around 500 mt in recent years due to the continuous reduction of fishing effort, especially for the deep-set fishery.

The proportion of estimated total catch of SMA for both coastal and other longline fisheries and the large-mesh driftnet fishery accounted for more than 89 % of annual total catch amounts except the catches in 2005 (83%) and 2022 (76%). The annual total coastal catch of SMA largely fluctuated between 151 mt and 638 mt throughout the period. After 2016, it continuously decreased through 2022 due to the reduction of catch for the large-mesh driftnet fishery.

#### *3.3.2. Chinese-Taipei (Taiwan)*

Taiwanese fisheries data were obtained primarily from two sources: 1) logbook data from the large-scale tuna longline (LTLL) fishery and 2) logbook data from the small-scale tuna longline (STLL) fishery. The large-scale tuna longline fishery operates in two areas: north of 25°N catching mainly albacore tuna (*Thunnus alalunga*) in more temperate waters and south of 25°N targeting bigeye tuna in equatorial waters. The estimated SMA catch in weight from the Taiwanese large-scale tuna longline fishery ranged from 0 mt in 1973 to 156 mt in 2015, decreasing thereafter, increasing to 183 mt in 2020, and subsequently decreasing in 2021 and 2022 (Liu et al., 2023).

The STLL fishery operates mainly in coastal waters. The large majority of SMA reported by Chinese Taipei from 2020 to 2022 are caught by the STLL fishery.

#### *3.3.3. Republic of Korea*

Major shark species were separately identified in catch statistics for the Republic of Korea longline fishery in the NPO from 2013 to 2019 with 100% observer data coverage. The catch amount of SMA in recent years is near zero, assumed to be due to conservation measures strengthened for Korean longline fisheries (e.g., sharks are now released prior to bringing on board the vessel). Since there was no update at the SHARKWG meeting, the SHARKWG used the official statistics submitted to the WCPFC.

#### *3.3.4. China*

The SHARKWG used official statistics provided to the WCPFC and IATTC as catches of SMA for China as no working paper was provided.

#### *3.3.5. Canada*

There is very little SMA catch (<100 sharks annually) in Canada's fisheries due to the limited overlap between SMA range and areas fished by Canadian vessels.

#### *3.3.6. USA*

There are a number of US fisheries operating in the NPO, either out of the US west coast or Hawai'i, which interact with SMA (Kinney et al., 2017). These fisheries include: a Hawai'i

based shallow-set longline fishery targeting swordfish, a Hawai'i based deep-set longline fishery targeting bigeye tuna, a California based longline (noting that the number of active vessels is greatly diminished in recent years), US west coast drift gillnet targeting swordfish and thresher sharks within the US EEZ, and recreational fisheries based out of the US west coast. The majority of SMA catch comes from the Hawai'i based longlines and the US west coast drift gillnet fishery.

Catches for the US Hawai'i deep-set and shallow-set longlines were provided based on observer data and are defined as the sum of retained catch, dead discards, and individuals discarded alive that experience post-release mortality (Ducharme-Barth et al., 2024). A design-based catch reconstruction (McCracken, 2019) was used for the years 2005-2022 to account for the lack of complete observer coverage. Shallow-set catch was highest in the early 1990s and remained high prior to a fishery closure in the early 2000s. Catch for the shallow-set remained low. Deep-set catches increase through 2017, after which a combination of gear changes by the fishery causes catch to go down.

#### *3.3.7. Mexico*

In Mexico, SMA are caught mainly by the medium sized longline fisheries that target pelagic sharks or swordfish, and by the artisanal fisheries. Mexican shark catch statistics by species were not available until 2006. Since 2006 the National Commission for Aquaculture and Fisheries (CONAPESCA) has reported total catches by the main shark species, so past SMA catches were estimated using different sources of information, assuming different proportions of the species in total catches that have been published in the scientific literature or estimated using more detailed local statistics. Catches that were landed in the past by the large size vessel longline fisheries and the drift gill net fisheries were taken into consideration to construct the historical series (Sosa-Nishizaki et al., 2017). Recent (2017-2022) SMA catches from Mexico's Pacific waters were provided by CONAPESCA (Fernandez-Mendez et al., 2023). Catches were aggregated into two distinct fisheries: 1) the fisheries from States of Baja California and Baja California Sur as northern catches, and 2) those from Sinaloa, Nayarit, and Colima as southern catches. However, from 2017-2022 the artisanal catch from these two fisheries was separated out into a distinct fishery since artisanal catch values were available by state. Since 2017 the proportion of total catch from Mexico attributed to artisanal sources is substantial (~74% on average).

#### *3.3.8. Inter-American Tropical Tuna Commission (IATTC)*

The number of SMAs caught in tuna purse seine fisheries was available for the period between 1971-2022 and was estimated from observer bycatch data (see appendix A in ISC 2018a). Some assumptions regarding the relative bycatch rates of SMAs were applied based on their temperate distribution, catch composition information, and estimates of SMA bycatch in tuna purse seine fisheries in the north EPO. Estimates were calculated separately by set type, year, and area. Small purse seine vessels, for which there are no observer data, were assumed to have the same

SMA bycatch rates by set type, year, and area, as those of large vessels.

#### *3.3.9. Western Central Pacific Fisheries Commission (WCPFC)*

Fleet-specific catch statistics of SMA caught in the western and central Pacific Ocean (WCPO) from 1950 to 2022 (not including fleets previously listed) were provided by the WCPFC data manager (Pacific Community, SPC). The catch statistics provided by Republic of Kiribati, Papua New Guinea, Republic of Palau, and Solomon Islands were not used as input data for the benchmark stock assessment in 2018 (ISC, 2018a), but these data were included in this assessment because they were deemed to be from the NPO.

### 3.4. Indices of relative abundance

Indices of relative abundance (CPUE) for SMA in the NPO and their corresponding coefficients of variation (CV) were developed with fishery data from four nations (Japan, USA, Chinese Taipei, and Mexico) (Figure 4; Table 5). The SHARKWG considered all available abundance indices provided by SHARKWG members based on the conceptual model. No fishery was identified to fully sample the entire NPO SMA stock or to adequately sample mature females, however multiple candidate indices were identified for further evaluation. The SHARKWG decided to set a minimum average CV of 0.2, and adjusted the average CV to at least this minimum level if the model estimated CV was more precise than this.

The SHARKWG also evaluated other available indices, such as Clarke et al. (2013), for suitability for inclusion in the stock assessment. The SHARKWG was concerned with the representativeness of the Clarke et al. (2013) index given the data going into the analysis (e.g., data from 1995-2004 are US data around Hawai'i, a shift from 2005-2011 to be from western equatorial waters which are believed to be poor SMA habitat based on the conceptual model, and lack of any data from the temperate western NPO which is a major part of the SMA distribution) along with the modeling approach used (e.g., lack of key covariates and limitations in ability to deal with spatial shifts in the data) and did not find it to be suitable for inclusion in the stock assessment.

#### *3.4.1. Japan*

Using the conceptual model, the SHARKWG identified a large overlap between the fishing grounds of the Japanese shallow-set longline fishery and the distribution of SMA in the NPO. Under the assumption of a well-mixed population in the NPO the Japanese shallow-set longline index should be representative of the population vulnerable to the fishing gear, and under a multi-stock hypothesis would be representative of the stock corresponding to the western parturition site.

To develop the shallow-set index, the set-by-set logbook data from Japanese offshore and distant water longline fishery was used to estimate the standardized CPUE of SMA in the western and central NPO over the period from 1994-2022 (Kai, 2023b). Since the catch data of sharks

caught by commercial tuna longline fishery is usually underreported due to discard of sharks, the logbook data were filtered using the simple filtering methods applied to BSH as in Kai (2021). The nominal CPUE of filtered shallow-set data was then standardized using a spatio-temporal generalized linear mixed model (GLMM) to provide the annual changes in the abundance of SMA in the northwestern Pacific. The author focused on seasonal and interannual variations of the density in the model to account for spatial and seasonal changes in the fishing location due to target changes between BSH and swordfish. The estimated annual changes in the CPUE of SMA revealed an upward trend from 1994 to 2014, and then downward trend until 2020. Thereafter the CPUE slightly increased in recent years. The best model (*S5 JP-OF-DW-SH-LL-M3*) was determined using Bayesian Information Criterion (BIC) and an alternative model (*S6 JP-OF-DW-SH-LL-M5*) determined using Akaike Information Criterion (AIC) was considered in a sensitivity analysis.

An index (*S7 JP-OF-DW-DE-LL-M7*) was also developed using Japanese research and training vessel data (Kai, 2023c). This is a deep-set longline fishery that typically operates to the southwest of the main Hawai'i islands. Sample sizes for this analysis were low, and the conceptual model indicated that this index would be a poor match to the presumed SMA distribution in the NPO. As a result, this index was only considered in a sensitivity analysis.

#### *3.4.2. Chinese-Taipei (Taiwan)*

The conceptual model identified that based on the presumed SMA distribution in the NPO, the Chinese-Taipei large-scale tuna longline (LTLL) fishery operating north of by 25 °N (e.g., targeting albacore tuna mostly in temperate waters) was more representative than the deep-set fishery fishing in more equatorial waters. To develop an index for use in the stock assessment model, the SMA catch and effort data from the logbook records of the LTLL fishing vessels operating in the NPO north of by 25 °N from 2005 to 2022 were analyzed to create an index of relative abundance for the Chinese Taipei longline fishery (*S4 TW-LA-LL-N*; Liu et al., 2023). Due to a significant percentage of zero SMA catch, a zero-inflated negative binomial model was used to standardize the CPUE, presenting the number of fish caught per 1,000 hooks. Both nominal and standardized CPUEs for SMA exhibited inter-annual fluctuations with two peaks in 2014 and 2020.

#### *3.4.3. USA*

Two data sources were available for the development of CPUE indices from US Hawai'i based longline vessels: shallow-set and deep-set. Using the conceptual model as a guide, the US identified that the deep-set sector may be more representative given that a) wire leaders were used through 2020 and b) satellite tagging data indicates larger individuals spend more time at deeper depths which could coincide with deep-set longline fishing practices. A preliminary analysis comparing catch-rates between deep-set and shallow-set from 5°x5° cells containing both gears appeared to show similar catch-rates and trends. Furthermore, the shallow-set fishery was subject to fishery closures due to bycatch concerns from 2002-2004 which limited the shallow-set data

available for analysis.

An annual standardized CPUE index for the US Hawai'i deep-set index was developed with spatio-temporal GLMM model (VAST) using observer data collected as a part of the Pacific Islands Regional Observer Program (PIROP) from 2000-2020 (Ducharme-Barth et al., 2024). The analysis window was restricted to this period due to low sample sizes prior to 2000 and likely catchability changes that occurred in 2020 (e.g., reduction in use of wire leaders and switch in bait type used from saury to milkfish). The window of analysis of data was further restricted to the 3rd quarter of the year in order to be more representative of sub-adult/adults as this coincided with the largest individuals being observed in the fishery (Ducharme-Barth et al., 2024). Two indices were developed, one which considered all 3rd quarter data (*S1 US-DE-LL-all*) and another 'core area' (*S2 US-DE-LL-core*) which contained the majority of the fishing effort since some 2020 values on the edge of the distribution appeared anomalously large and impacted the index trend in the terminal year. The final models indicated a generally increasing trend up through 2017, after which the model either declined or bounced back to 2017 levels depending on if possibly anomalous predictions were used for the index calculation. The model predicted large CVs (>1) however these were later determined to be model artifacts due to modeling some catchability terms using cubic splines. Re-running the standardization models either by removing these catchability terms or modeling the covariate as a linear effect did not change the trend of the standardized index but reduced the estimated CV to a mean ~0.33. Accordingly, this lower mean CV value was used in the stock assessment for these indices.

The SHARKWG also evaluated a fisheries-independent juvenile shark survey index from the Southern California Bight as a possible recruitment index for the eastern NPO parturition site (Runcie et al., 2016), and this index (*S3 Juvenile-Survey-LL*) was evaluated in a sensitivity analysis.

#### *3.4.4. Mexico*

Standardized CPUE of SMA caught in the Mexican pelagic longline fishery operating in the NPO off northwestern Mexico was estimated for the period between 2006 and 2022. The analysis used data obtained through the Mexican pelagic longline observer program and a generalized linear model (GLM) approach (Fernandez-Mendez et al., 2023). Individual longline set CPUE data, collected by scientific observers, were analyzed to assess effects of environmental factors such as sea surface temperature (SST), distance from land (including islands) and time-area factors, year, area fished, quarter and fraction of night hours in the fishing set. Standardized catch rates were estimated by applying hurdle (delta) models. This analysis resulted in stable index trends for most of the analyzed period, with lower values in the last year of the series. Given the large targeting shifts that occurred in the Mexican longline during the period of the analysis, the SHARKWG decided that the Mexican index should only be included in a sensitivity analysis.

### 3.5. Size composition

Raw size compositions were provided by SHARKWG members. Some fisheries from Japan raised these observations to the catch. Sex-specific size composition data were reported in the observed measurement units (FL – fork length, TL – total length, AL – alternate length, which is the length from the leading edge of the first dorsal fin to the leading edge of the second dorsal fin) which were subsequently converted to PCL using fishery specific conversion equations (ISC, 2018a).

#### *3.5.1. Japan*

Japan provided SMA size data from several sources including port sampling data from the offshore shallow-set longline, small-scale longline (mostly coastal) and driftnet fishery. Size data from research data comes from the shallow-set and deep-set longline survey, research and training vessels, and the observer program. Generally, coastal fisheries including the driftnet fishery, shallow-set longline research vessels, and small-scale longline operate in the western NPO (west of the dateline) and catch larger amounts of juveniles (< 150 cm PCL) compared to deep-set longline research which mainly operates in the area east of the dateline. Regarding the ratio of juveniles, 86-95% of males and almost 100% of females were juveniles in these coastal fisheries, while 58% of males and 4.7% of females were adults in deep-set longline research. The Kinkai-shallow commercial fishery also catches mainly juveniles smaller than 150 cm PCL, but 20% of males were adults while females were almost entirely juveniles. Different size structures were also observed, depending on data sources even if the same fishery and operation type were used in the same area. Fine-scale differences in the pattern of landing and reporting between commercial vessels and research vessels and reduced overlap of the operation area when considering fine-scale data may explain this difference. There does not appear to be an obvious trend in mean size in either the Kinkai-Shallow commercial landing data, deep-set longline research data or driftnet fishery. From the perspective of data availability, the Kinkai-Shallow commercial fishery has provided a large volume of observations, while the number of samples from the deep-set longline research vessels have deteriorated in recent years.

#### *3.5.2. Chinese-Taipei (Taiwan)*

Size composition data were available for two types of Chinese Taipei tuna longline vessels: LTLL (≧100 GRT) and STLL (＜100 GRT). The size composition data were obtained by converting recorded measurements to PCL using available conversion equations. For STLL, spanning from 1989 to 2019 in the NPO, female shortfin mako sizes ranged from 61 to 338 cm PCL (n = 116,281), and males ranged from 60 to 262 cm PCL (n = 108,505). The logbook data for LTLL from 2005 to 2019 included 11,173 individuals (sexes combined) with sizes ranging from 61 to 303 cm PCL. Size distribution analysis revealed bimodal patterns in STLL catches, indicating a prevalence of immature fish (female < 228 cm, male < 172 cm PCL). The capture of a high

proportion of immature sharks poses sustainability concerns for the fishery.

#### *3.5.3. Republic of Korea*

There are no size data available from fishery catches by the Republic of Korea.

#### *3.5.4. China*

There are no size data available from fishery catches by China.

#### *3.5.5. Canada*

Given the negligible level of catch, there are no size data available from fishery catches by Canada.

#### *3.5.6. USA*

Size frequency data were available for a number of US fisheries. Length-frequency observations for the US Hawai'i based deep-set and shallow-set longline were taken from PIROP observer data (Ducharme-Barth et al., 2024). Only records with lengths given as total length (TL), fork length (FL), and PCL were retained. These lengths were then all converted to PCL where appropriate. The aggregate deep-set distribution was unimodal while the shallow-set distribution was bimodal. Separating the distribution by sex and month indicated seasonal patterns where larger individuals were typically encountered in the summer months (e.g., 3$^{rd}$ quarter). As a note, sample size diminished greatly over the modelled period. This could be linked to non-retention measures (e.g., cutting off sharks prior to decking and/or reduction in use of wire-leaders) and/or increasing use of electronic monitoring.

Size frequency data were also available for the US California based drift gillnet fishery (Kinney et al., 2017). Sex-specific size data for this fishery collected by observers were available from 1990-2018. Port based size sampling was also available from 1981-1990 but sex was not recorded for the majority of port samples, so these data were kept separate from observer data.

Size frequency data were available for the fisheries-independent juvenile shark survey index (Runcie et al., 2016).

#### *3.5.7. Mexico*

Sex-specific length composition data were collected by onboard observers in Mexican pelagic longline fisheries based in Ensenada, Baja California and Mazatlán, Sinaloa between 2006 and 2022. Observed measurements given as total length (TL) were converted to PCL using available specific conversion equations.

#### *3.5.8. IATTC/Non-ISC*

There are no size data available from fishery catches by non-ISC fleets operating in the IATTC convention area.

#### *3.5.9. WCPFC/Non-ISC*

There are no size data available from fishery catches by non-ISC fleets operating in the WCPFC convention area.

## 4. MODELING APPROACH

Modeling took place in multiple distinct phases. The initial plan by the SHARKWG, and first phase of the analysis, was to build on the 2018 assessment (ISC, 2018a) and developed an integrated age-structured model using SS3 (Methot Jr. and Wetzel, 2013). The proposed initial model period was 1975 – 2022 and included updated fishery data (e.g., catch, size composition and CPUE indices) and additional fishery structure to match the data provided by SHARKWG members. This model would be used to explore a number of scenarios, in a hierarchical fashion, corresponding to key uncertainties identified in the conceptual model. The first level of the planned hierarchy would have been stock and fleet structures and would have developed models fitting to different combinations of abundance indices depending on the hypothesized stock structure. The next level of the hierarchy would have been biological uncertainty (growth, natural mortality, reproduction, and steepness).

A key decision by the SHARKWG in developing the SS3 model was to remove the early period (1975-1993) CPUE index from the model given the concerns referenced in Section 2.1. This decision was made early in model development, and it became apparent very quickly that the SS3 model, as configured, was unable to reconcile the updated catches (lower pre-1994 and increasing throughout 1975-2022), post-1994 CPUE trends (increasing), and assumed biological characteristics. In order to try and find a viable configuration, the SHARKWG converted the integrated age-structured model into an Age-Structured Production Model (ASPM), staying within the SS3 framework. The full SS3 model was simplified (e.g., fisheries that shared selectivity were aggregated into a single fisheries definition), run with a high data-weight placed on the size composition to get reasonable estimates for selectivity which were then held fixed. Using the ASPM configuration alternative initial conditions (e.g., initial fishing mortality, F) and model start years (e.g., 1994, 1975, or 1952) were tested and none yielded a model that converged. Additionally, given the uncertainties related to catch, alternative model configurations were attempted where the F values required to the fit the catch was iteratively solved for numerically (hybrid approach; Methot Jr. and Wetzel, 2013) or where F values were free parameters that were estimated by fitting to the catch with error. Neither of these approaches proved successful.

Following these investigations, the SHARKWG was unable to use the ASPM to define a stationary production function given the biological assumptions, the increasing catch and the increasing indices. The SHARKWG concluded that the inability to define a stationary production function using the ASPM implied that one (or some) of the following was likely to be true:

- The increasing CPUE trends imply a recovery. Under a stationary production model hypothesis, the stock must previously have been depleted. Therefore, the early period catches (pre-1994) are under reported/estimated since they must have been large enough (and larger than post-1994 catches) to cause the population to be depleted in

the early period and subsequently recover.

- The catch could be correct and the trends in the abundance indices could be wrong.
- The assumed stock productivity (e.g., natural mortality, maturity, litter size, reproductive cycle & steepness) is wrong
- The stock production function is non-stationary. Increases in catch and CPUE could both be correct and stock productivity/carrying capacity have increased over time due to ecosystem changes.

Given the uncertainties identified during the conceptual modeling exercise, it was acknowledged that both the catch and biological assumptions in the ASPM could be inappropriate. The SHARKWG considered the increasing CPUE trend to be most plausible given that this trend was seen in indices developed independently using data from Japan, Chinese-Taipei and the US. Further investigation of a model with a non-stationary production function was considered to be of limited utility since it would be difficult to evaluate stock status relative to reference points.

Despite the large-quantity of data post-1994, the SHARKWG determined that NPO SMA was in a data limited situation due to the lack of species-specific catch and CPUE data pre-1994; and uncertainties in the catch, CPUE and biological assumptions. Additionally, the dome-shaped selectivity of all fisheries (e.g., large females are rarely captured) reduces the ability of the model to use length composition data to inform estimates of fishing mortality and help set population scale unless the descending limb of the selectivity curve is held fixed. The SHARKWG acknowledged that a SS3 model was not possible at this stage, and that a strategic pivot to a more simplified model was needed in order to thoroughly explore the data conflicts and provide stock status information.

A Bayesian state-space surplus production model (BSPM) was developed to model the population from 1994-2022 in order to provide stock status information, while also accounting for the uncertainties identified during the conceptual modeling process. Use of BSPMs have precedence in shark stock assessments in the WCPFC. Neubauer et al. (2019) developed a BSPM as an alternative model which showed similar results as the SS3 model for oceanic whitetip shark, *Carcharhinus longimanus* (Tremblay-Boyer et al., 2019). The SHARKWG also notes the recommendation from SC19 that given challenges facing shark assessments, data-limited approaches (such as a BSPM) be developed concurrently to an integrated age-structured assessment model so that advice on stock status can still be provided even if the integrated assessment approach fails (WCPFC, 2023). One advantage of the BSPM approach is that an informative prior could be developed for initial population depletion in 1994. This allowed for the estimation of stock status from 1994-2022 while also accounting for the uncertainty in fishery impacts prior to 1994.

Simplifying the dynamics through the use of a BSPM makes the evaluation of data conflicts

more efficient as the number of parameters governing the population dynamics are much fewer and makes the provision of stock status possible. However, such simplification could lead to bias if there is a long lag to maturity (Kokkalis et al., 2024) and/or if the indices used in the model are not representative of the reproductive component of the population (e.g., a dome-shaped selectivity for a large majority of juvenile and sub-adults). In order to evaluate the potential bias, an age-structured model (ASM) simulation was developed as an operating model to generate simulated data representative of NPO SMA population dynamics and the fisheries operating in the NPO. Fitting the BSPM to the simulated data (where the true stock status is known from the operating model) allowed for the calculation of the likely bias in depletion relative to the unfished condition.

Details on the model configuration for the three modeling phases (SS3, BSPM & ASM simulation) are provided in the following sections.

### 4.1. Stock Synthesis (SS3)

The initial SS3 model followed the same structure as the 2018 assessment (ISC, 2018a). A brief summary of the model was provided in Section 2.1 and readers are directed to the 2018 assessment report for a full description of the model structure and configuration (ISC, 2018a). However, a few key changes were made to the data-inputs and model structure in the initial development of the 2024 stock assessment model:

- the SS3 executable was upgraded to version 3.30.22.1
- a typo in the length-weight relationship was corrected (the correct values were listed in the 2018 assessment report but not in the SS3 control file)
- the Japanese early (1975-1993) index was removed from the model
- the model assumed a well-mixed stock hypothesis and fit to three indices: the US Hawai'i deep-set longline all (*S1 US-DE-LL-all*), US juvenile shark survey index (*S3 Juvenile-Survey-LL*), and Japanese shallow-set longline index (*S5 JP-OF-DW-SH-LL-M3*)
- historical catch was updated based on revised analyses
- the model period was extended to 2022
- new fisheries structures (Table 1) were developed to account for new catch and size composition information (including equivalent 'simplified' fishery structure which aggregated fisheries with shared selectivity; Table 2).

### 4.2. Bayesian State-Space Surplus Production Model (BSPM)

A series of BSPM models spanning the period 1994-2022 were developed in the Stan probabilistic programming language (Stan Development Team, 2024a) using code from the *bdm* package (Edwards, 2024) in R (R Core Team, 2023) as a starting point for the BSPM model code. Development of the BSPM followed the approach of (Neubauer et al., 2019) and used recent best

practices for surplus production models (Kokkalis et al., 2024) and Bayesian workflows for stock assessment (Monnahan, 2024) as guides for the development, analysis and presentation of BSPM stock assessment models. BSPMs were implemented in Stan rather than JABBA (Winker et al., 2018) in order take advantage of enhanced diagnostics, greater efficiency in posterior sampling, and greater flexibility with model configuration/prior specification.

Stan is a state-of-the-art and high-performance platform that allows for full Bayesian statistical inference. Markov Chain Monte Carlo (MCMC) sampling of the posterior parameter distributions is implemented using the no-U-turn (NUTS) Hamiltonian Monte Carlo (HMC) algorithm (Betancourt and Girolami, 2013). Implementation in R using the *rstan* package (Stan Development Team, 2024b) allows connection to an ecosystem of additional R packages (*bayesplot* Gabry and Mahr, 2024*;* and *loo* Vehtari et al., 2024) for visualizing, diagnosing and validating Stan models (Gabry et al., 2019).

#### *4.2.1. Input data*

Input data for the BSPM models depended on the model structure of the BSPM (described in Section 4.2.2) and varied depending on how catch was treated in each model. Four primary indices of relative abundance were fit within individual models (multiple indices were never fit within the same model, differing trends were dealt with using a model ensemble approach), and an additional six indices were evaluated in sensitivity runs. Input values for catch, effort and indices of relative abundance are shown in Table 5 and Table 6.

##### **4.2.1.1. Catch**

The BSPM models tracked the evolution of the population over time in terms of numbers of individuals. Accordingly, catch or population removals were required to be in numbers. SHARKWG members provided catch values in a mix of numbers and metric tons. Catch provided in metric tons were converted to numbers using a SS3 model where this conversion accounts for fisheries selectivity, growth, variability in the growth curve, and the length-weight relationship. SS3 model 08 – 2022simple (described in Section 5.1), which had reasonable selectivity estimates and fits to size composition data, was used for the conversion. This catch time series (Table 6) was used directly as removals when catch was treated as fixed (Section 4.2.2.1) or was fit to with lognormal error when F was estimated directly to produce estimated population removals (Section 4.2.2.3). Catch generally increased over the modeled period from ~50,000 individuals per year in 1994 to ~80,000 individuals per year in 2022 (~94,000 individuals per year, average 2018-2022). Note that catch was used as numbers in the BSPM rather than 1000s of numbers as listed in the table.

When estimated population removals were mostly driven using longline effort (Section 4.2.2.2), the component of catch attributed to longline fisheries was subtracted from the catch time series (Table 6). In these models' population removals were a combination of fixed non-longline

removals and estimated longline removals driven by a time-series of longline effort (Section 4.2.1.2). Non-longline catch was largely consistent at between 6,000 – 10,000 individuals per year from 1994-2012, after which non-longline catch increased rapidly to ~55,000 individuals per year over 2018-2022. This rapid increase is likely due to the Mexican artisanal catch being split out from the Mexican longline catch in recent years (2017-2022) as this catch is substantial (~44,000 individuals per year from 2017-2022).

#### 4.2.1.2. Effort

An effort time-series was used to drive the estimation of longline removals (Section 4.2.2.2). Public longline effort data from all flags operating north of 10°N in the NPO were combined from WCPFC and IATTC databases. The 10°N cut-off was selected based on the conceptual model to identify longline effort that would likely encounter SMA. Prior to being used in the BSPM to estimate longline removals, the time-series of longline effort was rescaled to a maximum value of one. Nominal longline effort increased from ~103 million hooks fished in 1994 to a peak of ~208 million hooks fished in 2008 before declining to ~121 million hooks fished in 2022 (Table 6).

#### 4.2.1.3. Indices of relative abundance

Four main indices of abundance were used in the BSPM: two US deep-set indices (Section 3.4.3 *S1 US-DE-LL-all* & *S2 US-DE-LL-core*), the Chinese-Taipei longline index operating north of 25°N (Section 3.4.2 *S4 TW-LA-LL-N*) and a Japanese shallow-set index (Section 3.4.1 *S5 JP-OF-DW-SH-LL-M3*). An additional six indices were considered in sensitivity analyses: the US juvenile shark survey (Section 3.4.3 *S3 Juvenile-Survey-LL*), an alternative Japanese shallow-set index (Section 3.4.1 *S6 JP-OF-DW-SH-LL-M5*), the Japanese deep-set research and training vessel index (Section 3.4.1 *S7 JP-OF-DW-DE-LL-M7*), a combined Mexican longline index (Section 3.4.4 *S8 MX-Com-LL*), an index for the Ensenada based Mexican longline (Section 3.4.4 *S9 MX-Com-LL-N*), and an index for the Mazatlán based Mexican longline (Section 3.4.4 *S10 MX-Com-LL-S*).

All indices and associated time-varying CV can be found in Table 5. Each index was re-scaled to a mean of 1. When the mean CV of an index was less than 0.2 it was increased to have a mean of at least 0.2 except for *S1 US-DE-LL-all* & *S2 US-DE-LL-core* which had a mean CV of at least 0.33.

### *4.2.2. Model structures*

The population dynamics, in numbers, of the BSPM are governed by Fletcher-Schaefer hybrid surplus production model equations (Winker et al., 2020; Edwards, 2024). A *random-effects* style parameterization of a state-space model was used to incorporate process error into the state dynamics. This parametrization is statistically equivalent in a Bayesian statistical framework (de

Valpine, 2002) to the *state* style parametrization of state-space models more commonly seen in the fisheries assessment literature (e.g., *JABBA*; Winker et al., 2018).

BSPM development progressed through a series of phases where additional components were freed up for estimation. Initial models assumed catch was known along with the shape, process error and observation error parameters, while carrying capacity, initial depletion and the intrinsic rate of increase were estimated. Estimation of the remaining parameters was progressively turned on as priors for these parameters were defined and refined. The final BSPM estimated all parameters and is generally given by the following equations:

State-dynamics

$$x_1 = x_0 \quad \text{Eq. 4.2.2.a}$$

$$x_t = \begin{cases} \left(x_{t-1} + R_{Max}x_{t-1}\left(1 - \frac{x_{t-1}}{h}\right) - C_{t-1}\right) \times \epsilon_{t-1}, & x_{t-1} \leq D_{MSY}; t > 1 \quad \text{Eq. 4.2.2.b} \\ (x_{t-1} + x_{t-1}(\gamma \times m)(1 - x_{t-1}^{n-1}) - C_{t-1}) \times \epsilon_{t-1}, & x_{t-1} > D_{MSY}; t > 1 \quad \text{Eq. 4.2.2.c} \end{cases}$$

$$\epsilon_t = \exp\left(\delta_t - \frac{\sigma_P^2}{2}\right) \quad \text{Eq. 4.2.2.d}$$

$$\delta_t \sim N(0, \sigma_P) \quad \text{Eq. 4.2.2.e}$$

Intermediate parameters

$$D_{MSY} = \left(\frac{1}{n}\right)^{\frac{1}{n-1}}; \text{depletion at MSY} \quad \text{Eq. 4.2.2.f}$$

$$h = 2D_{MSY} \quad \text{Eq. 4.2.2.g}$$

$$m = \frac{R_{Max}h}{4}; \text{ MSY} \quad \text{Eq. 4.2.2.h}$$

$$\gamma = \frac{n^{\frac{n}{n-1}}}{n-1} \quad \text{Eq. 4.2.2.i}$$

where the leading parameters are $n$ (shape parameter of the production function[2] and controls $D_{MSY}$), $x_0$ (initial depletion of the population relative to carrying capacity $K$), $R_{Max}$ (intrinsic rate of increase), and $\sigma_P$ (process error). The population variable $x_t$ is modelled as the depletion relative to $K$. Population removals are given by $C_t$ where $C_t$ is defined as the proportion of $x_t$

[2] Note that when $n = 2$ the model is a Schaefer surplus production model with $D_{MSY} = 0.5$.

relative to $K$ that is removed. The alternative model structures only differ in their treatment of removals and further detail on these differences are provided in the following sections. Population carrying capacity $K$ is given in numbers.

#### 4.2.2.1. Catch (Fixed)

When catch is fixed, the observed levels of total catch ($C_t^*$) are removed directly from the population where population removals are defined as:

$$C_t = \begin{cases} \frac{C_t^*}{K}, & \frac{C_t^*}{K} < x_t \quad \text{Eq. 4.2.2.1.a} \\ x_t, & \frac{C_t^*}{K} \geq x_t \quad \text{Eq. 4.2.2.1.b} \end{cases}$$

subject to the constraint that population removals cannot be greater than the population.

#### 4.2.2.2. Catch (Estimated – Longline effort)

When catch is estimated and driven by longline effort, total population removals ($C_t''$) are a combination of fixed non-longline removals ($C_t'$) and estimated longline removals driven by a time-series of scaled longline effort ($E_t$):

$$F_t^{LL} = qE_t \quad \text{Eq. 4.2.2.2.a}$$

$$F_t^{noLL} = \frac{C_t'}{x_t K} \quad \text{Eq. 4.2.2.2.b}$$

$$U_t = 1 - \exp\left(-(F_t^{LL} + F_t^{noLL})\right) \quad \text{Eq. 4.2.2.2.c}$$

$$C_t'' = U_t \times (x_t K) \quad \text{Eq. 4.2.2.2.d}$$

$$C_t = \begin{cases} \frac{C_t''}{K}, & \frac{C_t''}{K} < x_t \quad \text{Eq. 4.2.2.2.e} \\ x_t, & \frac{C_t''}{K} \geq x_t \quad \text{Eq. 4.2.2.2.f} \end{cases}$$

where $q$ is the catchability for scaled longline effort and $U_t$ is the proportion of $x_t$ that is exploited in a given time step. Please note that in writing the stock assessment report an error was discovered in Eq. 4.2.2.2.b where the fishing mortality associated with non-longline catch ($F_t^{noLL}$) was defined using the discrete rather than continuous[3] equation for fishing mortality $F$. This is inappropriate given that $F_t^{noLL}$ is combined with $F_t^{LL}$ (defined as continuous $F$) in Eq. 4.2.2.2.c.

[3] The continuous definition of fishing mortality for non-longline catch is $F_t^{noLL} = -\log\left(-\left(\frac{C_t'}{x_t K}\right)+1\right)$.

An assessment of the impacts of this error on model outputs and management advice is described in the Appendix. However, correcting this error resulted in negligible differences in model estimates.

#### 4.2.2.3. Catch (Estimated – F)

When catch is estimated and the $F$ is directly estimated the population dynamics are given by the following equations:

$$x_1 = x_0 \quad \text{Eq. 4.2.2.3.a}$$

$$x_t = \begin{cases} \left(x_{t-1} + R_{Max}x_{t-1}\left(1 - \frac{x_{t-1}}{h}\right)\right) \times \exp(-F_{t-1}) \times \epsilon_{t-1}, & x_{t-1} \le D_{MSY}; t > 1 \quad \text{Eq. 4.2.2.3.b} \\ \left(x_{t-1} + x_{t-1}(\gamma \times m)(1 - x_{t-1}^{n-1})\right) \times \exp(-F_{t-1}) \times \epsilon_{t-1}, & x_{t-1} > D_{MSY}; t > 1 \quad \text{Eq. 4.2.2.3.c} \end{cases}$$

$$F_t \sim N^+(0, \sigma_F) \quad \text{Eq. 4.2.2.3.d}$$

where the population in time $t$ is the population from time $t-1$ plus/minus any surplus production that survives from fishing mortality ($\exp(-F)$), and $\sigma_F$ is the variability in $F$. Estimated catch based on the estimated $F$ is given by:

$$C_t = \begin{cases} \left(x_t + R_{Max}x_t\left(1 - \frac{x_t}{h}\right)\right) \times (1 - \exp(-F_t)) \times \epsilon_t \times K, & x_{t-1} \le D_{MSY} \quad \text{Eq. 4.2.2.3.e} \\ \left(x_t + x_t(\gamma \times m)(1 - x_t^{n-1})\right) \times (1 - \exp(-F_t)) \times \epsilon_t \times K, & x_{t-1} > D_{MSY} \quad \text{Eq. 4.2.2.3.f} \end{cases}$$

### *4.2.3. Developing priors*

Descriptions for the development of priors for leading model parameters ($R_{Max}$, $x_0$, $n$, $K$, $\sigma_P$, $\sigma_{O_{Add}}$, $q$, and $\sigma_F$) are found in the following sections and are compiled in Table 7.

#### 4.2.3.1. Intrinsic rate of increase $R_{Max}$

A prior for the maximum intrinsic rate of population increase ($R_{Max}$) was developed using an age-structured numerical simulation following (Pardo et al., 2016, 2018). Developing the prior for $R_{Max}$ requires solving the Euler-Lotka equation:

$$\sum_{a=1}^{A_{Max}} l_a b_a \exp(-R_{Max} \times a) = 1 \quad \text{Eq. 4.2.3.1.a}$$

where $A_{Max}$ is the maximum age, $l_a$ is the proportion of females that survive to age $a$, and $b_a$ is the reproductive output (average number of pups produced per year) of an average female of age $a$. The proportion of females that survive and the average reproductive output are defined by:

$$l_a = \begin{cases} \exp(-M_a), & a = 1 \\ l_{a-1} \times \exp(-M_a), & a > 1 \end{cases}$$ Eq. 4.2.3.1.b

Eq. 4.2.3.1.c

$$b_a = \frac{\psi_a \phi_a \alpha}{\rho}$$ Eq. 4.2.3.1.d

where $M_a$ is the natural mortality at age $a$, $\psi_a$ is the proportion of females that are mature at age $a$, $\phi_a$ is the fecundity or average number of pups per litter for a female of age $a$, $\alpha$ is the female sex-ratio at birth (e.g., 50%), and $\rho$ is the reproductive cycle (e.g., two or three years).

When setting up the numerical simulations, the SHARKWG considered a number of scenarios for natural mortality $M_a$, maturity $\psi_a$, fecundity $\phi_a$ and reproductive-cycle $\rho$. Additionally, both the maximum age and the sex-ratio were allowed to vary randomly for each simulation, $A_{Max} \sim \text{Lognormal}(\log(32), 0.15)$ and $\alpha \sim \text{Normal}(0.5, 0.05)$.

For natural mortality $M_a$ the SHARKWG first decided the level of adult natural morality for females based on the three options described in Section 2.2.5 (US aging scenario, JP aging scenario or based solely on maximum age). The adult $M$ was allowed to vary randomly with Lognormal error and a lognormal standard deviation of ~0.32 following (Teo et al., 2024). Next the SHARKWG considered if juvenile natural mortality should apply to age 1 or if the adult $M$ should be applied to all ages. If juvenile natural morality was applied, this was also allowed to vary proportionately for the three different adult $M$ scenarios based on the ratio between the three female adult $M$ values from Section 2.2.5 and the median natural mortality from Mucientes et al. (2023).

Maturity at age $\psi_a$ was calculated based on the maturity at length equation from Semba et al. (2017) and converted to age using the average length at age based on either the US aging or JP aging scenarios (Kinney et al., 2024). Maturity at age $\psi_a$ was allowed to vary randomly for each simulation by incorporating the estimated parameter uncertainty in the maturity at length relationship from Semba et al. (2017) and by allowing for variability in length at age by drawing growth parameters from the posterior distributions from Kinney et al. (2024).

Three fecundity scenarios were considered: constant across female body size (~12 pups per litter based on Mollet et al., 2000), increasing with a linear relationship with female body size (Semba et al., 2011), or increasing with a power relationship with female body size (Fletcher, 1978). Fecundity at length was converted to fecundity at age $\phi_a$ using the average length at age based on either the US aging or JP aging scenarios (Kinney et al., 2024). In each simulation, random variability was introduced by scaling the entire fecundity at age vector up or down using a normally distributed random deviate with a coefficient of variation of 0.15. Variability in length

at age was incorporated in the same way as for maturity at age $\psi_a$. Lastly, two scenarios were considered for reproductive cycle $\rho$ either two or three years.

A total of 1,036,800 simulations were conducted using a grid approach. The total number of simulations was determined based on 15 replicates for each of the full factorial combinations of: growth type (US or JP aging), natural mortality type (combined or maximum age based), inclusion of juvenile natural mortality (True or False), fecundity relationship with length (constant, linear, or power), reproductive cycle (two or three), and posterior sample for the growth parameters (n=1440). Distributions of the leading parameters across all simulations are shown in Figure 5.

The Euler-Lotka equation was solved numerically for each simulation resulting in a distribution of potential $R_{Max}$ values. This distribution of $R_{Max}$ values was further refined using a catch only numerical simulation following the approach of Neubauer et al. (2019). Briefly, a deterministic Schaefer surplus production model (Equations 4.2.2.a - 4.2.2.e where $n = 2$ and $\sigma_P = 0$) conditioned on the observed catch (Section 4.2.1.1) was used to simulate 10,000 population trajectories given the $R_{Max}$ distribution and broad priors for initial depletion $x_0 \sim \text{Uniform}(0.05, 0.80)$ and carrying capacity $K \sim \text{Lognormal}(\log(1.5 \times 10^7), 0.4)$. Given that the main CPUE indices (Section 4.2.1.3) show an increase over the model period, the resultant simulated population trajectories were filtered (Baseline filter: Trajectories that showed a 20% increase between the average depletion level from 1994-1998 to the average depletion level from 2018-2022) to develop a *baseline* distribution for $R_{Max}$. The *baseline* distribution of $R_{Max}$ was converted to a lognormal prior by solving for the mean and lognormal standard deviation that fit the distribution ($R_{Max} \sim \text{Lognormal}(-2.52, 0.41)$). However, the CPUE indices show a more dramatic increase than 20% over the model period so an alternative filter (Extreme filter: Trajectories that showed a 200% increase between the average depletion level from 1994-1998 to the average depletion level from 2018-2022) was applied to the simulated trajectories to develop an *extreme* distribution for $R_{Max}$. The *extreme* distribution of $R_{Max}$ was converted to a lognormal prior by solving for the mean and lognormal standard deviation that fit the distribution ($R_{Max} \sim \text{Lognormal}(-2.10, 0.20)$). The resultant prior distributions are shown in Figure 6.

Filtering the simulated population trajectories based on long-term viability ($R_{Max}$ must be greater than 0 to avoid extinction), and the two filtering criteria (baseline and extreme) showed selection of demographic traits that made up the numerical simulations. As each successive filter step is applied, the $R_{Max}$ distribution pushes to the right indicating a preference for a more productive stock. In general, this is characterized by selection for larger female body size, younger age at maturity, and lower levels of female natural mortality (Figure 5). Larger values of $R_{Max}$ are associated with greater reproductive output which can be achieved by having more individuals within the reproductive window (e.g., earlier maturation with faster growth and higher adult survival).

#### 4.2.3.2. Initial depletion $x_0$

Priors for initial depletion $x_0$ were developed from the identical numerical simulation and filtering as described for $R_{Max}$ in Section 4.2.3.1. The *baseline* distribution of $x_0$ was converted to a lognormal prior by solving for the mean and lognormal standard deviation that fit the distribution ($x_0 \sim \text{Lognormal}(-1.10, 0.59)$). The *extreme* distribution of $x_0$ was converted to a lognormal prior by solving for the mean and lognormal standard deviation that fit the distribution ($x_0 \sim \text{Lognormal}(-2.04, 0.39)$). The resultant prior distributions are shown in Figure 7.

#### 4.2.3.3. Shape $n$

Priors for shape $n$ were developed from the same age-structured simulations used to develop the $R_{Max}$ prior distributions in Section 4.2.3.1. Using the same input parameter combinations (e.g., those shown in Figure 5) that corresponded to the *baseline* and *extreme* distributions of $R_{Max}$, distributions for the inflection point of the production function $D_{MSY}$ were derived using the following relationship from Fowler (1988):

$$D_{MSY} = 0.633 - 0.187 \times \log\left(G_T R_{Max}\right) \quad \text{Eq. 4.2.3.2.a}$$

where $G_T$ is the generation time as defined by Grant and Grant (1992).

$$G_T = \frac{1}{SPR} \sum_{a=1}^{A_{Max}} a l_a b_a \quad \text{Eq. 4.2.3.2.b}$$

$$\text{SPR} = \sum_{a=1}^{A_{Max}} l_a b_a \quad \text{Eq. 4.2.3.2.c}$$

The *baseline* and *extreme* distributions of $D_{MSY}$ values were converted to shape $n$ by numerically solving Eq. 4.2.2.f. The *baseline* distribution of $n$ was converted to a lognormal prior by solving for the mean and lognormal standard deviation that fit the distribution ($n \sim \text{Lognormal}(1.02, 0.43)$). The *extreme* distribution of $n$ was converted to a lognormal prior by solving for the mean and lognormal standard deviation that fit the distribution ($n \sim \text{Lognormal}(0.60, 0.22)$). The resultant prior distributions are shown in Figure 8.

#### 4.2.3.4. Carrying capacity $K$

Initially, the same numerical simulation approach and filtering described in Section 4.2.3.1 to develop priors for $R_{Max}$ and $x_0$ was used to develop a prior for carrying capacity $K$. However, unlike for $R_{Max}$ and $x_0$ there appeared to be little information in such a prior pushforward approach for which to set population scale. Multiple priors were tested, and though results were sensitive to the choice of prior there was little to no posterior update, again indicating

the limited information content in the data to estimate population scale. In theory, there is information on the low-end of population scale as the population has to be large enough to support the catches, however defining a plausible upper bound is largely arbitrary. A broad uniform prior was tested, $\text{Uniform}(5e6,3e7)$, however the hard boundaries of the uniform prior caused convergence issues. Ultimately, a broad lognormal prior, $\text{Lognormal}(16,1)$, was used as this was able to cover a range of carrying capacity values without issues with model convergence.

#### 4.2.3.5. Process error $\sigma_P$

A lognormal prior was used for the standard deviation of the process error where the parameters were converted from the JABBA default prior for process error (Winker et al., 2018). JABBA assumed an inverse gamma prior for process error $\sigma_P^2 \sim \frac{1}{Gamma(4,0.01)}$. The corresponding lognormal distribution for $\sigma_P$ was $\text{Lognormal}(-2.93,0.27)$. Sensitivity to this choice of prior was tested, and a broad half-Normal prior, $\text{Normal}^+(0,1)$, was also investigated.

#### 4.2.3.6. Additional observation error $\sigma_{O_{Add}}$

A half-Normal prior, $\text{Normal}^+(0,0.2)$, was used for the additional observation error component $\sigma_{O_{Add}}$ which was in addition to the input time-varying, fixed observation error for each index $\sigma_{O_{Fixed},t}$. Initially a naïve half-Normal prior, $\text{Normal}^+(0,1)$, was used. However, this prior was refined to avoid placing too much prior weight on values of $\sigma_{O_{Add}}$ that were not supported by the data, and the prior distribution of $\text{Normal}^+(0,0.2)$ was selected to be broader than the posterior distribution of $\sigma_{O_{Add}}$.

#### 4.2.3.7. Longline catchability $q$

Initially a naïve half-Normal prior, $\text{Normal}^+(0,1)$, was used for the longline catchability $q$. However, a prior pushforward analysis, similar to the one described in Section 4.2.3.1 but using the population dynamics equations from Section 4.2.2.2 showed that the overwhelming majority of simulated population trajectories assuming the naïve prior went extinct (Figure 9). Subsequently, a more refined prior was developed based on deriving the parameters of lognormal distribution that fit the distribution of $q$ values where the population trajectory did not go extinct and was increasing (given that the available CPUEs all show an increase). This lognormal prior for $q$ was $\text{Lognormal}(-2.32,0.51)$.

#### 4.2.3.8. Fishing mortality error $\sigma_F$

Setting an appropriate prior for the variability in fishing mortality $\sigma_F$ can be challenging (Best and Punt, 2020), and in this case a relationship was seen between the broadness in the $\sigma_F$ prior and the estimated level of depletion. Initially a naïve half-Normal prior, $\text{Normal}^+(0,1)$, was used for the variability in fishing mortality $\sigma_F$. When applying this model with the population dynamics equations described in Section 4.2.2.3, this resulted in an almost exact fit to the catch

(as expected) but at a more pessimistic level of depletion relative to an equivalent model that treated catch as fixed. It was hypothesized that broad priors for $\sigma_F$ may give too much prior support to large values of $F$ and drive stock status down since smaller population sizes relative to $K$ are needed to produce the same levels of observed catch. Therefore, the prior for $\sigma_F$ was tuned such that it produced estimates of $F$ that were on a similar scale to the derived values of $F$ when catch was treated as fixed within the model. The baseline prior for $\sigma_F$ was half-Normal, $\text{Normal}^{+}(0,0.0125)$. In order to account for the sensitivity to model results based on the $\sigma_F$ prior and for the fact that observed SMA catch could be under-estimated, two alternative $\sigma_F$ priors were developed $\text{Normal}^{+}(0,0.025)$ and $\text{Normal}^{+}(0,0.05)$.

#### *4.2.4. Likelihood components*

BSPMs fit to two available data sources depending on the model structure. All models fit to an index of relative abundance. Models that directly estimated fishing mortality $F$ (Section 4.2.2.3) did so by also fitting to the observed catch. Details of these two likelihood components are provided in the following sections.

##### 4.2.4.1. Index of relative abundance

A lognormal likelihood was used to fit the indices of relative abundance,

$$\mu_{I,t} = \log(q_I \times x_t) - \frac{\sigma_{O,t}^2}{2} \quad \text{Eq. 4.2.4.1.a}$$

$$\sigma_{O,t}^2 = \left(\sigma_{O_{Fixed},t} + \sigma_{O_{Add}}\right)^2 \quad \text{Eq. 4.2.4.1.b}$$

$$I_t \sim \text{Lognormal}(\mu_{I,t}, \sigma_{O,t}) \quad \text{Eq. 4.2.4.1.c}$$

where the total observation error $\sigma_{O,t}$ associated with the index $I$ in time-step $t$ is the sum of the fixed input time-varying observation error for each index $\sigma_{O_{Fixed},t}$ and the estimated additional observation error component $\sigma_{O_{Add}}$. The expected value of the index is bias-corrected such that the mean of the lognormal distribution is $\log(q_I \times x_t)$ where $q_I$ is the catchability that scales the index $I$ to the population trajectory $x$. The catchability $q_I$ is analytically derived from its maximum posterior density assuming an uninformative uniform prior (Edwards, 2024):

$$q_I = \exp\left(\frac{1}{T}\sum_{t=1}^{T}\left((log(I_t) - log(x_t)) + \frac{\sigma_{O,t}^2}{2}\right)\right) \quad \text{Eq. 4.2.4.1.d}$$

##### 4.2.4.2. Catch

A lognormal likelihood was used to fit the observed catch for models where fishing mortality $F$ was directly estimated (Section 4.2.2.3),

$$\mu_{C,t} = \log(C_t^*) - \frac{\sigma_C^2}{2} \quad \text{Eq. 4.2.4.2.a}$$

$$C_t \sim \text{Lognormal}(\mu_{C,t}, \sigma_C) \quad \text{Eq. 4.2.4.2.b}$$

where $C_t^*$ is the observed total catch, $C_t$ is the predicted total catch, and $\sigma_C$ is a fixed parameter specifying the uncertainty in the catch time series. The expected value of the catch is bias-corrected such that the mean of the lognormal distribution is $\log(C_t^*)$. The uncertainty in the catch time series was assumed to be large, $\sigma_C = 0.5$. This value was selected given that there are important uncertainties that are likely unaccounted for in the observed total catch (e.g., incomplete reporting of discards, and uncertainties in the conversion of catch weight to numbers using SS3), and also because penalizing the model to fit tightly to catch can cause model convergence issues. Sensitivity to the choice of $\sigma_C$ was evaluated.

#### *4.2.5. Parameter estimation*

BSPMs were implemented in Stan through R using the *rstan* package. Sampling of the posterior distribution was done using 5 chains, with random starting points for all estimated parameters. A total of 3,000 samples were drawn from each chain with the first 1,000 samples serving as a 'warm-up' period. During the warm-up period the HMC sampling algorithm was tuned based on an *adapt_delta* = 0.99 and *max_treedepth* = 15. The 2,000 post warm-up samples from each chain were thinned to keep every 10$^{th}$ sample such that 200 posterior samples remained per chain. Posterior samples were combined across chains resulting in a combined 1,000 posterior samples per model.

#### *4.2.6. Model diagnostics*

BSPM performance was evaluated based on Stan model convergence criteria, fits to the data, posterior predictive checks, retrospective analysis, and hindcast cross-validation.

##### **4.2.6.1. Convergence**

Conventional Stan model diagnostics and thresholds were used to identify if posterior distributions were likely to be biased based on non-representative sampling of the posterior distribution. Models were assumed to have 'converged' to a stable, un-biased posterior distribution if the potential scale reduction statistic $\hat{R}$ was less than 1.01 for all leading model parameters, the bulk effective samples size was greater than 500 for all leading model parameters, and no divergent transitions were indicated (Monnahan, 2024).

##### **4.2.6.2. Data fits**

BSPM fits to the different data sources, index of relative abundance and/or observed catch, are given as the normalized root-mean-squared error (NRMSE),

$$RMSE = \sqrt{\frac{\sum_{i=1}^{n}(y_i - \hat{y}_i)^2}{n}} \quad \text{Eq. 4.2.6.2.a}$$

$$NRMSE = \frac{RMSE}{\left(\frac{\sum_{i=1}^{n} y_i}{n}\right)} \quad \text{Eq. 4.2.6.2.b}$$

where $y_i$ are the observations of either the index or the catch and $\hat{y}_i$ are the model predictions of either the index or the catch. The average NRMSE across all posterior samples is reported for each data component.

#### 4.2.6.3. Posterior Predictive Checks

Posterior predictive checks are conducted to see if the observed data could have been generated by the estimation model. This is done by generating simulated observations given the posterior parameter estimates and the data-likelihoods and comparing the distributions of simulated observations to the actual observations. Results are assessed visually.

#### 4.2.6.4. Retrospectives

Retrospective analysis was conducted for each model by sequentially peeling off a year from the terminal end of the fitted index and re-running the model. Data were removed for each year up to seven years from 2022 to 2016. Estimates of $x$ in the terminal year of each retrospective peel were compared to the corresponding estimate of $x$ from the full model run to better understand any potential biases or uncertainty in terminal year estimates. The Mohn's $\rho$ statistic (Mohn, 1999) was calculated and presented. This statistic measures the average relative difference between an estimated quantity from an assessment (e.g., depletion in final year) with a reduced time-series of information and the same quantity estimated from an assessment using the full time-series. Additionally, based on the recommendation from Kokkalis et al. (2024) we calculated the proportion of retrospective peels where the relative exploitation rate ($^{U}/_{U_{MSY}}$) and relative depletion ($^{D}/_{D_{MSY}}$) were inside the credible intervals of the full model run.

#### 4.2.6.5. Hindcast cross-validation

Hindcast cross-validation (Kell et al., 2021) was conducted for each index to determine the performance of the model to predict the observed CPUE $I$ one-step-ahead into the future relative to a naïve predictor. Briefly, the 'model-free' approach to hindcast cross-validation was used, and made use of the same set of seven retrospective peels described in Section 4.2.6.4. The 'model-free' hindcast calculation is described using the model from the last peel $BSPM_{2016}$ as an

example. This model fit to index data through 2016 but included catch through 2022. The model estimates of predicted CPUE in 2017 based on $BSPM_{2016}$ (which only fit to the index through 2016) is the 'model-free' hindcast for 2017, $\hat{I}_{2017}$. The naïve prediction of CPUE in 2017 is simply the observed CPUE from 2016, $I_{2016} = \ddot{I}_{2017}$. The absolute scaled error (ASE) of the prediction is:

$$ASE_{2017} = \frac{\left|I_{2017} - \hat{I}_{2017}\right|}{\left|I_{2017} - \ddot{I}_{2017}\right|} \qquad \text{Eq. 4.2.6.5.a}$$

Repeating this calculation across all retrospective peels for years 2017-2022 and taking the average across ASE values gives the mean ASE or MASE for the model. An MASE value less than one indicates that the model has greater predictive skill than the naïve predictor.

### *4.2.7. Projections*

#### 4.2.7.1. Retrospective

Though the BSPM modeled the period 1994 – 2022, fishing impacted the NPO SMA stock prior to 1994. However, the nature of these impacts is uncertain, so a retrospective projection was used to recreate possible historical trajectories of the stock from 1945 to 1993. Historical fishing impacts to the stock were driven by longline effort and high-seas driftnet effort.

Historical effort trajectories for longline $E_{LL_H}$ and high seas driftnet $E_{DFN_H}$ were compiled from publicly available sources. Using the same longline effort databases as in Section 4.2.1.2, public longline effort data from all flags operating north of 10°N in the NPO were combined from WCPFC and IATTC databases for the period 1952-1994. Longline effort was assumed to be negligible (e.g., 500 hooks) in the last year of World War II in 1945 so exponential interpolation was used to interpolate values from 1945 to the first full year of effort records in 1952.

Incomplete information existed for effort levels for high-seas driftnet fisheries, and effort information in number of tans fished was only available for the Japanese high-seas squid driftnet fishery (1982 - 1990) and the Korean high-seas squid driftnet fishery (1983 – 1990). Even though information was missing from the Chinese Taipei high-seas squid driftnet fishery or any of the high-seas large-mesh driftnet fisheries, the available effort data from Japan and The Republic of Korea is enough to get the relative pattern of effort needed to drive historical fishing mortality in the retrospective projection. The high-seas driftnet fisheries were assumed to operate from 1977 to 1992, so an exponential interpolation was used to interpolate values from negligible levels in 1977 (0.5 tans) to the first year of data for each country. The 1990 value was replicated for years 1991 – 1992 for each country, and then the effort levels for both countries were combined to get the total effort pattern for the period.

Prior to running the retrospective projection or historical reconstruction, catchability

coefficients were numerically derived to scale the fishing mortality associated with the two different effort time series (longline and driftnet) to the population. This was done in an iterative process for each sampled set of population dynamics parameters from the posterior distribution of the BSPM. The first step was to numerically calculate the historical longline catchability coefficient $q_{LL_H}$ by solving for the $q_{LL_H}$ that produced a simulated population trajectory which was approximately un-depleted in 1945 and that had a depletion in 1994 equal to the sampled $x_0$ value from the BSPM. The following population dynamics equations (slightly modified from Section 4.2.2.2) were used to solve for $q_{LL_H}$:

$$x_{1945} = \epsilon_{1945} \quad \text{Eq. 4.2.7.1.a}$$

$$\text{For t} \in 1946{:}\,1994$$

$$x_t = \begin{cases} \left(x_{t-1} + R_{Max}x_{t-1}\left(1 - \frac{x_{t-1}}{h}\right) - C_{t-1}\right) \times \epsilon_t, & x_{t-1} \leq D_{MSY}; t > 1 \quad \text{Eq. 4.2.7.1.b} \\ (x_{t-1} + x_{t-1}(\gamma \times m)(1 - x_{t-1}^{n-1}) - C_{t-1}) \times \epsilon_t, & x_{t-1} > D_{MSY}; t > 1 \quad \text{Eq. 4.2.7.1.c} \end{cases}$$

$$F_t^{LL_H} = (q_{LL_H}E_{LL_{H_t}}) \times \epsilon_{LL_t} \quad \text{Eq. 4.2.7.1.d}$$

$$U_t = 1 - \exp\left(-\left(F_t^{LL_H}\right)\right) \quad \text{Eq. 4.2.7.1.e}$$

$$C_t'' = U_t \times (x_t K) \quad \text{Eq. 4.2.7.1.f}$$

$$C_t = \begin{cases} \frac{C_t''}{K}, & \frac{C_t''}{K} < x_t \quad \text{Eq. 4.2.7.1.g} \\ x_t, & \frac{C_t''}{K} \geq x_t \quad \text{Eq. 4.2.7.1.h} \end{cases}$$

where $R_{Max}$, $D_{MSY}$, $h$, $n$, $\gamma$, and $m$ were all sampled jointly from the posterior distribution of the BSPM model. The historical process errors $\epsilon_t$ were also resampled from the estimated $\epsilon_t$ given that posterior sample. The simulated variability $\epsilon_{LL_t}$ in historical longline fishing mortality $F_t^{LL_H}$ was given by a lognormal random-walk.

With an initial estimate of historical longline catchability $q_{LL_H}$ solved for, the second step was to numerically solve for the historical longline driftnet catchability $q_{DFN_H}$. This was done by solving for the $q_{LL_H}$and $q_{DFN_H}$ that produced a simulated population trajectory which was approximately un-depleted in 1945, that had a depletion in 1994 equal to the sampled $x_0$ value from the BSPM, and that produced removals in 1994 equal to the 1994 removals from the BSPM.

The population dynamics equation (Eq. 4.2.7.1.e) was slightly modified to account for the additional historical driftnet fishing mortality:

$$F_t^{DFN_H} = (q_{DFN_H} E_{DFN_{H_t}}) \times \epsilon_{DFN_t} \quad \text{Eq. 4.2.7.1.i}$$

$$U_t = 1 - \exp\left(-\left(F_t^{LL_H} + F_t^{DFN_H}\right)\right) \quad \text{Eq. 4.2.7.1.j}$$

where the simulated variability $\epsilon_{DFN_t}$ in historical longline fishing mortality $F_t^{DFN_H}$ was given by a lognormal random-walk. This step was repeated twice to allow the numerically solved catchability covariates to converge to stable solutions.

Once the two catchability covariates were derived for each set of parameters from the posterior distribution, they were used with Equations 4.2.7.1.a – 4.2.7.1.j to generate a distribution of historical population trajectories.

#### 4.2.7.2. Future

The SHARKWG used 4 exploitation rate ($U$) based scenarios to conduct 10-year future projections for NPO SMA: the average $U$ from 2018-2021 $U_{2018-2021}$, $U_{2018-2021} + 20\%$, $U_{2018-2021} - 20\%$, and the $U$ that produces MSY $U_{MSY}$. Future projections were conducted from each set of parameters from the posterior distribution of BSPM models using the population dynamics equations from Section 4.2.2. The population removals in the future periods were given by the following equation:

$$C_t = x_{t-1} U \quad \text{Eq. 4.2.7.1.i}$$

where $U$ corresponds to the appropriate exploitation rate scenario. Additionally, process error $\epsilon_t$ in the forecast period was resampled from the estimated values of process error $\epsilon_t$ from the posterior distribution.

### 4.3. Age-structured simulation

As mentioned previously, there is the potential for bias in estimates of stock status when applying surplus production models to species that have a long lag time to maturity (age at 50% maturity for females is ~10-15 years depending on the growth curve used), and/or when age-specific processes are important (e.g., age-specific patterns in mortality or index selectivity). Additionally, rates of increase seen from a surplus production modeling approach might be overly optimistic given the simplifications made to the population dynamics. As a result, an age-structured simulation model, similar to the approach taken by Winker et al. (2020), was developed to: a) evaluate if the age-structured biological and fisheries characteristics of NPO SMA could produce the observed rates of increase implied by the standardized CPUE indices, and b) serve as an

operating model so that the potential bias in terminal depletion estimates (stock status relative to unfished conditions) from the BSPM could be calculated.

#### *4.3.1. Model structure*

A two-sex fully age-structured model was implemented in R by extracting the features of the SS3 (Methot Jr. and Wetzel, 2013) model that was developed for NPO SMA (described in Section 4.1). This model was used to simulate age-structured NPO SMA population dynamics from 1994 -2022. Briefly this is a single-season, annual model with two growth morphs (one for each sex), and a plus group for maximum age. Fisheries are defined with a double-Normal length-specific selectivity shared between sexes. Continuous fishing mortality is implemented where the hybrid approach is used to numerically calculate the fishing mortality to produce the observed catch for each fishery. Catch can be provided in terms of weight (mt) or numbers, though for simplicity catch was only provided in numbers. Key biological quantities were sex-specific: natural mortality, and growth. Additionally, maturity and fecundity were determined as functions of length. Length based quantities (growth, length-weight, selectivity, maturity, fecundity) were converted to age using an internal age-length-key accounting for variability in length at age. A low-fecundity stock recruit relationship (Taylor et al., 2013) was assumed to prevent recruitment from being greater than total reproductive output. For additional detail, including equations for the calculation of the population dynamics and fishing mortality, readers are referred to Methot Jr. and Wetzel (2013) and Appendix A of Methot Jr. and Wetzel (2013) as the same equations were used in the current model.

The initial conditions of the age-structured simulation model were specified a little differently than SS3, here initial age structure depended on assumptions for both initial fishing mortality, and initial levels of population depletion $x_{1994}$. Initial 1994 population numbers by sex $s$ were defined based on the following equations:

$$N_{s,1,1994} = \alpha S_{LFSR}(x_{1994}\beta_0)\beta_0 x_{1994}\epsilon_{1994} \quad \text{Eq. 4.3.1.a}$$

$$N_{s,a,1994} = N_{s,a-1,1994} \times \exp\left(Z_{s,a-1,1994}\right); A_{max} > a > 1 \quad \text{Eq. 4.3.1.b}$$

where $\alpha$ is the female sex-ratio at birth, $S_{LFSR}$ is the survival of recruits given the low-fecundity stock recruit relationship, $\beta_0$ is the total pups produced at unfished equilibrium, $x_{1994}$ is the initial level of population depletion in 1994, $\epsilon_{1994}$ is the process error associated with recruitment survival in 1994, and $Z_{s,a,1994}$ is the age and sex-specific instantaneous total mortality (sum of age and sex-specific initial fishing mortality and natural mortality). The initial plus-group was calculated following Methot Jr. and Wetzel (2013) as were the remaining population dynamics for years 1995 – 2022.

#### *4.3.2. Model conditioning*

Using this age-structured population model 1,000 simulated population trajectories for NPO SMA were generated from the period 1994 – 2022 using representative values for the biology and the fishery characteristics. The model defined 17 extraction fisheries based on the 17 fisheries from the simplified SS3 model (SS3 08 – 2022simple) described in Section 4.1 which had non-zero catch for the period 1994 – 2022 (Table 2). The catch in numbers from each fishery is the same that was aggregated together to form the input catch for the BSPM (see Section 4.2.1.1). The selectivity parameters for each fishery were taken from the same SS3 model used to convert catch in weight to catch in numbers (SS3 08 – 2022simple). The selectivity pattern of Fishery F6_JPN_SS_II from Table 2 was used to set the initial fishing mortality used to define the initial population numbers at age (Eq. 4.3.1.b). Initial (apical) fishing mortality was taken as a random multiplier, $\text{Uniform}(0.01,1.5)$, of natural mortality. Initial population depletion in 1994 was also random, $x_{1994} \sim \text{Uniform}(0.05,1)$. The population dynamics in each year were conditioned on the observed levels of catch by calculating, using the hybrid approach, the apical fishing mortality for each fishery needed to remove the observed catch. The apical fishing mortality was translated to fishing mortality at age using the fixed selectivity curves.

The model assumed the same NPO SMA biological assumptions (e.g., maximum age, maturity, growth, and reproductive cycle) and random variation in these biological assumptions as described in Section 4.2.3.1. Differences in assumptions and/or additional assumptions required for the age-structured model are described in the following paragraphs. To parametrize the low-fecundity stock recruit relationship, the total pups produced at equilibrium $\beta_0$ was calculated using NPO SMA biological assumptions following (Taylor et al., 2013) and assuming random variability in the number of surviving recruits at equilibrium $R_0 \sim \text{Uniform}(5e5,7.5e6)$. Random variability in the key input parameters to the low-fecundity stock recruit relationship were also assumed following (Taylor et al., 2013): $z_{frac} \sim \text{Uniform}(0,1)$, and $\beta_{LFSR} \sim \text{Uniform}(0.2,2.2)$. The process error associated with recruitment survival was also allowed to vary randomly $\epsilon \sim Lognormal\left(\log\left(\frac{-0.025^2}{2}\right), 0.025\right)$.

The natural mortality scenarios described in Section 4.2.3.1 applied for this simulation as well with the exception that higher juvenile natural mortality was always assumed to occur. Random variation in adult natural mortality for males and females was included by independently drawing from the sex specific distributions from Teo et al. (2024) corresponding to the appropriate scenario. Juvenile natural mortality (applied to ages 0 and 1) was drawn from a distribution of natural mortality inferred from Mucientes et al. (2023) given the estimated survival and proportion of mortality attributed to fishing. Since all three natural mortalities were drawn independently, a constraint was put in place such that the adult natural mortality for females was the lowest natural

mortality rate of the three and that the juvenile natural mortality rate was the highest of the three.

With regards to female spawning output, two changes were made to the assumptions from Section 4.2.3.1. Only two fecundity relationships were considered: constant as a function of female body length and linear as a function of female body length. The power relationship was not considered for this simulation as it tended to give similar aggregate results as the constant fecundity relationship. The fecundity scenario was randomly selected for each simulated population. Random variability in the sex-ratio at birth was reduced for the age-structured simulation, $\alpha \sim \text{Normal}(0.5, 0.01)$.

The same length-weight relationship as listed in the 2018 stock assessment report (ISC, 2018a) was specified for the age-structured simulation. However, this relationship never entered into the calculations since catches were input in terms of numbers.

A simulated index of relative abundance was developed for each simulated population, depending on the fishery selectivity used to index the stock. The simulated index was given by the vulnerable numbers (combined across age and sex) based on the fishery selectivity used. To match the indices used in the BSPM, the simulation used the selectivities from the SS3 model associated with the *US-DE-LL-all*, *TW-LA-LL-N* and *JP-OF-DW-SH-LL-M3* fisheries to develop indices. Lognormal observation error was added to each index to approximate the average level of observation error estimated from the BSPM for each index. Additionally, the availability of each simulated index matched the availability of the actual index (e.g., the simulated *US-DE-LL-all* index was also only available from 2000 – 2020).

#### *4.3.3. Bias calculation*

For each of the 1,000 simulated SMA population trajectories, 18 different BSPM estimation models were fit to the simulated index and the observed SMA catch in numbers (see Section 5.3). Recent depletion $D_{2019-2022}$ for the age-structured simulation model was calculated in terms of total numbers ($D_N$; total numbers relative to total numbers at the unfished equilibrium), and spawning output ($D_{SSO}$; number of pups produced relative to the total number of pups produced at the unfished equilibrium). Depletion for the BSPM is calculated in terms of total population numbers relative to the population numbers at carrying capacity. In either case depletion was calculated both as terminal year depletion and recent depletion (average depletion over the years 2019-2022).

Using the depletion values from the age-structured simulation models as the 'truth', bias in the estimate from the BSPMs relative to the true simulated value was calculated in one of two ways. Bias was calculated conventionally $B_C$ as:

$$B_C = D_{BSPM}/D_{AS} \qquad \text{Eq. 4.3.3.a}$$

where $D_{BSPM}$ is the median estimate of depletion from the posterior distribution of depletion from

the BSPM and $D_{AS}$ is the 'true' simulated depletion from the age-structured simulation model. Values greater than 1 indicate that the BSPM over-estimates depletion relative to the simulated truth, and values less than 1 indicate that the BSPM under-estimates depletion relative to the simulated truth. An alternative calculation defined bias $B_{ECDF}$ as where the $D_{AS}$ was located (e.g., the percentile) within the empirical cumulative distribution function (ECDF) created from the posterior distribution of depletion from the BSPM. This produces values of $B_{ECDF}$ bounded between 0 and 1. A $B_{ECDF}$ value of 0 indicates that $D_{AS}$ falls outside and below the posterior distribution of $D_{BSPM}$, while a $B_{ECDF}$ value of 1 indicates that $D_{AS}$ falls outside and above the posterior distribution of $D_{BSPM}$. An unbiased model would have a $B_{ECDF}$ of 0.5.

### 4.4. Uncertainty characterization

Uncertainty in BSPM outputs were quantified using credible intervals based on model posterior distributions. Additionally, a model ensemble was constructed from multiple BSPM runs to integrate across important sources of uncertainty. Unfortunately, it was not possible to develop all model weights *a priori* as it was not decided to include some alternative scenarios until later on in the modeling process. In most cases, alternative scenarios were given equal weight. However, when model weights were not equal between alternative scenarios, the SHARKWG decided the weighting based on the plausibility of the scenario relative to the alternatives.

## 5. MODEL RUNS

### 5.1. SS3

Though the focus of this assessment report is on the BSPM results, a few key SS3 models are described here as they set the foundation for the BSPM approach. Each model builds on a previous model in a series of steps. Results from these models are explored in more detail in Section 6.1.

- SS3 00 – 2018base: The 2018 benchmark stock assessment model (ISC, 2018a)
- SS3 01 – newSS3: Transition to SS3 version 3.30.22.1
- SS3 02 – correctLW: Apply the correct length-weight relationship.
- SS3 03 – early&late: Remove all CPUE indices except for the Japanese early (1975-1993) and the Japanese research and training vessel index (1994-2016). This model was developed to explore the impact of only using a single index for the 1994-2016 period. The Japanese research and training vessel index was selected as an update of this index was available for the current assessment.
- SS3 04 – lateOnly: Only fit to the Japanese research and training vessel index (1994-2016). This model was developed to see the impact of removing the early period (1975-1993) index from the model.
- SS3 05 – earlyOnly: Only fit to the Japanese early index (1975-1993). This model

was developed to see the impact of removing all late (1994-2016) period indices from the model.

- SS3 06 – 2022data: Update data files to 2022. This includes removing the Japanese early (1975-1993), fitting to three indices in the recent period from 1994-2022 (*S1 US-DE-LL-all*, *S3 Juvenile-Survey-LL*, and *S5 JP-OF-DW-SH-LL-M3*), revising the historical 1975-1993 driftnet catch, and developing new fishery definitions to account for new catch and size composition information. This model made a lot of changes and was never intended to be a single stepwise step. It was initially done in aggregate to evaluate the performance of a model that incorporated the initial modelling approach for the SHARKWG: namely updating catch values and fitting to key 'representative' indices.
- SS3 07 – 2022dataASPM: Fix the estimated selectivities and turn off the likelihood components for the size composition data to turn the model into an age-structured production model (ASPM). The assumption of a production function is central to the stock assessments of most species. Simplifying the integrated model to an ASPM was done to try and investigate a model configuration that could define a production function capable of reconciling the revised catch estimates and recent (1994-2022) period indices.
- SS3 08 – 2022simple: The fisheries definitions of the ASPM were simplified such that catch from fisheries that shared selectivity were aggregated together. This was a neutral change as aggregating the catch from fisheries that shared selectivity did not fundamentally change the fisheries characteristics or population dynamics. However, it was done to reduce the computational overhead (e.g., reduce the dimensionality of the model) in an attempt to more efficiently find a suitable model configuration.

A number of additional SS3 runs were also developed (e.g., start year, uncertainty in catch, initial conditions, method used to calculate fishing mortality). However, given that they did not successfully converge their configurations and results are not described in further detail.

## 5.2. BSPM

### *5.2.1. Model ensemble*

A model ensemble was developed to provide stock status and conservation information for NPO SMA using BSPMs. The model ensemble was constructed as the full-factorial combination of three key axes: CPUE index, treatment of the catch, and choice of prior for key parameters ($x_0, R_{Max}$, and $n$).

Despite all showing some level of increase, choice of CPUE index was considered to be a

major uncertainty as the implied rates of increase were different for each of the indices. Additionally, each candidate index had issues with representativeness. Rather than select a single index to base the assessment on (which would under-represent uncertainty) or fit to the indices simultaneously (which would likely result in poor fits to some or all the indices), the SHARKWG elected to use an ensemble modelling approach and fit to each index in turn. Four CPUE scenarios were included in the ensemble: two US deep-set indices (Section 3.4.3 *S1 US-DE-LL-all* & *S2 US-DE-LL-core*), the Chinese-Taipei longline index operating north of 25°N (Section 3.4.2 *S4 TW-LA-LL-N*) and a Japanese shallow-set index (Section 3.4.1 *S5 JP-OF-DW-SH-LL-M3*). Given that the two US indices represent the same scenario, models fitting to these indices were given half the weight of models fitting to other indices in order to not over represent the US CPUE index in the ensemble.

From the beginning of the assessment process catch was known to also be a major source of uncertainty. Rather than model catch in the historic period, the SHARKWG elected to begin the model in 1994 and estimate the initial depletion $x_0$. However, catch in the recent period, post-1994, is uncertain given that fleet-specific catches are often model reconstructions in their own right due to incomplete levels of logbook reporting for sharks and the lack of comprehensive observer coverage for many fisheries. It was important for the SHARKWG to make sure that this uncertainty in recent catches was reflected in the model ensemble. Three alternative model configurations were developed in order to reflect the uncertainty in catch (Section 4.2.2): fixed catch (Section 4.2.2.1), estimated catch using longline effort (Section 4.2.2.2), and estimated catch using direct estimation of fishing mortality (Section 4.2.2.3). The fixed catch BSPMs showed model convergence issues (presence of divergent transitions[4]) and were not included in the ensemble. Given the uncertainty in SMA logbook reporting, the SHARKWG considered that longline effort could be more reliably reported. Accordingly, the longline effort model configuration was developed to estimate the catch needed to fit the CPUE index given the pattern in longline effort and a constant catchability assumption. An additional model configuration was developed where catch was fit in a likelihood context via the direct estimation of fishing mortality needed to fit the catch. This approach had the benefit of incorporating uncertainty in catch through the likelihood and choice of $\sigma_C$, and by relaxing the restriction of fitting to catch exactly. It also resolved the model convergence issues observed with the fixed catch models. However, fitting to catch in this way produces catch estimates that are, on average, equal to the observed catch, which may not address the potential uncertainty in the magnitude of catches due to under-reporting.

[4] It has been suggested that treating catch as fixed may place an implicit constraint on the population dynamics, particularly at low stock sizes, that may be incompatible with the assumed parameter prior distributions and thus lead to the observed model convergence issues (P. Neubauer, *personal communication*, April 23, 2024).

Additionally, the direct estimation of fishing mortality is sensitive to the prior for the random effects variance $\sigma_F$. Three different priors for $\sigma_F$ were considered in the model ensemble to account for uncertainty in an appropriate prior for $\sigma_F$. Furthermore, the magnitude of the estimated fishing mortality varied depending on the choice of $\sigma_F$ which served the dual purpose of also integrating over potential uncertainty in fishing impacts due to under-reporting. Lastly, the 4 catch treatments were not assigned equal weight in the model ensemble. Preliminary results with the BSPM that estimated catch using longline effort indicated that this resulted in estimated fishery removals that were much larger than observed, particularly in recent years. As a result, the SHARKWG considered this scenario to represent a theoretical upper limit to fishing mortality and gave it a weight of 5% (e.g., commensurate with the probability of a value drawn from the tail of a distribution) relative to the scenario that catch was estimated through the direct estimation of fishing mortality which received 95% weight. Given that there were three models for the direct estimation of fishing mortality scenario, these each received a weight of ~31.7% so that the total weights for all 4 catch treatments summed to 100%.

Lastly, uncertainty in the level of prior used for key parameters of the BSPM, $x_0, R_{Max}$, and $n$, was included as a component of the ensemble given that model outcomes differed slightly when alternative priors were evaluated. Two prior types were considered, those developed under the *baseline* filtering or the *extreme* filtering described in Section 4.2.3.1. Each scenario was given equal weight in the model ensemble.

All told, 32 models (combination of 4 CPUE scenarios, 4 catch treatments, and 2 prior types) were included in the final ensemble Table 9. This final version of the model ensemble was influenced by earlier versions of the ensemble which suggested that the fixed catch scenario had convergence issues, and that the choice of prior for process error variability $\sigma_P$ did not meaningfully impact results. Model code and input data for replicating the model ensemble can be found online at a GitHub repository. Please contact the current SHARKWG chair for access information.

### *5.2.2. Sensitivity analyses*

#### 5.2.2.1. Indices of relative abundance

Six alternative CPUE indices were evaluated as sensitivity analyses: : the US juvenile shark survey (Section 3.4.3 *S3 Juvenile-Survey-LL*), an alternative Japanese shallow-set index (Section 3.4.1 *S6 JP-OF-DW-SH-LL-M5*), the Japanese deep-set research and training vessel index (Section 3.4.1 *S7 JP-OF-DW-DE-LL-M7*), a combined Mexican longline index (Section 3.4.4 *S8 MX-Com-LL*), an index for the Ensenada based Mexican longline (Section 3.4.4 *S9 MX-Com-LL-N*), and an index for the Mazatlán based Mexican longline (Section 3.4.4 *S10 MX-Com-LL-S*). These were evaluated in a one-off sensitivity to a reference BSPM that treated the catch as fixed, used the $K$ prior specified in Section 4.2.3.4, assumed the $\sigma_P$ specified in Section 4.2.3.5, the

$\sigma_{O_{Add}}$ prior specified in Section 4.2.3.6 and the *baseline* level of priors for $x_0, R_{Max},$ and $n$.

#### 5.2.2.2. Fixed catch scenarios

For sensitivity analyses related to the scale of the fixed catch, 9 scenarios were developed (including the baseline fixed catch scenario described in the Section 4.2.1.1). A full-factorial design was used to develop the 9 scenarios between 3 average catch levels and 3 historical under-reporting scenarios and under-estimating (hereafter under-reporting) scenarios (Table 8). For the 3 average catch scenarios the overall magnitude of the catch for 1994-2022 was increased by 0%, 50% or 100%. For the 3 historical under-reporting scenarios, 1994 catches in the first year of the BSPM were increased by 0%, 50% or 100% relative to catches observed in 2022. A linear relationship was used to increase catches from 1995-2021 relative to baseline levels (e.g., 1994 = +50%, 1995 = +48.2%, 1996 = +46.4%, …, 2021 = +1.8%, 2022 = +0%). These were evaluated in a one-off sensitivity to a reference BSPM that fit to the Japanese shallow-set index (Section 3.4.1 *JP-OF-DW-SH-LL-M3*), used a lognormal prior for $K \sim Lognormal(\log(16.524), 0.6)$, assumed the $\sigma_P$ specified in Section 4.2.3.5, the $\sigma_{O_{Add}}$ prior specified in Section 4.2.3.6 and the *baseline* level of priors for $x_0, R_{Max},$ and $n$.

#### 5.2.2.3. Catch error $\sigma_C$

In order to understand how the choice for the level of error in the catch likelihood $\sigma_C$ impacted estimates of catch. Sensitivity to the level selected for $\sigma_C$ (either 0.01, 0.025, 0.05, or 0.1) was evaluated in a one-off sensitivity to a reference BSPM that fit to the Japanese shallow-set index (Section 3.4.1 *S5 JP-OF-DW-SH-LL-M3*), used a lognormal prior for $K \sim Lognormal(\log(16.524), 0.6)$, assumed the $\sigma_P$ specified in Section 4.2.3.5, the $\sigma_{O_{Add}}$ prior specified in Section 4.2.3.6, a naïve half-normal prior for $\sigma_F \sim \text{Normal}^+(0,1)$, and the *extreme* level of priors for $x_0, R_{Max},$ and $n$.

#### 5.2.2.4. Process error prior

Sensitivity to the choice of process error variability $\sigma_P$ is demonstrated using a one-off sensitivity. A BSPM with a naïve half-normal prior for $\sigma_P \sim \text{Normal}^+(0,1)$, is compared to a reference BSPM that treated catch as fixed, fit to the Japanese shallow-set index (Section 3.4.1 *S5 JP-OF-DW-SH-LL-M3*), used a lognormal prior for $K \sim Lognormal(\log(16.524), 0.6)$, the $\sigma_{O_{Add}}$ prior specified in Section 4.2.3.6, and the *extreme* level of priors for $x_0, R_{Max},$ and $n$.

### 5.3. Age-structured simulation

The age-structured simulation model was used to simulate 1,000 population trajectories representative of the biology and fisheries characteristics of NPO SMA. For each simulated population trajectory, a subset of the model ensemble (18 BSPM estimation models) was fit to the simulated data in order to calculate the level of bias in depletion. Configuration of the estimation model depended on 3 different factors: the simulated index used (US, JP or TW), the type of prior

for $x_0, R_{Max}$ and $n$ (baseline or extreme), and the treatment of catch (estimated using longline effort, estimated with F & $\sigma_F = 0.0125$, or estimated with F & $\sigma_F = 0.05$). The BSPM estimation models were evaluated with the same convergence criteria as described in Section 4.2.6.1. Presentation of the results focus on simulated population trajectories that indicated an increase in the simulated index of 50% (similar to what is observed in the actual CPUE indices), and with estimation models that met convergence criteria.

# 6. MODEL RESULTS

## 6.1. SS3

Updating the 2018 base case SS3 model to the new executable (SS3 01 – newSS3) resulted in negligible change to key model outputs (Figure 10). Despite making a large correction to the length-weight relationship (SS3 02 – correctLW; Figure 11), and the scale of the population; fishing mortality and management quantities relative to MSY are essentially unchanged (Figure 10). Fishing mortality stays the same because the catch in numbers is scaled down at the same rate as the population, the catch in numbers is reduced now that males weigh more at length and it takes fewer numbers of fish to equal the same tonnage of catch (Figure 12). Reducing the number of late period (1994-2016) indices that the model fits to and only fitting to the Japanese research and training vessel index (SS3 03 – early&late) results in negligible change to the model (Figure 10). This indicates that model dynamics are not influenced by the late period indices that were removed from the model. Fitting only to the late period (1994-2016) Japanese research and training vessel index results in a model (SS3 04 – lateOnly) that is unable to converge, and with estimates of virgin recruitment going to the upper bound (~3.2 billion individuals). However, removing all late period indices and including the Japanese early index as the only index in the model (SS3 05 – earlyOnly) results in key model outputs that have very similar temporal dynamics albeit with a slightly lower scale (Figure 10). These results, in conjunction with the failures from the SS3 04 – lateOnly model, indicate that the overall population dynamics of the 2018 assessment are largely driven by the interaction between the 1975-1993 catch and index. The contrast between 1975-1993 catch and index define the production function for the model since the high catches coincide with a decrease in the index, and the decreases in catch coincide with an increase in the early period index (see ISC, 2018a Figure 11 reproduced here as Figure 13). The 1994-2016 catch for these models is relatively flat by comparison and has little information in the composition data (e.g., dome shaped selectivity with estimated descending limb) to inform fishing mortality so it has minimal impacts on model outputs. This model result is problematic since the 1975-1993 catch and index are two components that the SHARKWG identified as being highly uncertain, and it sets the stage for the difficulty in developing a SS3 model that excludes this index.

Given these results, updating the data through 2022 and removing the early index resulted

in models with predictably poor results (e.g., convergence and population scale estimates). As such presentations of models with updated data will focus on how the updated catch compares to the catch used in the previous assessment, fits to the size composition data, and the associated fishery selectivity curves. Updating the catch through 2022 also included revising the 1975-1993 catches, looking at the catches from the terminal SS3 model (SS3 08 – 2022simple) it is apparent (Figure 12) that pre-1994 catches are dramatically lower than what was used in the last assessment. Given that CPUE trends are generally increasing post-1994 this implies, under a stationary production model hypothesis, that pre-1994 catch must have been large enough to deplete the population and trigger a recovery under the current catch levels. However, this is not the case. This result was critical in illustrating to the SHARKWG that inconsistencies existed between the available data inputs and the biological assumptions, and prompted the strategic move to the BSPM approach.

Model fits to the size composition data are shown for model SS3 06 – 2022data. Nominal sample sizes were used resulting in a high weight on the composition data, and fits to the sex-specific size composition data were generally pretty good (Figure 14) given the estimated selectivity curves (Figure 15). These selectivity curves were fixed when developing the SS3 07 – 2022dataASPM, and then used to define the simplified fisheries structure (SS3 08 – 2022simple) based on fisheries that shared selectivity curves. These fishery selectivity curves from SS3 08 – 2022simple were used to condition the age-structured simulation model. Note that the female length at 50% maturity $L_{\text{Maturity}}@50\%$, is well in the tail of the selectivity curve for all fisheries.

## 6.2. BSPM

### *6.2.1. Model ensemble*

Diagnostics across the model ensemble were good (Table 9) with only 4 of 32 models failing to meet the convergence criteria. Additionally, no model exceeded the pre-specified maximum tree depth or showed low Bayesian fraction of missing information (Stan model diagnostics). These models were excluded from the calculation of stock status and management reference points. However, including these models would not have meaningfully changed the conclusions drawn from the aggregate model ensemble. Fits to the indices were reasonable in terms of RMSE (Table 9). Models fit to the *S4 TW-LA-LL-N* index showed worse fits relative to the other models, though these fits are in line with the estimated observation error. Posterior predictive checks indicated that the estimation models used were able to replicate the observed indices (Figure 16). Estimated catch for models that fit to catch using a likelihood also showed consistency across models despite different assumptions for $\sigma_F$, and observed catches were well within the predicted interval (Figure 17). However, there did appear to be a slight over estimation of catch towards the later part of the time series. Overall retrospective bias seemed low (Table 9; Figure 18 shows the retrospective analysis from a representative subset of models), and estimates of the relative exploitation rate ($^{U}/_{U_{MSY}}$) and

relative depletion ($^{D}/_{D_{MSY}}$) were inside the credible intervals of the full model run 100% of the time (Table 9). Hindcast cross-validation performance was poor, with 8 of 28 converged models (Table 9; Figure 19 shows hindcast cross-validation from a representative subset of models) showing a better ability to predict the one-step ahead observed CPUE than a naïve predictor (e.g., MASE < 1). Only models fitting to the *S4 TW-LA-LL-N* index outperformed the naïve predictor. This is not completely unsurprising given that the models estimate lower process error than observation error and are less responsive to deviations in the observed CPUE. A Shiny app for more completely interrogating model results can be found online. Please contact the current SHARKWG chair for access information.

Investigation of posterior parameter estimates for leading parameters ($R_{Max}$, $x_0$, $n$, $K$, $\sigma_P$, $\sigma_{O_{Add}}$, $q$, and $\sigma_F$), relative to their assumed prior distributions showed several patterns (Table 10; Figure 20). Both the shape $n$ and the process error variability $\sigma_P$ show minimal posterior update indicating either that there is no information in the data for which to estimate this parameter or that the data is already consistent with the prior. With respect to shape $n$ it is likely to be the former given that it usually difficult to estimate (Fletcher, 1978). The process error variability $\sigma_P$ prior may be consistent with the data given that sensitivity analyses (example shown in Section 6.2.2.4) indicated that using a significantly less informative prior resulted in similar posterior estimates. There appeared to be a trade-off between estimated exploitation rate and estimated population scale (e.g., carrying capacity $K$). Models with higher estimated exploitation rate (using longline effort to estimate removals, models 1-8 or having a larger prior on $\sigma_F$, models 9-16) tended to estimate lower population scale. Models estimating the lowest exploitation rate (smallest prior on $\sigma_F$, models 25-32) showed the largest estimates of population scale. Estimates of $R_{Max}$ were fairly consistent and estimated to be relatively close to the prior. This is an expected result given that the priors considered were developed to generate increasing populations under the observed catch levels. Estimates of initial depletion $x_0$ showed a large posterior update when the broader baseline prior was used which indicates that the data (e.g., relative abundance indices) support a more depleted initial condition. Models fitting to the *S4 TW-LA-LL-N* showed large estimates of additional observation error $\sigma_{O_{Add}}$ needed to reconcile the rapid increase seen in the middle portion of this index. Estimates of $\sigma_F$ tended to follow the prior indicating limited information in the data for which to estimate this parameter. Interpreting this result with the estimates for $K$ shows that there is little information in the model to estimate overall population scale. Longline catchability $q$ indicated that there was data in the model to support smaller estimates, translating to lower levels of exploitation rate than indicated by the prior.

Distributions of management reference points ($MSY$, $U_{MSY}$, $D_{MSY}$, $U_{2018-2021}$, $U_{2018-2021}/U_{MSY}$, $D_{2019-2022}$, and $D_{2019-2022}/D_{MSY}$: Table 11) across the weighted ensemble

were unchanged when models that failed to converge were excluded (Figure 21). Models that fit to the *S5 JP-OF-DW-SH-LL-M3* index showed more optimistic outcomes, while models fitting to either of the two US indices showed the most pessimistic outcomes (Figure 22). Models that assumed the 'extreme' prior level showed more pessimistic outcomes than models that assumed the 'baseline' prior level (Figure 23). This is likely a product of the initial depletion $x_0$ prior being more depleted under the 'extreme' prior level. Estimating removals using longline effort resulted in the most pessimistic outcomes, as did models fitting to catch with the largest prior for $\sigma_F$ (Figure 24). Imposing a more restrictive prior on $\sigma_F$ tended to result in more optimistic estimates of stock status.

### *6.2.2. Sensitivity analyses*

#### 6.2.2.1. Indices of relative abundance

A number of indices were prepared and considered by the SHARKWG; however, a subset were not considered by the SHARKWG for the BSPM ensemble (e.g., lack of representativeness of overall stock dynamics). For information purposes only, BSPM fits to these indices are shown in Figure 25 and BSPM estimated time-series quantities are shown in Figure 26.

#### 6.2.2.2. Fixed catch scenarios

Catch uncertainty was a key uncertainty identified by the SHARKWG and a number of alternative fixed catch scenarios were investigated (see Table 8). While the alternative scenarios showed some impact in terms of exploitation rates (larger catches resulted in greater exploitation), depletion estimates were largely constant across models (Figure 27). This indicates that the model is likely trading exploitation rate for population scale and is indicative of the lack of information in the data to estimate this quantity.

#### 6.2.2.3. Catch error

Catch error models, where catch was fit to with error in a likelihood context and fishing mortality was directly estimated as a free parameter, were developed to alleviate convergence issues seen with the fixed catch models. Across the range of $\sigma_C$ values trialed, results were very consistent between all catch error formulations (Figure 28), and the level of $\sigma_C$ did not appear to impact median estimates or the estimated credible intervals for management quantities. Additionally, the catch was fit exactly and without bias. This is a slightly different result than what was seen in the model ensemble where catch estimates showed a slight bias towards the end of the estimation period. Future analyses should investigate this further as there may be an interaction between the assumed value for $\sigma_C$, particularly at larger values, and the assumption made for the $\sigma_F$ prior.

#### 6.2.2.4. Process error prior

An informative prior for $\sigma_P$ based on Winker et al. (2018) was used in the model ensemble.

Sensitivity to this assumption was investigated by also trialing an uninformative prior $\sigma_P \sim \text{Normal}^{+}(0,1)$. Posterior modal and median estimates of $\sigma_P$ were consistent between the two priors (Figure 29) indicating that the model has information from which to estimate this parameter, and that it appears consistent with the Winker et al. (2018) prior. However, variability in the posterior distribution was greater with the uninformative Half-Normal prior. This additional variability at the parameter level did not translate to additional variability in management quantities (Figure 30).

#### *6.2.3. Projections*

##### 6.2.3.1. Retrospective

Retrospective projections driven by historical longline and driftnet effort indicated that the stock appeared to be substantially impacted by driftnet activity. Based on these simulations, a large amount of fishing mortality in the 1980s was required to deplete the stock in order to match the rebuilding trends implied by the recent (1994 – 2022) period relative abundance indices (Figure 31). However, prior to the 1980s, longline fisheries were also simulated to have a non-trivial impact on the stock.

##### 6.2.3.2. Future

Under the 4 scenarios considered by the SHARKWG ($U_{2018-2021}$, $U_{MSY}$, $U_{2018-2021} + 20\%$, and $U_{2018-2021} - 20\%$), scenarios based on multipliers of recent exploitation ($U_{2018-2021}$) are not predicted to cause the stock to deviate from the existing rebuilding trajectory (Figure 32). Increasing future exploitation to MSY levels is predicted to drive the stock down towards the $D_{MSY}$. However, this would represent a substantial increase in fishery removals relative to current best estimates.

### 6.3. Age-structured simulation

Conditioning the age-structured simulation on NPO SMA biological assumptions, observed levels of catch, and the fishery specific selectivity curves produced 140 scenarios that were able to reasonably replicate the observed CPUE trends seen in the *S1 US-DE-LL-all*, *S4 TW-LA-LL-N* and *S5 JP-OF-DW-SH-LL-M3* indices (Figure 33).

Of the 2520 estimation models fit to the 140 simulated populations of NPO SMA, 935 estimation models met the convergence criteria. These models indicated that the 'true' recent depletion $D_{2019-2022}$ defined in total numbers ($D_N$) fell within the credible interval of the converged estimation models 92.8% of the time. Averaging across the converged estimation models using a similar weighting scheme as described in Section 5.2.1 resulted in a median $B_{ECDF} = 0.65$ and a median $B_C = 0.85$. Both of these bias definitions indicate that the BSPM tended to underestimated $D_{2019-2022}$ relative to the simulated 'truth' when depletion was defined using total numbers.

Recent depletion defined in terms of spawning stock output (SSO) $D_{SSO}$ is typically more informative for management given that it tracks the reproductive component of the population. However, this quantity is expected to be challenging for a BSPM to estimate given that the index selectivities do not select for this component of the population, and there is a long lag to maturity. The 'true' recent depletion $D_{2019-2022}$ defined in total numbers ($D_{SSO}$) fell within the credible interval of the converged estimation models 97.2% of the time. Averaging across the converged estimation models using a similar weighting scheme as described in Section 5.2.1 resulted in a median $B_{ECDF} = 0.47$ and a median $B_C = 1.073$. These metrics indicate a slight over-estimate (7.3%) of $D_{2019-2022}$ relative to the simulated 'truth' when depletion was defined using spawning output, and suggest that despite the *a priori* concerns, the BSPM is able to provide a reasonable estimate of spawning output $D_{2019-2022}$.

# 7. STOCK STATUS AND CONSERVATION INFORMATION

## 7.1. Status of the stock

The current assessment provides the best scientific information available on NPO SMA stock status. Results from this assessment should be considered with respect to the management objectives of the Western and Central Pacific Fisheries Commission (WCPFC) and the Inter-American Tropical Tuna Commission (IATTC), the organizations responsible for management of pelagic sharks caught in international fisheries for tuna and tuna-like species in the Pacific Ocean. Target and limit reference points have not been established for pelagic sharks in the Pacific Ocean. In this assessment, stock status is reported in relation to maximum sustainable yield (MSY).

A BSPM ensemble was used for this assessment, so the reproductive capacity of this population was characterized using total depletion rather than spawning abundance as in the previous assessment. Total depletion (D) is the total number of SMA divided by the unfished total number (i.e., carrying capacity). Recent D ($D_{2019-2022}$) was defined as the average depletion over the period 2019-2022. Exploitation rate (U) was used to describe the impact of fishing on this stock. The exploitation rate is the proportion of the SMA population that is removed by fishing. Recent U ($U_{2018-2021}$) is defined as the average U over the period 2018-2021.

During the 1994-2022 period, the median depletion (D) of the model ensemble in the initial year was estimated to be 0.19 (95% CI: credible intervals = 0.08-0.44), and steadily improved over time and $D_{2019-2022}$ was 0.60 (95% CI = 0.23-1.00) (Table 12 and Figure 34). Although there are large uncertainties in the estimated population scale, the best available data for the stock assessment are the four standardized abundance indices from the longline fisheries of Japan, Taiwan, and the US, and all four indices indicate a substantial (>100%) increase in the population during the assessment period. The population was likely heavily impacted prior to the start of the modeled period, after which it has been steadily recovering. It is hypothesized that the fishing

impact prior to the modeled period was likely due to the high-seas drift gillnet fisheries operating from the late 1970s until it was banned in 1993, though specific impacts from this fishery on SMA are uncertain. Consistent with the estimated trends in depletion, the exploitation rates were estimated to be gradually decreasing from 0.023 (95% CI = 0.004-0.09) in 1994 to the recent estimated exploitation rate ($U_{2018-2021}$) of 0.018 (95% CI = 0.004-0.07). The decreasing trends in estimated exploitation rates were likely due to the increase in estimated population size being greater than increases in the observed catch.

The median of recent D ($D_{2019-2022}$) relative to the estimated D at MSY ($D_{MSY}$ = 0.51, 95% CI = 0.40-0.70) was estimated to be 1.17 (95% CI = 0.46-1.92) (Table 12 and Figure 35). The recent median exploitation rate ($U_{2018-2021}$) relative to the estimated exploitation rate at MSY ($U_{MSY}$ = 0.05, 95% CI =0.03-0.09) was estimated to be 0.34 (95% CI = 0.07-1.20) (Table 12 and Figure 35). Surplus production models are a simplification of age-structured population dynamics and can produce biased results if this simplification masks important components of the age-structured dynamics (e.g., index selectivities are dome shaped or there is a long-time lag to maturity). Simulations suggest that under circumstances representative of the observed SMA fishery and population characteristics (e.g., dome-shaped index selectivity, long lag to maturity, and increasing indices), the BSPM ensemble may produce biased results. Representative simulations suggested that the $D_{2019-2022}$ estimate has a positive bias of approximately 7.3 % (median). The historical trajectories of stock status from the model ensemble revealed that North Pacific SMA had experienced a high level of depletion in this historical period and was likely overfished in the 1990s and 2000s, relative to MSY reference points (Figure 35).

The following information on the status of the North Pacific SMA are provided:

**1. No biomass-based or fishing mortality-based limit or target reference points have been established for NPO SMA by the IATTC or WCPFC;**

**2. Recent median D ($D_{2019-2022}$) is estimated from the model ensemble to be 0.60 (95% CI = 0.23-1.00). The recent median $D_{2019-2022}$ is 1.17 times $D_{MSY}$ (95% CI = 0.46-1.92) and the stock is likely (66% probability) not in an overfished condition relative to MSY-based reference points.**

**3. Recent U ($U_{2018-2021}$) is estimated from the model ensemble to be 0.018 (95% CI = 0.004-0.07). $U_{2018-2021}$ is 0.34 times (95% CI = 0.07-1.20) $U_{MSY}$ and overfishing of the stock is likely not occurring (95% probability) relative to MSY-based reference points.**

**4. The model ensemble results show that there is a 65% joint probability that the North Pacific SMA stock is not in an overfished condition and that overfishing is not occurring relative to MSY based reference points.**

**5. Several uncertainties may limit the interpretation of the assessment results**

**including uncertainty in catch (historical and modeled period) and the biology and reproductive dynamics of the stock, and the lack of CPUE indices that fully index the stock.**

### 7.2. Conservation information

Stock projections of depletion and catch of North Pacific SMA from 2023 to 2032 were performed assuming four different harvest policies: $U_{2018-2021}$, $U_{MSY}$, $U_{2018-2021} + 20\%$, and $U_{2018-2021} - 20\%$ and evaluated relative to MSY-based reference points (Figure 32). Based on these findings, the following conservation information is provided:

**1. Future projections in three of the four harvest scenarios ($U_{2018-2021}$, $U_{2018-2021} + 20\%$, and $U_{2018-2021} - 20\%$) showed that median D in the North Pacific Ocean will likely (>50% probability) increase; only the $U_{MSY}$ harvest scenario led to a decrease in median D.**

**2. Median estimated D of SMA in the North Pacific Ocean will likely (>50% probability) remain above $D_{MSY}$ in the next ten years for all scenarios except $U_{MSY}$; harvesting at $U_{MSY}$ decreases D towards $D_{MSY}$.**

**3. Model projections using a surplus-production model may over simplify the age-structured population dynamics and as a result could be overly optimistic.**

## 8. DISCUSSION

### 8.1. General remarks

The current stock assessment of NPO SMA estimates that the stock is unlikely to be overfished and that overfishing is unlikely to be occurring, based on MSY based reference points derived from the current ensemble modeling approach. Stock status appears to be trending in an increasingly positive direction based on estimates from the last five years of the model period. However, current MSY based reference points are based on a BSPM which aggregate the population dynamics into a single population component which can impact inference on MSY (and associated levels of fishing pressure and stock status at MSY) if there are important age-based processes that occur since MSY is influenced by fisheries selectivity curves (Scott and Sampson, 2011). While previous simulation study (Winker et al., 2020) indicated that a correctly specified surplus-production model could provide reasonably accurate estimates of MSY based reference points relative to those defined by age-structured dynamics, that study assumed logistic selectivity. Available observations from fisheries interacting with SMA in the NPO indicate that the majority of fishery related removals occur on juveniles, which implies a strong dome shaped selectivity curve. Relative to a logistic selectivity shape, a strongly dome shaped selectivity curve could be expected to shift the fishing mortality that produces MSY to lower values (Scott and Sampson, 2011). Additionally, as seen using the current age-structured simulation, given that the indices track

the juvenile component of the population there is a lag before increases in juvenile abundance translate to the reproductive component of the population. As a result, the BSPM tends to slightly overestimate the rate of increase and recent depletion levels of the reproductive component of the population.

Relative to the 2018 assessment (ISC, 2018a), the current assessment produces similar top level stock status (unlikely to be overfished and overfishing is unlikely to be occurring) despite a much different model structure and treatment of the data. However, the uncertainty associated with the current assessment outcomes is larger and the risk of being overfished is greater in the current assessment. This greater uncertainty and risk level is not unexpected given that a model ensemble in now used to provide management advice. Additionally, while the previous assessment presented model estimation uncertainty using the Delta method, a number of population dynamics parameters were held fixed (e.g., growth, natural mortality, steepness, etc.) which could artificially increase the precision of model estimates. Even though the BSPM simplifies the population dynamics, all key parameters are estimated with the help of priors. Directly estimating $R_{Max}$ implicitly integrates over the uncertainty in those population dynamics parameters that were previously held fixed in the 2018 assessment and can provide a more appropriate representation of the uncertainty.

Stochastic projections based on the BSPM ensemble indicate that the stock is projected to keep increasing under most scenarios other than the $U_{MSY}$ scenario which would represent a dramatic increase in fishery removals from current observed levels. However, as previously mentioned, these projections are based on simplified population dynamics which do not explicitly account for lags between recruitment and maturity and may be overly optimistic. Furthermore, observed catches were highest in recent years and their impacts on the population may not be fully observed.

The next stock assessment for NPO SMA is tentatively scheduled for 2029, with an indicator analysis planned in the intervening year (i.e., 2027). Expectations in the availability of data for assessing the future status of NPO SMA are not promising. Conservation measures put in place at the international and national levels (e.g., non-retention measures and gear restrictions) ostensibly are put in place for the conservation of the species and to reduce the number of interactions between fishing operations and SMA. However, reductions in interactions and/or observations of interactions (e.g., increasing use of electronic monitoring may impact detectability of non-retained interactions; and/or sharks are released prior to species identification) can degrade the quality of fisheries dependent data. Catch estimates could become more uncertain and there could be reduced ability to collect size frequency or biological samples to improve biological understanding. Additionally, the CITES Appendix II listing has made collecting and sharing of biological samples between scientific institutes difficult, particularly at the international level, which can impede legitimate research activity that could improve understanding of the stock and potentially lead to

better management outcomes. This is not to say that conservation measures should not be put in place when warranted. However, they can have a real impact on the quality and availability of assessment input data and future assessments will have to adjust accordingly (either with the development of alternative inputs or pivoting to alternative assessment approaches) to continue to be able to provide managers with stock status and conservation advice.

### 8.2. Improvements to the assessment

Despite stepping back to a more simplified modelling approach, this assessment is an improvement on the 2018 assessment in several aspects (ISC, 2018a). Beginning the assessment process with a formalized conceptual model allowed the SHARKWG to organize an understanding of the species, identify knowledge gaps/key uncertainties, and identify alternative hypotheses to explain the identified knowledge gaps. This process was instrumental in guiding decisions in the development of model inputs and for determining the most appropriate modelling approach and configuration. Building on the 2022 NPO BSH assessment (ISC, 2022), a model ensemble approach was used to propagate uncertainties identified in the conceptual model through to the provision of stock status and management advice. Lastly, applying a Bayesian approach allowed for a more complete use of information on NPO SMA to be incorporated into the assessment through the use of priors. Using a Bayesian approach with priors (along with a simplified model) allowed for the estimation of all population dynamics parameters and integrated over their uncertainty. Estimation of initial population conditions for a model beginning in 1994 was also facilitated by applying a Bayesian approach. Given the uncertainties in pre-1994 data, beginning the model in 1994 while also acknowledging that significant fisheries depletion occurred prior to 1994 is likely an improvement.

### 8.3. Challenges, limitations & key uncertainties

The current assessment was not without its challenges, and while it represents the best scientific information available there is reason for caution when interpreting model results. One of the chief limitations of the assessment is the lack of age-structure in the estimation. While there were benefits to simplifying the assessment approach, it implicitly assumes that there are no age-specific population dynamics. This is a strong assumption to make given the long lag to maturity/reproduction (~10-15 years for females depending on the growth curve; length at 50% maturity for females is ~233 cm PCL), and the observation that fisheries almost exclusively operate on immature individuals for females. Additionally, the indices in a BSPM are implicitly assumed to index the reproductive component of the population which we know is likely not the case given the fishery characteristics. Lastly, SMA are believed to be long-lived with observations of maximum age of at least 30 years and have a long lag to maturity as mentioned previously. With an assessment period from 1994-2022, this represents a relatively short window relative to

generation time. It wouldn't be until the 2010s before annual cohorts are fully informed by adults born after the start of the model period. As a result, assessment outcomes will be highly sensitive to assumptions relating to the fisheries impacts and age-structure of the population prior to the start of the model. In a BSPM these impacts are captured in the initial depletion and the intrinsic rate of increase parameters. Modeling the population using an age-structured model and including informative size composition for the initial model years can help inform the initial age structure. It is for these reasons that an age-structured simulation was developed to assess likely bias in the BSPM. However, even though the estimated bias in depletion appeared low (< ~10%) development of an age-structured assessment model is needed to provide a more accurate understanding of stock status relative to yield based reference points.

Estimates of absolute population scale are highly uncertain and sensitive to the choice of prior. While there may be some information to inform scale on the low end (it must be sufficiently large to support the observed catches) there is little information in the data to provide information on how large the population is. Both the indices and catch time series tend to increase over the model period, and while this is able to provide some information on initial depletion and the intrinsic rate of increase when constrained by biological priors, it does not provide information on scale. Accordingly, relative statements about the status of the stock are likely to be more accurate than statements that refer to the absolute scale of stock status. Even moving the estimation into an integrated age-structured framework and incorporating size composition data may not necessarily help, as the dome-shaped nature of the fisheries selectivity curves reduces the information content of these data.

Many assessment modelling approaches make the simplifying assumption that catch is known with a high degree of confidence, as it increases model complexity and becomes more difficult to make statements about stock status when catch is unknown. However, for incidentally encountered species including sharks this is a difficult assumption to make given uncertainty in discard levels and logbook reporting. Knowledge of catch is further compounded for NPO SMA by the lack of species-specific shark catch pre-1994 for key fisheries. Additionally, there appears to be an important component of recent catch coming from Mexican artisanal fisheries which make data-collection difficult given the lack of monitoring, difficulty with species identification and remoteness of some fishing operations (Santana-Morales et al., 2020). Reducing catch uncertainty going forward will be key to improving the accuracy and precision of stock assessment models, however this is not likely to be a trivial task.

One of the initial challenges in developing the SS3 integrated age-structured model was the inability to reconcile observed catches with the increasing trends seen in several fishery dependent indices. Multiple hypotheses (Section 4) were developed to explain the lack of a production function, each dealing with the credibility of underlying data. Given the uncertainties in catch and

lack of information in the size composition, it was determined that the increase seen in the fishery dependent indices was the most credible data available due to the replication of the increase across several fisheries. Assessment outcomes are largely conditioned on the assumption that these indices are representative. However, there are multiple factors which can undermine confidence in the representativeness of these indices:

- no fishery indexes the entire spatial distribution of the population in the NPO,
- as with any fishery dependent index it is likely that despite standardization there are unaccounted for changes in catchability (Ward 2008 suggests that catchability for SMA has likely decreased due to gear changes, better targeting of target species, and avoidance of sharks),
- and the lack of observations of large individuals (particularly mature females) does limit the utility of the indices.

The likely dome-shaped selectivity of the indices, implicitly assumes limited fishing impacts to the largest individuals and makes assessment outcomes dependent on the existence of a cryptic reproductive component of the stock. The inability to effectively index this component of the population makes future projection uncertain.

Lastly, key uncertainties remain with respect to stock structure in the NPO (is it a single well-mixed stock or do the distinct parturition sites engender more complex regional dynamics?) and understanding of basic biological processes (e.g., age, growth and reproduction). The current assessment assumed a single-well mixed stock given the constraints of the available information however this assumption could produce biased outcomes if multiple stocks exist, connectivity between them is limited, and fishing pressure is not homogenous. At a more basic level, uncertainty in age, growth and reproduction creates uncertainty in the production function or the population's ability to cope with fishing pressure, and impacts understanding of stock status relative to yield based reference points.

### 8.4. Future stock assessment modeling considerations

In order to address some of the challenges and limitations identified with the current assessment (Section 8.3), the following modelling considerations should be made. Future assessment efforts should build back up to an age-structured estimation model (either using SS3 or otherwise). This would allow concerns with the BSPM to be addressed by explicitly considering age-structured population processes and fisheries selectivity. As an example, the age-structured simulation code could be transformed from an operating model to an estimation model by allowing for the estimation of leading parameters and adding in the likelihood components for the indices and size composition data. Furthermore, given parameter uncertainties, such an age-structured model should be estimated in a Bayesian context as was done for the BSPM. Developing

informative priors following Monnahan (2024) can be useful for stabilizing model estimation (given the number of parameters needed in an age-structured model) and for properly accounting for uncertainty in parameter values (rather than leaving them as fixed). Additionally, following a principled approach to developing priors can also assist in defining reasonable priors for biological relationships that are difficult to directly observe, such as the low-fecundity stock-recruit relationship. Transitioning to a Bayesian age-structured model would also allow for key processes such as growth to be estimated internally to the assessment which can incorporate the effect of fisheries selectivity into growth estimates. Internal estimation of growth should be done using conditional age-at-length of standardized ages, and take into account the associated error in the standardized ages.

The current assessment attempted to deal with the uncertainty in catch by modelling fishery removals in three different ways: fixed catch with alternative scenarios, direct estimation conditioned on effort, and direct estimation of fishing mortality. However, all three approaches leave room for improvement as the fixed catch models faced convergence issues, the effort conditioned estimates produced estimates of total catch that were inconsistent with observed catch levels, and the estimates directly estimated using fishing mortality were very sensitive to the choice of prior for the random effects variability. Additionally, fitting to catch with error using a likelihood produces catch estimates that are approximately equivalent to the observed catch on average which may not capture the full uncertainty in catch if alternative catch trends or magnitudes need to be investigated. The current assessment was able to investigate alternative catch magnitudes via proxy (using alternative priors for the variability in fishing mortality), investigation of alternative catch scenarios may be best accomplished by treating catch as fixed and using a Monte Carlo Bootstrap approach (Ducharme-Barth and Vincent, 2021). An alternative model parameterization may be needed to improve convergence for fixed catch scenarios. Additional work could also be done to improve the effort-based approach, either by refining the input time series of effort and/or anchoring estimates by fitting to observed catch values. It could also be useful to revisit how the prior variance for fishing mortality is developed if this approach for dealing with catch uncertainty is used again.

### 8.5. Research recommendations

Assessment of NPO SMA is challenging (Section 8.3), however these challenges provide no shortage of research opportunities through which improvements to the assessment can be made. One of the biggest challenges is the lack of large females in fisheries observations which limits our ability to say meaningful things about the reproductive component of the population using traditional methods. More advanced approaches such as close-kin mark-recapture (CKMR: Skaug, 2001; Bravington et al., 2016) could provide some of the missing information needed to address

this challenge. In CKMR, parents genetically mark their offspring such that estimates of adult abundance, trend and survival rate can be derived from the prevalence of half-sibling pairs in genetic samples of juvenile individuals (Hillary et al., 2018). In addition to providing information about adults CKMR could also help resolve challenges related to the scale and trend of the population, which would be difficult to resolve based on fisheries data alone. Furthermore, CKMR could help resolve an additional challenge by helping to identify the metapopulation structure for NPO SMA (Feutry et al., 2020; Trenkel et al., 2022).

While CKMR could potentially transform our understanding of NPO SMA and dramatically improve the quality of future stock assessments, the approach is not a 'silver-bullet'. CKMR approaches rely on accurate aging of samples in order to correctly assign a birth year for the calculation of kinship probabilities. If direct ages of samples are unobtainable, age is derived by converting length to age using a growth curve or using samples from known age individuals (e.g., pups or young-of-year with umbilical scars). Aging for NPO SMA is uncertain, especially for larger individuals so using a growth curve to convert lengths to age is unlikely to be viable unless improvements to the aging are made. Furthermore, applying a naïve CKMR analysis could provide biased outputs if intermittent breeding dynamics, like those believed to exist for NPO SMA, are not taken into account (Swenson et al., 2024). A targeted sampling effort to obtain young-of-year samples, paired with a CKMR model that accounts for the reproductive dynamics of NPO SMA integrated into an age-structured model (Punt et al., 2024) could be a viable way forward. It is recommended that a scoping study be conducted to evaluate the feasibility of implementing such a sampling plan and the number of samples needed for a CKMR analysis to provide useful information.

In addition to exploring the feasibility of CKMR, improving aging estimates is a critical area of future research. Kinney et al. (2024) suggest that in the NPO, differences in growth curves may be due to methodological differences in the detection of vertebral band-pairs. Additionally, there is increasing evidence to suggest that deposition of vertebral band-pairs may not correlate linearly with time but are rather a function of somatic growth (Natanson et al., 2018). Alternative aging methodologies that do not rely on detecting vertebral band-pairs is crucial. In particular, efforts should be made to evaluate the feasibility of applying emerging aging and validation techniques being used for teleosts, such as developing a bomb radiocarbon chronometer using eye lenses (Patterson and Chamberlin, 2023), amino acid racemization using eye lenses (Boye et al., 2020; Chamberlin et al., 2023), and DNA methylation using biopsied tissue samples (Piferrer and Anastasiadi, 2023). However, these emerging methods all currently depend on calibration with known age fish or comparison with a validated aging approach, both of which remain problematic for NPO SMA.

Assessment models can only ever be as good as their input data, and steps should be made to

improve the quality of inputs prior to the next assessment. Improvements can focus on three key areas: catch, indices, and size composition data. As mentioned, several times throughout this report, catch uncertainty is a key issue. The revision of early catch estimates from the values used in the previous assessment caused issues in the development of the current assessment model. Improvements to these estimates are needed however this may not be feasible given the limited data available from which to reconstruct pre-1994 catch. With respect to the post-1994 catch, it is imperative that all fishery removals are accounted for along with any uncertainty in catch estimates. Fishery removals should be calculated as the sum of landed catch, dead discards, and live discards which eventually succumb to release mortality for all fleets which interact with NPO SMA. With respect to the index, one of the challenges identified is that no fleet samples the complete spatial distribution of SMA in the NPO. It is recommended that a joint spatiotemporal analysis (Hoyle et al., 2024) of operational longline data be conducted in order to improve the spatial representativeness of the index. Lastly, if size-composition is to be used in an integrated assessment it must be representative of either the fishery removals or the index. The methods used to collect size composition data need to be evaluated for all fisheries, and if size composition data are collected non-representatively they should be appropriately standardized (Maunder et al., 2020).

## 9. ACKNOWLEDGEMENTS

Completion of the SMA stock assessment was a collaborative effort by the ISC Shark Working Group. Those who contributed to the assessment and participated in SHARKWG meetings included Carvalho, F., Dahl, K., Ducharme-Barth, N., Fernandez-Mendez, I., Gonzalez-Ania, L., Hutchinson, M., Kai, M. (SHARKWG Chair), Kanaiwa, M., King, J., Kinney, M. (SHARKWG Vice-Chair), Lee, H.H., Liu, K.M., Minte-Vera, C., Ovando, D., Ramírez-Soberón, G., Rodríguez-Madrigal, J.A., Semba, Y., Sosa-Nishizaki, O., Teo, S., and Tovar-Ávila, J. Ducharme-Barth, N. was the lead modeler. Observers to the SHARKWG meetings also helped to improve the models including Davies, N., Kim, K., Neubauer, P., and Soto, E.A. Research to develop the age-structured simulation model, and estimation of bias correction was greatly facilitated using services provided by the OSG Consortium (OSG, 2006; Pordes et al., 2007; Sfiligoi et al., 2009; OSG, 2015), which is supported by the National Science Foundation awards #2030508 and #1836650.

## 10. REFERENCES


Abascal, F.J., Quintans, M., Ramos-Cartelle, A., Mejuto, J., 2011. Movements and environmental preferences of the shortfin mako, Isurus oxyrinchus, in the southeastern Pacific Ocean. Mar Biol 158, 1175–1184. https://doi.org/10.1007/s00227-011-1639-1

Allendorf, F.W., Phelps, S.R., 1981. Use of Allelic Frequencies to Describe Population Structure. Can. J. Fish. Aquat. Sci. 38, 1507–1514. https://doi.org/10.1139/f81-203

Ardizzone, D., Cailliet, G.M., Natanson, L.J., Andrews, A.H., Kerr, L.A., Brown, T.A., 2006. Application of bomb radiocarbon chronologies to shortfin mako (Isurus oxyrinchus) age validation. Environ Biol Fish 77, 355–366. https://doi.org/10.1007/s10641-006-9106-4

Best, J.K., Punt, A.E., 2020. Parameterizations for Bayesian state-space surplus production models. Fisheries Research 222, 105411. https://doi.org/10.1016/j.fishres.2019.105411

Betancourt, M.J., Girolami, M., 2013. Hamiltonian Monte Carlo for Hierarchical Models. https://doi.org/10.48550/ARXIV.1312.0906

Bishop, S.D.H., Francis, M.P., Duffy, C., Montgomery, J.C., 2006. Age, growth, maturity, longevity and natural mortality of the shortfin mako shark (Isurus oxyrinchus) in New Zealand waters. Mar. Freshwater Res. 57, 143. https://doi.org/10.1071/MF05077

Boggs, C.H., Ito, R., 1993. Hawaii's Pelagic Fisheries. Marine Fisheries Review 55, 69–82.

Boye, T.K., Garde, E., Nielsen, J., Hedeholm, R., Olsen, J., Simon, M., 2020. Estimating the Age of West Greenland Humpback Whales Through Aspartic Acid Racemization and Eye Lens Bomb Radiocarbon Methods. Front. Mar. Sci. 6, 811. https://doi.org/10.3389/fmars.2019.00811

Bravington, M.V., Grewe, P.M., Davies, C.R., 2016. Absolute abundance of southern bluefin tuna estimated by close-kin mark-recapture. Nature Communications 7. https://doi.org/10.1038/ncomms13162

Carreón-Zapiain, M.T., Favela-Lara, S., González-Pérez, J.O., Tavares, R., Leija-Tristán, A., Mercado-Hernández, R., Compeán-Jiménez, G.A., 2018. Size, Age, and Spatial–Temporal Distribution of Shortfin Mako in the Mexican Pacific Ocean. Mar Coast Fish 10, 402–410. https://doi.org/10.1002/mcf2.10029

Casey, J., Kohler, N., 1992. Tagging studies on the Shortfin Mako Shark (Isurus oxyrinchus) in the Western North Atlantic. Mar. Freshwater Res. 43, 45. https://doi.org/10.1071/MF9920045

Cerna, F., Licandeo, R., 2009. Age and growth of the shortfin mako (Isurus oxyrinchus) in the south-eastern Pacific off Chile. Mar. Freshwater Res. 60, 394. https://doi.org/10.1071/MF08125

Chamberlin, D.W., Shervette, V.R., Kaufman, D.S., Bright, J.E., Patterson, W.F., 2023. Can amino acid racemization be utilized for fish age validation? Can. J. Fish. Aquat. Sci. 80, 642–647. https://doi.org/10.1139/cjfas-2022-0161

Charnov, E.L., Berrigan, D., 1990. Dimensionless numbers and life history evolution: Age of maturity versus the adult lifespan. Evol Ecol 4, 273–275. https://doi.org/10.1007/BF02214335

Clarke, S.C., Harley, S.J., Hoyle, S.D., Rice, J.S., 2013. Population Trends in Pacific Oceanic Sharks and the Utility of Regulations on Shark Finning. Conservation Biology 27, 197–209. https://doi.org/10.1111/j.1523-1739.2012.01943.x

Corrigan, S., Kacev, D., Werry, J., 2015. A case of genetic polyandry in the shortfin mako *Isurus oxyrinchus*. Journal of Fish Biology 87, 794–798. https://doi.org/10.1111/jfb.12743

Corrigan, S., Lowther, A.D., Beheregaray, L.B., Bruce, B.D., Cliff, G., Duffy, C.A., Foulis, A., Francis, M.P., Goldsworthy, S.D., Hyde, J.R., Jabado, R.W., Kacev, D., Marshall, L., Mucientes, G.R., Naylor, G.J.P., Pepperell, J.G., Queiroz, N., White, W.T., Wintner, S.P., Rogers, P.J., 2018. Population Connectivity of the Highly Migratory Shortfin Mako (Isurus oxyrinchus Rafinesque 1810) and Implications for Management in the Southern Hemisphere. Front. Ecol. Evol. 6, 187. https://doi.org/10.3389/fevo.2018.00187

De Deckker, P., 2016. The Indo-Pacific Warm Pool: critical to world oceanography and world climate. Geosci. Lett. 3, 20. https://doi.org/10.1186/s40562-016-0054-3

de Valpine, P., 2002. Review of methods for fitting time-series models with process and observation error and likelihood calculations for nonlinear, non-gaussian state-space models. Bulletin of Marine Science 70, 455–471.

Ducharme-Barth, N.D., Kinney, M., Teo, S., Carvalho, F., 2024. Catch, length-frequency and standardized CPUE of shortfin mako from the US Hawai'i longline fisheries through 2022 (No. ISC/24/SHARKWG-1/03).

Ducharme-Barth, N.D., Vincent, M.T., 2021. Focusing on the front end: A framework for incorporating uncertainty in biological parameters in model ensembles of integrated stock assessments (No. WCPFC-SC17-2021/SA-WP-05).

Edwards, C., 2024. Bdm: Bayesian biomass dynamics model (No. R package version 0.0.0.9036).

Fernandez-Mendez, J.I., Gonzalez-Ania, L.V., Ramirez-Soberon, G., Castillo-Géniz, J.L., Haro-Avalos, H., 2023. Update on standardized catch rates for mako shark (*Isurus oxyrinchus*) in the 2006-2022 Mexican Pacific longline fishery based upon a shark scientific observer program (No. ISC/24/SHARKWG-1/11).

Feutry, P., Devloo-Delva, F., Tran Lu Y, A., Mona, S., Gunasekera, R.M., Johnson, G., Pillans, R.D., Jaccoud, D., Kilian, A., Morgan, D.L., Saunders, T., Bax, N.J., Kyne, P.M., 2020. One panel to rule them all: DArTcap genotyping for population structure, historical demography, and kinship analyses, and its application to a threatened shark. Molecular Ecology Resources 20, 1470–1485. https://doi.org/10.1111/1755-0998.13204

Fletcher, R.I., 1978. Time-dependent solutions and efficient parameters for stock-production

models. Fish. Bull. 76, 377–388.
Fowler, C.W., 1988. Population dynamics as related to rate of increase per generation. Evol Ecol 2, 197–204. https://doi.org/10.1007/BF02214283
Francis, M.P., Lyon, W.S., Clarke, S.C., Finucci, B., Hutchinson, M.R., Campana, S.E., Musyl, M.K., Schaefer, K.M., Hoyle, S.D., Peatman, T., Bernal, D., Bigelow, K., Carlson, J., Coelho, R., Heberer, C., Itano, D., Jones, E., Leroy, B., Liu, K., Murua, H., Poisson, F., Rogers, P., Sanchez, C., Semba, Y., Sippel, T., Smith, N., 2023. Post-release survival of shortfin mako ( *ISURUS OXYRINCHUS* ) and silky ( *CARCHARHINUS FALCIFORMIS* ) sharks released from pelagic tuna longlines in the Pacific Ocean. Aquatic Conservation 33, 366–378. https://doi.org/10.1002/aqc.3920
Francis, M.P., Shivji, M.S., Duffy, C.A.J., Rogers, P.J., Byrne, M.E., Wetherbee, B.M., Tindale, S.C., Lyon, W.S., Meyers, M.M., 2019. Oceanic nomad or coastal resident? Behavioural switching in the shortfin mako shark (Isurus oxyrinchus). Mar Biol 166, 5. https://doi.org/10.1007/s00227-018-3453-5
Fujinami, Y., Kanaiwa, M., Kai, M., 2021a. Blue shark catches in the Japanese large-mesh driftnet fishery in the North Pacific Ocean from 1973 to 1993 (No. ISC/21/SHARKWG-1/08).
Fujinami, Y., Kanaiwa, M., Kai, M., 2021b. Estimation of annual catch for blue shark caught by Japanese high seas squid driftnet fishery in the North Pacific Ocean from 1981 to 1992 (No. ISC/21/SHARKWG-1/07).
Gabry, J., Mahr, T., 2024. bayesplot: Plotting for Bayesian Models (No. R package version 1.11.1).
Gabry, J., Simpson, D., Vehtari, A., Betancourt, M., Gelman, A., 2019. Visualization in Bayesian Workflow. Journal of the Royal Statistical Society Series A: Statistics in Society 182, 389–402. https://doi.org/10.1111/rssa.12378
Graham, J.B., Dewar, H., Lai, N.C., Lowell, W.R., Arce, S.M., 1990. Aspects of Shark Swimming Performance Determined Using a Large Water Tunnel. Journal of Experimental Biology 151, 175–192. https://doi.org/10.1242/jeb.151.1.175
Grant, P.R., Grant, B.R., 1992. Demography and the Genetically Effective sizes of Two Populations of Darwin's Finches. Ecology 73, 766–784. https://doi.org/10.2307/1940156
Hamel, O.S., Cope, J.M., 2022. Development and considerations for application of a longevity-based prior for the natural mortality rate. Fisheries Research 256, 106477. https://doi.org/10.1016/j.fishres.2022.106477
Hanan, D.A., Coan, A.L., Holts, D.B., 1993. The California Drift Gill Net Fishery For Sharks and Swordfish, 1981–82 Through 1990–91 (State of California Department of Fish and Game No. Fish Bulletin 175).
Heist, E.J., Musick, J.A., Graves, J.E., 1996. Genetic population structure of the shortfin mako ( *Isurus oxyrinchus* ) inferred from restriction fragment length polymorphism analysis of

mitochondrial DNA. Can. J. Fish. Aquat. Sci. 53, 583–588. https://doi.org/10.1139/f95-245

Hillary, R.M., Bravington, M.V., Patterson, T.A., Grewe, P., Bradford, R., Feutry, P., Gunasekera, R., Peddemors, V., Werry, J., Francis, M.P., Duffy, C.A.J., Bruce, B.D., 2018. Genetic relatedness reveals total population size of white sharks in eastern Australia and New Zealand. Sci Rep 8, 2661. https://doi.org/10.1038/s41598-018-20593-w

Hoyle, S.D., Campbell, R.A., Ducharme-Barth, N.D., Grüss, A., Moore, B.R., Thorson, J.T., Tremblay-Boyer, L., Winker, H., Zhou, S., Maunder, M.N., 2024. Catch per unit effort modelling for stock assessment: A summary of good practices. Fisheries Research 269, 106860. https://doi.org/10.1016/j.fishres.2023.106860

ISC, 2022. Stock assessment and future projections of blue shark in the north Pacific Ocean through 2020 (No. ISC/22/ANNEX/12).

ISC, 2021. Report of the Indicator-based Analysis for Shortfin Mako Shark in the North Pacific Ocean (No. ISC/21/ANNEX/05).

ISC, 2020. Report of the twentieth meeting of the international scientific committee for tuna and tuna-like species in the North Pacific Ocean.

ISC, 2018a. Stock assessment of shortfin mako shark in the North Pacific Ocean through 2016 (No. ISC/18/ANNEX/15).

ISC, 2018b. Report of the shark working group workshop (No. ISC/18/ANNEX/06).

ISC, 2018c. Report of the third shark age and growth workshop (No. ISC/18/ANNEX/05).

ISC, 2015. Indicator-based analysis of the status of shortfin mako shark in the north Pacific Ocean (No. ISC/15/ANNEX/12).

Joung, S.-J., Hsu, H.-H., 2005. Reproduction and Embryonic Development of the Shortfin Mako, *Isurus oxyrinchus* Rafinesque, 1810, in the Northwestern Pacific. Zoological Studies 44, 487–496.

Kai, M., 2023a. Update of annual catches for shortfin mako caught by Japanese offshore and distant water longliner in the North Pacific Ocean from 1994 to 2022 (No. ISC/23/SHARKWG-1/05).

Kai, M., 2023b. Spatio-temporal model for CPUE standardization: Application to shortfin mako caught by Japanese offshore and distant water shallow-set longliner in the western and central North Pacific (No. ISC/23/SHARKWG-1/02).

Kai, M., 2023c. Spatio-temporal model for CPUE standardization: Application to shortfin mako caught by longline of Japanese research and training vessels in the western and central North Pacific (No. ISC/23/SHARKWG-1/03).

Kai, M., 2021. Spatio-temporal model for CPUE standardization: Application to blue shark caught by Japanese offshore and distant water shallow-set longliner in the western North Pacific (No. ISC/18/SHARKWG-2/01).

Kai, M., Kanaiwa, M., 2018. Standardized CPUE of shortfin mako caught by Japanese shallow-set longline fisheries from 1975 to 1993 (No. ISC/18/SHARKWG-2/02).

Kai, M., Liu, K.-M., 2018. Estimation of initial equilibrium catch for North Pacific shortfin mako (No. ISC/18/SHARKWG-2/01).

Kai, M., Shiozaki, K., Ohshimo, S., Yokawa, K., 2015. Growth and spatiotemporal distribution of juvenile shortfin mako (Isurus oxyrinchus) in the western and central North Pacific. Mar. Freshwater Res. 66, 1176. https://doi.org/10.1071/MF14316

Kai, M., Thorson, J.T., Piner, K.R., Maunder, M.N., 2017a. Predicting the spatio-temporal distributions of pelagic sharks in the western and central North Pacific. Fisheries Oceanography 26, 569–582. https://doi.org/10.1111/fog.12217

Kai, M., Thorson, J.T., Piner, K.R., Maunder, M.N., 2017b. Spatiotemporal variation in size-structured populations using fishery data: an application to shortfin mako ( *Isurus oxyrinchus* ) in the Pacific Ocean. Can. J. Fish. Aquat. Sci. 74, 1765–1780. https://doi.org/10.1139/cjfas-2016-0327

Kai, M., Yano, T., 2023. Updated annual catches of shortfin mako caught by Japanese coastal fisheries in the North Pacific Ocean from 1994 to 2022 (No. ISC/23/SHARKWG-1/04).

Kell, L.T., Sharma, R., Kitakado, T., Winker, H., Mosqueira, I., Cardinale, M., Fu, D., 2021. Validation of stock assessment methods: is it me or my model talking? ICES Journal of Marine Science 78, 2244–2255. https://doi.org/10.1093/icesjms/fsab104

Kinney, M., Ducharme-Barth, N.D., Takahashi, N., Kai, M., Semba, Y., Kanaiwa, M., Liu, K.-M., Rodriguez-Madrigal, J., Tovar-Avila, J., 2024. Mako Age and Growth, Meta-analysis Revisited (No. ISC/24/SHARKWG-1/01).

Kinney, M.J., Carvalho, F., Teo, S.L.H., 2017. Length composition and catch of shortfin mako sharks in U.S. commercial and recreational fisheries in the North Pacific (No. ISC/17/SHARKWG-3/04).

Kinney, M.J., Wells, R.J.D., Kohin, S., 2016. Oxytetracycline age validation of an adult shortfin mako shark *Isurus oxyrinchus* after 6 years at liberty. Journal of Fish Biology 89, 1828–1833. https://doi.org/10.1111/jfb.13044

Kohler, N.E., Casey, J.G., Turner, P.A., 1996. Length-Length and Length-Weight Relationships for 13 Shark Species from the Western North Atlantic (No. NOAA Tech. Memo. NMFS-NE 110).

Kokkalis, A., Berg, C.W., Kapur, M.S., Winker, H., Jacobsen, N.S., Taylor, M.H., Ichinokawa, M., Miyagawa, M., Medeiros-Leal, W., Nielsen, J.R., Mildenberger, T.K., 2024. Good practices for surplus production models. Fisheries Research 275, 107010. https://doi.org/10.1016/j.fishres.2024.107010

LaFreniere, B.R., Sosa-Nishizaki, O., Herzka, S.Z., Snodgrass, O., Dewar, H., Miller, N., Wells,

R.J.D., Mohan, J.A., 2023. Vertebral Chemistry Distinguishes Nursery Habitats of Juvenile Shortfin Mako in the Eastern North Pacific Ocean. Mar Coast Fish 15, e10234. https://doi.org/10.1002/mcf2.10234

Liu, K.-M., Su, K.Y., Chin, C.P., Tsai, W.P., 2023. Updated standardized CPUE and historical catch estimate of the shortfin mako shark caught by Taiwanese large-scale tuna longline fishery in the North Pacific Ocean (No. ISC/23/SHARKWG-1/11).

Liu, S.Y.V., Wen-Pei Tsai, Mengshan Lee, Hsiu-Wen Chien, 2020. Accessing Multiple Paternity in the Shortfin Mako Shark (Isurus oxyrinchus). Zoological Studies 無. https://doi.org/10.6620/ZS.2020.59-49

Maunder, M.N., Thorson, J.T., Xu, H., Oliveros-Ramos, R., Hoyle, S.D., Tremblay-Boyer, L., Lee, H.H., Kai, M., Chang, S.-K., Kitakado, T., Albertsen, C.M., Minte-Vera, C.V., Lennert-Cody, C.E., Aires-da-Silva, A.M., Piner, K.R., 2020. The need for spatio-temporal modeling to determine catch-per-unit effort based indices of abundance and associated composition data for inclusion in stock assessment models. Fisheries Research 229, 105594. https://doi.org/10.1016/j.fishres.2020.105594

McCracken, M., 2019. Sampling the Hawaii deep-set longline fishery and point estimators of bycatch. https://doi.org/10.25923/2PSA-7S55

McKinnell, S., Seki, M.P., 1998. Shark bycatch in the Japanese high seas squid driftnet fishery in the North Pacific Ocean. Fisheries Research 39, 127–138. https://doi.org/10.1016/S0165-7836(98)00179-9

Methot Jr., R.D., Wetzel, C.R., 2013. Stock synthesis: A biological and statistical framework for fish stock assessment and fishery management. Fisheries Research 142, 86–99. https://doi.org/10.1016/j.fishres.2012.10.012

Miyaoka, I., 2004. Case One: Driftnet Fishing, in: Legitimacy in International Society. Palgrave Macmillan UK, London, pp. 49–73. https://doi.org/10.1057/9781403948199_4

Mohn, R., 1999. The retrospective problem in sequential population analysis: An investigation using cod fishery and simulated data. ICES Journal of Marine Science 56, 473–488. https://doi.org/10.1006/jmsc.1999.0481

Monnahan, C.C., 2024. Toward good practices for Bayesian data-rich fisheries stock assessments using a modern statistical workflow. Fisheries Research 275, 107024. https://doi.org/10.1016/j.fishres.2024.107024

Mucientes, G., Fernández-Chacón, A., Queiroz, N., Sims, D.W., Villegas-Ríos, D., 2023. Juvenile survival and movements of two threatened oceanic sharks in the North Atlantic Ocean inferred from tag-recovery data. Ecology and Evolution 13, e10198. https://doi.org/10.1002/ece3.10198

Musyl, M., Brill, W., Curran, D., Fragoso, N., McNaughton, L., Nielsen, A., Kikkawa, B., Moyes,

C., 2011. Postrelease survival, vertical and horizontal movements, and thermal habitats of five species of pelagic sharks in the central Pacific Ocean. Fish. Bull. 109, 341–368.

Nakano, H., Okada, K., Watanabe, Y., Uosaki, K., 1993. Outline of the Large-Mesh Driftnet Fishery of Japan (No. Bulletin Number 53 (I)), Driftnet Fisheries of the North Pacific Ocean. International North Pacific Fisheries Commission.

Nasby-Lucas, N., Dewar, H., Sosa-Nishizaki, O., Wilson, C., Hyde, J.R., Vetter, R.D., Wraith, J., Block, B.A., Kinney, M.J., Sippel, T., Holts, D.B., Kohin, S., 2019. Movements of electronically tagged shortfin mako sharks (Isurus oxyrinchus) in the eastern North Pacific Ocean. Anim Biotelemetry 7, 12. https://doi.org/10.1186/s40317-019-0174-6

Natanson, L.J., Kohler, N.E., Ardizzone, D., Cailliet, G.M., Wintner, S.P., Mollet, H.F., 2006. Validated age and growth estimates for the shortfin mako, Isurus oxyrinchus, in the North Atlantic Ocean. Environ Biol Fish 77, 367–383. https://doi.org/10.1007/s10641-006-9127-z

Natanson, L.J., Skomal, G.B., Hoffmann, S.L., Porter, M.E., Goldman, K.J., Serra, D., 2018. Age and growth of sharks: do vertebral band pairs record age? Mar. Freshwater Res. 69, 1440. https://doi.org/10.1071/MF17279

Neubauer, P., Richard, Y., Tremblay-Boyer, L., 2019. Alternative assessment methods for oceanic whitetip shark (No. WCPFC-SC15-2019/SA-WP-13).

O'Brien, J., Sunada, J., 1994. A review of the southern California experimental drift longline fishery for sharks, 1988-1991 (No. CalCOFI Rep., Vol. 35).

OSG, 2015. Open Science Data Federation. https://doi.org/10.21231/0KVZ-VE57

OSG, 2006. OSPool. https://doi.org/10.21231/906P-4D78

Pardo, S.A., Cooper, A.B., Reynolds, J.D., Dulvy, N.K., 2018. Quantifying the known unknowns: estimating maximum intrinsic rate of population increase in the face of uncertainty. ICES Journal of Marine Science 75, 953–963. https://doi.org/10.1093/icesjms/fsx220

Pardo, S.A., Kindsvater, H.K., Reynolds, J.D., Dulvy, N.K., 2016. Maximum intrinsic rate of population increase in sharks, rays, and chimaeras: the importance of survival to maturity. Can. J. Fish. Aquat. Sci. 73, 1159–1163. https://doi.org/10.1139/cjfas-2016-0069

Patterson, W.F., Chamberlin, D.W., 2023. Application of the bomb radiocarbon chronometer with eye lens core $\Delta^{14}$C for age validation in deepwater reef fishes. Can. J. Fish. Aquat. Sci. cjfas-2023-0003. https://doi.org/10.1139/cjfas-2023-0003

Piferrer, F., Anastasiadi, D., 2023. Age estimation in fishes using epigenetic clocks: Applications to fisheries management and conservation biology. Front. Mar. Sci. 10, 1062151. https://doi.org/10.3389/fmars.2023.1062151

Pordes, R., Petravick, D., Kramer, B., Olson, D., Livny, M., Roy, A., Avery, P., Blackburn, K., Wenaus, T., Würthwein, F., Foster, I., Gardner, R., Wilde, M., Blatecky, A., McGee, J.,

Quick, R., 2007. The open science grid. J. Phys.: Conf. Ser. 78, 012057. https://doi.org/10.1088/1742-6596/78/1/012057

Pratt Jr., H.L., Casey, J.G., 1983. Age and Growth of the Shortfin Mako, *Isurus oxyrinchus* , Using Four Methods. Can. J. Fish. Aquat. Sci. 40, 1944–1957. https://doi.org/10.1139/f83-224

Punt, A.E., Thomson, R., Little, L.R., Bessell-Browne, P., Burch, P., Bravington, M., 2024. Including close-kin mark-recapture data in statistical catch-at-age stock assessments and management strategies. Fisheries Research 276, 107057. https://doi.org/10.1016/j.fishres.2024.107057

R Core Team, 2023. R: A Language and Environment for Statistical Computing (No. v 4.3.1). R Foundation for Statistical Computing, Vienna, Austria.

Ramirez-Amaro, S.R., Cartamil, D., Galvan-Magaña, F., Gonzalez-Barba, G., Graham, J.B., Carrera-Fernandez, M., Escobar-Sanchez, O., Sosa-Nishizaki, O., Rochin-Alamillo, A., 2013. The artisanal elasmobranch fishery of the Pacific coast of Baja California Sur, Mexico, management implications. Sci. Mar. 77, 473–487. https://doi.org/10.3989/scimar.03817.05A

Runcie, R., Holts, D., Wraith, J., Xu, Y., Ramon, D., Rasmussen, R., Kohin, S., 2016. A fishery-independent survey of juvenile shortfin mako (Isurus oxyrinchus) and blue (Prionace glauca) sharks in the Southern California Bight, 1994–2013. Fisheries Research 183, 233–243. https://doi.org/10.1016/j.fishres.2016.06.010

Santana-Morales, O., Cartamil, D., Sosa-Nishizaki, O., Zertuche-Chanes, R., Hernández-Gutiérrez, E., Graham, J., 2020. Artisanal elasmobranch fisheries of northwestern Baja California, Mexico. Cienc. Mar. 46. https://doi.org/10.7773/cm.v46i1.3023

Schrey, A.W., Heist, E.J., 2003. Microsatellite analysis of population structure in the shortfin mako ( *Isurus oxyrinchus* ). Can. J. Fish. Aquat. Sci. 60, 670–675. https://doi.org/10.1139/f03-064

Scott, R.D., Sampson, D.B., 2011. The sensitivity of long-term yield targets to changes in fishery age-selectivity. Marine Policy 35, 79–84. https://doi.org/10.1016/j.marpol.2010.08.005

Semba, Y., Aoki, I., Yokawa, K., 2011. Size at maturity and reproductive traits of shortfin mako, Isurus oxyrinchus, in the western and central North Pacific. Mar. Freshwater Res. 62, 20. https://doi.org/10.1071/MF10123

Semba, Y., Kai, M., 2023. Reconsideration of catch of shortfin mako (*Isurus oxyrinchus*) caught by Japanese large-mesh driftnet fishery between 1975 and 1993 in the North Pacific (No. ISC/23/SHARKWG-1/8).

Semba, Y., Kanaiwa, M., Kai, M., 2023. Estimate of catch of shortfin mako caught by Japanese squid driftnet fishery between 1981 and 1992 in the North Pacific (No. ISC/23/SHARKWG-1/09).

2685 Semba, Y., Liu, K.-M., Su, S.-H., 2017. Revised integrated analysis of maturity size of shortfin
2686 mako (*Isurus oxyrinchus* in the North Pacific (No. ISC/17/SHARKWG-3/22).
2687 Semba, Y., Nakano, H., Aoki, I., 2009. Age and growth analysis of the shortfin mako, Isurus
2688 oxyrinchus, in the western and central North Pacific Ocean. Environ Biol Fish 84, 377–
2689 391. https://doi.org/10.1007/s10641-009-9447-x
2690 Sepulveda, C.A., Graham, J.B., Bernal, D., 2007. Aerobic metabolic rates of swimming juvenile
2691 mako sharks, Isurus oxyrinchus. Mar Biol 152, 1087–1094.
2692 https://doi.org/10.1007/s00227-007-0757-2
2693 Sepulveda, C.A., Kohin, S., Chan, C., Vetter, R., Graham, J.B., 2004. Movement patterns, depth
2694 preferences, and stomach temperatures of free-swimming juvenile mako sharks, Isurus
2695 oxyrinchus, in the Southern California Bight. Marine Biology 145.
2696 https://doi.org/10.1007/s00227-004-1356-0
2697 Sfiligoi, I., Bradley, D.C., Holzman, B., Mhashilkar, P., Padhi, S., Wurthwein, F., 2009. The Pilot
2698 Way to Grid Resources Using glideinWMS, in: 2009 WRI World Congress on Computer
2699 Science and Information Engineering. Presented at the 2009 WRI World Congress on
2700 Computer Science and Information Engineering, IEEE, Los Angeles, California USA, pp.
2701 428–432. https://doi.org/10.1109/CSIE.2009.950
2702 Sippel, T., Wraith, J., Kohin, S., Taylor, V., Holdsworth, J., Taguchi, M., Matsunaga, H., Yokawa,
2703 K., 2011. A summary of blue shark (*Prionace glauca*) and shortfin mako shark (*Isurus*
2704 *oxyrinchus*) tagging data available from the North and Southwest Pacific Ocean (No.
2705 ISC/11/SHARKWG-2/04).
2706 Skaug, H.J., 2001. Allele-Sharing Methods for Estimation of Population Size. Biometrics 57, 750–
2707 756. https://doi.org/10.1111/j.0006-341X.2001.00750.x
2708 Sosa-Nishizaki, O., García-Rodríguez, E., Morales-Portillo, C.D., Pérez-Jiménez, J.C., Rodríguez-
2709 Medrano, M.D.C., Bizzarro, J.J., Castillo-Géniz, J.L., 2020. Fisheries interactions and the
2710 challenges for target and nontargeted take on shark conservation in the Mexican Pacific,
2711 in: Advances in Marine Biology. Elsevier, pp. 39–69.
2712 https://doi.org/10.1016/bs.amb.2020.03.001
2713 Sosa-Nishizaki, O., Saldana-Ruiz, L.E., Corro-Espinosa, D., Tovar-Avila, J., Castillo-Géniz, J.L.,
2714 Santana-Hernandez, H., Marquez-Farias, J.F., 2017. Estimations of the shortfin mako shark
2715 (*Isurus oxyrinchus*) catches by Mexican Pacific fisheries, An update (1976-2016) (No.
2716 ISC/17/SHARKWG-3/19).
2717 Stan Development Team, 2024a. Stan Modeling Language Users Guide and Reference Manual, v
2718 2.32.6.
2719 Stan Development Team, 2024b. RStan: the R interface to Stan (No. R package version 2.32.6).
2720 Stevens, J.D., 1983. Observations on Reproduction in the Shortfin Mako Isurus oxyrinchus.

Copeia 1983, 126. https://doi.org/10.2307/1444706
Stillwell, C.E., Kohler, N.E., 1982. Food, Feeding Habits, and Estimates of Daily Ration of the Shortfin Mako ( *Isurus oxyrinchus* ) in the Northwest Atlantic. Can. J. Fish. Aquat. Sci. 39, 407–414. https://doi.org/10.1139/f82-058
Swenson, J.D., Brooks, E.N., Kacev, D., Boyd, C., Kinney, M.J., Marcy-Quay, B., Sévêque, A., Feldheim, K.A., Komoroske, L.M., 2024. Accounting for unobserved population dynamics and aging error in close-kin mark-recapture assessments. Ecology and Evolution 14, e10854. https://doi.org/10.1002/ece3.10854
Takahashi, N., Kai, M., Semba, Y., Kanaiwa, M., Liu, K.-M., Rodriguez-Madrigal, J., Tovar-Avila, J., Kinney, M., Taylor, J., 2017. Meta-analysis of Growth Curve for Shortfin Mako Shark in the North Pacific (No. ISC/17/SHARKWG-3/05).
Taylor, I.G., Gertseva, V., Methot, R.D., Maunder, M.N., 2013. A stock–recruitment relationship based on pre-recruit survival, illustrated with application to spiny dogfish shark. Fisheries Research 142, 15–21. https://doi.org/10.1016/j.fishres.2012.04.018
Teo, S.L.H., Ducharme-Barth, N.D., Kinney, M.J., 2024. Developing natural mortality priors for North Pacific shortfin mako sharks (No. ISC/24/SHARKWG-1/02).
Then, A.Y., Hoenig, J.M., Hall, N.G., Hewitt, D.A., 2015. Evaluating the predictive performance of empirical estimators of natural mortality rate using information on over 200 fish species. ICES Journal of Marine Science 72, 82–92. https://doi.org/10.1093/icesjms/fsu136
Tremblay-Boyer, L., Carvalho, F., Neubauer, P., Pilling, G., 2019. Stock assessment for oceanic whitetip shark in the western and central pacific ocean (No. WCPFC-SC15-2019/SA-WP-06).
Trenkel, V.M., Charrier, G., Lorance, P., Bravington, M.V., 2022. Close-kin mark–recapture abundance estimation: practical insights and lessons learned. ICES Journal of Marine Science 79, 413–422. https://doi.org/10.1093/icesjms/fsac002
Vaudo, J., Wetherbee, B., Wood, A., Weng, K., Howey-Jordan, L., Harvey, G., Shivji, M., 2016. Vertical movements of shortfin mako sharks Isurus oxyrinchus in the western North Atlantic Ocean are strongly influenced by temperature. Mar. Ecol. Prog. Ser. 547, 163–175. https://doi.org/10.3354/meps11646
Vehtari, A., Gabry, J., Magnusson, M., Yao, Y., Burkner, P., Paananen, T., Gelman, A., 2024. loo: Efficient leave-one-out cross-validation and WAIC for Bayesian models (No. R package version 2.7.0).
Ward, P., 2008. Empirical estimates of historical variations in the catchability and fishing power of pelagic longline fishing gear. Rev Fish Biol Fisheries 18, 409–426. https://doi.org/10.1007/s11160-007-9082-6
WCPFC, 2023. SC19 Summary Report (No. WCPFC20-2023-SC19).

Wells, R.J.D., Smith, S.E., Kohin, S., Freund, E., Spear, N., Ramon, D.A., 2013. Age validation of juvenile Shortfin Mako (Isurus oxyrinchus) tagged and marked with oxytetracycline off southern California. FB 111, 147–160. https://doi.org/10.7755/FB.111.2.3

Winker, H., Carvalho, F., Kapur, M., 2018. JABBA: Just Another Bayesian Biomass Assessment. Fisheries Research 204, 275–288. https://doi.org/10.1016/j.fishres.2018.03.010

Winker, H., Mourato, B., Chang, Y., 2020. Unifying parameterizations between age-structured and surplus production models: An application to atlantic white marlin (*Kajiki albidia*) with simulation testing. Collect. Vol. Sci. Pap. ICCAT 76, 219–234.

Yatsu, A., Hiramatsu, K., Hayase, S., 1993. Outline of the Japanese Squid Driftnet Fishery with Notes on the By-Catch (No. Bulletin Number 53 (I)), Driftnet Fisheries of the North Pacific Ocean. International North Pacific Fisheries Commission.

## 11. TABLES

*Table 1.* Fleet-specific definitions, original units of catch, and selectivity assumptions used in the SS3 models (Models: *SS3 06 – 2022data* and *SS3 07 – 2022dataASPM*) updated with data through 2022 for North Pacific shortfin mako. The selectivity curves for fisheries lacking size composition were assumed to be the same (i.e., mirror fishery) as a related fishery.

| Fishery number | Fishery name | Type | Catch units | Catch start | Catch end | Selectivity assumption | Mirror fishery |
|---|---|---|---|---|---|---|---|
| 1 | F1_US_Survey | Extraction | Numbers (1000s) | - | - | Double-normal-24 | Estimated |
| 2 | F2_US_CA_LL | Extraction | mt | 1981 | 1994 | Mirrored | 1 |
| 3 | F3_US_HI_SS_LL | Extraction | Numbers (1000s) | 1985 | 2022 | Double-normal-24 | Estimated |
| 4 | F4_US_HI_DS_LL | Extraction | Numbers (1000s) | 1975 | 2022 | Double-normal-24 | Estimated |
| 5 | F5_US_DGN | Extraction | mt | 1981 | 2022 | Double-normal-24 | Estimated |
| 6 | F6_US_REC | Extraction | Numbers (1000s) | 2005 | 2022 | Mirrored | 3 |
| 7 | F7_JPN_SS_II | Extraction | Numbers (1000s) | 1994 | 2022 | Double-normal-24 | Estimated |
| 8 | F8_JP_DS_II | Extraction | Numbers (1000s) | 1992 | 2022 | Double-normal-24 | Estimated |
| 9 | F9_JPN_DGN_II | Extraction | mt | 1994 | 2022 | Double-normal-24 | Estimated |
| 10 | F10_JPN_CST | Extraction | mt | 1994 | 2022 | Double-normal-24 | Estimated |
| 11 | F11_JPN_DS_I | Extraction | mt | 1975 | 1991 | Mirrored | 8 |
| 12 | F12_JPN_DGN_I | Extraction | mt | 1975 | 1992 | Mirrored | 9 |
| 13 | F13_JPN_OTH | Extraction | mt | 1994 | 2022 | Mirrored | 10 |
| 14 | F14_JPN_SS_I | Extraction | mt | 1975 | 1993 | Mirrored | 7 |
| 15 | F15_JPN_SS_DISC | Extraction | Numbers (1000s) | 1994 | 2022 | Double-normal-24 | Estimated |
| 16 | F16_JP_SML_DGN | Extraction | Numbers (1000s) | 1981 | 1992 | Mirrored | 7 |
| 17 | F17_JPN_SS_III | Extraction | Numbers (1000s) | 2014 | 2016 | Double-normal-24 | Estimated |
| 18 | F18_JPN_CST_DISC | Extraction | mt | 1994 | 2022 | Mirrored | 10 |
| 19 | F19_TW_LRG_N | Extraction | Numbers (1000s) | 1975 | 2022 | Double-normal-24 | Estimated |
| 20 | F20_TW_LRG_S | Extraction | Numbers (1000s) | 1975 | 2022 | Double-normal-24 | Estimated |
| 21 | F21_TW_SML | Extraction | Numbers (1000s) | 1989 | 2022 | Double-normal-24 | Estimated |
| 22 | F22_TW_LRG_DGN | Extraction | mt | 1987 | 1992 | Mirrored | 9 |
| 23 | F23_TW_SML_DGN | Extraction | mt | 1981 | 1992 | Mirrored | 7 |
| 24 | F24_MEX_NOR | Extraction | mt | 1976 | 2022 | Double-normal-24 | Estimated |
| 25 | F25_MEX_SOU | Extraction | mt | 1976 | 2022 | Double-normal-24 | Estimated |
| 26 | F26_MEX_ART | Extraction | mt | 2017 | 2022 | Mirrored | 5 |
| 27 | F27_CANADA | Extraction | mt | 1980 | 2014 | Mirrored | 5 |
| 28 | F28_CHINA | Extraction | Numbers (1000s) | 2002 | 2022 | Mirrored | 8 |

*Table 1 (continued).* Fleet-specific definitions, original units of catch, and selectivity assumptions used in the SS3 models (Models: *SS3 06 – 2022data* and *SS3 07 – 2022dataASPM*) updated with data through 2022 for North Pacific shortfin mako. The selectivity curves for fisheries lacking size composition were assumed to be the same (i.e., mirror fishery) as a related fishery.

| Fishery number | Fishery name | Type | Catch units | Catch start | Catch end | Selectivity assumption | Mirror fishery |
|---|---|---|---|---|---|---|---|
| 29 | F29_KR | Extraction | Numbers (1000s) | 2010 | 2022 | Mirrored | 8 |
| 30 | F30_KR_SML_DGN | Extraction | mt | 1981 | 1992 | Mirrored | 7 |
| 31 | F31_WCPFC_LL | Extraction | Numbers (1000s) | 2003 | 2022 | Mirrored | 8 |
| 32 | F32_IATTC_PS | Extraction | mt | 1975 | 2022 | Mirrored | 3 |
| 33 | F33_IATTC_LL | Extraction | Numbers (1000s) | 2008 | 2022 | Mirrored | 8 |
| 34 | S1:US-DE-LL-all | Index | Numbers (1000s) | - | - | Double-normal-24 | Estimated |
| 35 | S2:US-DE-LL-core | Index | Numbers (1000s) | - | - | Mirrored | 34 |
| 36 | S3:Juvenile-Survey-LL | Index | Numbers (1000s) | - | - | Mirrored | 1 |
| 37 | S4:TW-LA-LL-N | Index | Numbers (1000s) | - | - | Mirrored | 7 |
| 38 | S5:JP-OF-DW-SH-LL-M3 | Index | Numbers (1000s) | - | - | Mirrored | 7 |
| 39 | S6:JP-OF-DW-SH-LL-M5 | Index | Numbers (1000s) | - | - | Mirrored | 7 |
| 40 | S7:JP-OF-DW-DE-LL-M7 | Index | Numbers (1000s) | - | - | Mirrored | 8 |
| 41 | S8:MX-Com-LL | Index | Numbers (1000s) | - | - | Mirrored | 24 |
| 42 | S9:MX-Com-LL-N | Index | Numbers (1000s) | - | - | Mirrored | 24 |
| 43 | S10:MX-Com-LL-S | Index | Numbers (1000s) | - | - | Mirrored | 25 |

*Table 2*. Fleet-specific definitions, original units of catch, and selectivity assumptions used in *SS3 08 – 2022simple* for North Pacific shortfin mako. The selectivity curves for fisheries lacking size composition were assumed to be the same (i.e., mirror fishery) as a related fishery. Fishery definitions from Table 1 are denoted in the *Former fishery* column.

| Fishery Number | Fishery name | Type | Catch units | Catch start | Catch end | Selectivity assumption | Mirror fishery | Former fishery |
|---|---|---|---|---|---|---|---|---|
| 1 | F1_US_Survey | Extraction | Numbers (1000s) | - | - | Double-normal-24 | Estimated | 1 |
| 2 | F2_US_CA_LL | Extraction | mt | 1981 | 1994 | Double-normal-24 | Estimated | 2 |
| 3 | F3_US_HI_SS_LL_+ | Extraction | Numbers (1000s) | 1985 | 2022 | Double-normal-24 | Estimated | 3,6 |
| 4 | F4_US_HI_DS_LL | Extraction | Numbers (1000s) | 1975 | 2022 | Double-normal-24 | Estimated | 4 |
| 5 | F5_US_DGN_+ | Extraction | mt | 1980 | 2022 | Double-normal-24 | Estimated | 5,27 |
| 6 | F6_JPN_SS_II | Extraction | Numbers (1000s) | 1994 | 2022 | Double-normal-24 | Estimated | 7 |
| 7 | F7_JP_SML_DGN | Extraction | Numbers (1000s) | 1981 | 1992 | Mirrored | 6 | 16 |
| 8 | F8_JP_DS_II_+ | Extraction | Numbers (1000s) | 1992 | 2022 | Double-normal-24 | Estimated | 8,28,29,31,33 |
| 9 | F9_JPN_DGN_II_+ | Extraction | mt | 1975 | 2022 | Double-normal-24 | Estimated | 9,12,22 |
| 10 | F10_JPN_CST_+ | Extraction | mt | 1994 | 2022 | Double-normal-24 | Estimated | 10,13,18 |
| 11 | F11_JPN_DS_I_+ | Extraction | mt | 1975 | 1991 | Mirrored | 8 | 11 |
| 12 | F12_JPN_SS_I_+ | Extraction | mt | 1975 | 1993 | Mirrored | 6 | 14,23,30 |
| 13 | F13_JPN_SS_DISC | Extraction | Numbers (1000s) | 1994 | 2022 | Double-normal-24 | Estimated | 15 |
| 14 | F14_JPN_SS_III | Extraction | Numbers (1000s) | 2014 | 2016 | Double-normal-24 | Estimated | 17 |
| 15 | F15_TW_LRG_N | Extraction | Numbers (1000s) | 1975 | 2022 | Double-normal-24 | Estimated | 19 |
| 16 | F16_TW_LRG_S | Extraction | Numbers (1000s) | 1975 | 2022 | Double-normal-24 | Estimated | 20 |
| 17 | F17_TW_SML | Extraction | Numbers (1000s) | 1989 | 2022 | Double-normal-24 | Estimated | 21 |
| 18 | F18_MEX_NOR | Extraction | mt | 1976 | 2022 | Double-normal-24 | Estimated | 24 |
| 19 | F19_MEX_SOU | Extraction | mt | 1976 | 2022 | Double-normal-24 | Estimated | 25 |
| 20 | F20_MEX_ART | Extraction | mt | 2017 | 2022 | Mirrored | 5 | 26 |
| 21 | F21_IATTC_PS | Extraction | mt | 1975 | 2022 | Mirrored | 3 | 32 |
| 22 | S1:US-DE-LL-all | Index | Numbers (1000s) | - | - | Double-normal-24 | Estimated | 34 |
| 23 | S2:US-DE-LL-core | Index | Numbers (1000s) | - | - | Mirrored | 22 | 35 |
| 24 | S3:Juvenile-Survey-LL | Index | Numbers (1000s) | - | - | Mirrored | 1 | 36 |
| 25 | S4:TW-LA-LL-N | Index | Numbers (1000s) | - | - | Mirrored | 15 | 37 |
| 26 | S5:JP-OF-DW-SH-LL-M3 | Index | Numbers (1000s) | - | - | Mirrored | 6 | 38 |

*Table 2 (continued)*. Fleet-specific definitions, original units of catch, and selectivity assumptions used in *SS3 08 – 2022simple* for North Pacific shortfin mako. The selectivity curves for fisheries lacking size composition were assumed to be the same (i.e., mirror fishery) as a related fishery. Fishery definitions from Table 1 are denoted in the *Former fishery* column.

| **Fishery Number** | **Fishery name** | **Type** | **Catch units** | **Catch start** | **Catch end** | **Selectivity assumption** | **Mirror fishery** | **Former fishery** |
|---|---|---|---|---|---|---|---|---|
| 27 | S6:JP-OF-DW-SH-LL-M5 | Index | Numbers (1000s) | - | - | Mirrored | 6 | 39 |
| 28 | S7:JP-OF-DW-DE-LL-M7 | Index | Numbers (1000s) | - | - | Mirrored | 8 | 40 |
| 29 | S8:MX-Com-LL | Index | Numbers (1000s) | - | - | Mirrored | 18 | 41 |
| 30 | S9:MX-Com-LL-N | Index | Numbers (1000s) | - | - | Mirrored | 18 | 42 |
| 31 | S10:MX-Com-LL-S | Index | Numbers (1000s) | - | - | Mirrored | 19 | 43 |

2780

2781 *Table 3*. Catch in numbers (1000s) of North Pacific shortfin mako for fisheries listed in *Table 1*.

| Year | 1 | 2 | 3 | 4 | 5 | 6 | 7 | 8 | 9 | 10 | 11 | 12 | 13 | 14 | 15 | 16 | 17 | 18 | 19 | 20 | 21 | 22 | 23 | 24 | 25 | 26 | 27 | 28 | 29 | 30 | 31 | 32 | 33 |
|---|---|---|---|---|---|---|---|---|---|---|---|---|---|---|---|---|---|---|---|---|---|---|---|---|---|---|---|---|---|---|---|---|---|
| 1974 | | | | | | | | | | | | | | 24.89 | | | | | | | | | | | | | | | | | | | |
| 1975 | | | | 0.05 | | | | | | | 2.90 | 5.98 | | 15.64 | | | | | 0.13 | 0.15 | | | | | | | | | | | | 0.00 | |
| 1976 | | | | 0.07 | | | | | | | 5.44 | 11.17 | | 21.95 | | | | | 0.01 | 0.01 | | | | 2.31 | 0.19 | | | | | | | 0.00 | |
| 1977 | | | | 0.08 | | | | | | | 7.38 | 18.41 | | 29.80 | | | | | 0.04 | 0.05 | | | | 2.22 | 0.21 | | | | | | | 0.00 | |
| 1978 | | | | 0.06 | | | | | | | 6.94 | 11.14 | | 24.13 | | | | | 0.05 | 0.05 | | | | 3.16 | 0.29 | | | | | | | 0.00 | |
| 1979 | | | | 0.03 | | | | | | | 9.81 | 8.17 | | 26.18 | | | | | 0.01 | 0.01 | | | | 1.46 | 0.55 | | | | | | | 0.00 | |
| 1980 | | | | 0.00 | | | | | | | 11.65 | 5.90 | | 24.77 | | | | | 0.03 | 0.03 | | | | 1.72 | 0.37 | | 0.00 | | | | | 0.00 | |
| 1981 | | 0.89 | | 0.00 | 6.68 | | | | | | 13.63 | 5.75 | | 21.76 | | 0.06 | | | 0.03 | 0.03 | | | 0.02 | 1.27 | 0.49 | | | | | 0.08 | | 0.00 | |
| 1982 | | 0.30 | | 0.01 | 14.00 | | | | | | 9.77 | 5.73 | | 13.56 | | 0.60 | | | 0.00 | 0.00 | | | 0.03 | 2.02 | 0.39 | | | | | 0.09 | | 0.00 | |
| 1983 | | 0.03 | | 0.03 | 8.80 | | | | | | 10.58 | 4.29 | | 10.77 | | 0.93 | | | 0.00 | 0.00 | | | 0.05 | 1.92 | 0.26 | | | | | 0.14 | | 0.00 | |
| 1984 | | 0.11 | | 0.01 | 6.40 | | | | | | 10.46 | 4.68 | | 8.36 | | 1.33 | | | | 0.00 | | | 0.10 | 1.33 | 0.26 | | | | | 0.31 | | 0.00 | |
| 1985 | | 0.00 | 0.00 | 0.02 | 6.05 | | | | | | 9.60 | 4.51 | | 7.41 | | 1.18 | | | 0.08 | 0.09 | | | 0.07 | 1.16 | 0.18 | | | | | 0.29 | | 0.00 | |
| 1986 | | 0.06 | 0.00 | 0.04 | 12.54 | | | | | | 7.04 | 5.00 | | 8.73 | | 1.37 | | | 0.09 | 0.10 | | | 0.04 | 1.88 | 0.74 | | 0.00 | | | 0.36 | | 0.00 | |
| 1987 | | 0.16 | 0.00 | 0.03 | 16.09 | | | | | | 6.04 | 4.44 | | 6.94 | | 1.12 | | | 0.04 | 0.04 | | 1.66 | 0.05 | 5.81 | 0.48 | | 0.00 | | | 0.40 | | 0.00 | |
| 1988 | | 7.31 | 0.01 | 0.04 | 6.86 | | | | | | 7.97 | 3.66 | | 6.20 | | 1.77 | | | 0.01 | 0.01 | | 2.98 | 0.04 | 7.59 | 0.41 | | | | | 0.65 | | 0.00 | |
| 1989 | | 0.22 | 0.03 | 0.19 | 10.21 | | | | | | 9.18 | 3.06 | | 5.69 | | 1.40 | | | 0.04 | 0.04 | 5.64 | 3.44 | 0.10 | 3.76 | 0.51 | | | | | 0.63 | | 0.00 | |
| 1990 | | 0.71 | 0.10 | 0.47 | 14.60 | | | | | | 6.27 | 3.08 | | 5.34 | | 0.79 | | | 0.14 | 0.16 | 5.98 | 8.48 | 0.06 | 8.50 | 0.77 | | | | | 0.60 | | 0.00 | |
| 1991 | | 1.09 | 0.39 | 0.46 | 7.98 | | | | | | 6.17 | 3.67 | | 6.93 | | 0.85 | | | 0.15 | 0.17 | 7.23 | 3.66 | 0.03 | 6.55 | 0.77 | | | | | 0.48 | | 0.00 | |
| 1992 | | 0.10 | 3.55 | 0.65 | 5.72 | | | 8.46 | | | | 3.47 | | 7.16 | | 0.48 | | | 0.05 | 0.06 | 7.77 | 10.03 | 0.01 | 11.60 | 0.67 | | 0.00 | | | 0.19 | | 0.00 | |
| 1993 | | 0.04 | 3.50 | 0.80 | 5.08 | | | 14.31 | | | | | | 9.04 | | | | | 0.04 | 0.04 | 5.80 | | | 11.94 | 2.30 | | | | | | | 0.00 | |
| 1994 | | 1.02 | 2.78 | 0.79 | 4.60 | | 7.17 | 14.55 | 3.31 | 1.65 | | | 0.52 | | 0.63 | | | 0.14 | 0.01 | 0.01 | 4.63 | | | 9.43 | 1.61 | | | | | | | 0.00 | |
| 1995 | | | 2.34 | 1.08 | 3.72 | | 8.44 | 17.44 | 2.79 | 1.59 | | | 0.37 | | 0.74 | | | 0.14 | 0.82 | 0.92 | 3.67 | | | 9.49 | 1.54 | | | | | | | 0.00 | |

*Table 3* (continued). Catch in numbers (1000s) of North Pacific shortfin mako for fisheries listed in *Table 1*.

| Year | 1 | 2 | 3 | 4 | 5 | 6 | 7 | 8 | 9 | 10 | 11 | 12 | 13 | 14 | 15 | 16 | 17 | 18 | 19 | 20 | 21 | 22 | 23 | 24 | 25 | 26 | 27 | 28 | 29 | 30 | 31 | 32 | 33 |
|---|---|---|---|---|---|---|---|---|---|---|---|---|---|---|---|---|---|---|---|---|---|---|---|---|---|---|---|---|---|---|---|---|---|
| 1996 | | | 2.20 | 1.04 | 3.71 | | 9.40 | 10.88 | 2.69 | 9.60 | | | 0.43 | | 0.82 | | | 0.84 | 0.35 | 0.40 | 12.51 | | | 11.29 | 1.99 | | | | | | | 0.00 | |
| 1997 | | | 2.63 | 1.16 | 5.13 | | 10.08 | 10.65 | 3.32 | 4.86 | | | 0.39 | | 0.88 | | | 0.42 | 0.32 | 0.36 | 6.82 | | | 10.71 | 1.87 | | | | | | | 0.00 | |
| 1998 | | | 2.48 | 1.41 | 3.79 | | 10.32 | 11.04 | 3.35 | 0.49 | | | 0.30 | | 0.90 | | | 0.04 | 0.37 | 0.42 | 5.98 | | | 10.72 | 1.41 | | | | | | | 0.00 | |
| 1999 | | | 2.44 | 1.40 | 2.25 | | 11.50 | 16.20 | 4.55 | 5.04 | | | 0.33 | | 1.01 | | | 0.44 | 0.78 | 0.87 | 11.43 | | | 11.48 | 2.14 | | | | | | | 0.00 | |
| 2000 | | | 1.92 | 1.34 | 3.04 | | 13.94 | 11.49 | 4.08 | 2.42 | | | 0.37 | | 1.22 | | | 0.21 | 0.72 | 0.80 | 7.52 | | | 14.38 | 2.76 | | | | | | | 0.00 | |
| 2001 | | | 0.46 | 1.67 | 1.69 | | 13.24 | 9.61 | 4.17 | 4.98 | | | 0.37 | | 1.16 | | | 0.44 | 0.75 | 0.85 | 8.73 | | | 14.48 | 1.83 | | | | | | | 0.00 | |
| 2002 | | | 0.41 | 1.74 | 3.40 | | 11.16 | 9.37 | 3.69 | 2.91 | | | 0.11 | | 0.98 | | | 0.25 | 1.02 | 1.14 | 9.89 | | | 13.65 | 2.56 | | | 0.02 | | | | 0.00 | |
| 2003 | | | 0.26 | 1.84 | 2.83 | | 11.11 | 9.35 | 6.93 | 0.47 | | | 0.14 | | 0.97 | | | 0.04 | 0.66 | 0.74 | 12.50 | | | 12.12 | 3.32 | | | 0.03 | | | 0.01 | 0.00 | |
| 2004 | | | 0.22 | 1.80 | 2.20 | | 13.15 | 7.17 | 4.03 | 0.64 | | | 0.02 | | 1.15 | | | 0.06 | 1.09 | 1.23 | 12.98 | | | 18.40 | 8.92 | | | 0.46 | | | 0.22 | 0.00 | |
| 2005 | | | 0.42 | 1.71 | 1.37 | 1.34 | 14.23 | 6.37 | 4.65 | 1.49 | | | 1.04 | | 1.25 | | | 0.13 | 0.60 | 1.19 | 7.79 | | | 13.36 | 5.85 | | | 0.19 | | | 0.02 | 0.00 | |
| 2006 | | | 0.27 | 1.63 | 1.81 | 1.87 | 14.92 | 7.96 | 5.29 | 0.23 | | | 0.14 | | 1.31 | | | 0.02 | 1.18 | 0.85 | 7.94 | | | 12.88 | 6.84 | | | 0.14 | | | 0.27 | 0.00 | |
| 2007 | | | 0.36 | 1.80 | 1.72 | 0.88 | 17.79 | 7.48 | 7.16 | 1.02 | | | 0.35 | | 1.56 | | | 0.09 | 0.64 | 0.68 | 8.79 | | | 11.48 | 8.96 | | | 0.06 | | | 0.23 | 0.00 | |
| 2008 | | | 0.38 | 2.18 | 1.26 | 0.63 | 14.20 | 4.52 | 6.19 | 2.85 | | | 0.32 | | 1.24 | | | 0.25 | 0.31 | 0.51 | 5.98 | | | 13.26 | 5.38 | | | 0.03 | | | 0.28 | 0.00 | 0.03 |
| 2009 | | | 0.48 | 1.95 | 1.19 | 0.72 | 18.10 | 2.62 | 8.57 | 8.00 | | | 0.03 | | 1.58 | | | 0.70 | 0.32 | 0.67 | 5.88 | | | 14.52 | 5.49 | | | 0.04 | | | 0.44 | 0.00 | 0.12 |
| 2010 | | | 0.61 | 1.36 | 0.83 | 0.40 | 17.54 | 3.16 | 7.97 | 3.54 | | | 0.46 | | 1.54 | | | 0.31 | 0.19 | 0.49 | 8.27 | | | 18.43 | 5.44 | | | 3.23 | 0.00 | | 0.14 | 0.00 | 0.53 |
| 2011 | | | 0.44 | 1.51 | 0.72 | 0.41 | 9.86 | 2.83 | 4.35 | 1.13 | | | 0.27 | | 0.86 | | | 0.10 | 0.41 | 1.17 | 6.98 | | | 17.85 | 6.23 | | | 13.82 | | | 0.29 | 0.00 | 1.93 |
| 2012 | | | 0.39 | 1.33 | 0.92 | 0.87 | 12.59 | 2.52 | 6.24 | 0.23 | | | 0.04 | | 1.10 | | | 0.02 | 0.26 | 0.71 | 6.44 | | | 17.16 | 6.04 | | | 5.65 | 0.03 | | 0.10 | 0.00 | 10.21 |
| 2013 | | | 0.35 | 1.45 | 1.23 | 0.92 | 10.08 | 1.37 | 10.52 | 1.15 | | | 0.23 | | 0.88 | | | 0.10 | 1.01 | 1.17 | 5.18 | | | 16.88 | 6.32 | | | 0.12 | 0.31 | | 0.79 | 0.00 | 14.70 |
| 2014 | | | 0.56 | 1.59 | 0.67 | 0.57 | | 2.70 | 7.96 | 0.18 | | | 0.08 | | 1.27 | | 14.56 | 0.02 | 1.35 | 1.33 | 4.58 | | | 31.93 | 14.50 | | 0.00 | 0.22 | 0.22 | | 1.39 | 0.00 | 9.25 |
| 2015 | | | 0.59 | 1.73 | 0.53 | 0.23 | | 3.92 | 9.90 | 0.05 | | | 0.27 | | 1.24 | | 14.19 | 0.00 | 0.51 | 1.81 | 7.65 | | | 41.87 | 10.45 | | | 1.60 | 0.07 | | 1.22 | 0.00 | 5.44 |
| 2016 | | | 0.42 | 2.40 | 0.74 | 0.21 | | 2.33 | 12.95 | 0.76 | | | 0.37 | | 1.51 | | 17.24 | 0.07 | 0.53 | 1.61 | 5.26 | | | 13.07 | 6.61 | | | 0.93 | 0.03 | | 1.51 | 0.00 | 0.82 |
| 2017 | | | 0.60 | 2.92 | 0.74 | 0.32 | 12.27 | 1.26 | 7.77 | 0.54 | | | 0.23 | | 1.07 | | | 0.05 | 0.14 | 0.52 | 5.53 | | | 9.80 | 1.56 | 21.60 | | 0.44 | 0.03 | | 2.84 | 0.00 | 4.03 |

*Table 3* (continued). Catch in numbers (1000s) of North Pacific shortfin mako for fisheries listed in *Table 1*.

| Year | 1 | 2 | 3 | 4 | 5 | 6 | 7 | 8 | 9 | 10 | 11 | 12 | 13 | 14 | 15 | 16 | 17 | 18 | 19 | 20 | 21 | 22 | 23 | 24 | 25 | 26 | 27 | 28 | 29 | 30 | 31 | 32 | 33 |
|---|---|---|---|---|---|---|---|---|---|---|---|---|---|---|---|---|---|---|---|---|---|---|---|---|---|---|---|---|---|---|---|---|---|
| 2018 | | | 0.27 | 3.14 | 0.67 | 0.34 | 13.91 | 1.38 | 6.34 | 0.44 | | | 0.64 | | 1.22 | | | 0.04 | 0.59 | 0.96 | 4.30 | | | 5.99 | 1.08 | 28.96 | | 2.75 | 0.01 | | 2.82 | 0.00 | 11.03 |
| 2019 | | | 0.31 | 2.38 | 1.11 | 0.23 | 12.42 | 1.39 | 6.06 | 0.35 | | | 0.07 | | 1.09 | | | 0.03 | 1.03 | 1.24 | 5.13 | | | 13.60 | 2.28 | 48.47 | | 2.26 | 0.07 | | 2.33 | 0.00 | 2.08 |
| 2020 | | | 0.65 | 1.96 | 0.27 | 0.08 | 8.28 | 0.96 | 5.57 | 0.09 | | | 0.36 | | 0.72 | | | 0.01 | 1.91 | 1.83 | 3.91 | | | 6.57 | 3.58 | 59.36 | | 1.23 | 0.02 | | 2.29 | 0.00 | 0.14 |
| 2021 | | | 0.38 | 1.30 | 0.31 | 0.05 | 6.70 | 0.85 | 3.90 | 0.37 | | | 0.52 | | 0.59 | | | 0.03 | 1.38 | 1.08 | 3.40 | | | 7.69 | 2.48 | 65.74 | | 0.11 | 0.02 | | 2.58 | 0.00 | 2.77 |
| 2022 | | | 0.45 | 0.73 | 0.19 | 0.16 | 8.96 | 0.42 | 4.74 | 0.11 | | | 1.27 | | 0.78 | | | 0.01 | 1.11 | 1.45 | 3.00 | | | 6.54 | 3.98 | 42.16 | | 0.33 | 0.04 | | 1.43 | 0.00 | 1.74 |

2782

*Table 4.* Catch in metric tons of North Pacific shortfin mako for fisheries listed in *Table 1.*

| Year | 1 | 2 | 3 | 4 | 5 | 6 | 7 | 8 | 9 | 10 | 11 | 12 | 13 | 14 | 15 | 16 | 17 | 18 | 19 | 20 | 21 | 22 | 23 | 24 | 25 | 26 | 27 | 28 | 29 | 30 | 31 | 32 | 33 |
|---|---|---|---|---|---|---|---|---|---|---|---|---|---|---|---|---|---|---|---|---|---|---|---|---|---|---|---|---|---|---|---|---|---|
| 1974 | | | | | | | | | | | | | | 1180 | | | | | | | | | | | | | | | | | | | |
| 1975 | | | | 4 | | | | | | | 232 | 200 | | 721 | | | | | 7 | 5 | | | | | | | | | | | | 0 | |
| 1976 | | | | 5 | | | | | | | 433 | 368 | | 1002 | | | | | 0 | 0 | | | | 66 | 7 | | | | | | | 0 | |
| 1977 | | | | 6 | | | | | | | 588 | 607 | | 1351 | | | | | 2 | 2 | | | | 64 | 8 | | | | | | | 0 | |
| 1978 | | | | 5 | | | | | | | 550 | 371 | | 1097 | | | | | 2 | 2 | | | | 92 | 11 | | | | | | | 0 | |
| 1979 | | | | 2 | | | | | | | 774 | 274 | | 1200 | | | | | 0 | 0 | | | | 43 | 21 | | | | | | | 0 | |
| 1980 | | | | 0 | | | | | | | 918 | 199 | | 1144 | | | | | 2 | 1 | | | | 51 | 14 | | 0 | | | | | 0 | |
| 1981 | | 19 | | 0 | 168 | | | | | | 1076 | 195 | | 1013 | | 3 | | | 1 | 1 | | | 1 | 38 | 19 | | | | | 4 | | 0 | |
| 1982 | | 6 | | 1 | 354 | | | | | | 774 | 196 | | 637 | | 28 | | | 0 | 0 | | | 1 | 61 | 15 | | | | | 4 | | 0 | |
| 1983 | | 1 | | 2 | 223 | | | | | | 842 | 147 | | 510 | | 44 | | | 0 | 0 | | | 2 | 58 | 10 | | | | | 7 | | 0 | |
| 1984 | | 2 | | 1 | 162 | | | | | | 836 | 160 | | 397 | | 63 | | | | 0 | | | 5 | 40 | 10 | | | | | 15 | | 0 | |
| 1985 | | 0 | 0 | 2 | 153 | | | | | | 769 | 154 | | 352 | | 56 | | | 4 | 3 | | | 3 | 35 | 7 | | | | | 14 | | 0 | |
| 1986 | | 1 | 0 | 3 | 319 | | | | | | 565 | 172 | | 416 | | 65 | | | 5 | 4 | | | 2 | 57 | 29 | | 0 | | | 17 | | 0 | |
| 1987 | | 4 | 0 | 2 | 410 | | | | | | 486 | 153 | | 333 | | 54 | | | 2 | 1 | | 57 | 3 | 177 | 19 | | 0 | | | 19 | | 0 | |
| 1988 | | 156 | 0 | 3 | 174 | | | | | | 645 | 126 | | 299 | | 85 | | | 0 | 0 | | 103 | 2 | 231 | 16 | | | | | 31 | | 0 | |
| 1989 | | 5 | 1 | 15 | 258 | | | | | | 747 | 105 | | 274 | | 68 | | | 2 | 1 | 240 | 118 | 5 | 114 | 20 | | | | | 31 | | 0 | |
| 1990 | | 15 | 5 | 36 | 368 | | | | | | 512 | 105 | | 257 | | 38 | | | 8 | 6 | 254 | 290 | 3 | 257 | 30 | | | | | 29 | | 0 | |
| 1991 | | 23 | 19 | 35 | 201 | | | | | | 505 | 126 | | 333 | | 41 | | | 8 | 6 | 307 | 125 | 2 | 198 | 30 | | | | | 23 | | 0 | |
| 1992 | | 2 | 175 | 51 | 144 | | | 694 | | | | 119 | | 344 | | 23 | | | 3 | 2 | 330 | 343 | 1 | 350 | 26 | | 0 | | | 9 | | 0 | |
| 1993 | | 1 | 168 | 62 | 125 | | | 1174 | | | | | | 431 | | | | | 2 | 2 | 245 | | | 354 | 89 | | | | | | | 0 | |
| 1994 | | 21 | 129 | 61 | 111 | | 336 | 1189 | 110 | 69 | | | 22 | | 6 | | | 6 | 0 | 0 | 193 | | | 274 | 61 | | | | | | | 0 | |
| 1995 | | | 108 | 82 | 91 | | 389 | 1416 | 93 | 65 | | | 15 | | 8 | | | 6 | 43 | 31 | 150 | | | 276 | 58 | | | | | | | 0 | |
| 1996 | | | 104 | 78 | 94 | | 435 | 875 | 91 | 399 | | | 18 | | 9 | | | 35 | 18 | 13 | 513 | | | 337 | 76 | | | | | | | 0 | |

*Table 4.* Catch in metric tons of North Pacific shortfin mako for fisheries listed in *Table 1.*

| Year | 1 | 2 | 3 | 4 | 5 | 6 | 7 | 8 | 9 | 10 | 11 | 12 | 13 | 14 | 15 | 16 | 17 | 18 | 19 | 20 | 21 | 22 | 23 | 24 | 25 | 26 | 27 | 28 | 29 | 30 | 31 | 32 | 33 |
|---|---|---|---|---|---|---|---|---|---|---|---|---|---|---|---|---|---|---|---|---|---|---|---|---|---|---|---|---|---|---|---|---|---|
| 1997 | | | 127 | 88 | 133 | | 476 | 851 | 114 | 206 | | | 17 | | 9 | | | 18 | 17 | 12 | 285 | | | 328 | 73 | | | | | | | 0 | |
| 1998 | | | 123 | 107 | 99 | | 496 | 885 | 117 | 21 | | | 13 | | 9 | | | 2 | 20 | 15 | 255 | | | 332 | 56 | | | | | | | 0 | |
| 1999 | | | 121 | 107 | 58 | | 560 | 1311 | 158 | 219 | | | 14 | | 10 | | | 19 | 42 | 31 | 492 | | | 353 | 85 | | | | | | | 0 | |
| 2000 | | | 94 | 104 | 76 | | 675 | 941 | 140 | 104 | | | 16 | | 12 | | | 9 | 39 | 28 | 322 | | | 431 | 108 | | | | | | | 0 | |
| 2001 | | | 22 | 130 | 41 | | 630 | 792 | 140 | 210 | | | 16 | | 11 | | | 18 | 40 | 29 | 368 | | | 422 | 70 | | | | | | | 0 | |
| 2002 | | | 19 | 134 | 82 | | 520 | 771 | 122 | 120 | | | 5 | | 10 | | | 11 | 54 | 38 | 408 | | | 392 | 96 | | | 1 | | | | 0 | |
| 2003 | | | 12 | 140 | 68 | | 511 | 762 | 229 | 19 | | | 6 | | 10 | | | 2 | 34 | 25 | 510 | | | 348 | 124 | | | 3 | | | 1 | 0 | |
| 2004 | | | 10 | 136 | 53 | | 602 | 579 | 134 | 26 | | | 1 | | 12 | | | 2 | 56 | 41 | 529 | | | 530 | 334 | | | 37 | | | 18 | 0 | |
| 2005 | | | 19 | 128 | 33 | 61 | 652 | 510 | 155 | 61 | | | 43 | | 13 | | | 5 | 31 | 39 | 318 | | | 388 | 220 | | | 15 | | | 2 | 0 | |
| 2006 | | | 12 | 121 | 45 | 86 | 689 | 635 | 178 | 10 | | | 6 | | 13 | | | 1 | 61 | 29 | 326 | | | 380 | 260 | | | 11 | | | 21 | 0 | |
| 2007 | | | 17 | 135 | 43 | 41 | 832 | 596 | 244 | 43 | | | 15 | | 16 | | | 4 | 33 | 23 | 365 | | | 344 | 345 | | | 5 | | | 18 | 0 | |
| 2008 | | | 18 | 164 | 32 | 30 | 673 | 362 | 212 | 121 | | | 14 | | 13 | | | 11 | 17 | 18 | 251 | | | 400 | 209 | | | 2 | | | 22 | 0 | 2 |
| 2009 | | | 23 | 148 | 30 | 35 | 864 | 211 | 294 | 342 | | | 1 | | 16 | | | 30 | 17 | 23 | 249 | | | 438 | 214 | | | 3 | | | 35 | 0 | 10 |
| 2010 | | | 29 | 104 | 21 | 19 | 839 | 256 | 272 | 151 | | | 20 | | 15 | | | 13 | 10 | 17 | 350 | | | 550 | 211 | | | 262 | 0 | | 11 | 0 | 43 |
| 2011 | | | 20 | 116 | 17 | 19 | 466 | 231 | 146 | 48 | | | 11 | | 9 | | | 4 | 22 | 40 | 293 | | | 520 | 238 | | | 1127 | | | 24 | 0 | 156 |
| 2012 | | | 18 | 101 | 22 | 39 | 583 | 205 | 206 | 10 | | | 2 | | 11 | | | 1 | 13 | 24 | 265 | | | 488 | 226 | | | 459 | 2 | | 8 | 0 | 830 |
| 2013 | | | 15 | 109 | 29 | 40 | 459 | 111 | 345 | 47 | | | 9 | | 9 | | | 4 | 52 | 38 | 210 | | | 478 | 234 | | | 10 | 25 | | 64 | 0 | 1194 |
| 2014 | | | 25 | 118 | 16 | 25 | | 216 | 263 | 7 | | | 3 | | 13 | | 558 | 1 | 69 | 44 | 185 | | | 925 | 542 | | 0 | 17 | 18 | | 111 | 0 | 752 |
| 2015 | | | 27 | 129 | 13 | 11 | | 311 | 334 | 2 | | | 11 | | 13 | | 557 | 0 | 26 | 61 | 313 | | | 1253 | 400 | | | 127 | 5 | | 97 | 0 | 442 |
| 2016 | | | 20 | 179 | 19 | 10 | | 185 | 446 | 32 | | | 16 | | 16 | | 694 | 3 | 28 | 55 | 220 | | | 401 | 259 | | | 74 | 2 | | 120 | 0 | 67 |
| 2017 | | | 30 | 221 | 19 | 16 | 592 | 100 | 271 | 23 | | | 10 | | 11 | | | 2 | 8 | 18 | 236 | | | 306 | 62 | 568 | | 35 | 2 | | 227 | 0 | 327 |
| 2018 | | | 14 | 241 | 18 | 17 | 684 | 111 | 223 | 19 | | | 28 | | 12 | | | 2 | 32 | 34 | 187 | | | 189 | 43 | 765 | | 223 | 1 | | 228 | 0 | 896 |
| 2019 | | | 16 | 187 | 29 | 12 | 621 | 115 | 214 | 15 | | | 3 | | 11 | | | 1 | 58 | 45 | 226 | | | 430 | 93 | 1273 | | 186 | 5 | | 192 | 0 | 169 |

*Table 4.* Catch in metric tons of North Pacific shortfin mako for fisheries listed in *Table 1*.

| Year | 1 | 2 | 3 | 4 | 5 | 6 | 7 | 8 | 9 | 10 | 11 | 12 | 13 | 14 | 15 | 16 | 17 | 18 | 19 | 20 | 21 | 22 | 23 | 24 | 25 | 26 | 27 | 28 | 29 | 30 | 31 | 32 | 33 |
|---|---|---|---|---|---|---|---|---|---|---|---|---|---|---|---|---|---|---|---|---|---|---|---|---|---|---|---|---|---|---|---|---|---|
| 2020 | | | 34 | 157 | 7 | 4 | 417 | 81 | 194 | 4 | | | 16 | | 7 | | | 0 | 108 | 66 | 174 | | | 205 | 145 | 1528 | | 103 | 2 | | 193 | 0 | 11 |
| 2021 | | | 20 | 106 | 8 | 3 | 335 | 72 | 133 | 16 | | | 23 | | 6 | | | 1 | 78 | 38 | 149 | | | 235 | 99 | 1658 | | 9 | 2 | | 220 | 0 | 225 |
| 2022 | | | 23 | 59 | 5 | 8 | 439 | 36 | 160 | 5 | | | 55 | | 8 | | | 0 | 62 | 50 | 129 | | | 197 | 157 | 1044 | | 28 | 4 | | 123 | 0 | 141 |

*Table 5.* Indices of relative abundance for North Pacific shortfin mako corresponding to the fisheries named in *Table 1.*

| Year | S1 | S1: CV | S2 | S2: CV | S3 | S3: CV | S4 | S4: CV | S5 | S5: CV | S6 | S6: CV | S7 | S7: CV | S8 | S8: CV | S9 | S9: CV | S10 | S10: CV |
|---|---|---|---|---|---|---|---|---|---|---|---|---|---|---|---|---|---|---|---|---|
| 1994 | | | | | 1.47 | 0.15 | | | 0.41 | 0.25 | 0.18 | 0.15 | 1.09 | 1.09 | | | | | | |
| 1995 | | | | | 1.24 | 0.07 | | | 0.51 | 0.23 | 0.27 | 0.15 | 0.99 | 0.99 | | | | | | |
| 1996 | | | | | 1.19 | 0.10 | | | 0.65 | 0.20 | 0.43 | 0.14 | 1.03 | 1.03 | | | | | | |
| 1997 | | | | | 0.94 | 0.10 | | | 0.63 | 0.19 | 0.42 | 0.14 | 1.03 | 1.03 | | | | | | |
| 1998 | | | | | | | | | 0.65 | 0.17 | 0.50 | 0.13 | 1.09 | 1.09 | | | | | | |
| 1999 | | | | | | | | | 0.66 | 0.17 | 0.48 | 0.12 | 1.33 | 1.33 | | | | | | |
| 2000 | 0.55 | 0.34 | 0.57 | 0.34 | 0.78 | 0.05 | | | 0.65 | 0.16 | 0.48 | 0.12 | 1.37 | 1.37 | | | | | | |
| 2001 | 0.85 | 0.33 | 0.87 | 0.32 | 1.18 | 0.10 | | | 0.73 | 0.15 | 0.58 | 0.12 | 1.01 | 1.01 | | | | | | |
| 2002 | 0.64 | 0.33 | 0.67 | 0.33 | 1.03 | 0.07 | | | 0.66 | 0.16 | 0.50 | 0.13 | 1.10 | 1.10 | | | | | | |
| 2003 | 0.71 | 0.33 | 0.72 | 0.33 | 0.97 | 0.05 | | | 0.75 | 0.13 | 0.62 | 0.11 | 1.17 | 1.17 | | | | | | |
| 2004 | 0.46 | 0.33 | 0.48 | 0.33 | 0.93 | 0.04 | | | 0.81 | 0.14 | 0.68 | 0.12 | 1.10 | 1.10 | | | | | | |
| 2005 | 0.74 | 0.33 | 0.74 | 0.33 | 0.97 | 0.07 | 0.54 | 0.06 | 0.96 | 0.12 | 0.86 | 0.11 | 1.09 | 1.09 | | | | | | |
| 2006 | 0.60 | 0.33 | 0.65 | 0.33 | 0.94 | 0.04 | 0.66 | 0.04 | 1.00 | 0.13 | 0.89 | 0.12 | 1.37 | 1.37 | 1.70 | 0.22 | 2.19 | 0.29 | 1.44 | 0.55 |
| 2007 | 0.81 | 0.33 | 0.81 | 0.33 | 0.92 | 0.07 | 0.51 | 0.05 | 1.06 | 0.12 | 0.95 | 0.11 | 1.74 | 1.74 | 0.85 | 0.47 | 0.79 | 0.19 | 0.86 | 0.38 |
| 2008 | 0.97 | 0.33 | 0.97 | 0.34 | 0.79 | 0.04 | 0.23 | 0.12 | 0.91 | 0.14 | 0.84 | 0.13 | 1.07 | 1.07 | 0.83 | 0.33 | 0.51 | 0.30 | 1.29 | 0.24 |
| 2009 | 0.93 | 0.33 | 0.92 | 0.33 | 0.84 | 0.05 | 0.40 | 0.12 | 1.21 | 0.12 | 1.10 | 0.12 | 0.86 | 0.86 | 0.75 | 0.39 | 1.14 | 0.18 | 0.78 | 0.58 |
| 2010 | 0.76 | 0.33 | 0.80 | 0.33 | 0.76 | 0.03 | 0.32 | 0.13 | 1.14 | 0.13 | 1.08 | 0.13 | 0.93 | 0.93 | 0.67 | 0.30 | 0.70 | 0.21 | 0.87 | 0.41 |
| 2011 | 0.96 | 0.33 | 0.90 | 0.33 | 0.84 | 0.03 | 0.70 | 0.12 | 1.30 | 0.15 | 1.33 | 0.15 | 0.67 | 0.67 | 1.21 | 0.25 | 0.72 | 0.44 | 1.91 | 0.40 |
| 2012 | 0.78 | 0.33 | 0.79 | 0.33 | 1.05 | 0.06 | 0.88 | 0.08 | 1.40 | 0.15 | 1.47 | 0.15 | 0.71 | 0.71 | 1.93 | 0.26 | 1.90 | 0.34 | 1.35 | 0.74 |
| 2013 | 1.04 | 0.33 | 1.03 | 0.33 | 1.16 | 0.08 | 1.36 | 0.03 | 1.16 | 0.16 | 1.12 | 0.16 | 0.34 | 0.34 | 1.03 | 0.28 | 0.81 | 0.45 | 1.81 | 0.41 |
| 2014 | 1.03 | 0.33 | 1.04 | 0.33 | | | 1.36 | 0.05 | 1.56 | 0.15 | 1.78 | 0.16 | 0.76 | 0.76 | 0.70 | 0.42 | 0.66 | 0.21 | 0.91 | 0.34 |
| 2015 | 1.25 | 0.33 | 1.26 | 0.33 | | | 1.16 | 0.06 | 1.52 | 0.15 | 1.86 | 0.17 | 1.32 | 1.32 | 1.02 | 0.23 | 0.71 | 0.16 | 0.67 | 0.39 |

*Table 5 (continued).* Indices of relative abundance for North Pacific shortfin mako corresponding to the fisheries named in *Table 1*.

| Year | S1 | S1: CV | S2 | S2: CV | S3 | S3: CV | S4 | S4: CV | S5 | S5: CV | S6 | S6: CV | S7 | S7: CV | S8 | S8: CV | S9 | S9: CV | S10 | S10: CV |
|---|---|---|---|---|---|---|---|---|---|---|---|---|---|---|---|---|---|---|---|---|
| 2016 | 1.36 | 0.33 | 1.38 | 0.33 | | | 1.17 | 0.05 | 1.42 | 0.16 | 1.73 | 0.18 | 1.09 | 1.09 | 0.72 | 0.09 | 0.83 | 0.21 | 0.84 | 0.36 |
| 2017 | 1.78 | 0.33 | 1.97 | 0.33 | | | 1.16 | 0.06 | 1.40 | 0.17 | 1.77 | 0.19 | 0.75 | 0.75 | 0.81 | 0.33 | 0.47 | 0.34 | 1.62 | 0.28 |
| 2018 | 1.63 | 0.33 | 1.63 | 0.33 | | | 1.46 | 0.03 | 1.39 | 0.19 | 2.03 | 0.21 | 0.85 | 0.85 | 0.34 | 0.41 | 0.32 | 0.09 | 0.41 | 0.26 |
| 2019 | 1.46 | 0.33 | 1.51 | 0.33 | | | 1.30 | 0.03 | 1.24 | 0.18 | 1.60 | 0.20 | 0.78 | 0.78 | 1.53 | 0.23 | 1.94 | 0.18 | 0.88 | 0.71 |
| 2020 | 1.70 | 0.33 | 1.29 | 0.33 | | | 2.14 | 0.03 | 0.98 | 0.18 | 1.00 | 0.18 | 0.67 | 0.67 | 0.58 | 0.48 | 0.75 | 0.14 | 0.60 | 0.44 |
| 2021 | | | | | | | 1.34 | 0.03 | 1.10 | 0.18 | 1.09 | 0.17 | 0.92 | 0.92 | 1.99 | 0.24 | 2.20 | 0.09 | 0.40 | 0.49 |
| 2022 | | | | | | | 1.31 | 0.03 | 1.15 | 0.18 | 1.35 | 0.20 | 0.79 | 0.79 | 0.33 | 0.44 | 0.38 | 0.08 | 0.35 | 0.32 |

*Table 6.* Bayesian state-space surplus production model (BSPM) inputs: removals and effort.

| Year | Total removals (1000s) | Removals: non-longline (1000s) | Effort (hooks, millions) | Effort (scaled) |
|---|---|---|---|---|
| 1994 | 52.83 | 8.43 | 103.90 | 0.50 |
| 1995 | 55.08 | 6.89 | 98.61 | 0.47 |
| 1996 | 68.17 | 6.83 | 90.09 | 0.43 |
| 1997 | 59.64 | 8.85 | 90.11 | 0.43 |
| 1998 | 53.05 | 7.44 | 90.12 | 0.43 |
| 1999 | 71.88 | 7.13 | 103.04 | 0.49 |
| 2000 | 66.24 | 7.48 | 85.58 | 0.41 |
| 2001 | 64.44 | 6.23 | 104.05 | 0.50 |
| 2002 | 62.33 | 7.20 | 101.48 | 0.49 |
| 2003 | 63.35 | 9.89 | 126.04 | 0.60 |
| 2004 | 73.75 | 6.25 | 143.45 | 0.69 |
| 2005 | 63.01 | 8.41 | 155.67 | 0.75 |
| 2006 | 65.57 | 9.11 | 159.13 | 0.76 |
| 2007 | 71.06 | 10.11 | 206.22 | 0.99 |
| 2008 | 59.83 | 8.41 | 208.35 | 1.00 |
| 2009 | 71.47 | 10.52 | 185.50 | 0.89 |
| 2010 | 74.47 | 9.67 | 147.60 | 0.71 |
| 2011 | 71.18 | 5.75 | 179.22 | 0.86 |
| 2012 | 72.87 | 8.07 | 159.99 | 0.77 |
| 2013 | 74.78 | 12.90 | 108.17 | 0.52 |
| 2014 | 94.94 | 23.85 | 140.24 | 0.67 |
| 2015 | 103.23 | 25.11 | 133.09 | 0.64 |
| 2016 | 69.30 | 31.51 | 141.40 | 0.68 |
| 2017 | 74.22 | 30.66 | 112.92 | 0.54 |
| 2018 | 86.83 | 36.95 | 110.29 | 0.53 |
| 2019 | 103.90 | 55.95 | 145.18 | 0.70 |
| 2020 | 99.73 | 65.64 | 125.94 | 0.60 |
| 2021 | 102.17 | 70.53 | 112.37 | 0.54 |
| 2022 | 79.52 | 48.52 | 121.34 | 0.58 |

*Table 7.* Priors used for leading parameters in the Bayesian state-space surplus production model (BSPM).

| Parameter | Type | | Prior |
|---|---|---|---|
| Intrinsic rate of increase $R_{Max}$ | Ensemble | Baseline | $R_{Max} \sim \text{Lognormal}(-2.52, 0.41)$ |
| | Ensemble | Extreme | $R_{Max} \sim \text{Lognormal}(-2.10, 0.20)$ |
| Initial depletion $x_0$ | Ensemble | Baseline | $x_0 \sim \text{Lognormal}(-1.10, 0.59)$ |
| | Ensemble | Extreme | $x_0 \sim \text{Lognormal}(-2.04, 0.39)$ |
| Shape $n$ | Ensemble | Baseline | $n \sim \text{Lognormal}(1.02, 0.43)$ |
| | Ensemble | Extreme | $n \sim \text{Lognormal}(0.60, 0.22)$ |
| Carrying capacity $K$ | Ensemble | | $K \sim \text{Lognormal}(16,1)$ |
| Process error $\sigma_P$ | Ensemble | | $\sigma_P \sim \text{Lognormal}(-2.93,0.27)$ |
| | Sensitivity | | $\sigma_P \sim \text{Normal}^{+}(0,1)$ |
| Additional observation error $\sigma_{O_{Add}}$ | Ensemble | | $\sigma_{O_{Add}} \sim \text{Normal}^{+}(0,0.2)$ |
| Longline catchability $q$ | Ensemble | | $q \sim \text{Lognormal}(-2.32,0.51)$ |
| Fishing mortality error $\sigma_F$ | Ensemble | Est. (F - L) | $\sigma_F \sim \text{Normal}^{+}(0,0.0125)$ |
| | Ensemble | Est. (F - M) | $\sigma_F \sim \text{Normal}^{+}(0,0.025)$ |
| | Ensemble | Est. (F - H) | $\sigma_F \sim \text{Normal}^{+}(0,0.05)$ |

2795 *Table 8.* Fixed catch sensitivity scenarios.

| Scenario label | Catch magnitude assumption | Historical under-reporting assumption |
|---|---|---|
| 1: bb | Observed levels | No under-reporting |
| 2: 50b | 50% higher than observed | `` |
| 3: 100b | 100% higher than observed | `` |
| 4: b50 | Observed levels | 1994 catches 50% higher than observed, linearly declining to match observed in 2022 |
| 5: 5050 | 50% higher than observed | `` |
| 6: 10050 | 100% higher than observed | `` |
| 7: b100 | Observed levels | 1994 catches 100% higher than observed, linearly declining to match observed in 2022 |
| 8: 50100 | 50% higher than observed | `` |
| 9: 100100 | 100% higher than observed | `` |

2796

*Table 9.* Model configuration, ensemble weight and diagnostics for each model in the Bayesian state-space surplus production model (BSPM) ensemble.

| Model | Weight (relative) | Index | Prior type | Catch | Divergences | $\widehat{R}$ | $N_{eff}$ | Converged | RMSE | Mohn's $\rho$ | Coverage ($D/D_{MSY}$) | Coverage ($U/U_{MSY}$) | MASE |
|---|---|---|---|---|---|---|---|---|---|---|---|---|---|
| 1 | 0.026 | 1 | Baseline | Est. (Longline) | 0 | 1.007 | 639 | Y | 0.202 | -0.011 | 100% | 100% | 1.821 |
| 2 | 0.026 | 2 | Baseline | Est. (Longline) | 0 | 1.006 | 876 | Y | 0.225 | 0.001 | 100% | 100% | 1.387 |
| 3 | 0.053 | 4 | Baseline | Est. (Longline) | 0 | 1.008 | 717 | Y | 0.312 | -0.018 | 100% | 100% | 0.763 |
| 4 | 0.053 | 5 | Baseline | Est. (Longline) | 0 | 1.003 | 754 | Y | 0.133 | -0.059 | 100% | 100% | 1.870 |
| 5 | 0.026 | 1 | Extreme | Est. (Longline) | 0 | 1.011 | 815 | N | 0.191 | -0.035 | 100% | 100% | 1.376 |
| 6 | 0.026 | 2 | Extreme | Est. (Longline) | 0 | 1.004 | 805 | Y | 0.215 | -0.045 | 100% | 100% | 1.164 |
| 7 | 0.053 | 4 | Extreme | Est. (Longline) | 0 | 1.004 | 667 | Y | 0.308 | 0.004 | 100% | 100% | 0.824 |
| 8 | 0.053 | 5 | Extreme | Est. (Longline) | 1 | 1.009 | 698 | N | 0.134 | 0.026 | 100% | 100% | 2.253 |
| 9 | 0.5 | 1 | Baseline | Est. (F - H) | 0 | 1.006 | 798 | Y | 0.202 | 0.036 | 100% | 100% | 1.721 |
| 10 | 0.5 | 2 | Baseline | Est. (F - H) | 0 | 1.007 | 789 | Y | 0.221 | 0.003 | 100% | 100% | 1.322 |
| 11 | 1 | 4 | Baseline | Est. (F - H) | 0 | 1.007 | 794 | Y | 0.326 | -0.007 | 100% | 100% | 0.772 |
| 12 | 1 | 5 | Baseline | Est. (F - H) | 0 | 1.012 | 630 | N | 0.136 | -0.100 | 100% | 100% | 1.962 |
| 13 | 0.5 | 1 | Extreme | Est. (F - H) | 0 | 1.005 | 807 | Y | 0.186 | -0.023 | 100% | 100% | 1.191 |
| 14 | 0.5 | 2 | Extreme | Est. (F - H) | 0 | 1.006 | 839 | Y | 0.212 | -0.014 | 100% | 100% | 1.116 |
| 15 | 1 | 4 | Extreme | Est. (F - H) | 0 | 1.008 | 772 | Y | 0.313 | -0.028 | 100% | 100% | 0.828 |
| 16 | 1 | 5 | Extreme | Est. (F - H) | 0 | 1.006 | 763 | Y | 0.138 | -0.060 | 100% | 100% | 2.688 |
| 17 | 0.5 | 1 | Baseline | Est. (F - M) | 0 | 1.006 | 769 | Y | 0.203 | 0.036 | 100% | 100% | 1.720 |
| 18 | 0.5 | 2 | Baseline | Est. (F - M) | 0 | 1.009 | 703 | Y | 0.221 | 0.042 | 100% | 100% | 1.333 |
| 19 | 1 | 4 | Baseline | Est. (F - M) | 0 | 1.007 | 767 | Y | 0.326 | 0.025 | 100% | 100% | 0.748 |
| 20 | 1 | 5 | Baseline | Est. (F - M) | 0 | 1.007 | 667 | Y | 0.137 | -0.105 | 100% | 100% | 1.916 |
| 21 | 0.5 | 1 | Extreme | Est. (F - M) | 0 | 1.006 | 600 | Y | 0.185 | 0.005 | 100% | 100% | 1.110 |

*Table 9 (continued).* Model configuration, ensemble weight and diagnostics for each model in the Bayesian state-space surplus production model (BSPM) ensemble.

| Model | Weight (relative) | Index | Prior type | Catch | Divergences | $\widehat{R}$ | $N_{eff}$ | Converged | RMSE | Mohn's $\rho$ | Coverage ($D/D_{MSY}$) | Coverage ($U/U_{MSY}$) | MASE |
|---|---|---|---|---|---|---|---|---|---|---|---|---|---|
| 22 | 0.5 | 2 | Extreme | Est. (F - M) | 0 | 1.007 | 813 | Y | 0.211 | 0.045 | 100% | 100% | 1.026 |
| 23 | 1 | 4 | Extreme | Est. (F - M) | 0 | 1.007 | 797 | Y | 0.312 | 0.007 | 100% | 100% | 0.831 |
| 24 | 1 | 5 | Extreme | Est. (F - M) | 0 | 1.007 | 842 | Y | 0.139 | -0.092 | 100% | 100% | 2.774 |
| 25 | 0.5 | 1 | Baseline | Est. (F - L) | 0 | 1.009 | 566 | Y | 0.203 | 0.051 | 100% | 100% | 1.731 |
| 26 | 0.5 | 2 | Baseline | Est. (F - L) | 0 | 1.006 | 768 | Y | 0.222 | 0.051 | 100% | 100% | 1.307 |
| 27 | 1 | 4 | Baseline | Est. (F - L) | 0 | 1.006 | 785 | Y | 0.325 | 0.010 | 100% | 100% | 0.756 |
| 28 | 1 | 5 | Baseline | Est. (F - L) | 0 | 1.005 | 785 | Y | 0.135 | -0.107 | 100% | 100% | 1.932 |
| 29 | 0.5 | 1 | Extreme | Est. (F - L) | 0 | 1.01 | 667 | Y | 0.186 | 0.013 | 100% | 100% | 1.115 |
| 30 | 0.5 | 2 | Extreme | Est. (F - L) | 0 | 1.012 | 696 | N | 0.212 | 0.023 | 100% | 100% | 1.014 |
| 31 | 1 | 4 | Extreme | Est. (F - L) | 0 | 1.006 | 789 | Y | 0.312 | -0.020 | 100% | 100% | 0.837 |
| 32 | 1 | 5 | Extreme | Est. (F - L) | 0 | 1.005 | 770 | Y | 0.14 | -0.103 | 100% | 100% | 2.795 |

*Table 10*. Model configuration, ensemble weight and median estimates of leading parameters for each model in the Bayesian state-space surplus production model (BSPM) ensemble.

| Model | Weight (relative) | Index | Prior type | Catch | Converged | $R_{Max}$ | $K$ | $x_0$ | $n$ | $\sigma_P$ | $q$ | $\sigma_{O_{Add}}$ | $\sigma_F$ |
|---|---|---|---|---|---|---|---|---|---|---|---|---|---|
| 1 | 0.026 | 1 | Baseline | Est. (Longline) | Y | 0.121 | 11,503,792 | 0.174 | 3.175 | 0.054 | 0.058 | 0.019 | |
| 2 | 0.026 | 2 | Baseline | Est. (Longline) | Y | 0.113 | 11,084,818 | 0.183 | 3.033 | 0.055 | 0.058 | 0.019 | |
| 3 | 0.053 | 4 | Baseline | Est. (Longline) | Y | 0.126 | 11,464,144 | 0.145 | 3.225 | 0.060 | 0.052 | 0.149 | |
| 4 | 0.053 | 5 | Baseline | Est. (Longline) | Y | 0.123 | 7,586,497 | 0.213 | 3.019 | 0.054 | 0.055 | 0.008 | |
| 5 | 0.026 | 1 | Extreme | Est. (Longline) | N | 0.132 | 10,827,525 | 0.110 | 1.867 | 0.053 | 0.062 | 0.018 | |
| 6 | 0.026 | 2 | Extreme | Est. (Longline) | Y | 0.131 | 10,745,383 | 0.112 | 1.859 | 0.053 | 0.066 | 0.017 | |
| 7 | 0.053 | 4 | Extreme | Est. (Longline) | Y | 0.139 | 9,924,718 | 0.097 | 1.886 | 0.057 | 0.057 | 0.140 | |
| 8 | 0.053 | 5 | Extreme | Est. (Longline) | N | 0.129 | 6,034,203 | 0.131 | 1.812 | 0.052 | 0.066 | 0.007 | |
| 9 | 0.5 | 1 | Baseline | Est. (F - H) | Y | 0.094 | 10,561,573 | 0.223 | 2.971 | 0.052 | | 0.018 | 0.026 |
| 10 | 0.5 | 2 | Baseline | Est. (F - H) | Y | 0.095 | 9,930,773 | 0.237 | 2.879 | 0.052 | | 0.018 | 0.027 |
| 11 | 1 | 4 | Baseline | Est. (F - H) | Y | 0.098 | 10,403,004 | 0.213 | 3.010 | 0.057 | | 0.158 | 0.027 |
| 12 | 1 | 5 | Baseline | Est. (F - H) | N | 0.107 | 9,380,736 | 0.288 | 2.902 | 0.051 | | 0.007 | 0.021 |
| 13 | 0.5 | 1 | Extreme | Est. (F - H) | Y | 0.122 | 9,575,731 | 0.132 | 1.823 | 0.052 | | 0.018 | 0.043 |
| 14 | 0.5 | 2 | Extreme | Est. (F - H) | Y | 0.122 | 9,702,316 | 0.137 | 1.845 | 0.050 | | 0.018 | 0.043 |
| 15 | 1 | 4 | Extreme | Est. (F - H) | Y | 0.123 | 10,140,157 | 0.129 | 1.826 | 0.054 | | 0.150 | 0.041 |
| 16 | 1 | 5 | Extreme | Est. (F - H) | Y | 0.123 | 8,107,936 | 0.178 | 1.735 | 0.052 | | 0.008 | 0.037 |
| 17 | 0.5 | 1 | Baseline | Est. (F - M) | Y | 0.087 | 13,441,071 | 0.243 | 2.827 | 0.053 | | 0.016 | 0.019 |
| 18 | 0.5 | 2 | Baseline | Est. (F - M) | Y | 0.086 | 13,409,960 | 0.252 | 2.904 | 0.052 | | 0.018 | 0.018 |
| 19 | 1 | 4 | Baseline | Est. (F - M) | Y | 0.090 | 12,930,570 | 0.222 | 2.999 | 0.057 | | 0.163 | 0.020 |
| 20 | 1 | 5 | Baseline | Est. (F - M) | Y | 0.104 | 10,762,256 | 0.303 | 2.925 | 0.051 | | 0.008 | 0.017 |
| 21 | 0.5 | 1 | Extreme | Est. (F - M) | Y | 0.118 | 12,565,512 | 0.143 | 1.812 | 0.052 | | 0.016 | 0.028 |

*Table 10 (continued).* Model configuration, ensemble weight and median estimates of leading parameters for each model in the Bayesian state-space surplus production model (BSPM) ensemble.

| Model | Weight (relative) | Index | Prior type | Catch | Converged | $R_{Max}$ | $K$ | $x_0$ | $n$ | $\sigma_P$ | $q$ | $\sigma_{O_{Add}}$ | $\sigma_F$ |
|---|---|---|---|---|---|---|---|---|---|---|---|---|---|
| 22 | 0.5 | 2 | Extreme | Est. (F - M) | Y | 0.114 | 12,595,141 | 0.142 | 1.800 | 0.051 | | 0.016 | 0.028 |
| 23 | 1 | 4 | Extreme | Est. (F - M) | Y | 0.119 | 13,467,789 | 0.134 | 1.810 | 0.054 | | 0.147 | 0.026 |
| 24 | 1 | 5 | Extreme | Est. (F - M) | Y | 0.120 | 10,106,643 | 0.199 | 1.755 | 0.051 | | 0.008 | 0.026 |
| 25 | 0.5 | 1 | Baseline | Est. (F - L) | Y | 0.083 | 17,817,997 | 0.257 | 2.959 | 0.052 | | 0.017 | 0.013 |
| 26 | 0.5 | 2 | Baseline | Est. (F - L) | Y | 0.082 | 16,932,888 | 0.268 | 2.863 | 0.051 | | 0.016 | 0.013 |
| 27 | 1 | 4 | Baseline | Est. (F - L) | Y | 0.087 | 18,749,846 | 0.234 | 2.926 | 0.058 | | 0.159 | 0.013 |
| 28 | 1 | 5 | Baseline | Est. (F - L) | Y | 0.102 | 15,204,333 | 0.316 | 2.873 | 0.051 | | 0.008 | 0.011 |
| 29 | 0.5 | 1 | Extreme | Est. (F - L) | Y | 0.115 | 18,998,009 | 0.159 | 1.817 | 0.052 | | 0.017 | 0.015 |
| 30 | 0.5 | 2 | Extreme | Est. (F - L) | N | 0.112 | 18,573,343 | 0.160 | 1.804 | 0.052 | | 0.016 | 0.015 |
| 31 | 1 | 4 | Extreme | Est. (F - L) | Y | 0.118 | 20,019,746 | 0.141 | 1.830 | 0.054 | | 0.150 | 0.015 |
| 32 | 1 | 5 | Extreme | Est. (F - L) | Y | 0.119 | 14,997,418 | 0.224 | 1.772 | 0.051 | | 0.008 | 0.015 |

*Table 11.* Model configuration, ensemble weight and median estimates of stock status and management reference points for each model in the Bayesian state-space surplus production model (BSPM) ensemble.

| Model | Weight (relative) | Index | Prior type | Catch | Converged | $MSY$ | $D_{MSY}$ | $U_{MSY}$ | $D_{2019-2022}$ | $U_{2018-2022}$ | $\frac{D_{2019-2022}}{D_{MSY}}$ | $\frac{U_{2018-2022}}{U_{MSY}}$ |
|---|---|---|---|---|---|---|---|---|---|---|---|---|
| 1 | 0.026 | 1 | Baseline | Est. (Longline) | Y | 384,575 | 0.588 | 0.060 | 0.553 | 0.047 | 0.954 | 0.781 |
| 2 | 0.026 | 2 | Baseline | Est. (Longline) | Y | 356,932 | 0.579 | 0.057 | 0.537 | 0.046 | 0.940 | 0.802 |
| 3 | 0.053 | 4 | Baseline | Est. (Longline) | Y | 404,345 | 0.591 | 0.063 | 0.620 | 0.042 | 1.058 | 0.694 |
| 4 | 0.053 | 5 | Baseline | Est. (Longline) | Y | 259,274 | 0.579 | 0.061 | 0.565 | 0.049 | 0.995 | 0.810 |
| 5 | 0.026 | 1 | Extreme | Est. (Longline) | N | 345,228 | 0.487 | 0.066 | 0.414 | 0.053 | 0.863 | 0.804 |
| 6 | 0.026 | 2 | Extreme | Est. (Longline) | Y | 356,537 | 0.486 | 0.066 | 0.412 | 0.053 | 0.856 | 0.814 |
| 7 | 0.053 | 4 | Extreme | Est. (Longline) | Y | 341,224 | 0.489 | 0.070 | 0.476 | 0.048 | 0.978 | 0.694 |
| 8 | 0.053 | 5 | Extreme | Est. (Longline) | N | 184,144 | 0.481 | 0.065 | 0.342 | 0.070 | 0.719 | 1.101 |
| 9 | 0.5 | 1 | Baseline | Est. (F - H) | Y | 271,753 | 0.576 | 0.047 | 0.590 | 0.021 | 1.039 | 0.465 |
| 10 | 0.5 | 2 | Baseline | Est. (F - H) | Y | 261,071 | 0.570 | 0.047 | 0.608 | 0.023 | 1.089 | 0.477 |
| 11 | 1 | 4 | Baseline | Est. (F - H) | Y | 278,584 | 0.578 | 0.049 | 0.623 | 0.022 | 1.096 | 0.452 |
| 12 | 1 | 5 | Baseline | Est. (F - H) | N | 263,965 | 0.571 | 0.053 | 0.718 | 0.019 | 1.273 | 0.365 |
| 13 | 0.5 | 1 | Extreme | Est. (F - H) | Y | 275,031 | 0.482 | 0.061 | 0.437 | 0.034 | 0.902 | 0.544 |
| 14 | 0.5 | 2 | Extreme | Est. (F - H) | Y | 280,086 | 0.484 | 0.061 | 0.417 | 0.035 | 0.861 | 0.590 |
| 15 | 1 | 4 | Extreme | Est. (F - H) | Y | 300,340 | 0.482 | 0.061 | 0.462 | 0.030 | 0.970 | 0.485 |
| 16 | 1 | 5 | Extreme | Est. (F - H) | Y | 232,400 | 0.472 | 0.062 | 0.464 | 0.034 | 0.995 | 0.567 |
| 17 | 0.5 | 1 | Baseline | Est. (F - M) | Y | 322,173 | 0.566 | 0.044 | 0.649 | 0.016 | 1.164 | 0.353 |
| 18 | 0.5 | 2 | Baseline | Est. (F - M) | Y | 323,773 | 0.571 | 0.043 | 0.646 | 0.015 | 1.136 | 0.360 |
| 19 | 1 | 4 | Baseline | Est. (F - M) | Y | 334,898 | 0.577 | 0.045 | 0.674 | 0.016 | 1.172 | 0.345 |
| 20 | 1 | 5 | Baseline | Est. (F - M) | Y | 309,016 | 0.573 | 0.052 | 0.769 | 0.015 | 1.336 | 0.294 |
| 21 | 0.5 | 1 | Extreme | Est. (F - M) | Y | 351,395 | 0.481 | 0.059 | 0.505 | 0.021 | 1.056 | 0.364 |

*Table 11 (continued).* Model configuration, ensemble weight and median estimates of stock status and management reference points for each model in the Bayesian state-space surplus production model (BSPM) ensemble.

| Model | Weight (relative) | Index | Prior type | Catch | Converged | $MSY$ | $D_{MSY}$ | $U_{MSY}$ | $D_{2019-2022}$ | $U_{2018-2022}$ | $\frac{D_{2019-2022}}{D_{MSY}}$ | $\frac{U_{2018-2022}}{U_{MSY}}$ |
|---|---|---|---|---|---|---|---|---|---|---|---|---|
| 22 | 0.5 | 2 | Extreme | Est. (F - M) | Y | 337,613 | 0.480 | 0.057 | 0.475 | 0.023 | 1.012 | 0.400 |
| 23 | 1 | 4 | Extreme | Est. (F - M) | Y | 381,637 | 0.481 | 0.060 | 0.537 | 0.019 | 1.119 | 0.322 |
| 24 | 1 | 5 | Extreme | Est. (F - M) | Y | 282,053 | 0.475 | 0.060 | 0.547 | 0.023 | 1.167 | 0.403 |
| 25 | 0.5 | 1 | Baseline | Est. (F - L) | Y | 418,310 | 0.575 | 0.042 | 0.717 | 0.011 | 1.253 | 0.264 |
| 26 | 0.5 | 2 | Baseline | Est. (F - L) | Y | 395,082 | 0.569 | 0.041 | 0.702 | 0.011 | 1.241 | 0.265 |
| 28 | 1 | 5 | Baseline | Est. (F - L) | Y | 454,686 | 0.573 | 0.043 | 0.742 | 0.010 | 1.295 | 0.227 |
| 29 | 0.5 | 1 | Extreme | Est. (F - L) | Y | 424,496 | 0.569 | 0.051 | 0.817 | 0.010 | 1.418 | 0.198 |
| 30 | 0.5 | 2 | Extreme | Est. (F - L) | N | 516,071 | 0.481 | 0.058 | 0.618 | 0.012 | 1.280 | 0.206 |
| 31 | 1 | 4 | Extreme | Est. (F - L) | Y | 568,037 | 0.483 | 0.059 | 0.640 | 0.011 | 1.325 | 0.179 |
| 32 | 1 | 5 | Extreme | Est. (F - L) | Y | 408,518 | 0.477 | 0.059 | 0.636 | 0.013 | 1.359 | 0.226 |

*Table 12*. Summary of reference points and management quantities for the model ensemble of North Pacific shortfin mako. Values in parentheses represent the 95% credible intervals when available. Note that exploitation rate is defined relative to the carrying capacity.

| **Reference points** | **Symbol** | **Median (95% CI)** |
|---|---|---|
| **Unfished conditions** | | |
| Carrying capacity | $K$ (1000s sharks) | 12,541 (4,164 - 52,684) |
| **MSY-based reference points** | | |
| Maximum Sustainable Yield (MSY) | $C_{MSY}$ (1000s sharks) | 338 (134 - 1,338) |
| Depletion at MSY | $D_{MSY}$ | 0.51 (0.40 - 0.70) |
| Exploitation rate at MSY | $U_{MSY}$ | 0.055 (0.027 - 0.087) |
| **Stock status** | | |
| Recent depletion | $D_{2019-2022}$ | 0.60 (0.23 - 1.00) |
| Recent depletion relative to MSY | $D_{2019-2022}/D_{MSY}$ | 1.17 (0.46-1.92) |
| Recent exploitation | $U_{2018-2021}$ | 0.018 (0.004-0.07) |
| Recent exploitation relative to MSY | $U_{2018-2021}/U_{MSY}$ | 0.34 (0.07-1.20) |

## 12. FIGURES

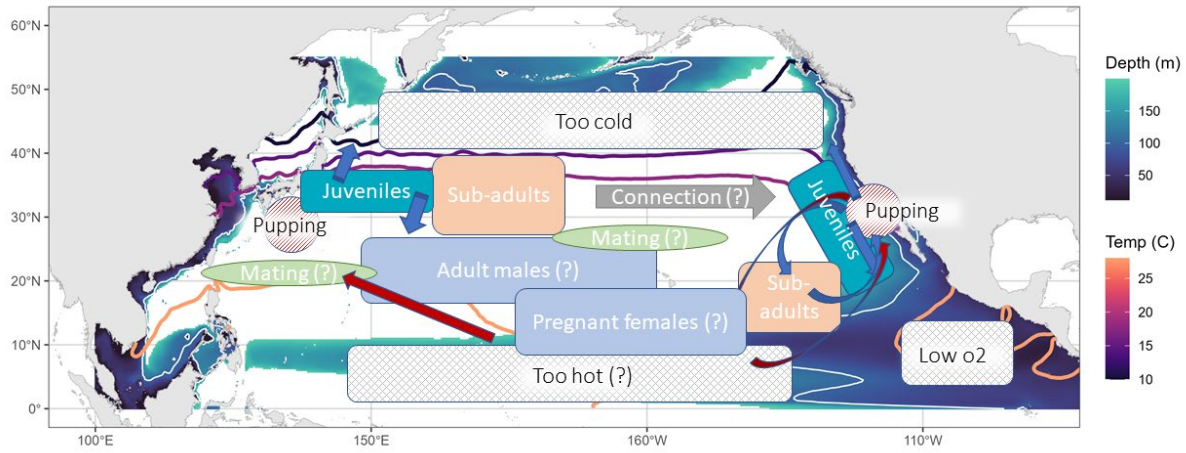


*Figure 1*. Conceptual model for North Pacific shortfin mako. Contour lines (warm colors) are shown for the average annual $10°, 15°, 18°,$ and $28°C$ sea surface temperature isotherms. Background shading (cooler colors) shows the depth of the oxygen minimum zone ($3\ mL/L$), a white isocline indicates a depth of 100m which could be limiting based on North Pacific shortfin mako vertical dive profiles.

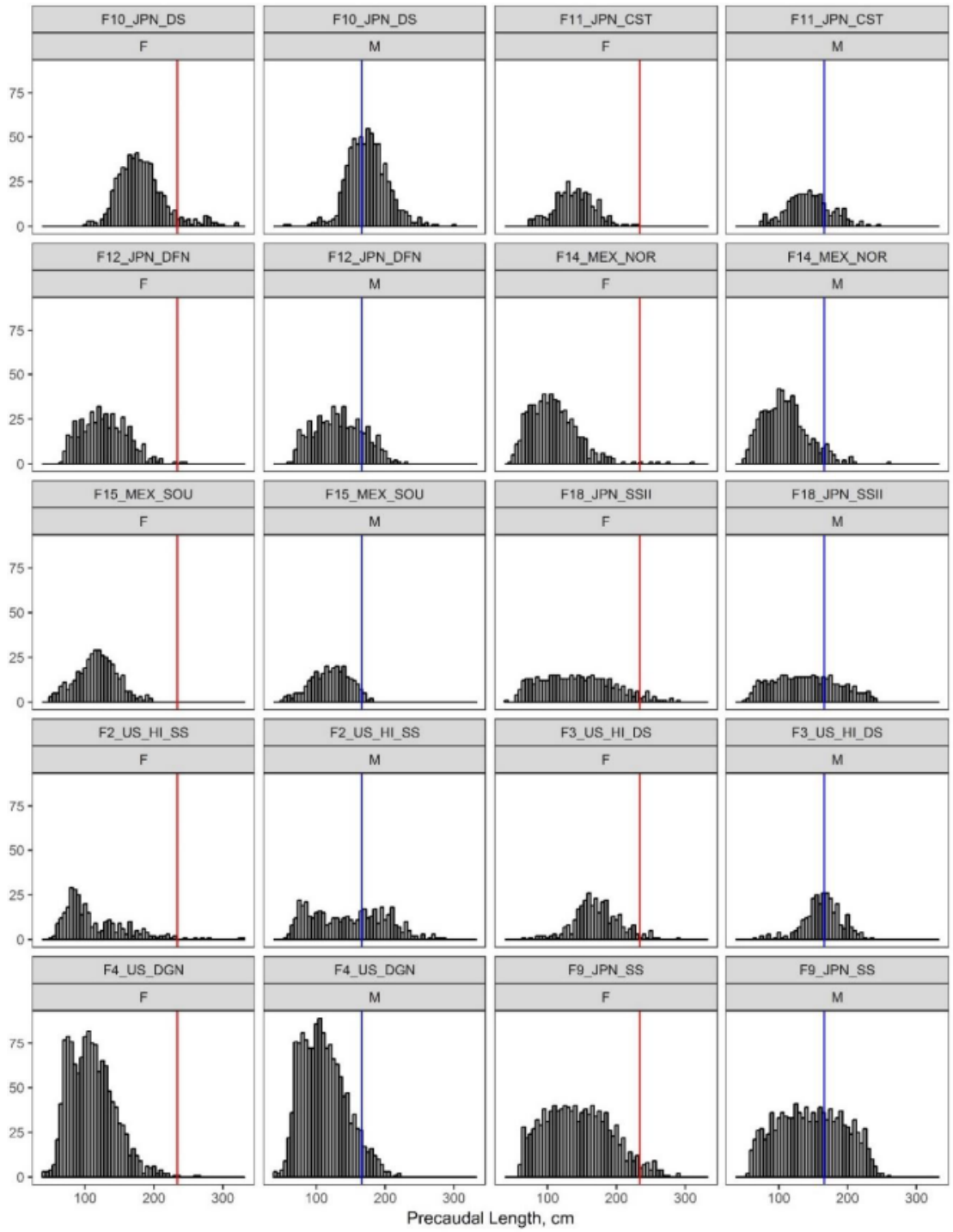


*Figure 2*. Frequency of sex-specific size data (Pre-caudal length; PCL in cm) by fleet for North Pacific shortfin mako. Colored solid vertical lines indicate size-at-50% maturity. F and M denotes female and male, respectively (Figure 4; ISC, 2018a).

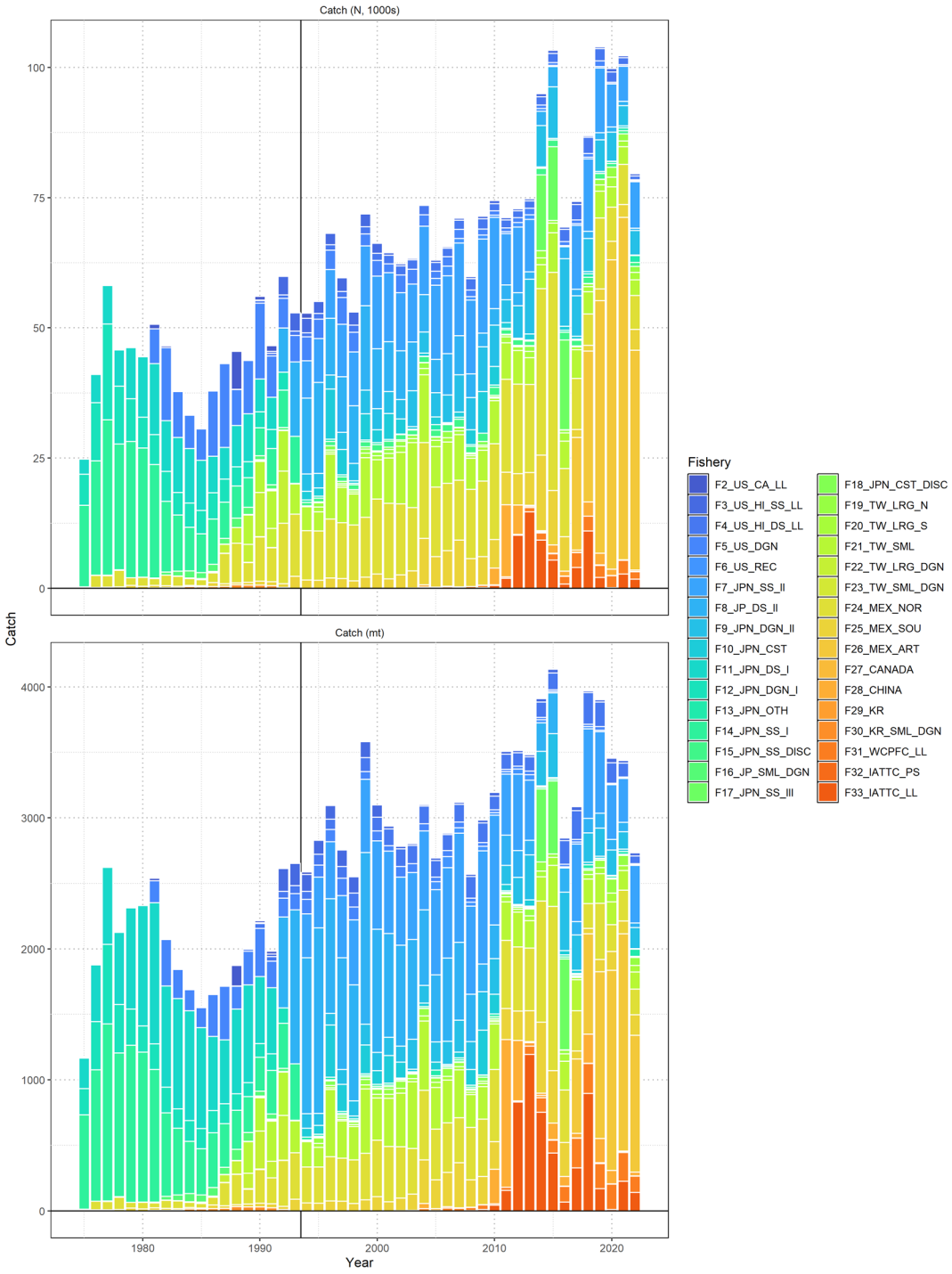


*Figure 3*. Catch of North Pacific shortfin mako by fishery as assembled by the SHARKWG. Upper panel is catch in numbers (1000s) and lower panel is catch in biomass (mt). The vertical black line indicates the start of the assessment period in 1994.

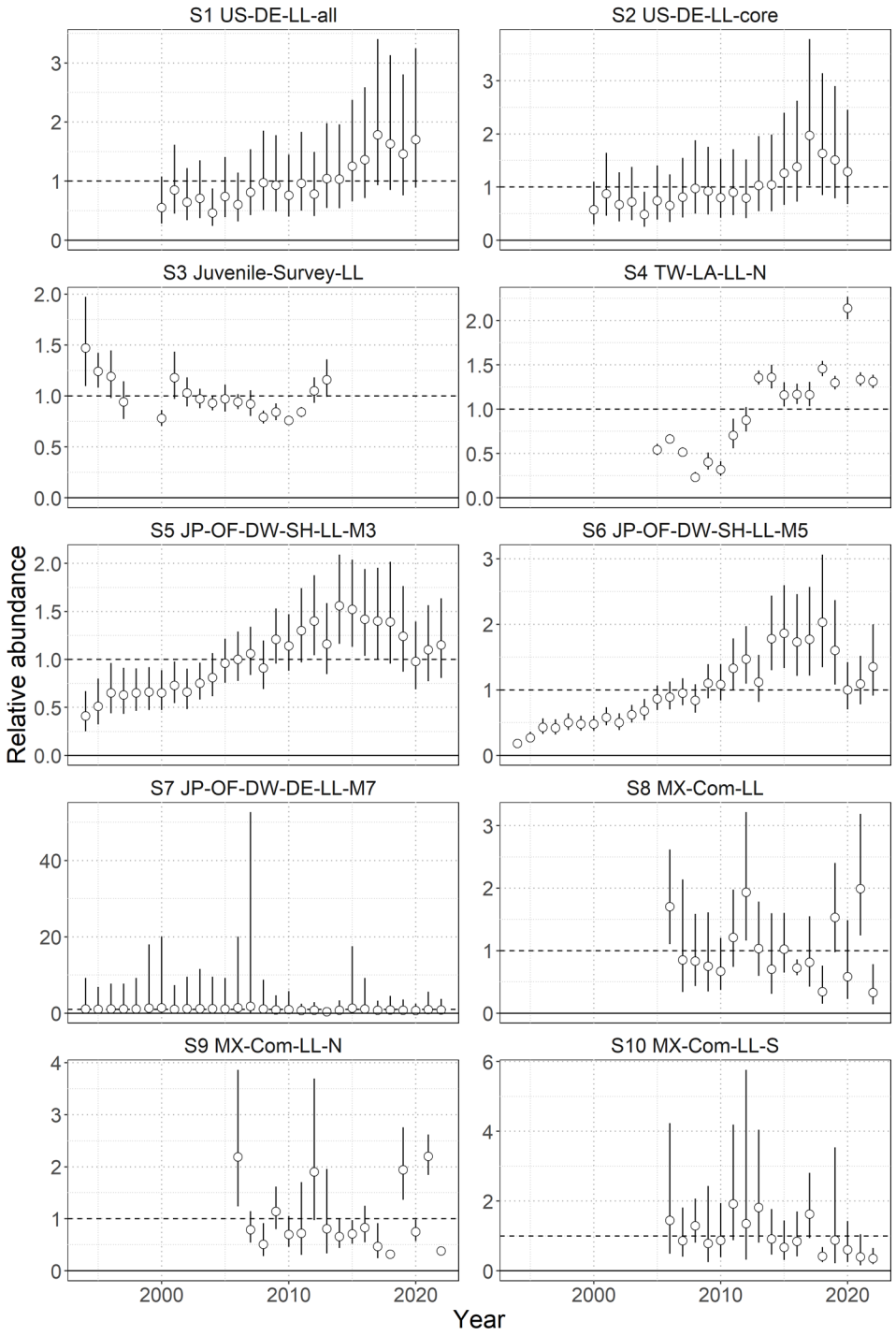


*Figure 4*. Standardized indices of relative abundance used in the stock assessment model ensemble and sensitivity analyses for North Pacific shortfin mako. Open circles show observed values (standardized to mean of 1; black horizontal line) and the vertical bars indicate the observation error (95% confidence interval).

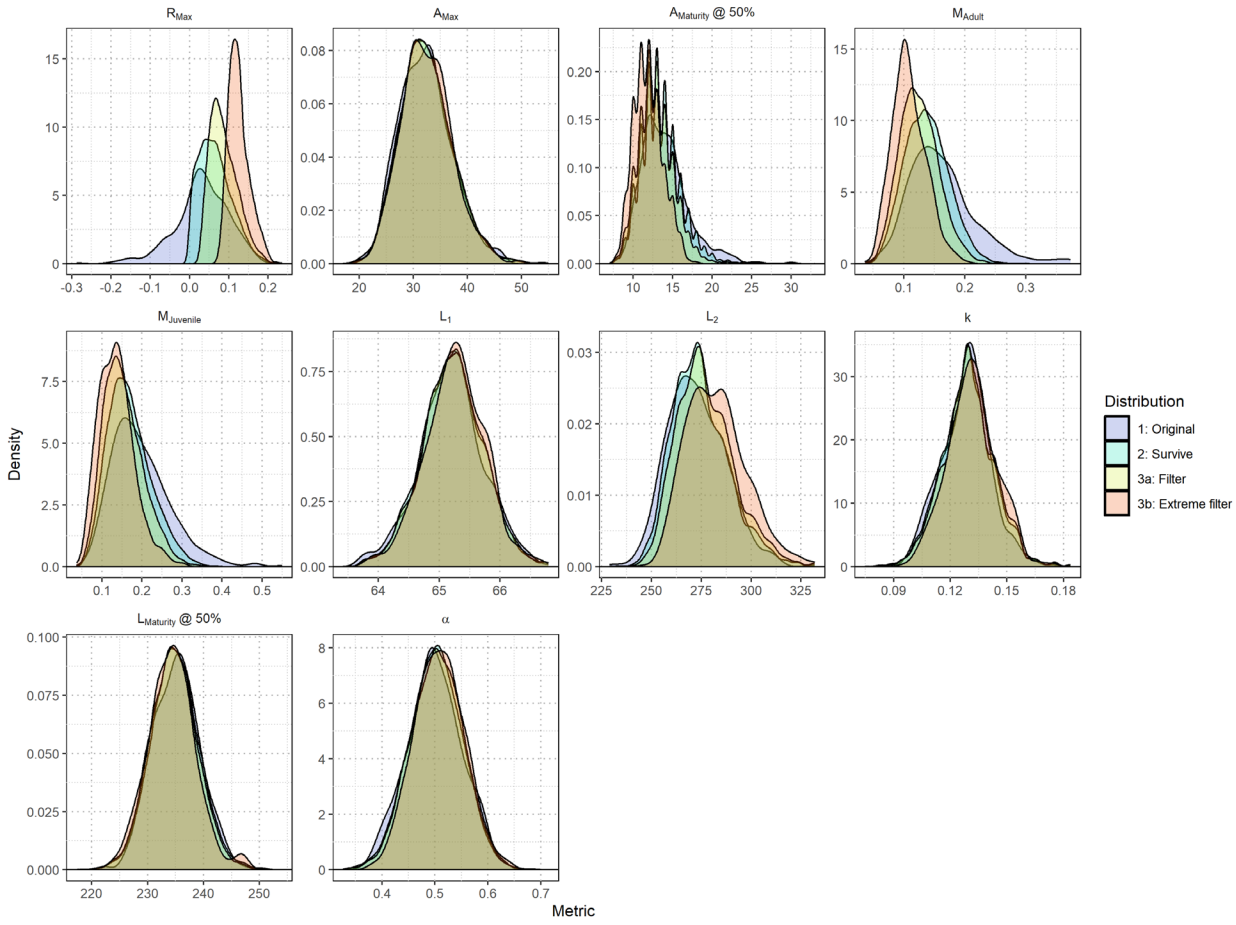


*Figure 5*. Initial distributions of biological parameters (maximum age $A_{Max}$, age at 50% maturity $A_{Maturity}$@50%, adult natural mortality $M_{Adult}$, juvenile natural mortality $M_{Juvenile}$, length at birth $L_1$, length at theoretical age 40 $L_2$, growth coefficient $k$, length at 50% maturity $L_{Maturity}$@50%, and female sex-ratio at birth $\alpha$) for North Pacific shortfin mako used in numerical simulations to develop the $R_{Max}$ prior (blue shading). Resultant distributions following filtering: simulated populations which were viable (Survive, aqua shading), baseline filter (Filter, yellow), extreme filter (orange).

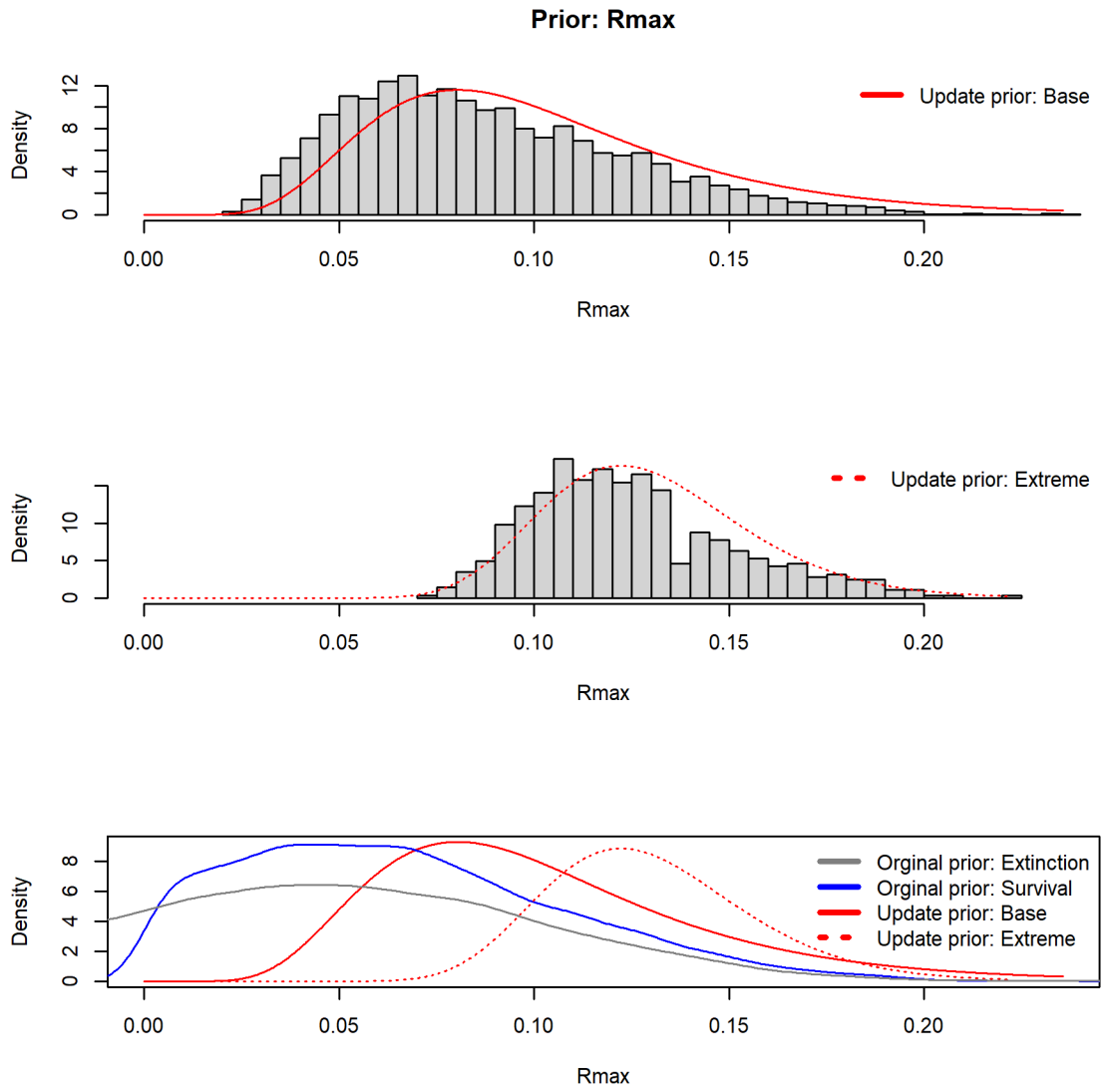


*Figure 6*. Prior distributions for maximum intrinsic rate of population increase $R_{Max}$ of North Pacific shortfin mako. *Upper panel*: Gray histogram is the $R_{Max}$ values from the numerical simulation which meet baseline filtering levels. Red line is fitted lognormal distribution. *Middle panel*: Gray histogram is the $R_{Max}$ values from the numerical simulation which meet extreme filtering levels. Dotted red line is fitted lognormal distribution. *Bottom panel*: Original distribution of $R_{Max}$ values from numerical simulation (gray), those from viable populations (blue), and the two lognormal priors (red).

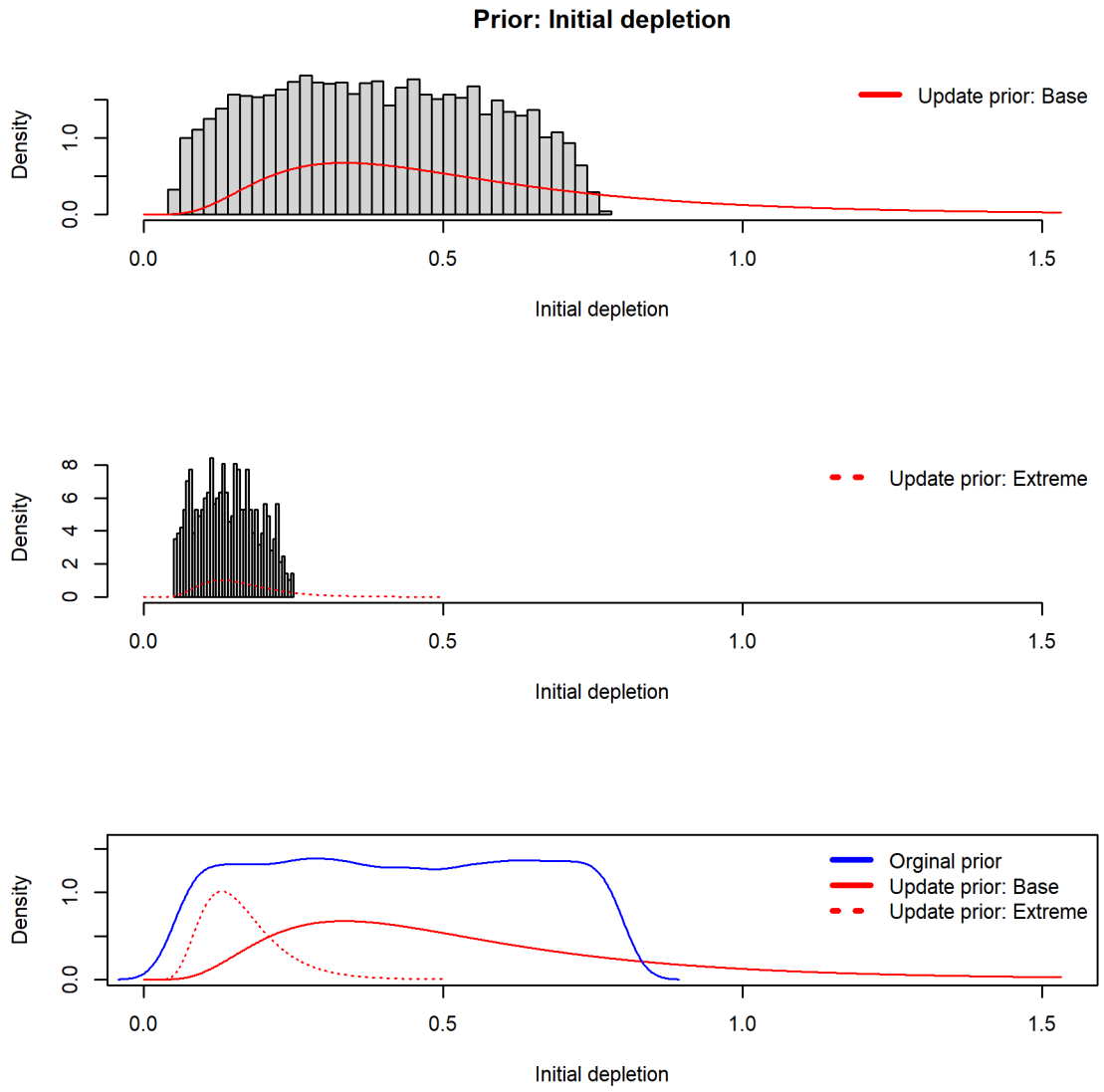


2854

2855 *Figure 7*. Prior distributions for initial depletion $x_0$ of North Pacific shortfin mako. *Upper*
2856 *panel*: Gray histogram is the $x_0$ values from the numerical simulation which meet baseline
2857 filtering levels. Red line is fitted lognormal distribution. *Middle panel*: Gray histogram is the $x_0$
2858 values from the numerical simulation which meet extreme filtering levels. Dotted red line is
2859 fitted lognormal distribution. *Bottom panel*: Original distribution of $x_0$ values from numerical
2860 simulation (gray), those from viable populations (blue), and the two lognormal priors (red).

2861

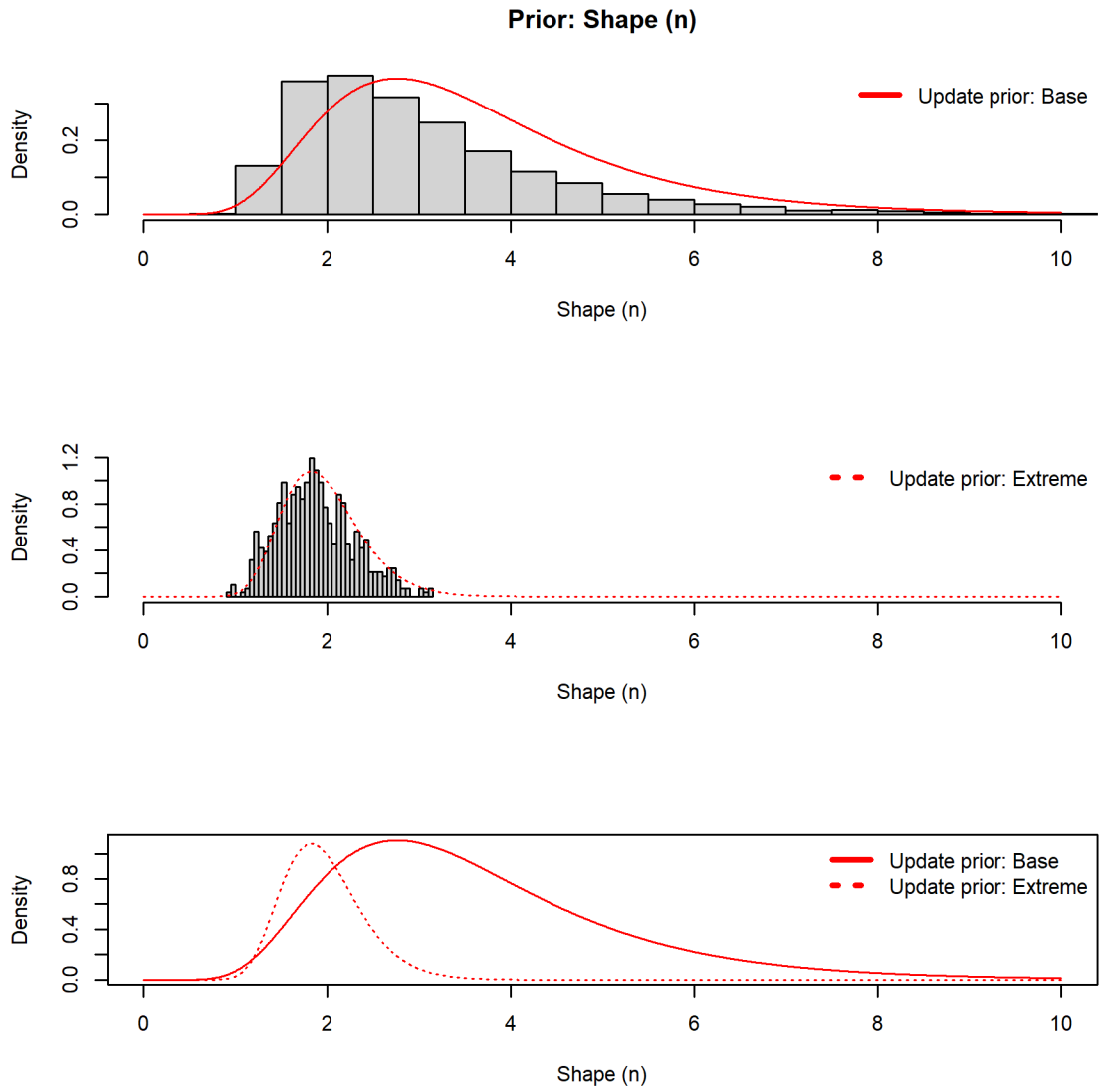


2862

2863 *Figure 8*. Prior distributions for shape $n$ of North Pacific shortfin mako. *Upper panel*: Gray
2864 histogram is the $n$ values from the numerical simulation which meet baseline filtering levels.
2865 Red line is fitted lognormal distribution. *Middle panel*: Gray histogram is the $n$ values from the
2866 numerical simulation which meet extreme filtering levels. Dotted red line is fitted lognormal
2867 distribution. *Bottom panel*: The two lognormal priors (red).

2868

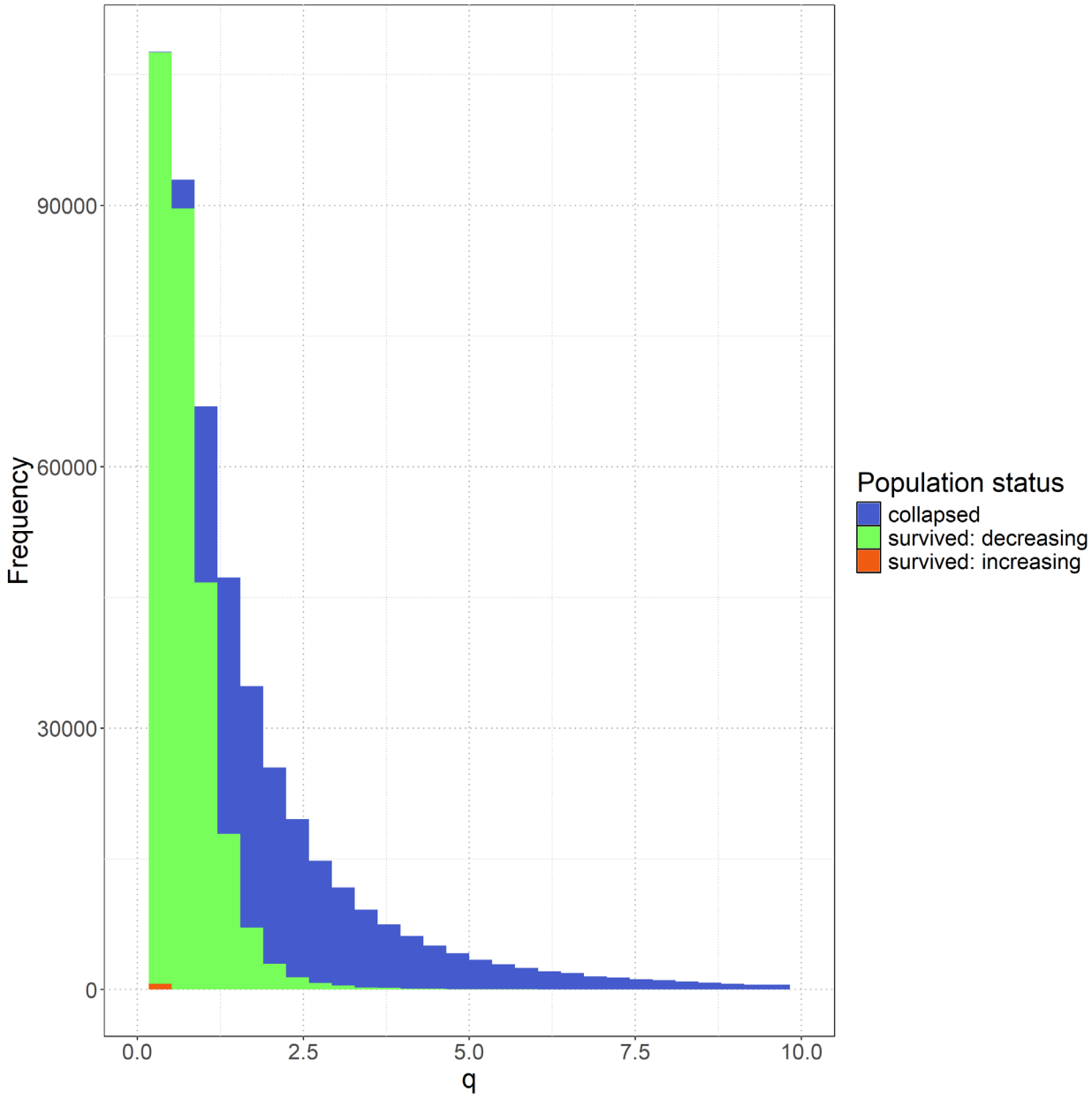


*Figure 9*. Histogram of population status (collapsed, survived with decreasing trend, and survived with increasing trend) of North Pacific shortfin mako from numerical simulations with a naïve half-Normal prior, $\text{Normal}^{+}(0,1)$, for longline catchability $q$.


*Figure 10*. Stepwise model output (spawning biomass SSB, fishing mortality F, recruitment, spawning biomass relative to spawning biomass at MSY $SSB/SSB_{MSY}$, and fishing mortality relative to fishing mortality that produces MSY $F/F_{MSY}$) for key SS3 models of North Pacific shortfin mako. Note *SS3 00 – 2018base* (blue) is overlaid by *SS3 01 – newSS3* (aqua).

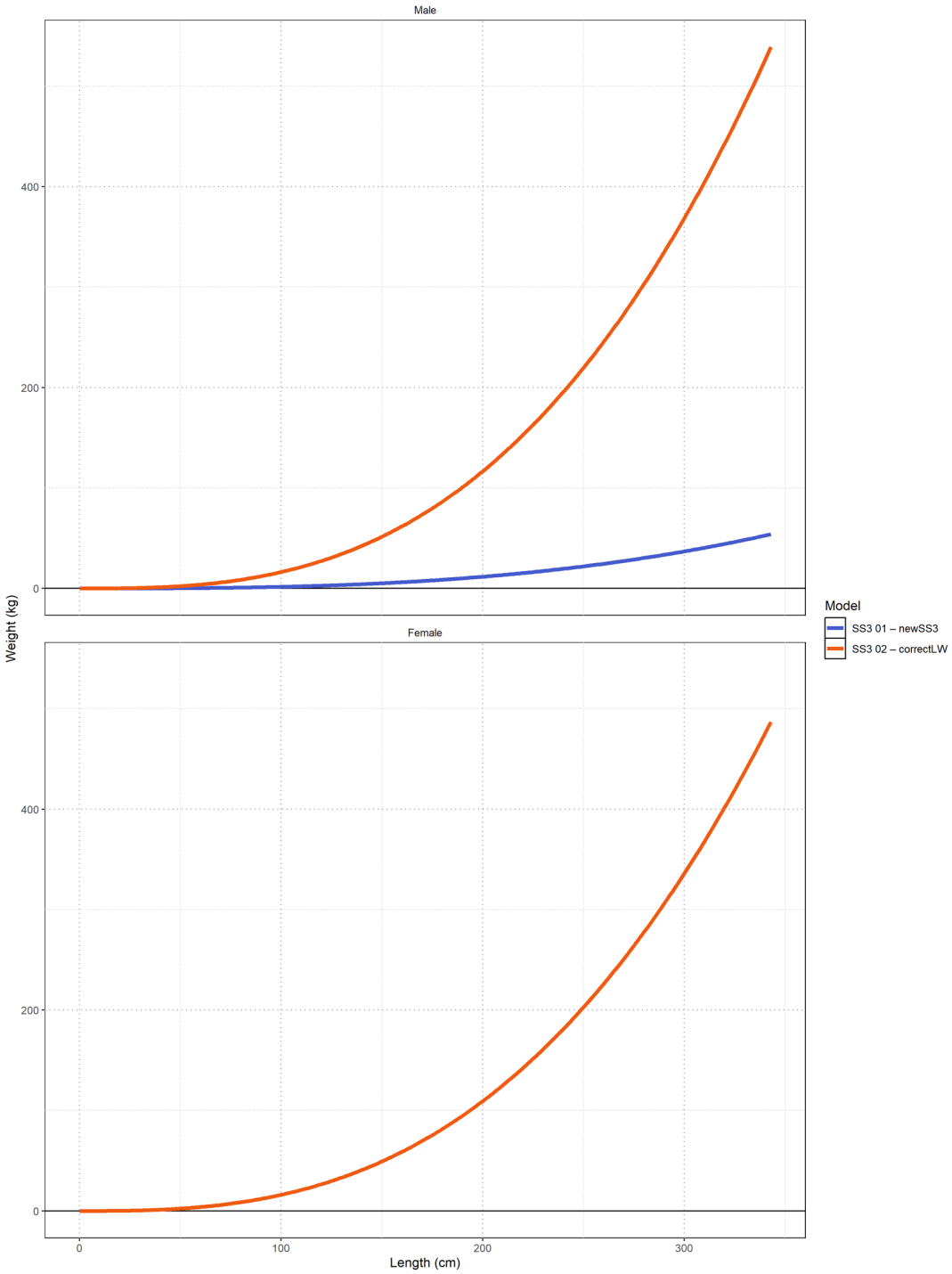


*Figure 11*. Length-weight relationships assumed in the SS3 models for males (top) and females (bottom) of North Pacific shortfin mako.

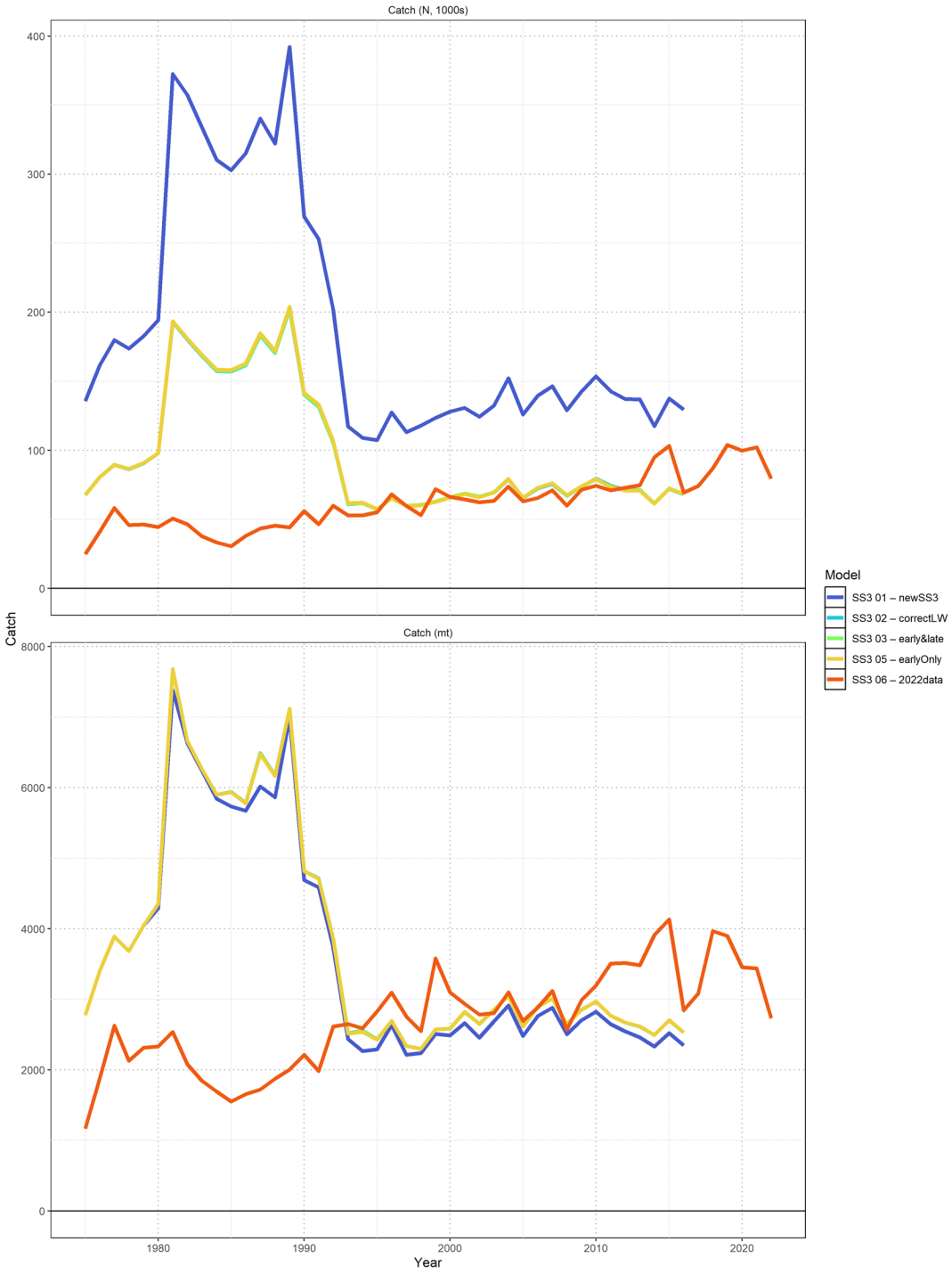


*Figure 12*. Stepwise model catch in numbers (1000s, top) and biomass (mt, bottom) of North Pacific shortfin mako for key SS3 models.

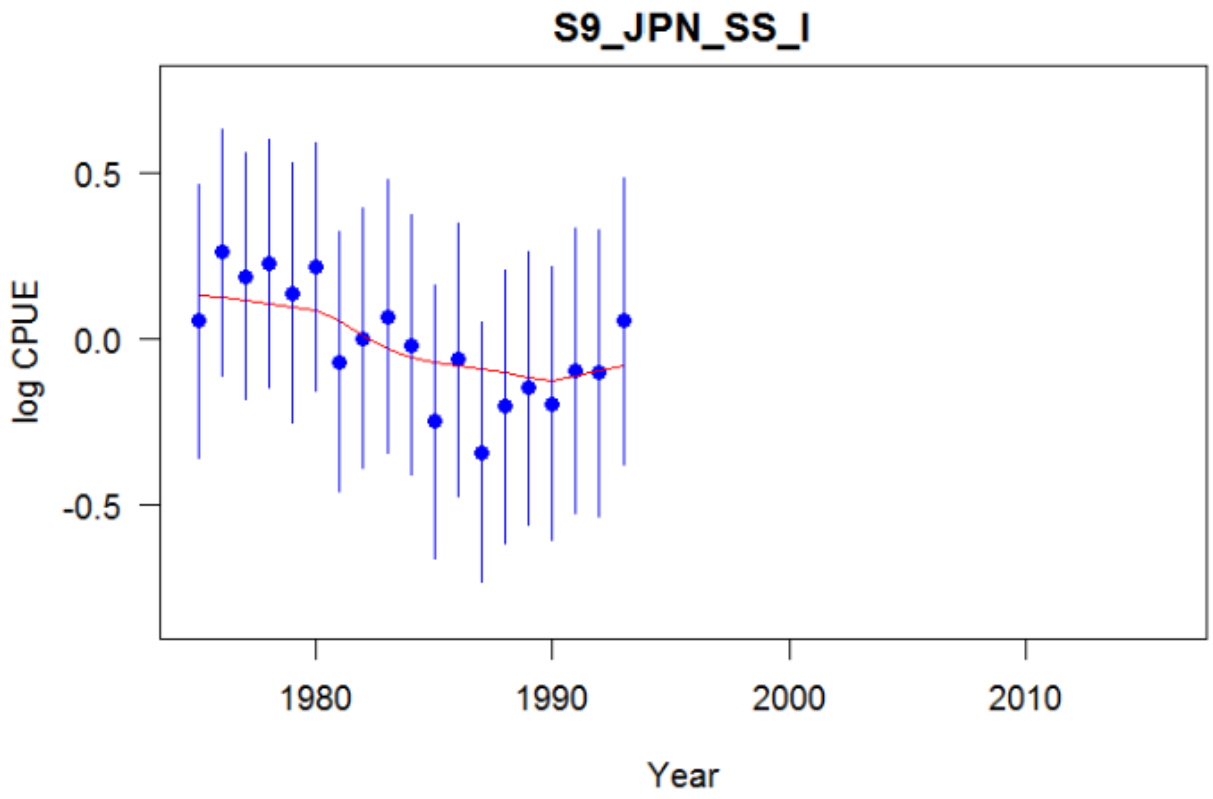


2888

2889 *Figure 13*. Early period (1975-1993) CPUEs of North Pacific shortfin mako used in the 2018
2890 assessment and initial SS3 models for the current assessment. Solid circles denote observed data
2891 values. Vertical blue lines represent the estimated confidence intervals (± 1.96 standard
2892 deviations) around the CPUE values and the red line is the 2018 assessment fit (Figure 11; ISC,
2893 2018a).

2894

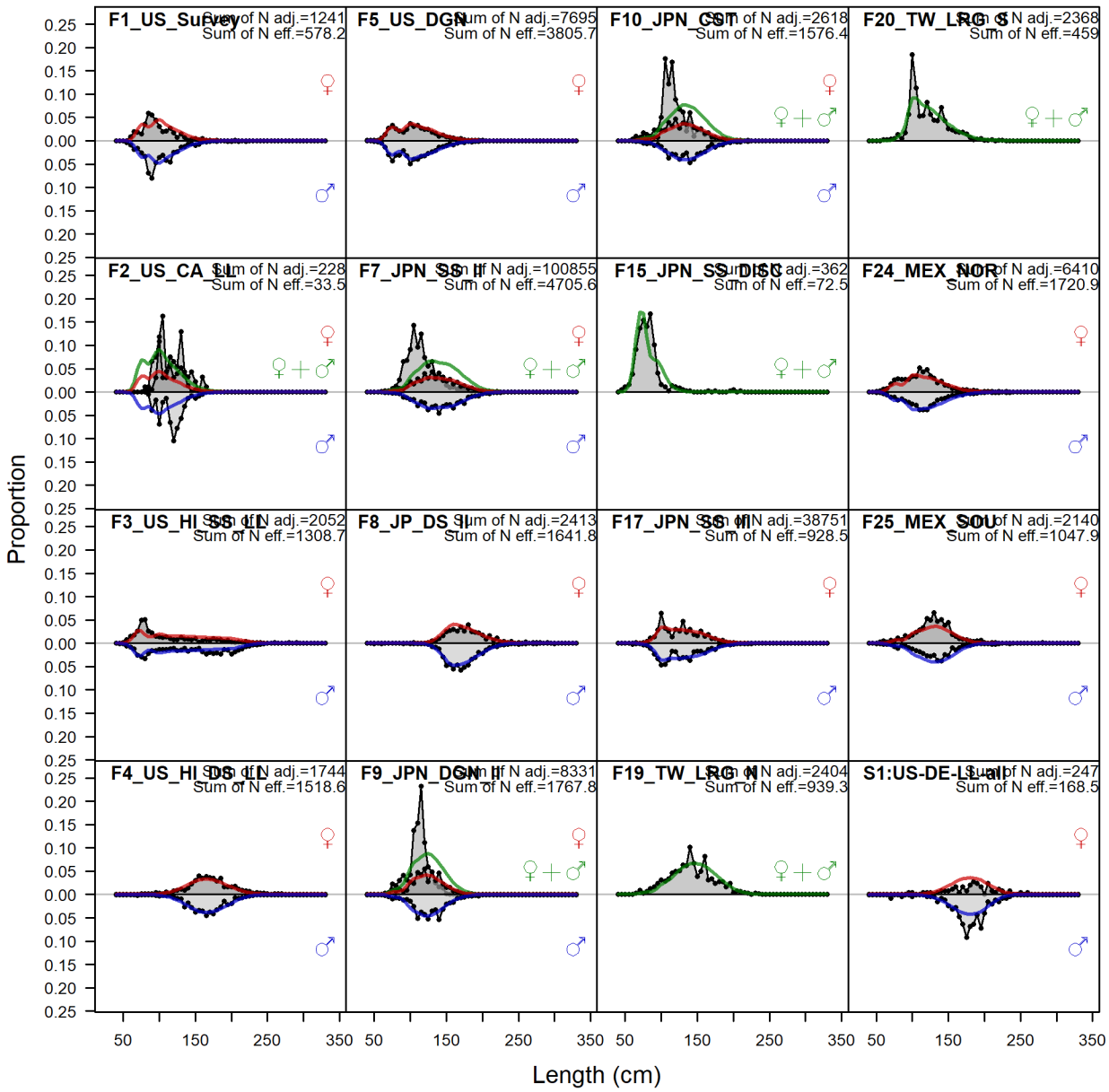


*Figure 14*. Sex specific comparison of observed (gray shaded area) and model predicted (colored solid lines; blue=male, red=female, green=un-sexed) length compositions (pre-caudal length in cm) of North Pacific shortfin mako for different fleets in the *SS3 06 – 2022data* model.

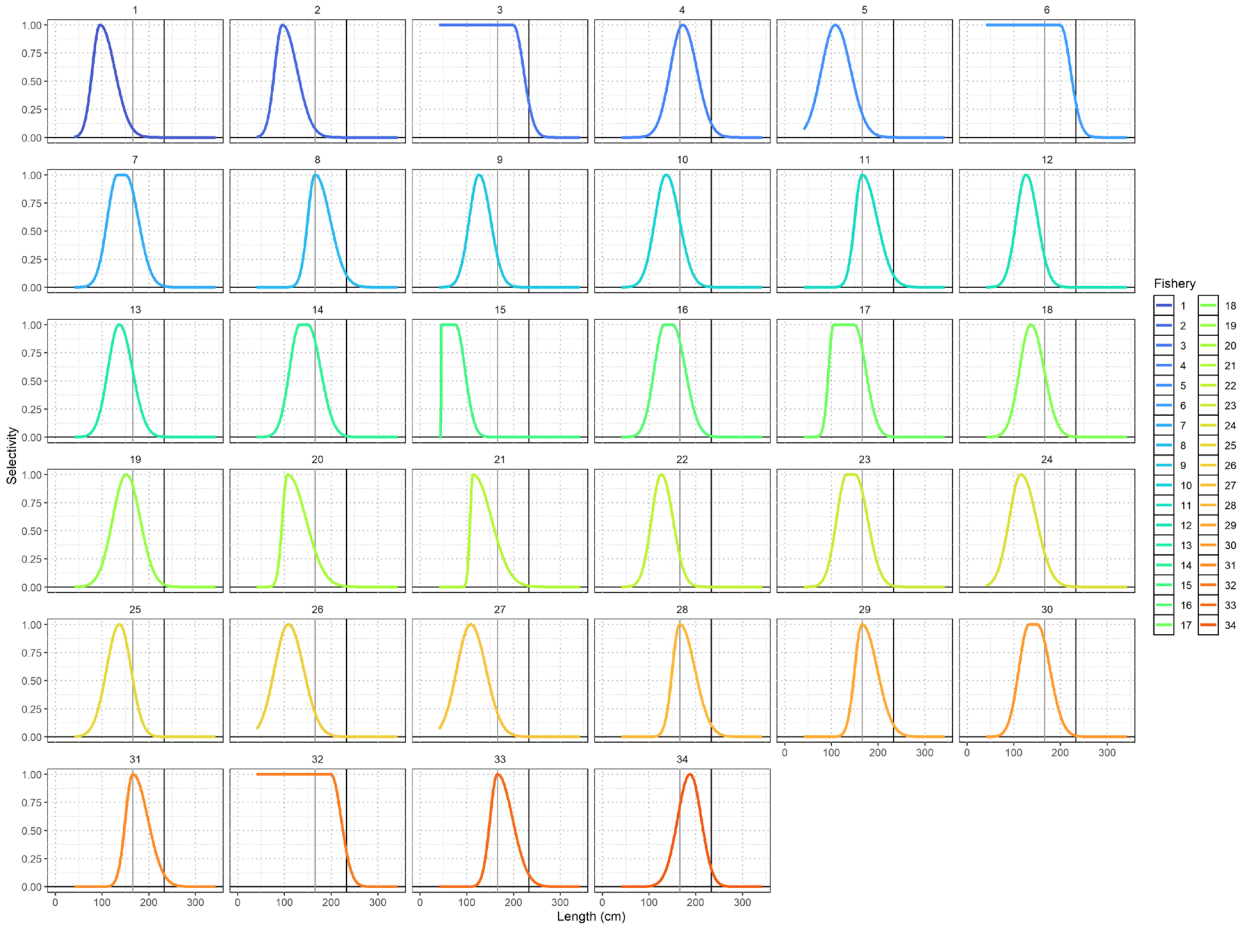


*Figure 15*. Estimated length-based selectivity curves of North Pacific shortfin mako for the *SS3 06 – 2022 data* model. Fisheries definitions can be found in *Table* 1. The vertical black line gives the female length at 50% maturity $L_{Maturity}@50\% = 233$cm PCL, and the vertical gray line gives the male $L_{Maturity}@50\% = 166$cm PCL.

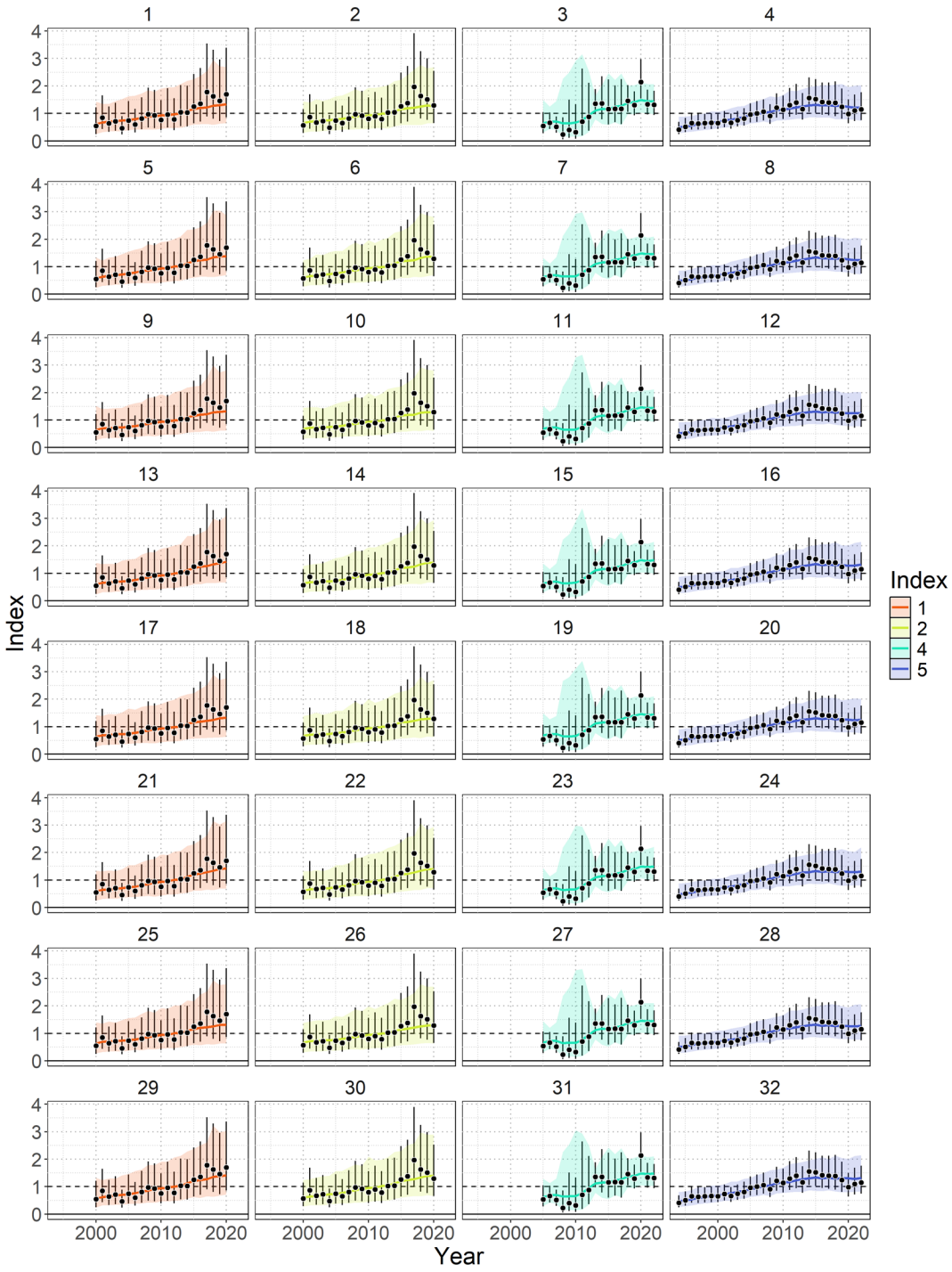


*Figure 16*. Posterior predicted CPUE (solid line – median, and 95% credible interval – shaded polygon) of North Pacific shortfin mako for all 32 models in the ensemble (*Table 9*). Observed CPUE is shown in the black circles and the estimated observation error (95% credible interval) is shown with the vertical black bars.

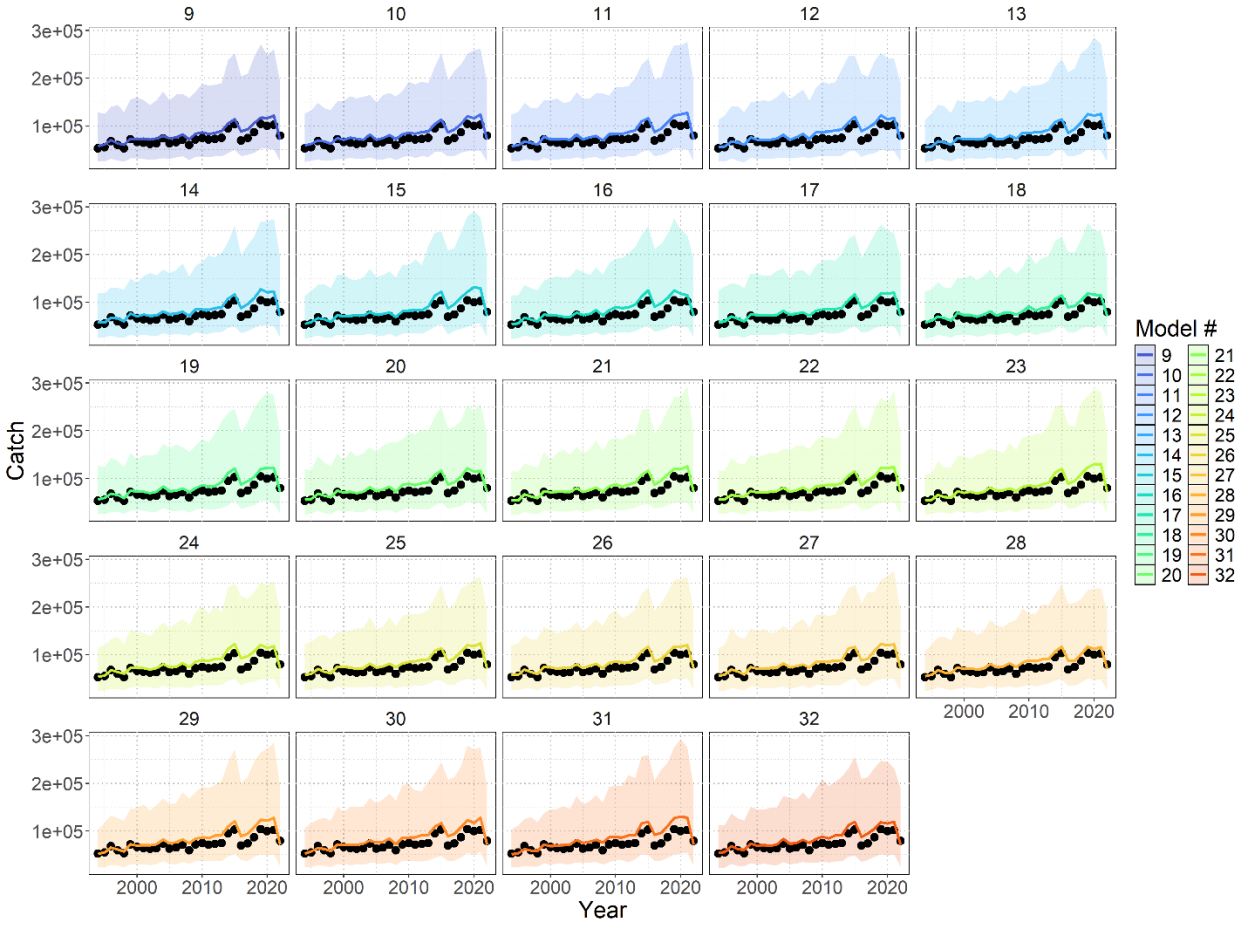


*Figure 17*. Posterior estimates of total removals or catch (solid line – median, and 95% credible interval – shaded polygon) of North Pacific shortfin mako for the 24 models in the ensemble (*Table 9*) that fit to the catch. Observed total removals is shown by the black circles.

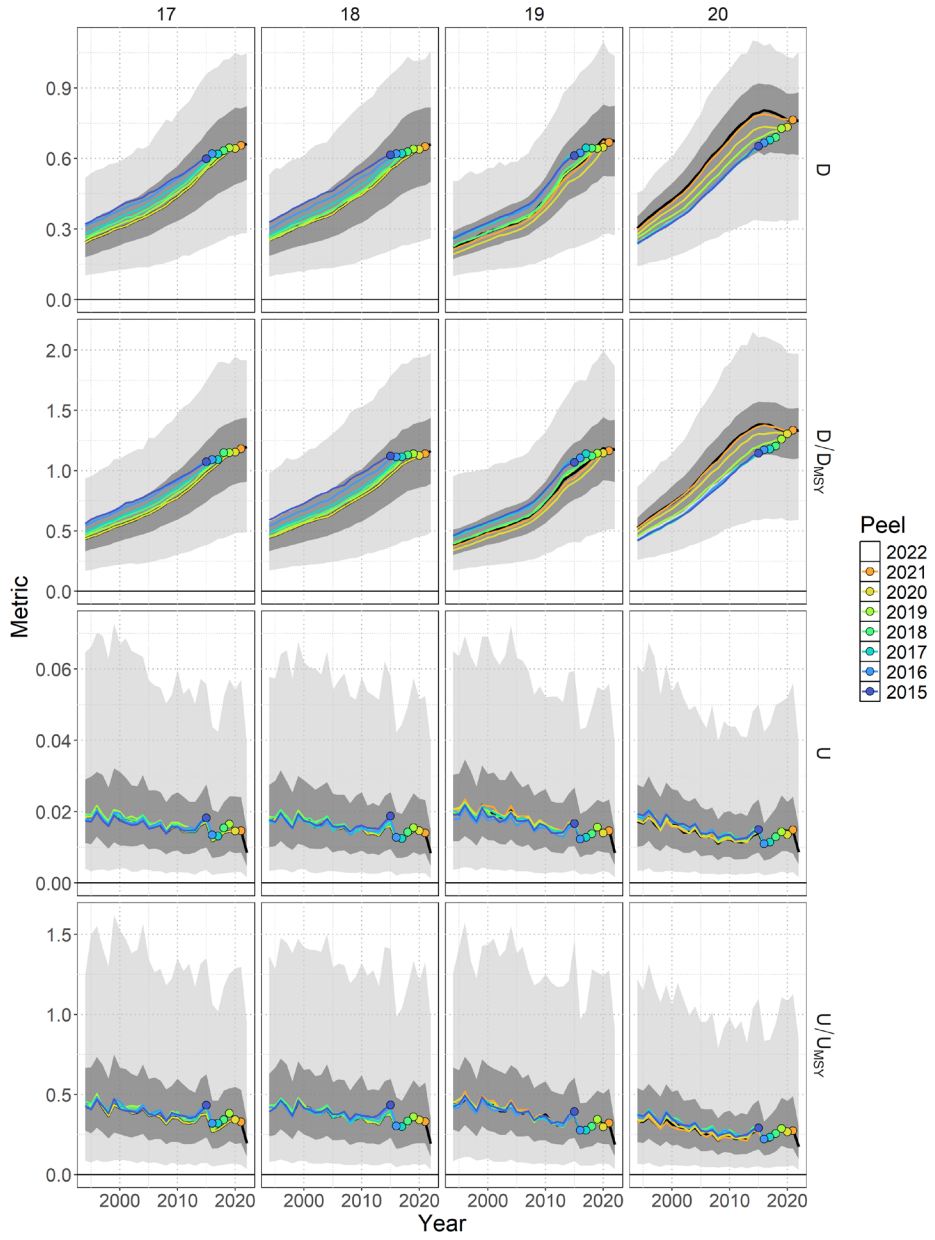


*Figure 18*. Example of retrospective analysis for 4 models in the ensemble (see *Table 9* for details regarding the model configuration of these example models) with respect to time series of depletion $D_t$, depletion relative to depletion at MSY $D_t/D_{MSY}$, exploitation rate $U_t$, and exploitation rate relative to the rate of exploitation that produces MSY $U_t/U_{MSY}$ for North Pacific shortfin mako. The base model with data included through 2022 (black line – median; dark shading – 50% credible interval; light shading – 95% credible interval) is shown relative to the retrospective models. Colored lines correspond to the last year of index data and the colored point indicates the estimate in the last year of the retrospective peel.

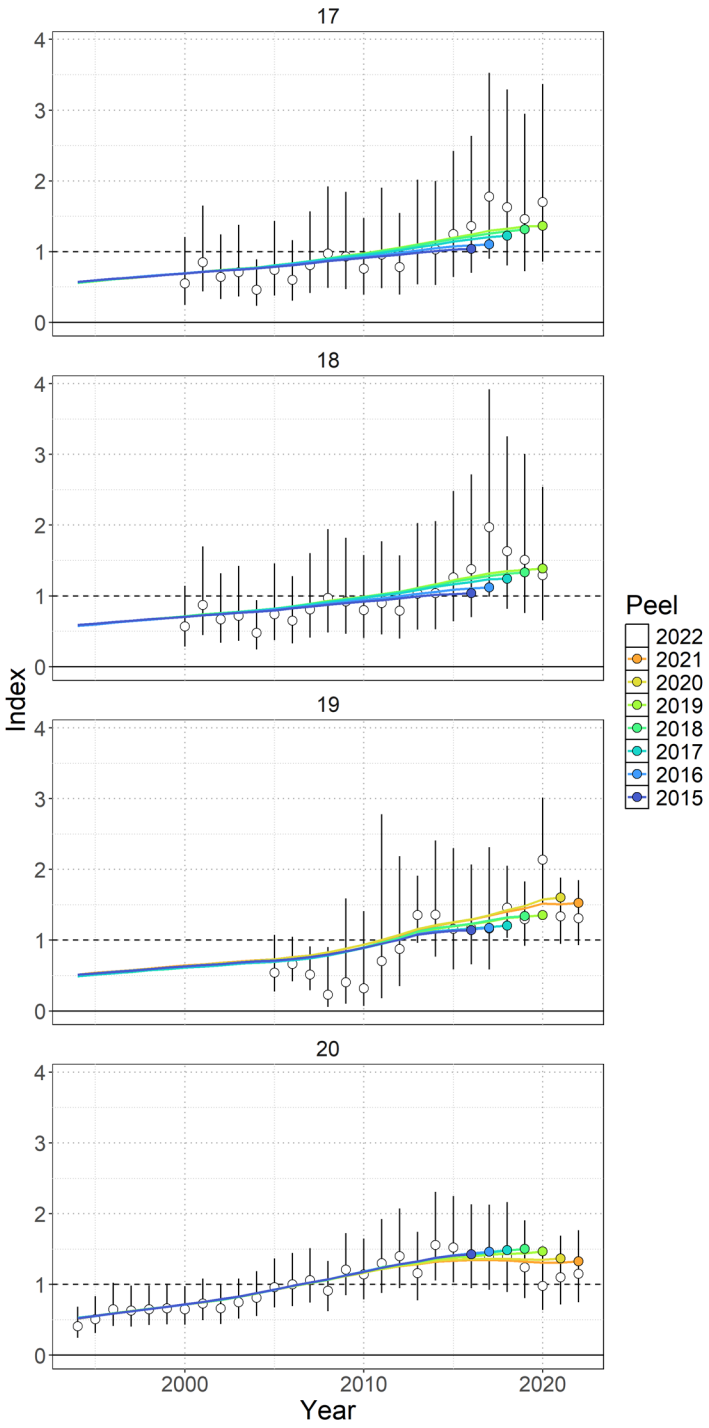


*Figure 19*. Standardized indices of relative abundance used in the stock assessment model ensemble for North Pacific shortfin mako. Open circles show observed values (standardized to mean of 1; black horizontal line) and the vertical bars indicate the observation error (95% confidence interval). One year ahead 'model-free' hindcast predictions are shown by the colored lines, where the color indicates the last year of index data seen by the model. The predicted value is shown one year-ahead with the colored point.

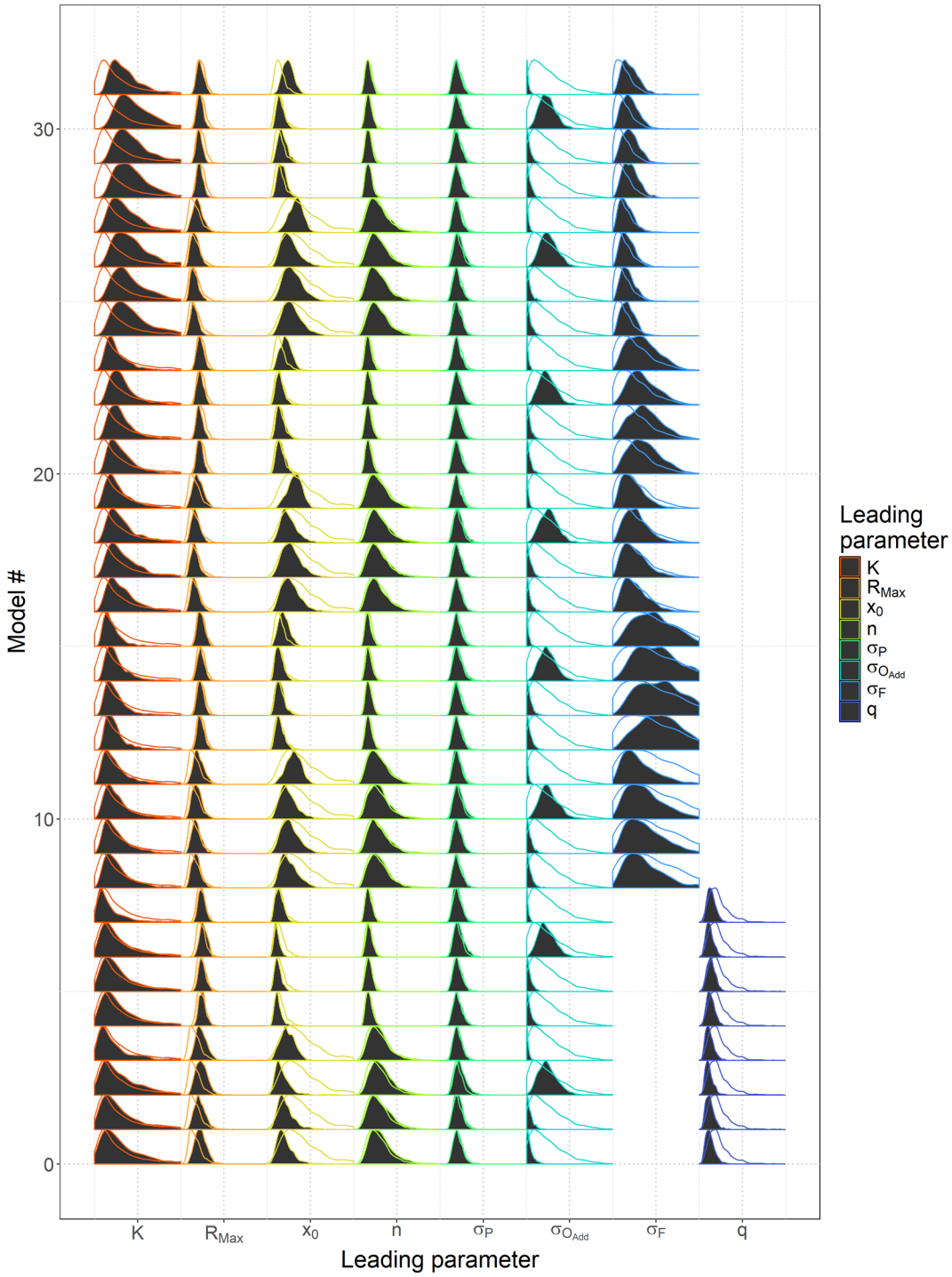


*Figure 20*. Posterior parameter distributions (filled polygon) for leading parameters ($R_{Max}$, $x_0$, $n$, $K$, $\sigma_P$, $\sigma_{O_{Add}}$, $q$, and $\sigma_F$), relative to their assumed prior distributions (colored line) for all 32 models of North Pacific shortfin mako in the ensemble.

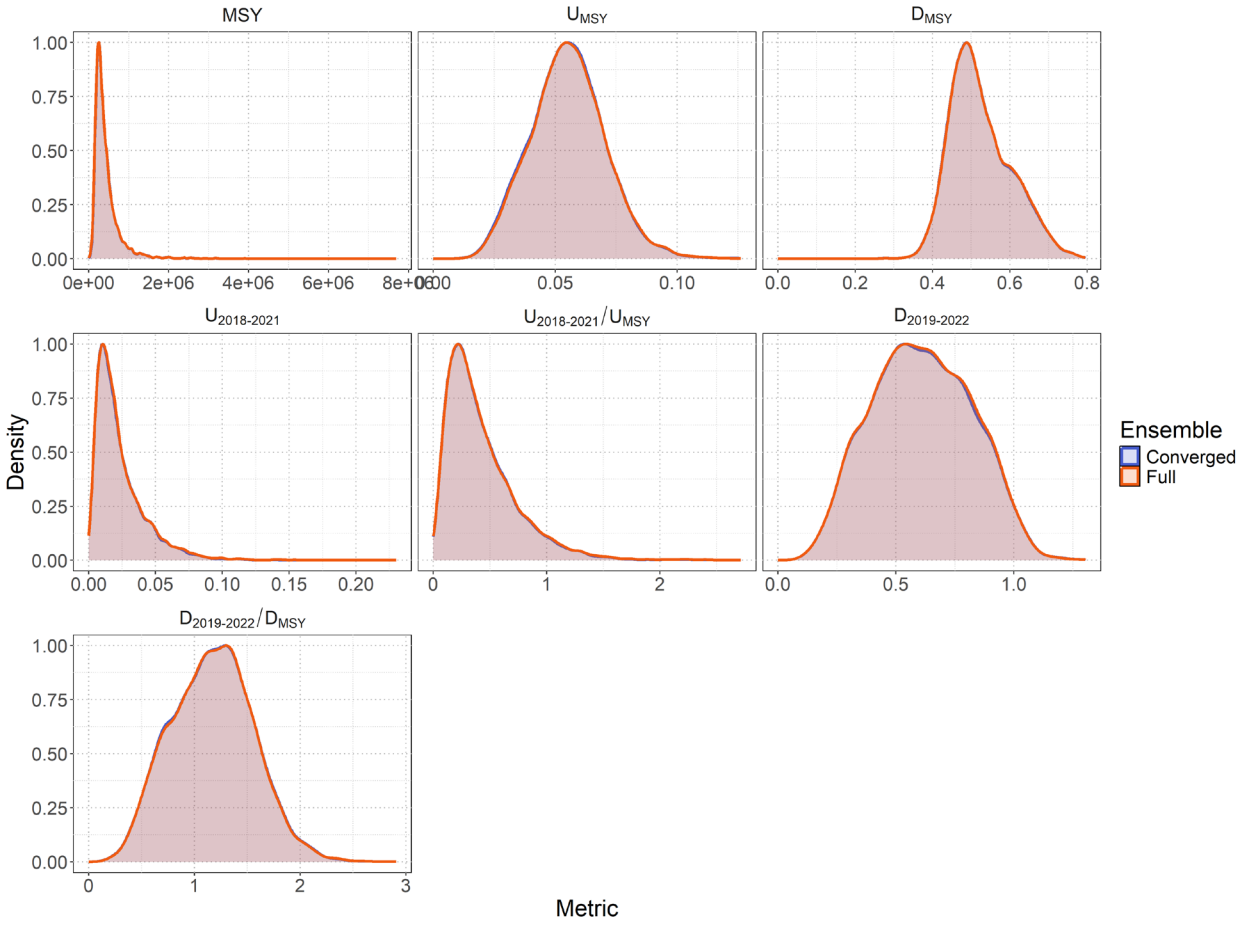


*Figure 21*. Posterior distributions of management reference points ($MSY$, $U_{MSY}$, $D_{MSY}$, $U_{2018-2021}$, $U_{2018-2021}/U_{MSY}$, $D_{2019-2022}$, and $D_{2019-2022}/D_{MSY}$) for all 32 models in the weighted ensemble (Full, orange distribution) and all 28 converged models in the weighted ensemble (Converged, blue distribution) for North Pacific shortfin mako.

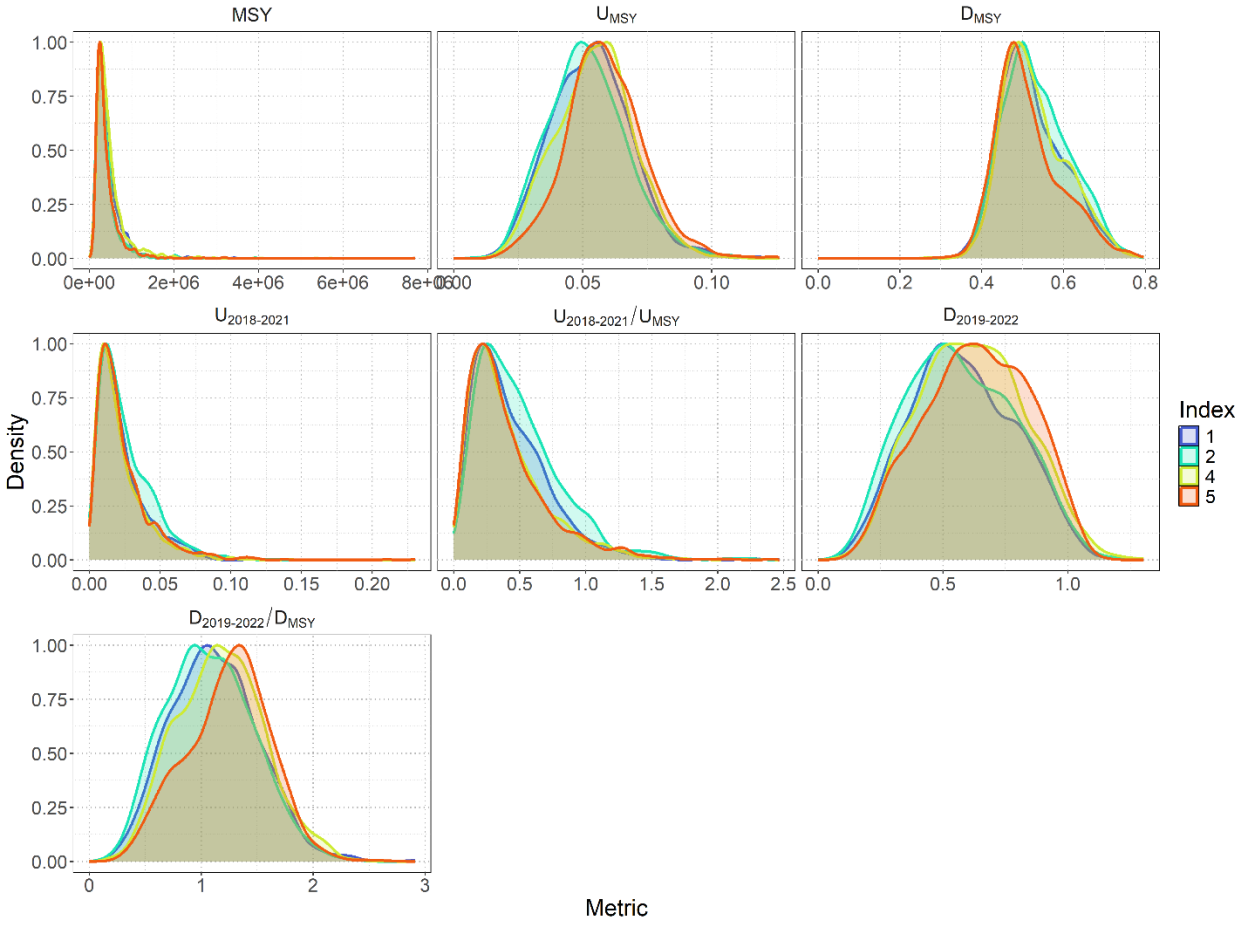


*Figure 22*. Posterior distributions of management reference points ($MSY$, $U_{MSY}$, $D_{MSY}$, $U_{2018-2021}$, $U_{2018-2021}/U_{MSY}$, $D_{2019-2022}$, and $D_{2019-2022}/D_{MSY}$) for all 28 converged models of North Pacific shortfin mako in the weighted ensemble. Distribution color indicates the index that the models were fit to (see *Table 9* for details).

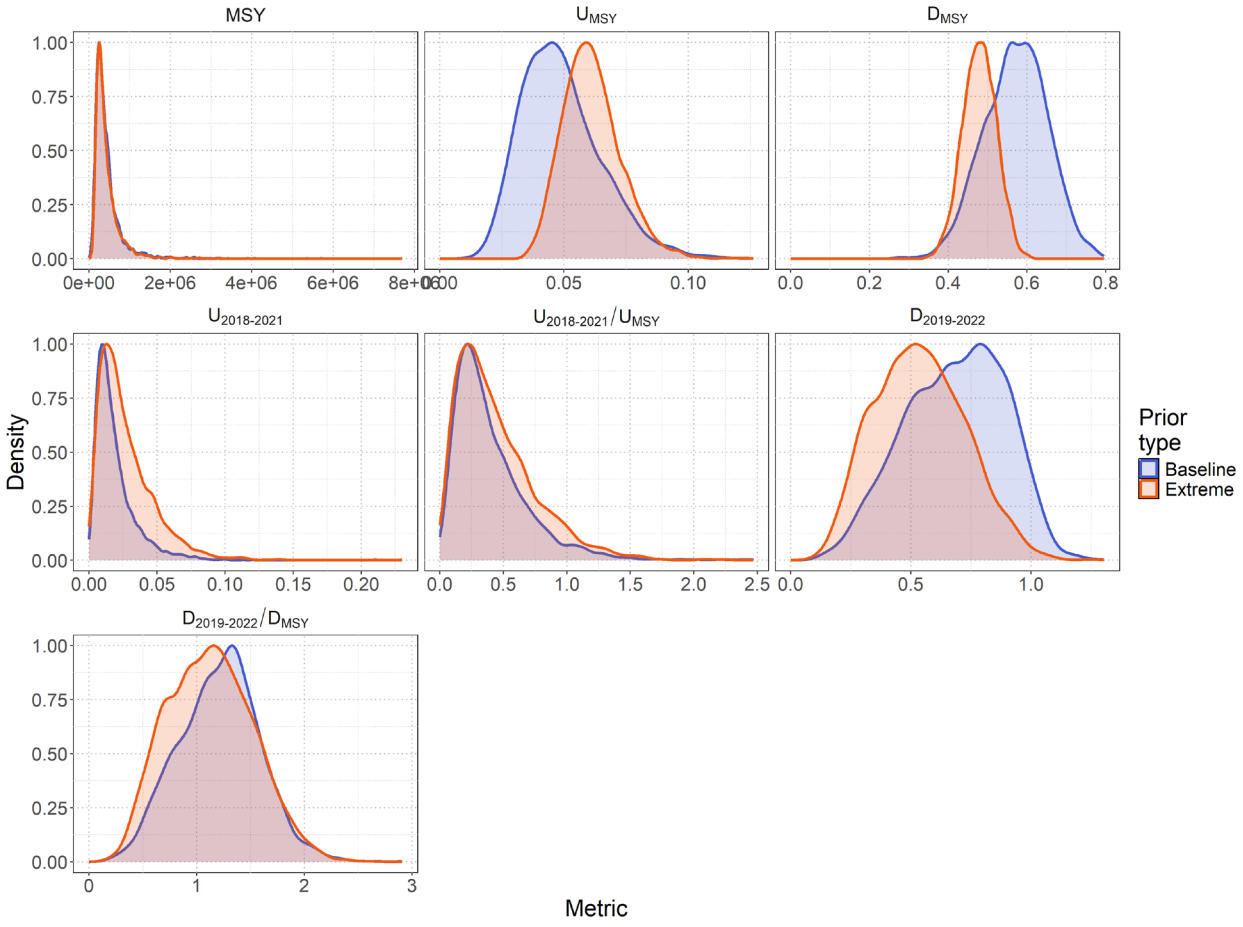


2951

2952 *Figure 23*. Posterior distributions of management reference points ($MSY$, $U_{MSY}$, $D_{MSY}$,
2953 $U_{2018-2021}$, $U_{2018-2021}/U_{MSY}$, $D_{2019-2022}$, and $D_{2019-2022}/D_{MSY}$) for all 28 converged models
2954 of North Pacific shortfin mako in the weighted ensemble. Distribution color indicates the prior
2955 type for $R_{Max}$, $x_0$, and $n$ that the models used (see *Table 9* for details).

2956

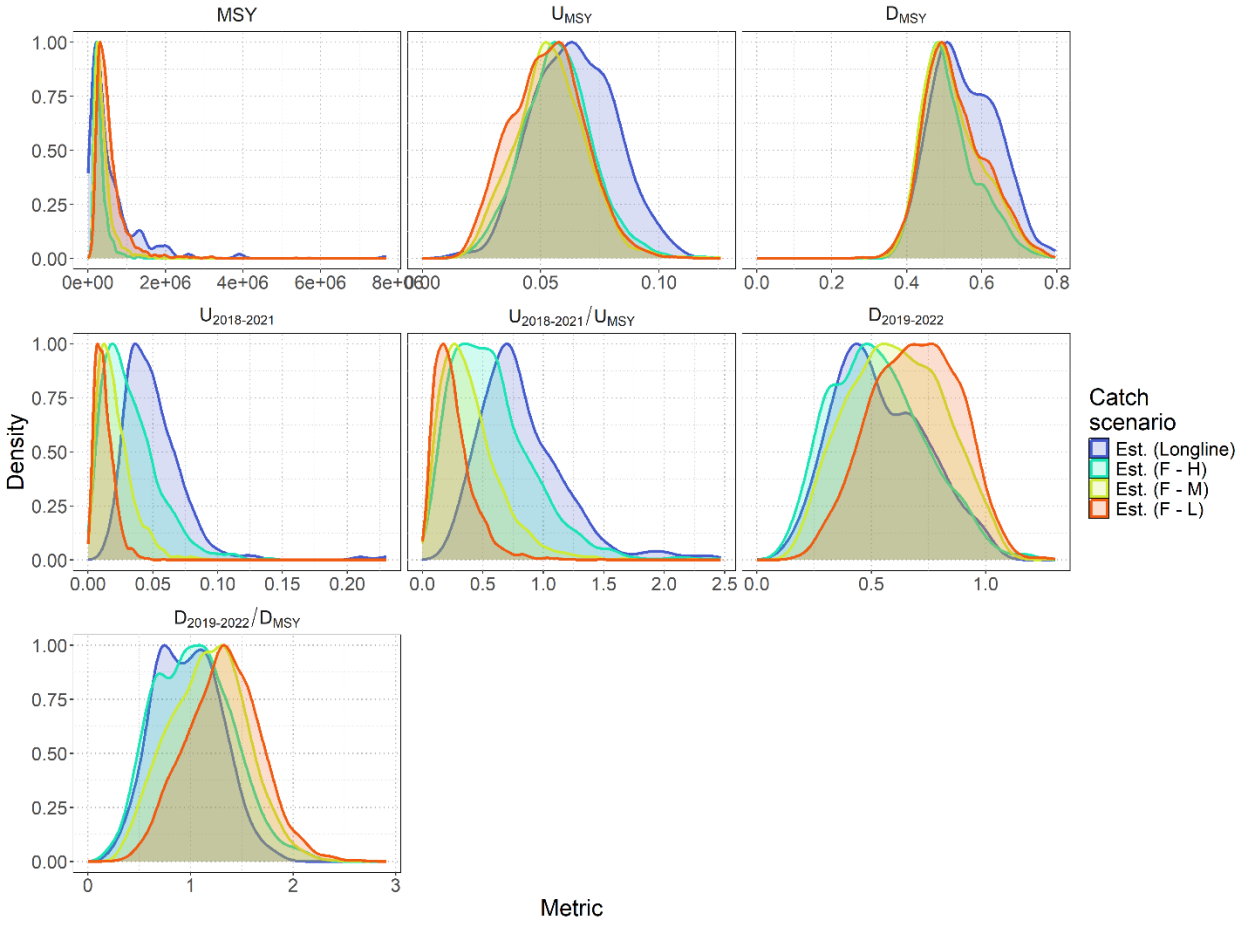


2957

2958 *Figure 24*. Posterior distributions of management reference points ($MSY$, $U_{MSY}$, $D_{MSY}$,
2959 $U_{2018-2021}$, $U_{2018-2021}/U_{MSY}$, $D_{2019-2022}$, and $D_{2019-2022}/D_{MSY}$) for all 28 converged models
2960 of North Pacific shortfin mako in the weighted ensemble. Distribution color indicates the
2961 treatment of catch that the models used (see *Table 9* for details).

2962

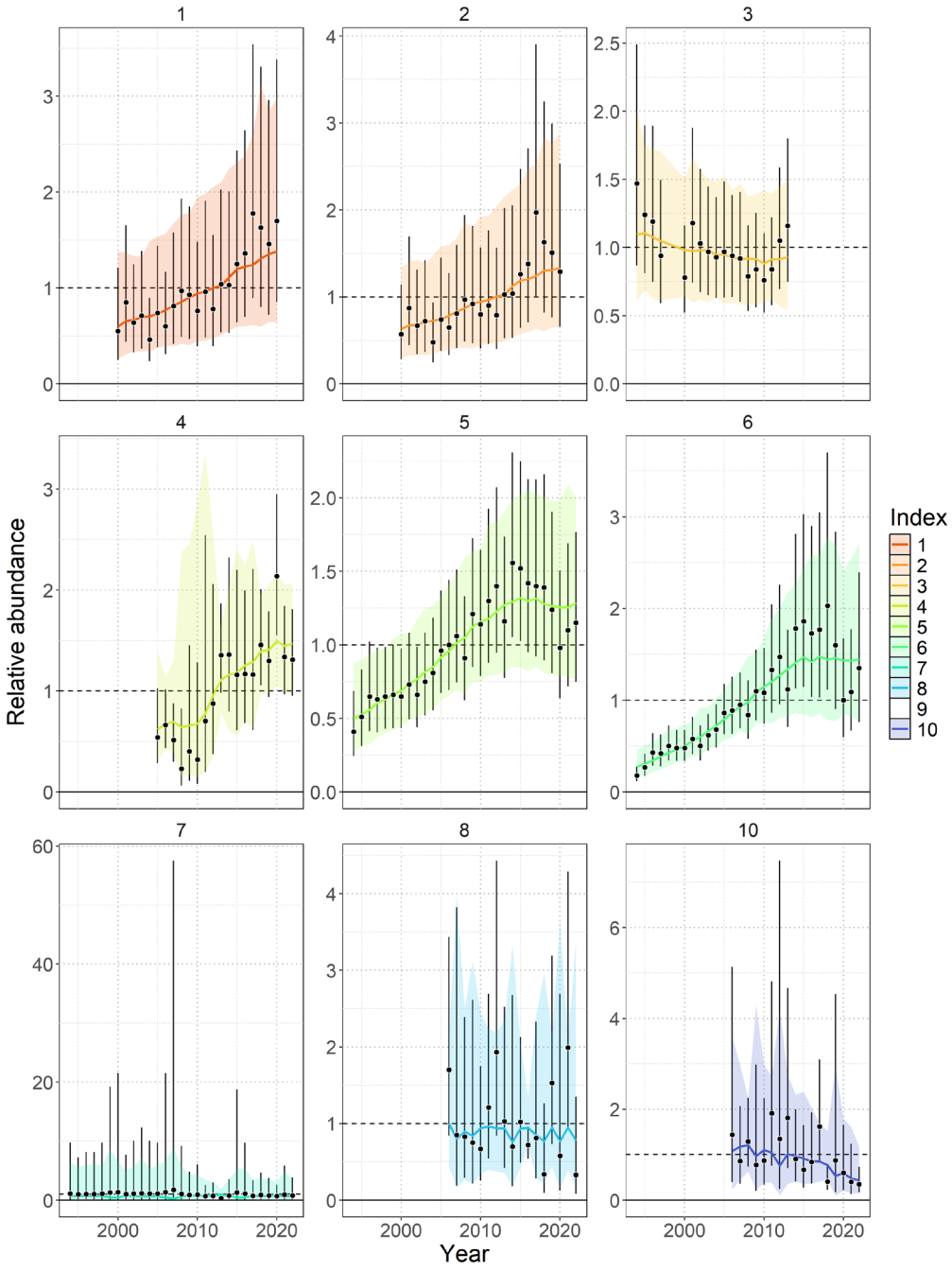


*Figure* 25. Posterior predicted CPUE (solid line – median, and 95% credible interval – shaded polygon) for 4 main indices (1,2, 4, and 5) and 6 sensitivity indices (3, 6, 7, 8, 9, and 10) of North Pacific shortfin mako. See *Table* 1 for details. Note that the model fitting to index 9 crashed and was unable to complete the estimation. Observed CPUE is shown in the black circles and the estimated observation error (95% credible interval) is shown with the vertical black bars. Colors correspond to each index.

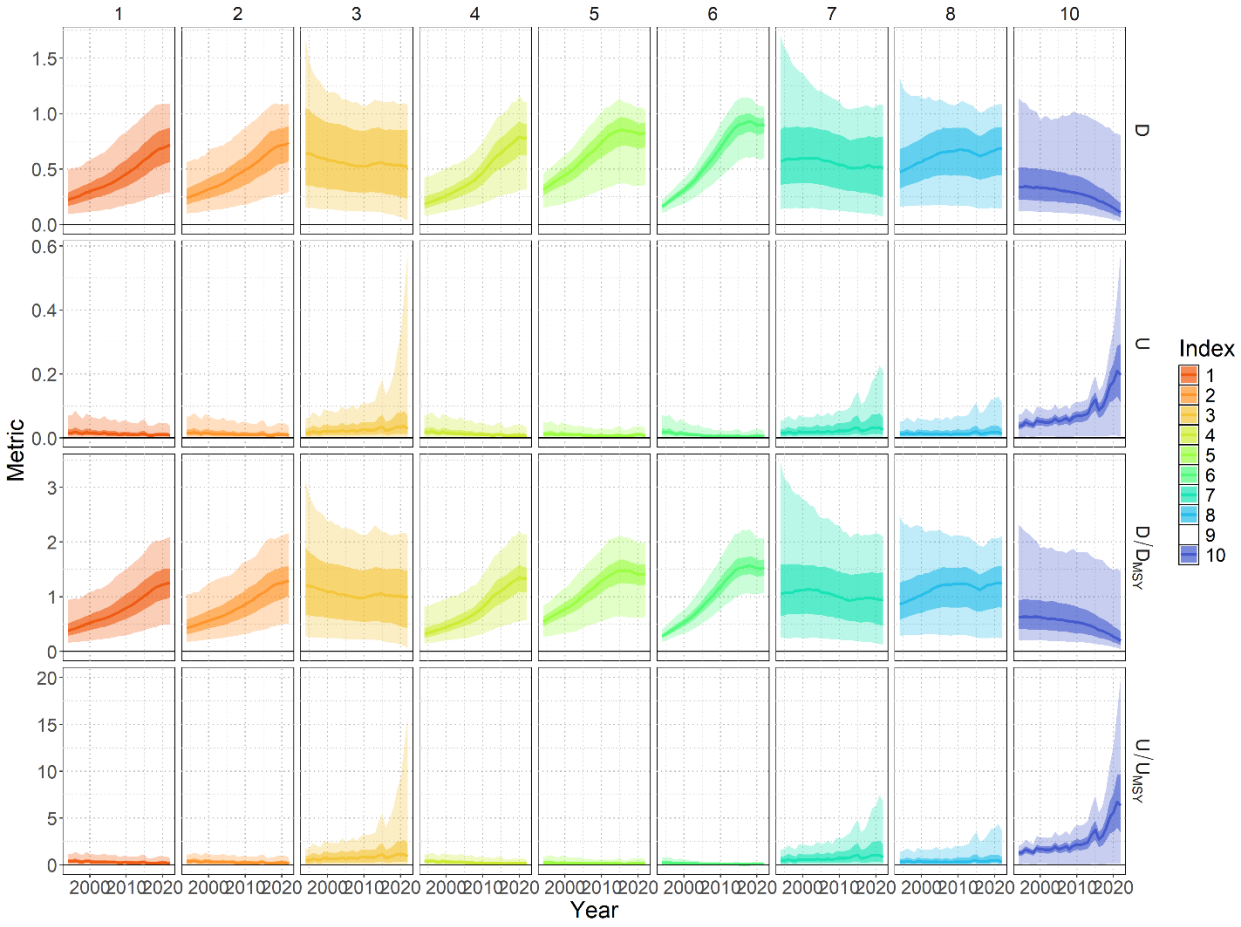


*Figure 26*. Time series (median - solid line) of management quantities ($D_t$, $U_t$, $D_t/D_{MSY}$, and $U_t/U_{MSY}$) for 4 main indices (1,2, 4, and 5) and 6 sensitivity indices (3, 6, 7, 8, 9, and 10) of North Pacific shortfin mako. See *Table* 1 for details. Darker shading indicates 50% credible interval and lighter shading indicates 95% credible interval. Colors correspond to each index.

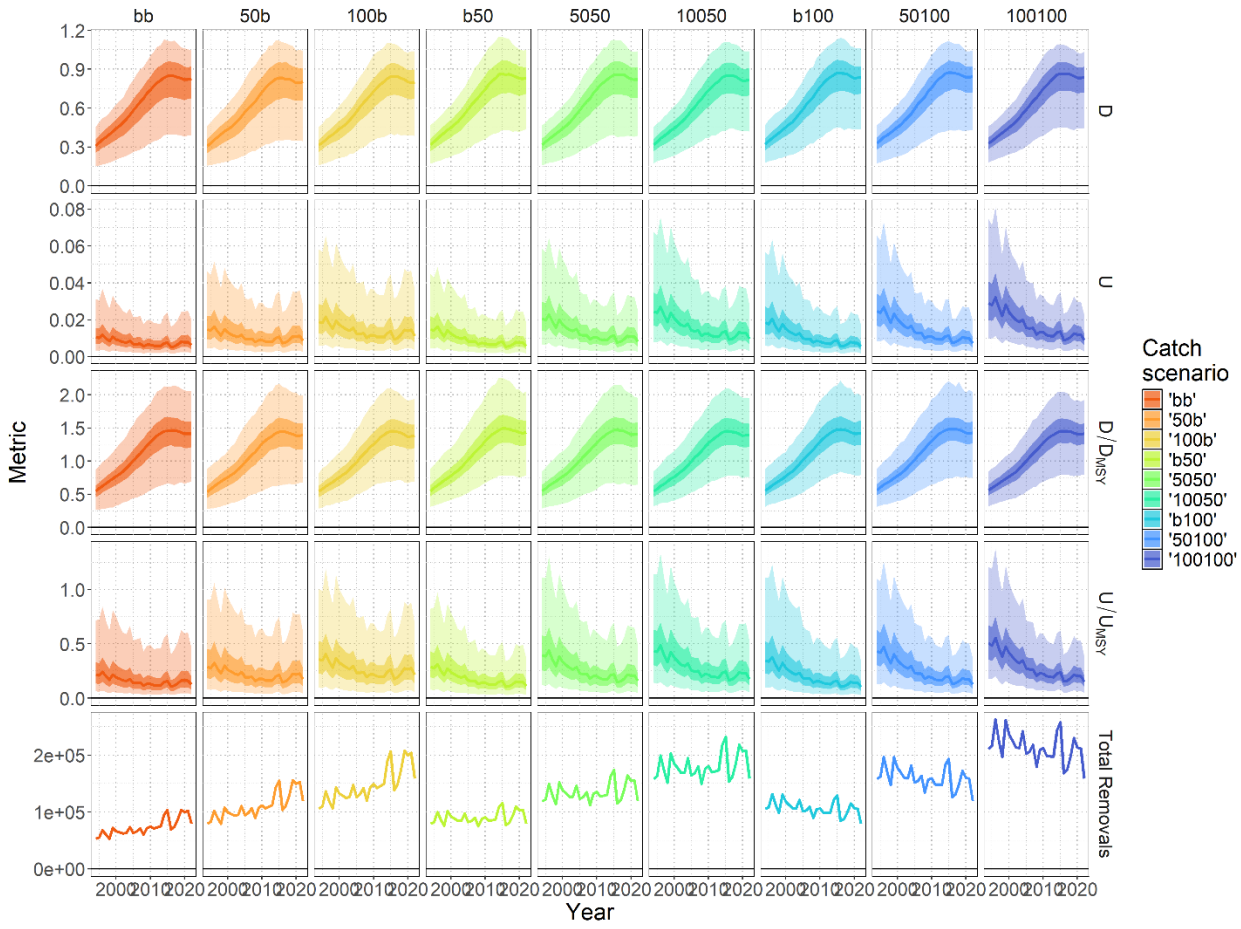


*Figure 27*. Time series (median - solid line) of management quantities ($D_t$, $U_t$, $D_t/D_{MSY}$, $U_t/U_{MSY}$, and total removals) for 9 fixed catch scenarios of North Pacific shortfin mako. See *Table 8* for details. Darker shading indicates 50% credible interval and lighter shading indicates 95% credible interval. Colors correspond to each catch scenario.

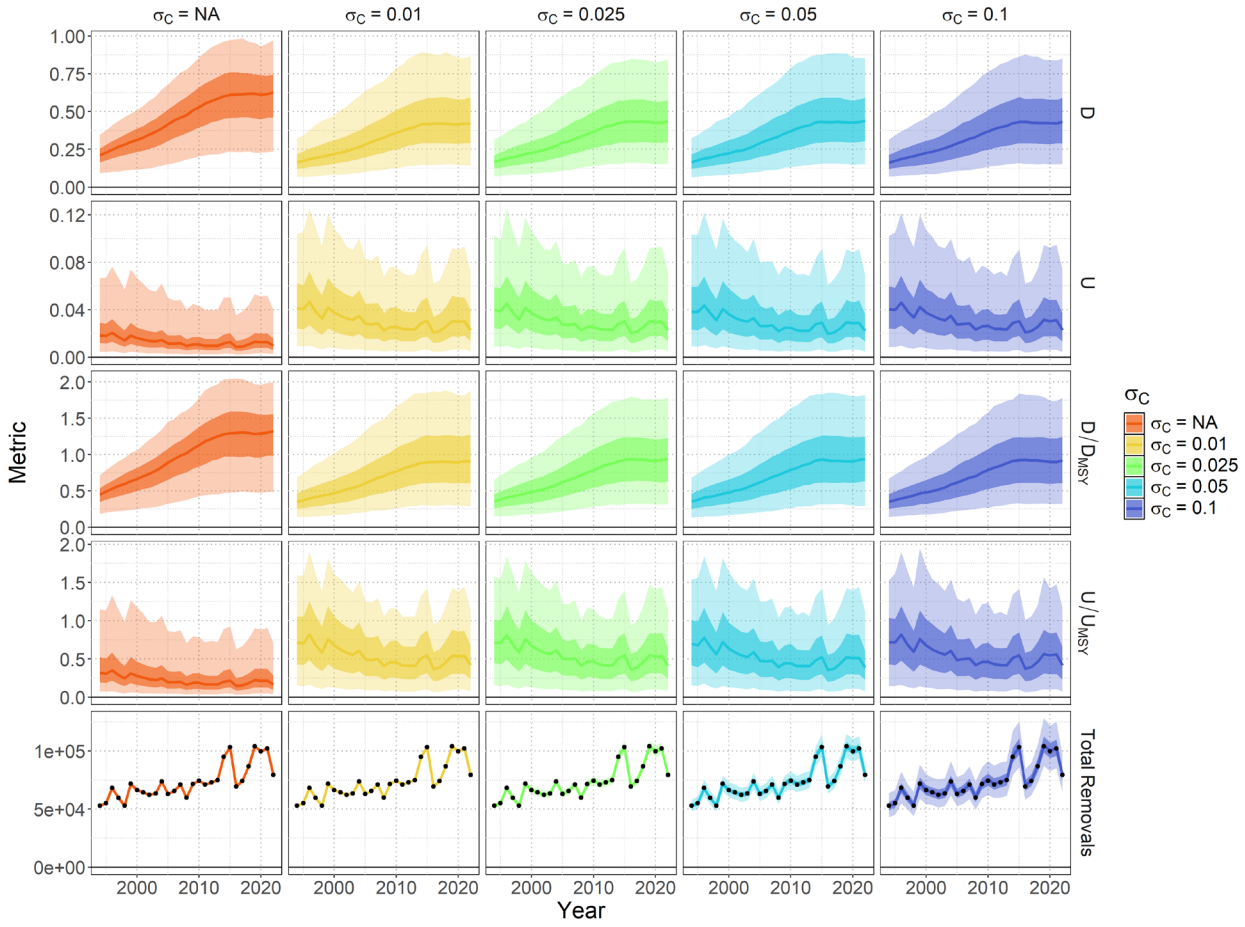


2982

2983 *Figure 28*. Time series (median - solid line) of management quantities ($D_t$, $U_t$, $D_t/D_{MSY}$,
2984 $U_t/U_{MSY}$, and total removals) of North Pacific shortfin mako for alternative assumptions of $\sigma_C$.
2985 Darker shading indicates 50% credible interval and lighter shading indicates 95% credible
2986 interval. Colors correspond to each $\sigma_C$ scenario. The black circles in the 'Total Removals'
2987 panels are the observations of catch that those models were fit to.

2988

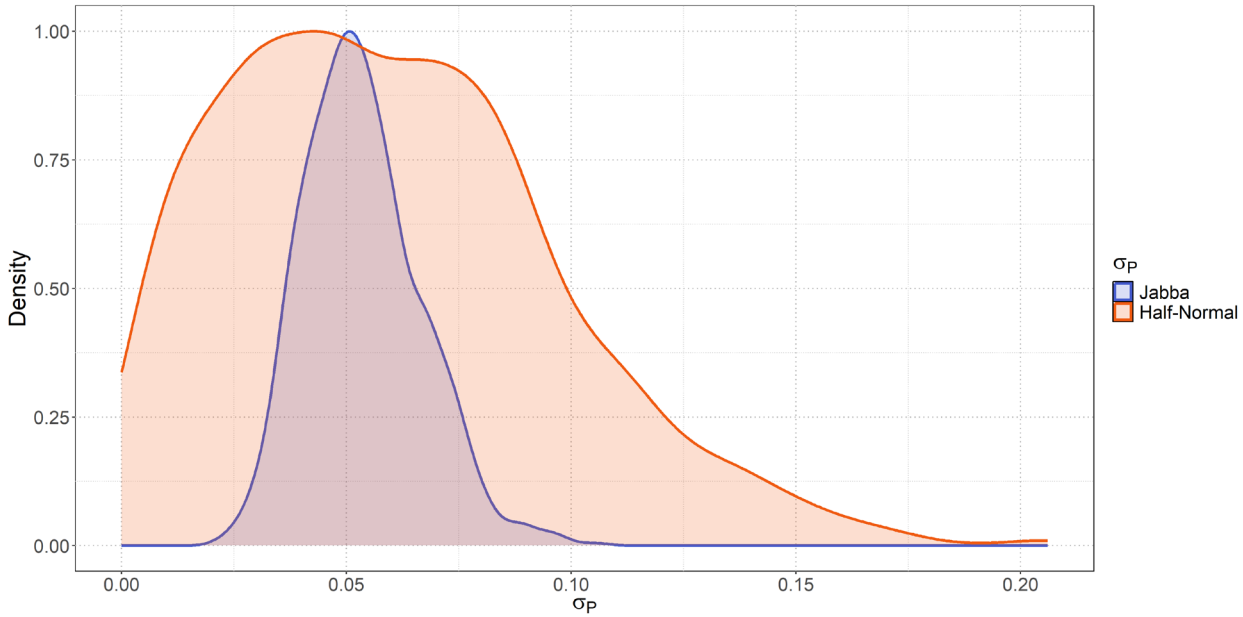


*Figure 29*. Estimated posterior distributions of process error $\sigma_P$ under two different prior distributions: JABBA *(Winker et al., 2018)*, and $\sigma_P \sim \text{Normal}^{+}(0,1)$, half-Normal for North Pacific shortfin mako.

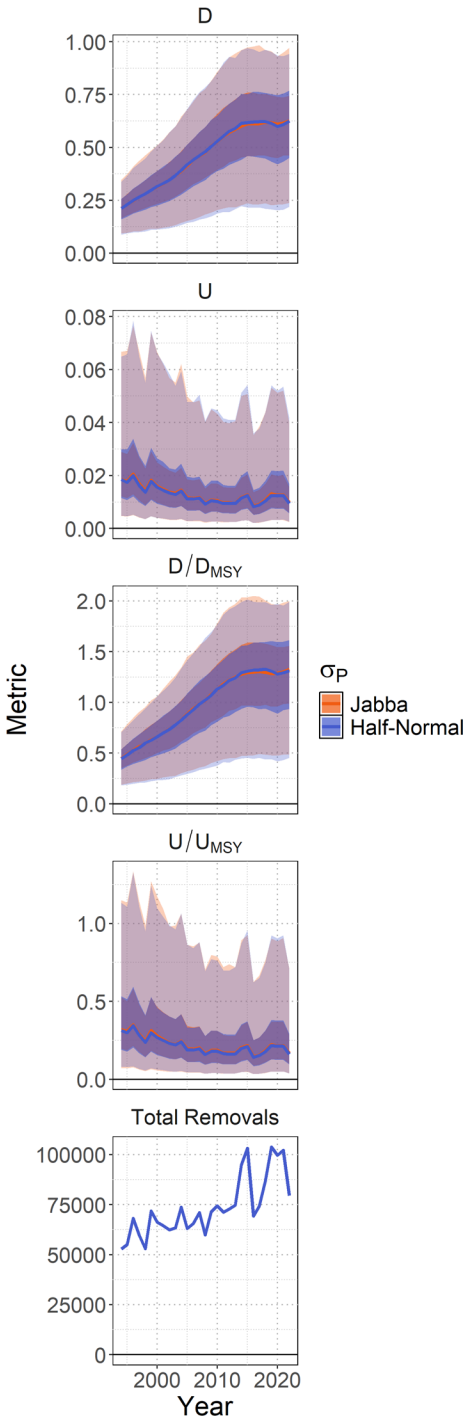


*Figure 30*. Time series (median - solid line) of management quantities ($D_t$, $U_t$, $D_t/D_{MSY}$, $U_t/U_{MSY}$, and total removals) of North Pacific shortfin mako for alternative priors for $\sigma_P$. Darker shading indicates 50% credible interval and lighter shading indicates 95% credible interval. Colors correspond to each $\sigma_P$ scenario.

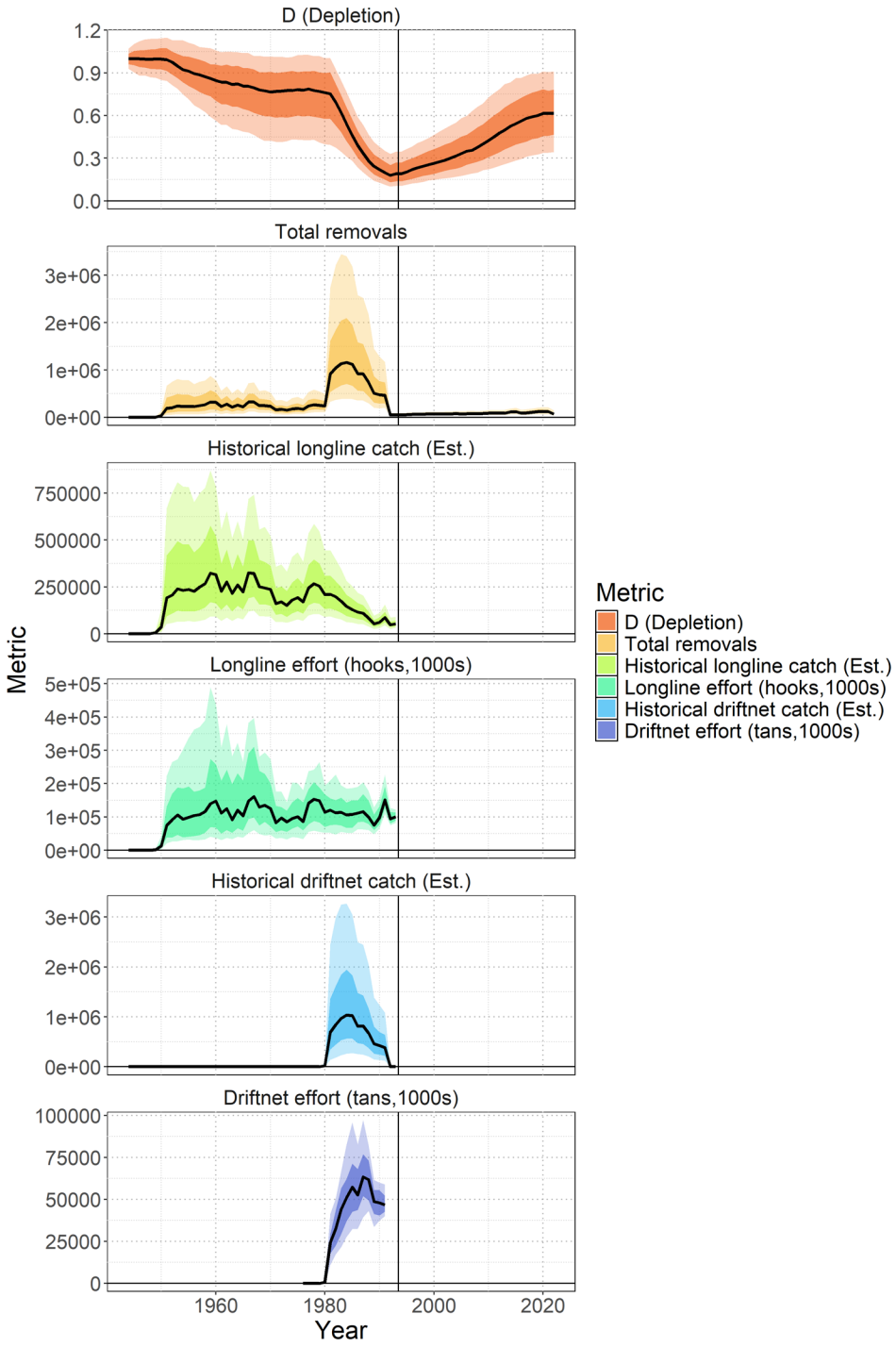


3000

3001 *Figure 31*. Historical simulated population trajectory, total removals, and catch (for longline and
3002 driftnet) based on retrospective projections across the converged, weighted ensemble for North
3003 Pacific shortfin mako. The effort time series used to drive the retrospective projections are
3004 shown with error. Median values are shown by the solid line. Darker shading indicates 50%

credible interval and lighter shading indicates 80% credible interval. Colors correspond to each metric.

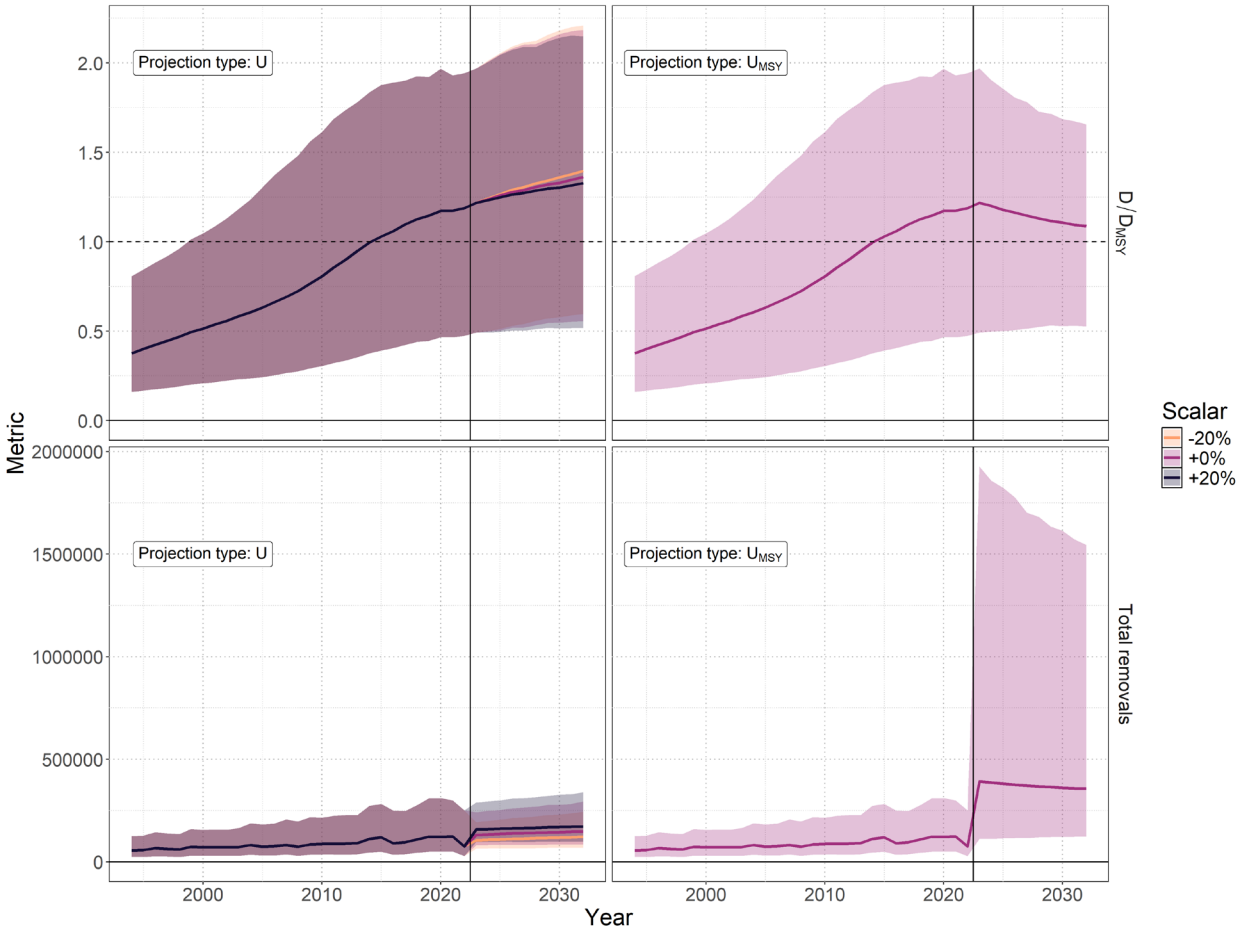


*Figure 32*. Stochastic stock projections of depletion relative to MSY ($D/D_{MSY}$) and catch (total removals) of North Pacific shortfin mako from 2023 to 2032 were performed assuming four different harvest policies: $U_{2018-2021}$, $U_{2018-2021} + 20\%$, $U_{2018-2021} - 20\%$, and $U_{MSY}$. The 95% credible interval around the projection is shown by the shaded polygon.

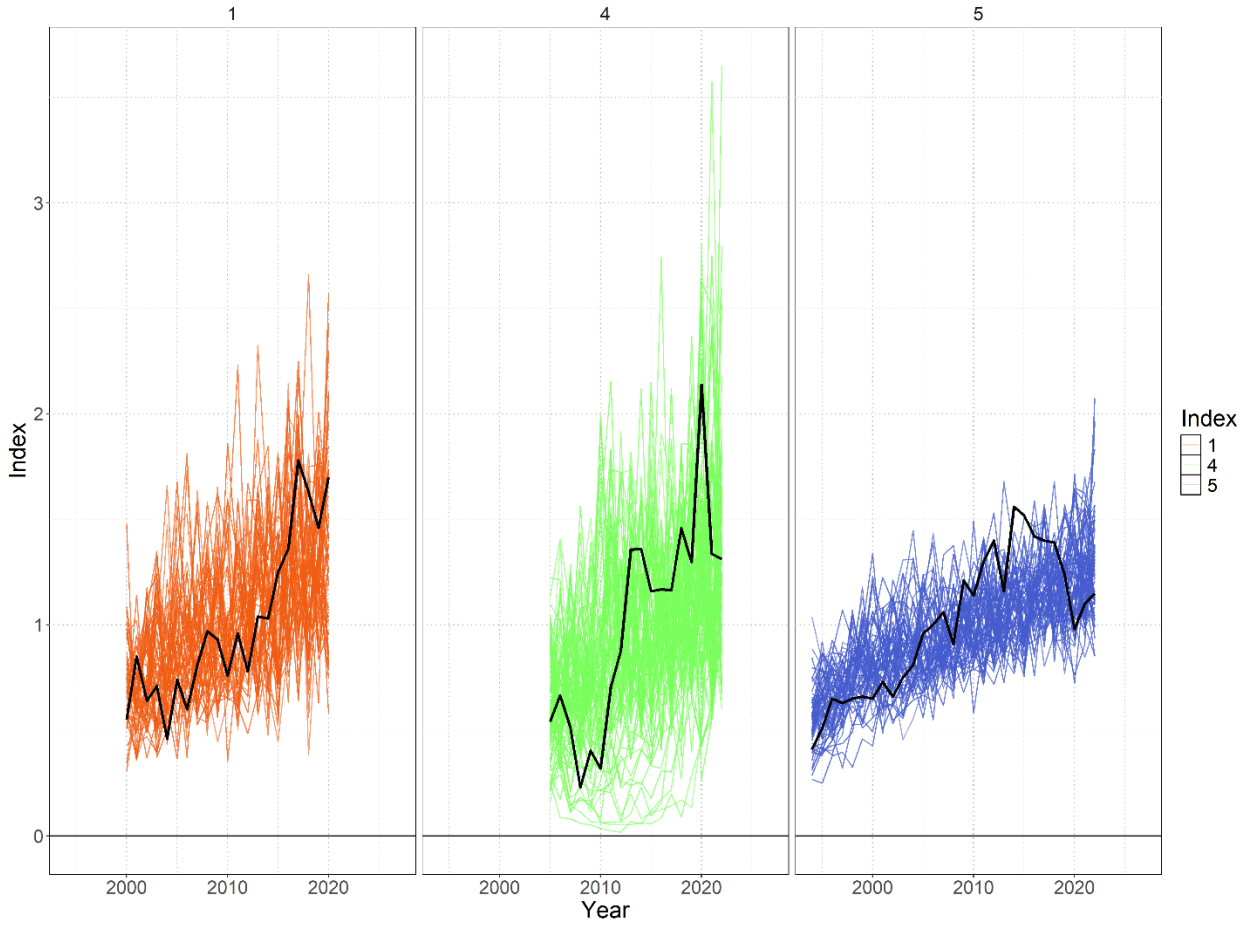


*Figure 33*. Simulated indices of North Pacific shortfin mako from the age-structured simulation model for the 140 scenarios that produced an index with at least a 50% increase over the model period. Simulated indices were constructed by applying the fisheries selectivity curve associated with indices S1, S4, or S5 to the simulated numbers at age. The black line in each panel is the observed index for S1, S4, or S5.

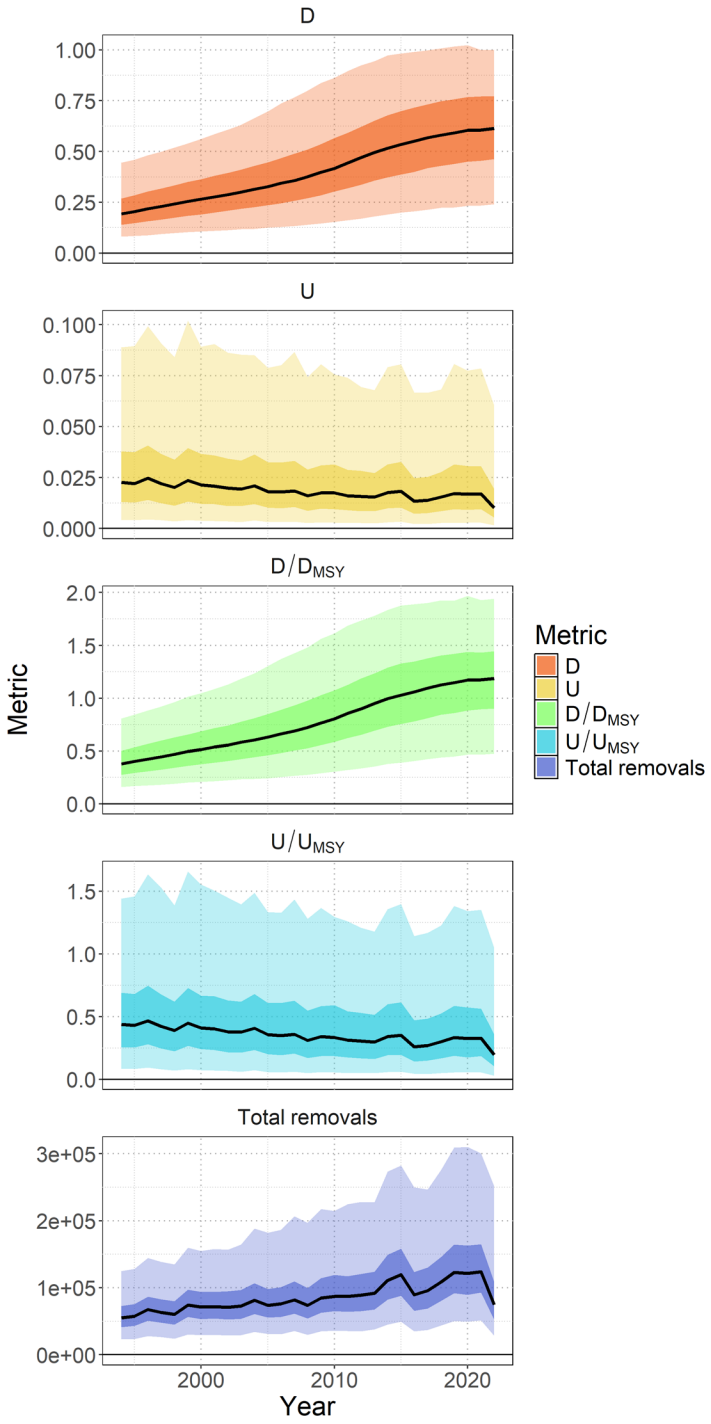


*Figure 34*. Time series (solid lines) of estimated: depletion (D), exploitation rate (U), depletion relative to the depletion at maximum sustainable yield ($D/D_{MSY}$), exploitation rate relative to the exploitation rate that produces MSY ($U/U_{MSY}$), and total fishery removals (numbers) for North Pacific shortfin mako. Darker shading indicates 50% credible interval and lighter shading indicates 95% credible interval.

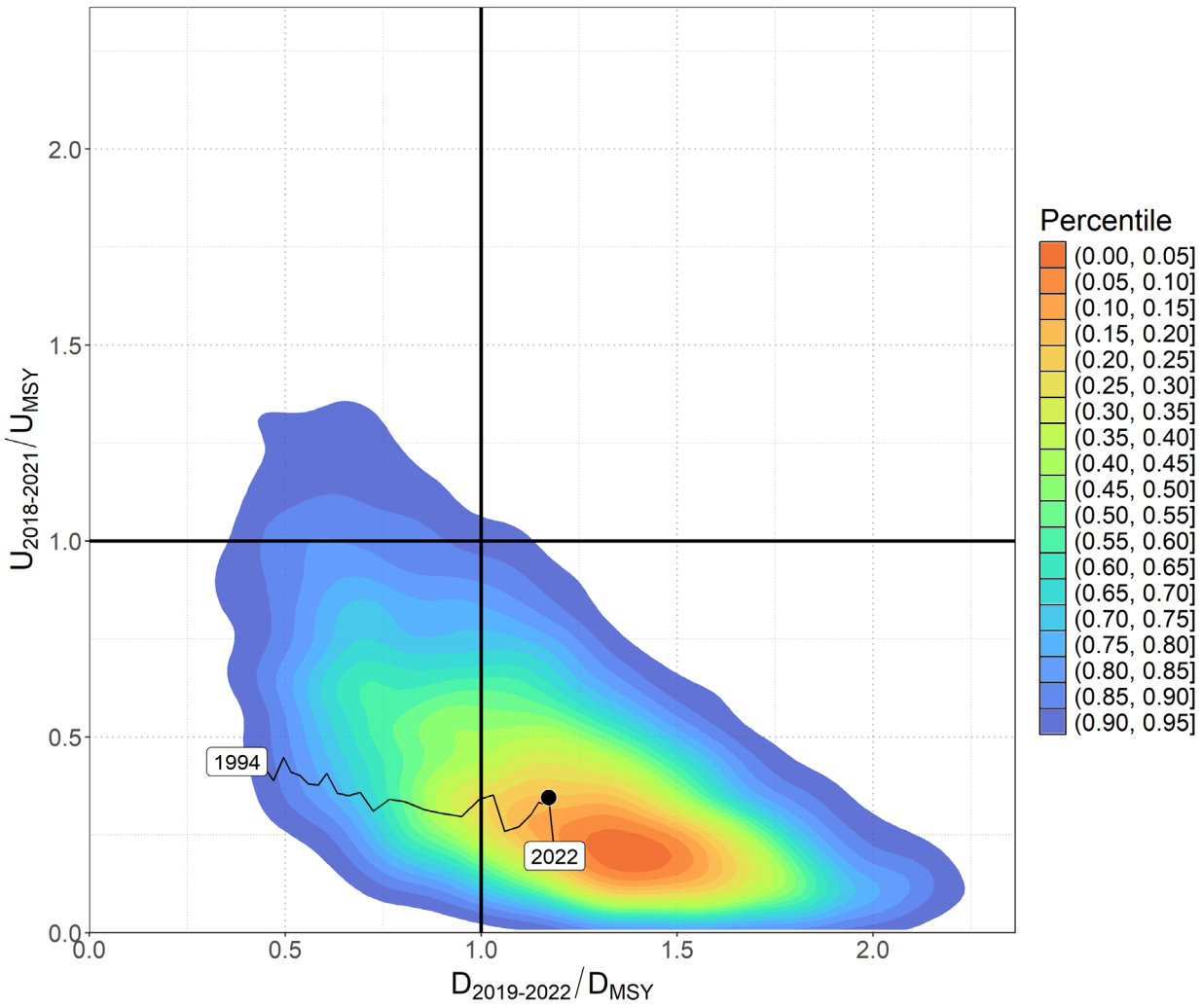


*Figure 35*. Kobe plot showing the bivariate distribution (shaded polygon) average recent depletion relative to the depletion at MSY ($D_{2019-2022}/D_{MSY}$) against the average recent exploitation rate relative to the exploitation rate at MSY ($U_{2018-2021}/U_{MSY}$) for North Pacific shortfin mako. The median of this bivariate distribution is shown with the solid black point. The time series of annual $D_t/D_{MSY}$ versus $U_t/U_{MSY}$ is shown from 1994 to 2022.

## 13. APPENDIX

As mentioned in Section 4.2.2.2, an error was discovered in Eq. 4.2.2.2.b where the fishing mortality associated with non-longline catch ($F_t^{noLL}$) was defined using the discrete rather than the continuous definition of fishing mortality.

$$F_t^{noLL} = \frac{C_t'}{x_t K};\ \text{Discrete}$$

$$F_t^{noLL} = -\log\left(-\left(\frac{C_t'}{x_t K}\right)+1\right);\ \text{Continuous}$$

The eight models in the BSPM ensemble that estimated removals using fishing mortality were re-run with a Stan executable that used the correct, continuous definition of fishing mortality. Comparing the estimates of time series of management quantities between the 8 models that used discrete versus continuous fishing mortality for Eq. 4.2.2.2.b showed negligible differences (Appendix Figure 1). Recalculating the weighted, ensemble posterior distributions using the 8 models with the correct, continuous definition of fishing mortality showed negligible differences (Appendix Figure 2).

These results are unsurprising given that estimated fishing mortality is small. When estimated fishing mortality is small differences between the two fishing mortality differences are minimized.

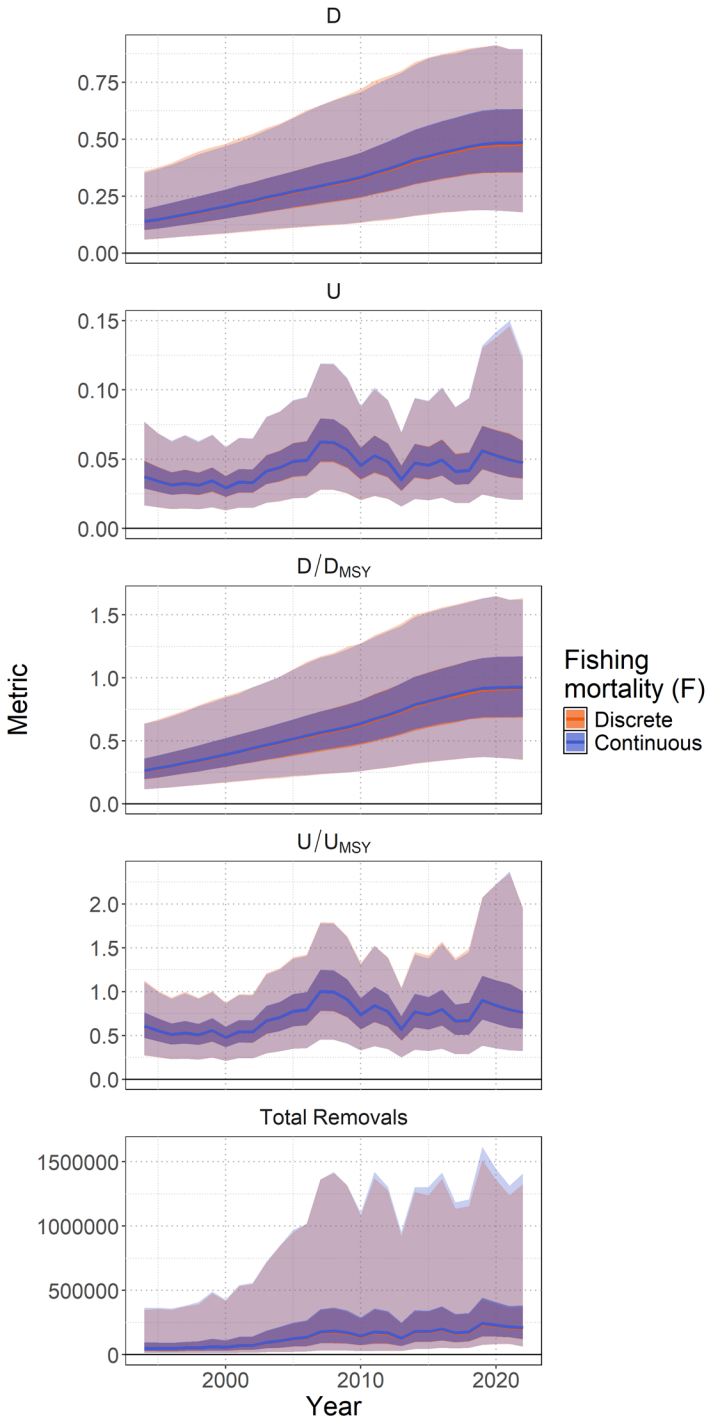


*Appendix Figure 1*. Time series (solid lines) of estimated: depletion (D), exploitation rate (U), depletion relative to the depletion at maximum sustainable yield ($D/D_{MSY}$), exploitation rate relative to the exploitation rate that produces MSY ($U/U_{MSY}$), and total fishery removals (numbers) for North Pacific shortfin mako. Darker shading indicates 50% credible interval and lighter shading indicates 95% credible interval. Color indicates which definition of fishing mortality was used.

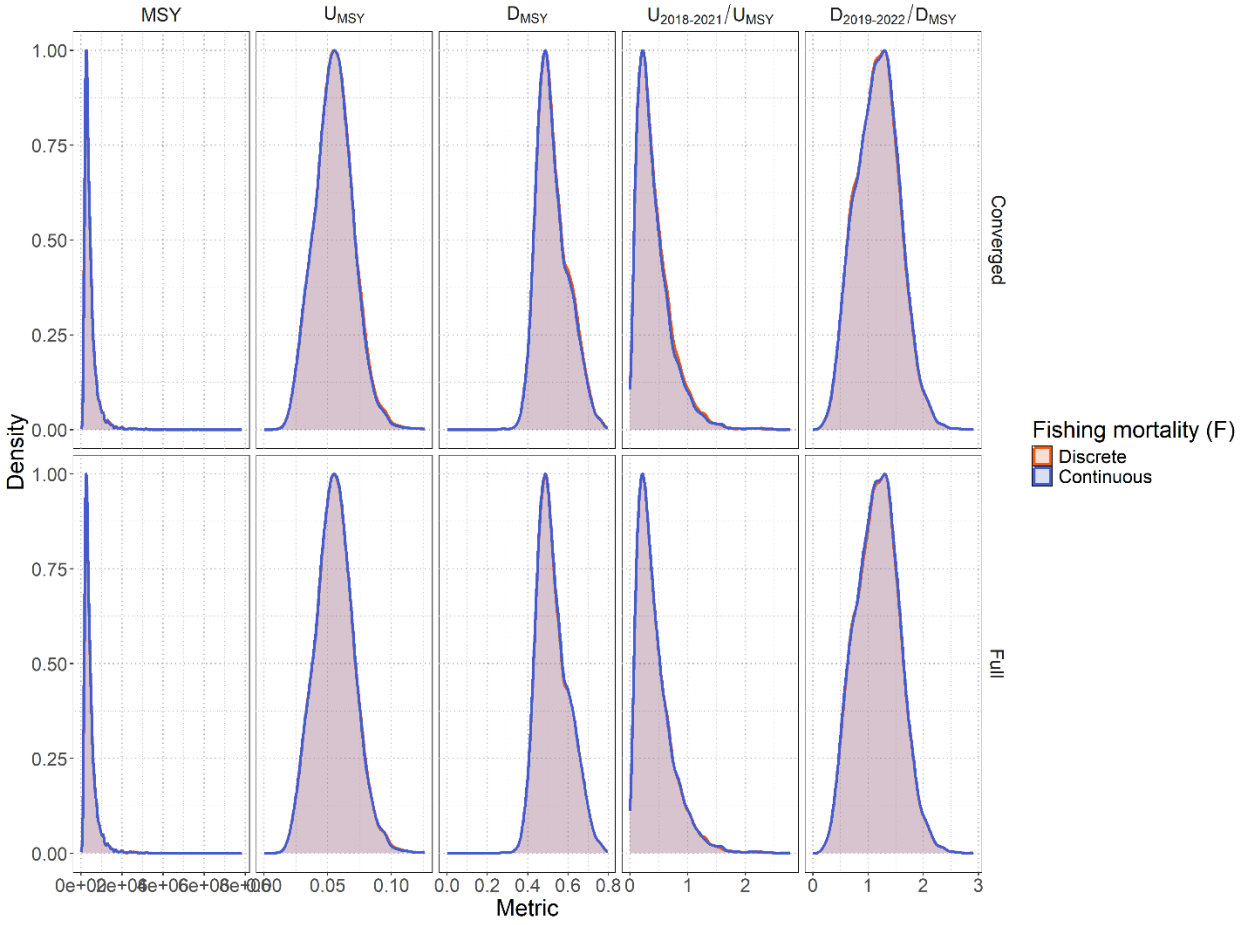


*Appendix Figure 2*. Posterior distributions of management reference points ($MSY$, $U_{MSY}$, $D_{MSY}$, $U_{2018-2021}/U_{MSY}$, and $D_{2019-2022}/D_{MSY}$) of North Pacific shortfin mako for all models in the weighted ensemble. The top row shows distributions only for converged models, the bottom row shows distributions for all models. Color indicates which definition of fishing mortality was used.